STRENGTHENING BRIDGES USING COMPOSITE MATERIALS

FHWA-OR-RD-98-08

RESEARCH UNIT

Oregon Department of Transportation

STRENGTHENING BRIDGES USING COMPOSITE MATERIALS

FHWA-OR-RD-98-08

by

Damian Kachlakev, PhD
Oregon State University
Civil Construction and Environmental Engineering Department
Corvallis, OR 97331

for

Oregon Department of Transportation
Research Unit
2950 State Street
Salem, OR 97310

and
Federal Highway Administration
Washington DC 20560

March 1998

Technical Report Documentation Page

1. Report No. FHWA-OR-RD-98-08	2. Government Accession No.	3. Recipient's Catalog No.
4. Title and Subtitle Strengthening Bridges Using Composite Materials		5. Report Date March 1998 6. Performing Organization Code
7. Author(s) Damian Kachlakev, PhD Oregon State University Civil Construction and Environmental Engineering Department Corvallis, OR 97330		8. Performing Organization Report No.
9. Performing Organization Name and Address Oregon Department of Transportation Research Unit 2950 State Street Salem, Oregon 97310		10. Work Unit No. (TRAIS) 11. Contract or Grant No.
12. Sponsoring Agency Name and Address Oregon Department of Transportation Research Unit 2950 State Street Salem, Oregon 97310 and Federal Highway Administration Washington DC 20560		13. Type of Report and Period Covered Synthesis 14. Sponsoring Agency Code

15. Supplementary Notes

16. Abstract

The objective of this research project is to outline methodologies for using Fiber Reinforced Polymer (FRP) composites to strengthen and rehabilitate reinforced concrete bridge elements.

Infrastructure deterioration and bridge strengthening techniques using FRP materials are discussed as background. Properties and classifications of different reinforcing fibers and resin matrices are provided, along with the mechanical properties of the FRP composites.

Basic concepts and design principles for composite FRP materials are introduced, and topics such as manufacturing processes, anisotropic elasticity, strength of anisotropic materials, and micro-mechanics are presented.

Techniques and concepts for strengthening concrete beams with FRP composites are discussed, as are flexural and shear strengthening design and construction methodologies. The worldwide research experience in the behavior of FRP strengthened beams under various conditions are summarized.

External reinforcement of concrete columns using FRP materials is examined. Theoretical background, factors influencing the performance of FRP wrapped columns, and various case studies are presented. Design methodologies and examples supplement the case studies for both beams and columns. Most FRP material systems available on the market today are summarized and evaluated.

Construction and durability requirements of the retrofitted systems are presented. Reliability assessment, condition evaluation methods, and factors influencing the strengthening quality are included. The various steps of the construction process, such as selection of a composite strengthening system, concrete surface preparation, and bond between FRP and concrete are summarized. Quality control, environmental durability of FRP composites, and cost effectiveness are presented.

17. Key Words BRIDGE, COMPOSITE, FIBER, FRP, POLYMER, REINFORCEMENT, STRENGTHENING	18. Distribution Statement		
19. Security Classif. (of this report) Unclassified	20. Security Classif. (of this page) Unclassified	21. No. of Pages 182	22. Price

Technical Report Form DOT F 1700.7 (8-72) Reproduction of completed page authorized

SI* (MODERN METRIC) CONVERSION FACTORS

APPROXIMATE CONVERSIONS TO SI UNITS

Symbol	When You Know	Multiply By	To Find	Symbol
		LENGTH		
in	inches	25.4	millimeters	mm
ft	feet	0.305	meters	m
yd	yards	0.914	meters	m
mi	miles	1.61	kilometers	km
		AREA		
in^2	square inches	645.2	millimeters	mm^2
ft^2	square feet	0.093	meters squared	m^2
yd^2	square yards	0.836	meters squared	m^2
ac	acres	0.405	hectares	ha
mi^2	square miles	2.59	kilometers	km^2
		VOLUME		
fl oz	fluid ounces	29.57	milliliters	mL
gal	gallons	3.785	liters	L
ft^3	cubic feet	0.028	meters cubed	m^3
yd^3	cubic yards	0.765	meters cubed	m^3
NOTE: Volumes greater than 1000 L shall be shown in m^3.				
		MASS		
oz	ounces	28.35	grams	g
lb	pounds	0.454	kilograms	kg
T	short tons (2000 lb)	0.907	megagrams	Mg
		TEMPERATURE (exact)		
°F	Fahrenheit temperature	5(F-32)/9	Celsius temperature	°C

APPROXIMATE CONVERSIONS FROM SI UNITS

Symbol	When You Know	Multiply By	To Find	Symbol
		LENGTH		
mm	millimeters	0.039	inches	in
m	meters	3.28	feet	ft
m	meters	1.09	yards	yd
km	kilometers	0.621	miles	mi
		AREA		
mm^2	millimeters squared	0.0016	square inches	in^2
m^2	meters squared	10.764	square feet	ft^2
ha	hectares	2.47	acres	ac
km^2	kilometers squared	0.386	square miles	mi^2
		VOLUME		
mL	milliliters	0.034	fluid ounces	fl oz
L	liters	0.264	gallons	gal
m^3	meters cubed	35.315	cubic feet	ft^3
m^3	meters cubed	1.308	cubic yards	yd^3
		MASS		
g	grams	0.035	ounces	oz
kg	kilograms	2.205	pounds	lb
Mg	megagrams	1.102	short tons (2000 lb)	T
		TEMPERATURE (exact)		
°C	Celsius temperature	1.8 + 32	Fahrenheit	°F

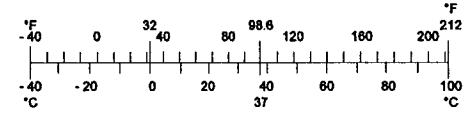

* SI is the symbol for the International System of Measurement

(4-7-94 jbp)

ACKNOWLEDGEMENTS

The author wishes to express his appreciation to Marty Laylor, Project Manager, and Galen McGill, Manager, both of the Research Unit of the Oregon Department of Transportation, for their valuable suggestions and many contributions to this project. The author also gratefully acknowledges the rest of the technical advisory committee for their direction and review of this work.

DISCLAIMER

STRENGTHENING BRIDGES USING COMPOSITE MATERIALS

TABLE OF CONTENTS

LIST OF FIGURES

LIST OF TABLES

STANDARD TERMINOLOGY RELATED TO COMPOSITE MATERIALS

Anisotropic Material – A material having properties that vary with direction or depend on the orientation of reference axes. Generally these material do not have planes of material property symmetry.

Fiber – A material characterized geometrically by its high length-to-diameter ratio.

Fiber Reinforced Polymers (FRP) – Composite materials that consist of high strength fibers bound together with an inert plastic resin.

Filler – In manufacturing carbon or glass product technology, particles comprising the base aggregate in an unbaked green-mix formulation. Generally a finely ground mineral that has been intimately mixed into a resin or resin component for the purpose controlling the rheology or extending the resin.

Hardness – The property of a material that resists deformation, particularly permanent deformation or indentation.

Heterogeneous Material – Also called **inhomogeneous**, a material having properties that vary from point to point or depend on location.

Homogeneous – A material having properties that are independent of location.

Hybrid Composite – Composite laminate containing lamina of two or more different types of materials.

Hybrid Structural Behavior – The response of hybrid structure, i.e., FRP-strengthened concrete.

Impregnation – Partial filling of the open pore structure with another material.

Isotropic Material – A material having the same properties in all directions which are independent of the orientation of the reference axes.

Lamina – Also called **ply**, is a plane (or curved) layer of fibers or woven fabric in a matrix. In the case of unidirectional fibers, it is referred to as **unidirectional lamina**.

Laminate – A sequence of two or more unidirectional laminae or plies bonded together at various orientations.

Lamination – The bonding or impregnating of superposed layers with resin and compressing under heat.

Lay-up – Installation of lamina to form a laminate; configuration of the laminate indicating its ply composition.

Macro-mechanics – A study of the composite material behavior wherein the material is presumed homogeneous and the effects of the constituent materials are detected only as average properties.

Micro-mechanics – A study of the composite behavior by examining the behavior and interaction of the constituent materials on a microscopic level.

Molded – Formed in a die by the application of external pressure.

Orthotropic Material – An orthogonally anisotropic material, i.e., having at least three mutually perpendicular planes of material property symmetry.

Phase – Constituent. Each constituent of a composite material, i.e. the fibers and the resin, is a phase. One phase, called reinforcement, is usually discontinuous and stronger, and the weaker phase is called a matrix.

Prepreg FRP – Pre-made materials which are cold laminated in place, by using a resin-fibers-resin lay-up technique to build up an appropriate thickness for the completed composite.

Pultruded Composite Plates – Plates, manufactured by pultrusion (as contrasted to extrusion) which are post-epoxy-bonded to the concrete structure.

Pultrusion – Manufacturing process for fiber-reinforced composites by pulling resin-impregnated fiber through a die.

Specially Orthotropic Material – Orthotropic material with axes of symmetry aligned with the material symmetry, i.e., "x " axis coincides with fiber direction.

Specific Modulus – Elastic modulus of the material divided by its density.

Specific Strength – Strength of the material divided by its density.

Structural Composite – A material system consisting of two or more phases on a macroscopic level, whose mechanical properties and performance are designed to be superior to those of the constituent materials acting independently.

Working Direction – The direction of fiber or the direction of applied force used in forming a solid body; which defines its physical properties and orientation at installation.

1.0 INTRODUCTION

1.1 BACKGROUND

In the present age, civil engineers are frequently faced with the problem of strengthening an existing structure to assure or to increase its structural safety. Reasons for such actions include changes in the use of structures as well as increased traffic loads on bridges. Due to ever increasing damage caused by environmental effects, corrosion of steel and deterioration of concrete reduce structural safety and lead to inconvenience for the users.

The aging of infrastructures is a great safety and economic concern throughout the world today. The European Community directed that all highway bridges in the United Kingdom must either be capable of carrying 40-ton vehicles by 1999 or have a weight restriction order placed on them. This directive led to a major bridge assessment program, resulting in the need to address deficiencies in over 10,000 of the 60,000 reinforced concrete bridges in the UK. Similar problems are observed all over the world.

The backbone of America's commerce and industry consists of constructed facilities including highways, bridges, airports, and transit systems. Most of the constructed facilities are deteriorating at a rate faster than we can renovate them. Recent studies indicate that over three trillion dollars, or $200 billion dollars per year *(Faza et al, 1994)*, will be needed during the next fifteen years to bring these facilities to adequate operating levels *(McConnell, 1993)*.

Many bridges across the United States are deteriorating due to problems associated with reinforced concrete. Factors contributing to this infrastructure deterioration include the effects of environment (i.e. harsh climate), de-icing fluids, seismic activity, and increase in both quantity and weight of traffic loads on structures. For example, 40 percent of the nation's 575,000 bridges are structurally deficient or structurally obsolete, and 25 percent are over 50 years old *(Marshall and Busel, 1996)*. Many of these bridges were designed for lower traffic volumes and lighter loads than are common today. This makes them under-designed for current or projected traffic needs. Therefore, rehabilitation to original specifications will not bring these bridges up to the current standards. Strengthening must be considered.

The infrastructure in Oregon needs significant attention. Approximately 75 percent of Oregon's bridges are over 50 years old. These bridges were designed for H-15 traffic loads and do not meet the requirements for the current H-25 load standard. Based on their theoretical capacity, many of Oregon's bridges are classified as under-designed.

In addition to increased or changing traffic demands, common bridge deficiencies include deck deterioration due to wear, freeze/thaw cycles, corrosion of structural steel members, corrosion of reinforcement in concrete structures, response problems under extreme wind or earthquake loads; and aging materials.

With the majority of the U.S. bridge inventory built in the 1950s and 1960s, many bridges are at an age where environmental deterioration, wear, and level of service dictate rehabilitation and upgrading *(Seible et al, 1995)*. Repair, strengthening, and/or retrofitting technologies are still at a stage where most applications are based on experience and trial and error, rather than on a sound scientific basis. In order to upgrade the bridge inventory to 21st century service levels, the large volume of rehabilitation work requires the development of new technologies based on new materials and new processes.

Restoring the structural integrity and enhancing the strength and stiffness capabilities of aging structures is a major challenge. The selection of proper methods to retrofit a structure is a complex task. Until recently, external post-tensioning and epoxy-bonded steel plates were the two alternative techniques used to retrofit structurally deficient structures.

External post-tensioning has been successfully used to increase strength of girders in existing bridges or buildings *(Klaiber et al, 1982; Saadatmanesh et al, 1989)*. However, this method has several practical difficulties such as providing anchorage for the post-tensioning strands, maintaining the lateral stability of the girders during post-tensioning, and protecting the exposed strands against corrosion *(Saadatmanesh and Ehsani, 1996)*. Additionally, post-tensioning requires considerable force to stress the concrete effectively, and may significantly reduce overhead clearance *(Dussek, 1980)*.

Epoxy-bonded steel plates have been used successfully in Europe, Japan, Australia, and South Africa for 25 years to increase the load-carrying capacity of existing reinforced concrete bridges *(Dussek, 1980; Chan and Tan, 1996; Yong et al, 1996)*. This strengthening technique has been found economical and efficient to apply. However, its application in the United States has been extremely rare *(Saadatmanesh et al, 1996)*.

The use of Fiber Reinforced Polymer (FRP) composites for rehabilitation and strengthening of civil engineering structures is very promising. FRP composites consist of high strength fibers bound together with an inert plastic resin. Epoxy resins curing at room temperature or specially developed resin systems are usually selected for this. The epoxy resins used for structural bonding of steel plates to concrete are suitable for the bonding of FRP plates as well *(Steiner, 1996)*.

FRP composites, primarily developed and used in the defense and aerospace industries, offer unique advantages in many applications where conventional materials cannot provide satisfactory service. Lightweight and natural corrosion resistance are among their main advantages over steel and metal alloys. Their high tensile strength is an excellent complement to concrete properties. Their impermeability and their ability to adhere to old concrete make FRP composites systems that outclass high-performance concrete *(Demers et al, 1996)*. Other advantages of FRP over steel include ease of surface preparation at installation, enhanced structural characteristics, and improved durability. When compared to conventional materials, the high strength-to-weight ratio, minor disruption of traffic during repair, and minimal maintenance requirements help make FRP composites an excellent candidate for rehabilitation and strengthening of reinforced concrete structures.

FRP composites are being explored worldwide as a promising material for new structures and rehabilitation/retrofit of aging facilities. In Germany and Switzerland, replacement of steel plates with FRP plates is viewed as a major improvement in externally bonded repair *(Meier and Kaiser, 1991)*. In the United States, Saadatmanesh and Ehsani *(1991, 1996)*, Ritchie *(1991)*, and Triantafillou and Plevris *(1992)* studied the behavior of reinforced concrete beams with externally bonded glass and carbon FRP. Fyfe *(1992)* first proposed a method for retrofitting bridge columns with glass FRP jackets. His work was followed by others *(Priestley et al, 1992)* and was supported by California Department of Transportation (Caltrans) in an effort to develop a method to enhance flexural and shear performance in critical regions of bridge columns during seismic retrofit. Of all countries, Japan has seen the largest research and development effort and the largest number of field applications using externally bonded FRP composites *(Nanni, 1995)*. The Japanese work is different from American and European approaches in that it makes use of thin FRP sheets rather than FRP plates.

Two approaches for the provision and application of FRP materials have been developed internationally. One is to employ pre-impregnation (prepreg) materials, which are cold laminated in place, by using a resin-fibers-resin lay-up technique to build up an appropriate thickness of the completed composite reinforcement. The second is to use "pultruded" composite plates, which are post-epoxy-bonded to the concrete structure. Both forms of material can be applied to either unstressed or prestressed concrete elements to take advantage of the high strength offered by FRP materials. The prepreg has the advantage of ensuring better "wetting" of the individual fibers, but has a disadvantage in terms of shelf life and curing because it requires a heating source and precautions for environmental protection.

FRP composites have the potential for tremendous impact on the construction industry internationally. Recent earthquakes in Southern California demonstrated the need for civil engineering structures with enhanced seismic protection. Applications of composite material systems to repair and/or upgrade structures may save billions of dollars, as well as many human lives.

While the advantages and limitations of conventional materials are well established, the advanced composite science and industry must clearly answer questions such as: What is a composite?; How much will it cost?; How long will it last?; and many more. Properly designed and manufactured composite material systems offer superior structural performance while being compatible with existing construction industry practices. Consensus standards and design guidelines are needed so that composite materials can enter the construction market on a large scale in the near future *(McConnell, 1995)*. Most importantly, selection and application of FRP materials for repair of structures should be used where the benefits of composites can be best realized.

Although strengthening of existing structures and construction of new facilities with FRP composites is a growing trend worldwide, many engineers are not aware that a significant body of knowledge exists. The existing knowledge can allow engineers to design retrofits and build new structures with composite materials based on sound engineering principles.

1.2 SCOPE AND OBJECTIVES

The objectives of this research project are to outline the methodologies that are needed for using FRP composites to strengthen and rehabilitate reinforced concrete bridge elements. This is achieved by examining the strengthening techniques and material properties of the available glass, carbon and aramid FRP composites. The most promising and cost effective composite systems and modeling techniques are recommended. Further consideration and potential use of composites for strengthening bridges in Oregon is recommended.

2.0 CONSTITUENT MATERIALS FOR COMPOSITES

2.1 DEFINITION OF FRP COMPOSITE MATERIALS FOR STRUCTURAL APPLICATIONS

A structural FRP composite is a material system that consists of two or more constituent materials or "phases", whose mechanical properties and performance are superior to those of the constituent materials acting independently. One of the phases is typically discontinuous, stiffer, and stronger and is called reinforcement or "fiber". The less stiff and weaker phase is continuous and is called matrix or "polymer". Sometimes, because of chemical interactions or other effects, an additional phase, called interphase, exists between the reinforcement and the matrix.

The constituent materials of the composite are typically homogeneous and isotropic, i.e.; their properties are not a function of position or orientation. On the other hand, FRP composites are typically heterogeneous and anisotropic, and their properties depend on position, orientation and reinforcement volume *(Kachlakev, 1997)*. On a macro-mechanical scale, their anisotropic behavior can be an advantage.

The average material behavior can be predicted and controlled by the properties of the constituents. However, the anisotropic analysis is complex and results often depend on the chosen computational procedure *(Daniel and Ishai, 1994)*. The degree of anisotropy of the most widely used composite materials is shown in Table 2.1, where E_1, E_2 are the elastic moduli in longitudinal and transverse direction, respectively, G_{12} is the shear modulus, and F_1, F_{2t} are the tensile strength values in the longitudinal and transverse direction, respectively.

Table 2.1: Degree of Anisotropy of FRP Composites

FRP Composite	E_1/E_2	E_1/G_{12}	F_1/F_{2t}
Steel	1.00	2.58	1.00
Vinyl Ester Epoxy	1.00	0.94	1.00
S-glass/Epoxy	2.44	5.06	28
E-glass/Epoxy	4.42	8.76	17.7
Carbon/Epoxy	13.64	19.1	41.4
UHM/Epoxy	40	70	90
Kevlar/Epoxy	15.3	27.8	260

(Daniel and Ishai, 1994)

Steel and epoxy, which are isotropic materials, are presented for comparative purposes. Note that the steel has the same elastic modulus in longitudinal and transverse direction, e.g. $E_1 = E_2$. The other materials are anisotropic. For example, the longitudinal elastic modulus of E-glass/epoxy composite is 4.42 times greater than its transverse elastic modulus.

When viewed on a micro-mechanical scale, composites have the advantage of high stiffness and strength. For example, ordinary plane glass fractures at stresses of only few thousand pounds per square inch, while glass fibers, in commercially available forms, have strengths 100 times that of plane glass. The paradox of a fiber having different properties from the bulk form is due to the more perfect structure of the fiber. The fibers usually have a low fracture toughness, which, in the FRP composite, is compensated for by the ductility of the matrix. The stress transfer capability of the matrix enables development of multi-site failure mechanisms, which results in the high strength of the composite.

2.2 PROPERTIES OF CONSTITUENT MATERIALS

Among the main reasons for using composites are: improved strength, stiffness, corrosion and wear resistance, fatigue life, reduced weight and improved thermal behavior of the resulting structure. One of the most important features of the composites is their "tailorable" behavior. Properly designed, they allow control of the properties of the material according to specific needs.

Properties of a composite material depend on the properties of the constituents, geometry, and distribution of the phases. One of the most important parameters is the volume (or weight) fraction of the reinforcement. The distribution of the reinforcement determines the homogeneity of the material system. The more non-uniform is the reinforcement, the more heterogeneous is the composite material and the higher is the probability of failure in the weakest area. The geometry and orientation of the reinforcement affect the anisotropy of the system.

The phases of the composite materials have different roles that depend on the type of material and application for the composite. In the case of low performance composites, the reinforcement, usually in form of short fibers, provides some stiffening but only local strengthening. The matrix is the main load-bearing constituent governing the mechanical properties and performance of the composite. In case of high performance structural composites, the reinforcement usually consists of continuous fibers, which determine the stiffness and strength of the composite system in the direction of fibers. In such cases, the matrix phase provides protection of the fibers and transfers local stresses from one fiber to another.

2.2.1 Classification and Properties of Reinforcing Fibers

A fiber is characterized geometrically by its high length-to-diameter ratio. A large variety of fibers are available for reinforcement. The desirable characteristics of most reinforcing fibers are high strength, high stiffness, and low density. Each type of fiber has its own advantages and disadvantages, depending upon their manufacturer and specific properties.

The most common types of fibers used in advanced composites for structural applications are glass, carbon, and aramid. The fibers can be chopped, woven or braided and occupy 50 to 70 percent of the composites volume.

Figure 2.1 shows the relationship between specific modulus and specific strength of some of the most common fibers. The specific strength and specific modulus of a material are defined as the ratios of the ultimate strength to material's density and elastic modulus to material's density, respectively.

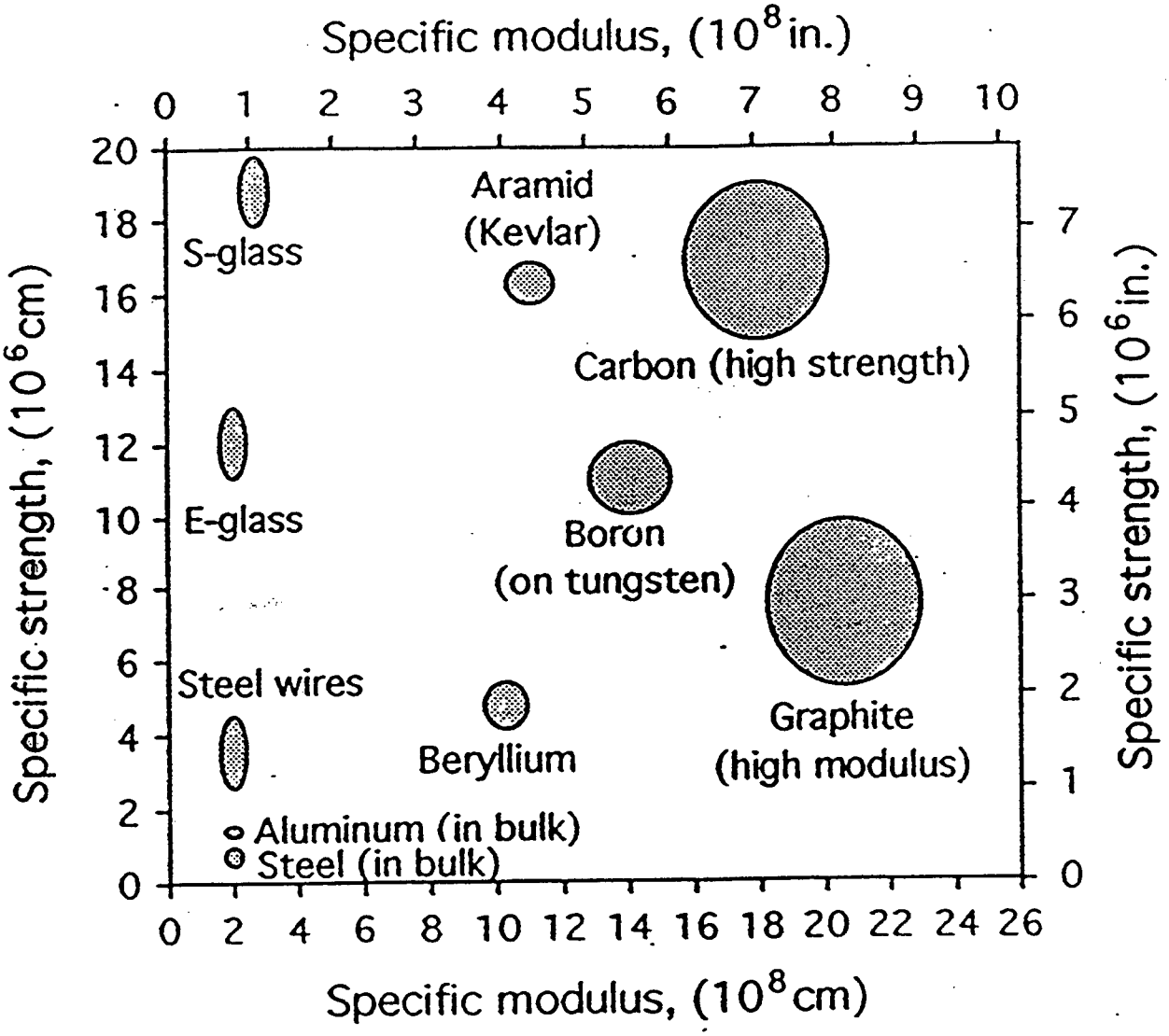

Figure 2.1: Performance Map of Fibers Used in Structural Composite Materials
(Daniel and Ishai, 1994)

Glass fibers are commonly used in structural composites because of their high tensile strength and low cost. They are limited for high performance applications due to their relatively low stiffness, and chemical degradation when exposed to severe hydrothermal conditions *(Daniel and Ishai, 1994)*. Glass fibers have good characteristics for civil engineering applications. However, if not properly coated with resin, their durability in high alkaline environment is unacceptable. E-glass and S-glass are the two types of fibers most widely used in civil engineering. S-glass fibers possess strength and elastic modulus superior to E-glass, mainly due to better quality control during manufacturing.

The aramid fibers are aromatic polyamides. Aramid fibers exhibit excellent fatigue and creep behavior. However, their chemical or mechanical bond with resin may be problematic. Kevlar 29 and Kevlar 49 are the two most commonly used aramid fibers for structural applications. Aramid (or Kevlar) fibers have higher stiffness and lower density then S glass fibers, but they are limited by their very low compressive strength in the composites and high moisture absorption *(Daniel and Ishai, 1994)*.

The graphite or carbon fibers are produced from three types of polymer precursors, polyacrylonitrile (PAN) fibers, rayon fibers, and pitch *(Tang, 1997)*. Although there are many carbon fibers available on the market, they are divided into three categories, high strength (HS), high modulus (HM), and ultra-high modulus UHM). In the case of UHM carbon fibers, the increase in stiffness is achieved at the expense of strength. Their fatigue and creep resistance is excellent. Table 2.2 shows typical properties of the most widely used fibers for structural composites.

Table 2.2: Typical Properties of Structural Fibers

Fiber Type	Density (g/cm^3)	Elastic Modulus (GPa)	Tensile Strength (GPa)	Elongation (%)
E-Glass	2.54	72.5	1.72-3.45	2.5
S-Glass	2.49	87	2.53-4.48	2.9
Kevlar 29	1.45	85	2.27-3.80	2.8
Kevlar 49	1.45	117	2.27-3.80	1.8
Carbon (HS)	1.80	227	2.80-5.10	1.1
Carbon (HM)	1.80-1.86	370	1.80	0.5
Carbon (UHM)	1.86-2.10	350-520	1.00-1.75	0.2

Most fibers behave linearly up to failure. Figure 2.2 shows the stress-strain behavior of some of the most popular fibers.

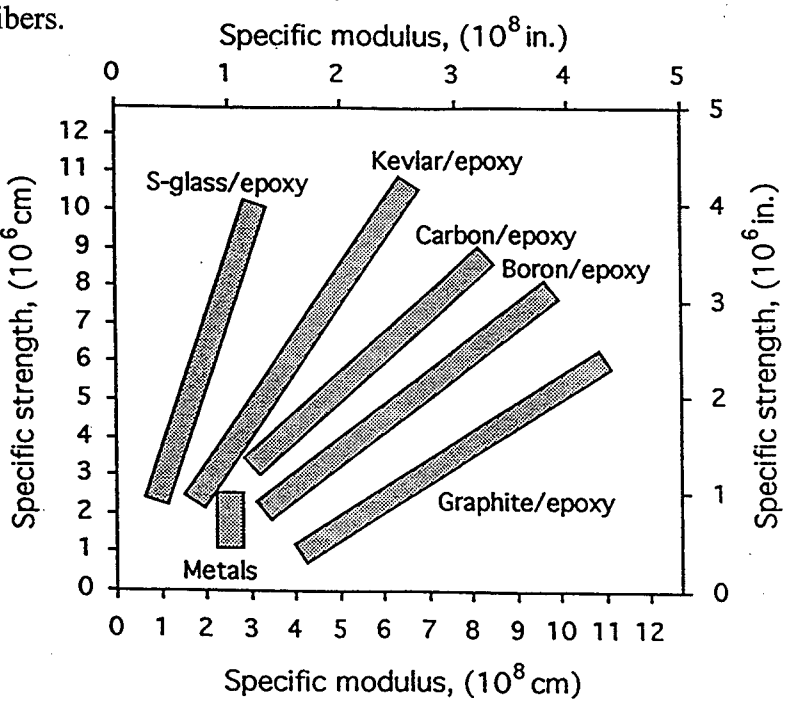

Figure 2.2: Stress-Strain Curves of Typical Reinforcing Fibers
(Daniel and Ishai, 1994)

The advantages and disadvantages of different types of reinforcing fibers are summarized in Table 2.3.

Table 2.3: Advantages and Disadvantages of Reinforcing Fibers

Fiber Type	Advantages	Disadvantages
E-glass, S-glass	High strength, low cost	Low stiffness, short fatigue life, temperature sensitivity
Aramid (Kevlar)	High tensile strength, low density	Low compressive strength, high moisture absorption
HS Carbon	High strength, high stiffness	High cost
UHM Carbon	Very high stiffness	Low strength, high cost

2.2.2 Classification and Properties of Resin Matrices

Epoxy resins are used widely in structural applications. Their attractive features for composite applications include adequate strength, chemical resistance, dimensional stability, low shrinkage compared to unsaturated polyesters, good adhesion to a variety of reinforcing fibers, and low material cost *(Billmeyer, 1984)*.

The resin matrix protects the reinforcing fibers, which are typically rigid and brittle. More importantly, it distributes an applied load and acts as a stress-transfer element, so that when an individual fiber fails, the composite system does not lose its load carrying capability. Durability, shear, compressive and transverse strength are also provided by the resin matrix. To fulfill these functions, fiber-matrix interface adhesion is of great importance. The physical properties of the matrix that are critical for the performance of the overall composite are its tensile, compressive and shear strength, elastic modulus, toughness, yield and ultimate elongation, as well as its thermal and moisture resistance. Table 2.4 summarizes some of the test methods used for determination of resin properties.

Table 2.4: Standards for Determination of Epoxy Resin Properties

Mechanical Property	Test Method
Shore Hardness	ASTM D-2583-87
Heat Distortion Temperature	ASTM D-641-96
Tensile Strength	ASTM D-638-89
Tensile Modulus	ASTM D-638-89
Tensile Elongation	ASTM D-638-89
Flexural Strength	ASTM D-790-86
Flexural Modulus	ASTM D-790-86
Viscosity, Krebs Units	ASTM D 2393-86 and ASTM D 445-96
Weight per Gallon	ASTM D 3892-77
Epoxy Content	ASTM D 1652-88
Water Absorption	ASTM D 570-81
Pot Life	ASTM D 2566-86
Specifications of Epoxy Resins	ASTM D 1763-88
Fire Resistance	ASTM D 635-88

The most commonly used resin matrices in composites are polymeric. Polymers are long molecules that essentially consist of repeating structural units. Polymers for resin matrices can be divided into two groups: thermosets and thermoplastics. Typical thermoset matrices are

epoxies, polyesters, and polyamides. Thermoplastics are represented by polysulfone and poly-ether-ketone. Thermosets develop their properties as the result of exothermic reactions and are used for quick-curing systems, while thermoplastics develop their properties on solidification by cooling, and are more compatible with hot forming and injection molding fabrication methods.

Thermoset resins are typically associated with expensive multi-step manufacturing processes. They often exhibit low toughness, high moisture sensitivity, short shelf life, and may require complex repair methods. However, they are generally harder and less flexible than thermoplastics. They are usually solvent resistant and do not melt when heated. They cannot be easily shaped after polymerization, and therefore are polymerized into the final shape in the mold rather than in lay-up work. The thermosets are preferred for structural applications. Table 2.5 summarizes some of the physical properties of the thermosetting resins. Specifications of thermosetting polyesters can be found in ASTM D 1201-81 (1987).

Table 2.5: Physical Properties of Some Thermosetting Resins Used in Structural Composites

Resin Type	Density (kg/m^3)	Tensile Strength (MPa)	Elongation (%)	Elastic Modulus (GPa)	Long Term Use Temp. (°C)
Polyester	1.2	50-65	2-3	3.0	120
Vinyl Ester	1.15	70-80	4-6	3.5	140
Epoxy	1.1-1.4	50-90	2-8	3.0	120-200
Phenolic	1.2	40-50	1-2	3.0	120-150

(Moukwa, 1996)

Thermoplastic resins offer single step processing, good toughness, almost no moisture absorption, simple repair methods, and multiple reforming processes. However, they do exhibit sudden changes in properties when heated. Thus, they are not suitable for civil engineering applications.

2.3 MECHANICAL PROPERTIES OF FIBER REINFORCED POLYMER COMPOSITES

Composite materials have many characteristics that are different from those of conventional engineering materials. Some characteristics are merely modifications of conventional materials, while others require new analytical and experimental procedures. Most common engineering materials are assumed to be homogeneous and isotropic. In contrast, composite materials are often both heterogeneous and anisotropic to such a degree that the differences cannot be ignored.

Some material properties, such as density, are described by a single value for both isotropic and anisotropic materials. Properties such as stiffness, strength, Poisson's ratio, moisture, thermal expansion, and electrical conductivity are associated with direction and are treated as anisotropic. The largest differences typically occur between properties in longitudinal and transverse directions.

The performance of composites is typically rated on the basis of specific strength and specific modulus as defined in Section 2.2.1. A representation of the performance of typical structural composites is shown in Figure 2.3.

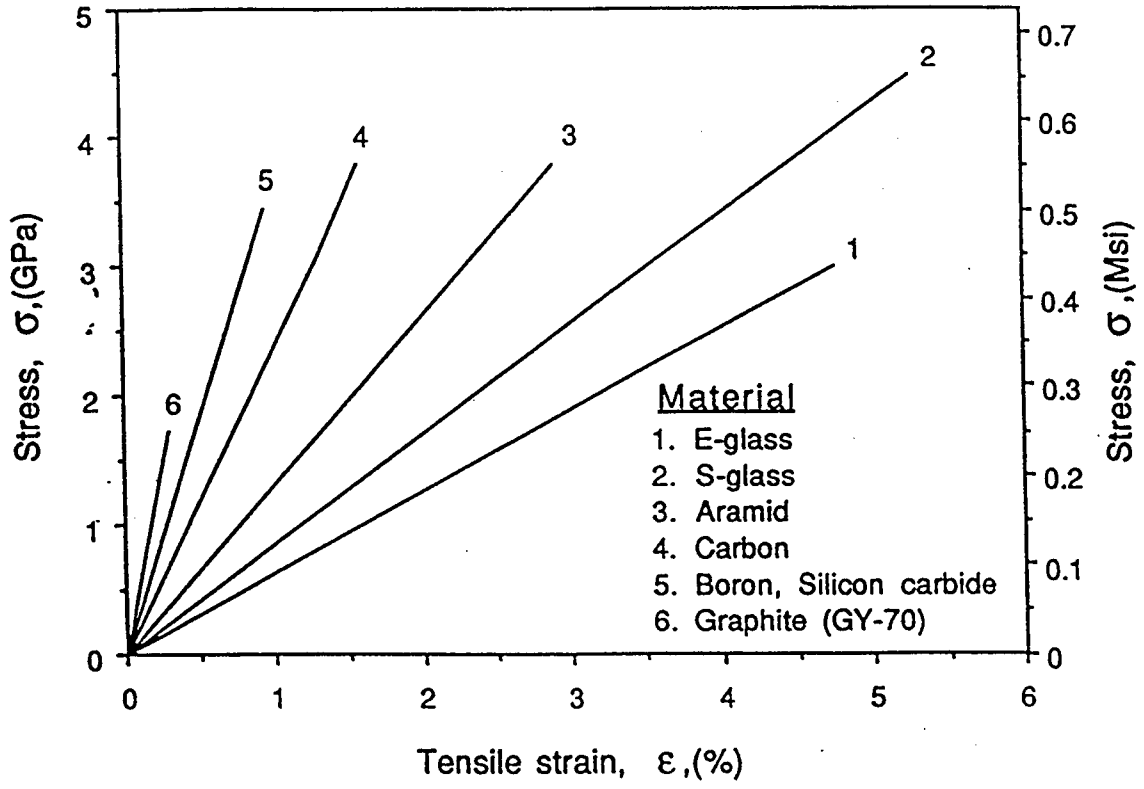

Figure 2.3: Performance Map of Structural Composites
(Daniel and Ishai, 1994)

The variation shown corresponds to the variation between quasi-isotropic and unidirectional laminates. As can be seen, most composites have higher specific modulus and specific strength than metals. The specific gravity of FRP composite reinforcement is one-fourth to one-seventh to that of steel reinforcement with equivalent diameter. The ratio of strength to mass density is 10 to 15 times greater than that of steel.

The structural properties of fiber reinforced laminates can be determined in accordance to the following standards:

Table 2.6: Structural Properties of FRP Reinforced Laminates

Structural Property	Test Method
Tensile Strength	ASTM D-638
Tensile Modulus	ASTM D-638
Flexural Strength	ASTM D-790
Flexural Modulus	ASTM D-790

Mechanical properties of some of the most widely used unidirectional composite materials are shown in Table 2.7.

Table 2.7: Properties of Typical Unidirectional Composite Materials

Property	E-Glass/Epoxy	S-Glass/Epoxy	Aramid/Epoxy	Carbon/Epoxy
Fiber Volume	0.55	0.50	0.60	0.63
Density, g/cm^3	2.10	2.00	1.38	1.58
Longitudinal Modulus, GPa	39	43	87	142
Transverse Modulus, GPa	8.6	8.9	5.5	10.3
Shear Modulus, GPa	3.8	4.5	2.2	7.2
Poisson's Ratio	0.28	0.27	0.34	0.27
Long. Tensile Strength, MPa	1080	1280	1280	2280
Compressive Strength, MPa	620	690	335	1440
Thermal Expansion Coeff.,10^6/°C	7.0	5.0	-2.0	-0.9
Moisture Expansion	0	0	0	0.001

(Jones, 1975; Daniel and Ishai, 1994)

Table 2.7 defines the stiffness, compressive and tensile strengths for the principal material directions. Thus, the degree of anisotropy of the composite material can be determined, similarly to that shown in Table 2.1. Therefore, the mechanical properties in the principal material directions can be combined in order to define the stiffness and strength parameters at an arbitrary orientation of the composite.

Shear strength and shear modulus are of particular importance for composites designed to work in a direction different than that of the principal material direction. With certain combinations of fiber-orientation, the corresponding elastic and shear moduli will define a material having superior properties than that of the constituent materials and improved performance of the reinforced structure.

Table 2.8 shows the elastic (E_i) and shear (G_i) moduli of some conventional metals and composites used for structural applications.

Table 2.8: Elastic and Shear Moduli, and Poisson Ratio's for Conventional Metals and Composites

Material	E_1	E_2	G_{12}	G_{13}	G_{23}
Aluminum	10.40	10.40	3.38	3.38	3.38
Copper	17.00	17.00	6.39	6.39	6.39
Steel	29.00	29.00	11.24	11.24	11.24
Carbon/Epoxy (AS/3501)	20.00	1.30	1.03	1.03	0.90
Carbon/Epoxy (T300/934)	19.00	1.50	1.00	0.90	0.90
Glass/Epoxy	7.80	2.60	1.25	1.25	0.50

(Daniel and Ishai, 1994)
Note: Values of the moduli are in msi = 1 million psi; 1 psi = 6.895 kN/m^2

Usually, fatigue behavior of FRP composites is very good. Carbon and aramid fiber reinforcement have a fatigue characteristics as much as three times higher than steel *(Kretsis, 1987)*. These FRP reinforcements do not fatigue when stressed to less than 1/2 of their ultimate strength. The fatigue strength of glass FRP reinforcement has not been researched in detail. Although the glass usually creeps under a sustained load, it can be designed to perform satisfactorily *(Tang, 1997)*.

The two main failure modes for FRP composites are fiber-dominated failure and matrix-dominated failure. Laminates with sufficient 0° degree layer, i.e. fibers oriented in load direction, will exhibit the fiber-dominated failure mode. This type of failure is essentially independent of the rate and frequency of loading. On the other hand, matrix-dominated failure mode is a rate/frequency dependent phenomenon due to the viscous matrix behavior *(Kujawski and Ellyin, 1995)*. The viscous-dependent matrix behavior plays an essential role in fatigue performance of FRP composites.

2.4 MATERIALS AND MANUFACTURING PROCESS SELECTION

Materials have to be chosen based on their properties and costs. Based on economics, glass FRP is the preferred reinforcing material for reinforced concrete, while carbon would only be used in critical areas.

Manufacturing processes, such as pultrusion, yield products in the $2 to $3 per pound range, with raw materials cost being as high as 80 percent of the overall cost *(Seible et al, 1995)*. Other methods of fiber placement can cost hundreds of dollars per pound, with material cost as low as 10 to 30 percent.

Additional considerations concerning the design purpose of the structural elements must be taken into account for any load carrying structural element. Shape factor is often forgotten. Shape factor is a dimensionless parameter characterizing the efficiency of a specific shape to carry a given load. It is clear that under tension the best performance is seen when the axial loading capacity at the lowest self-weight is realized. This is obtained by maximizing E/ρ, where E is the Young's modulus and ρ is the density *(Seible et al, 1995)*. Similarly, in flexure, the highest factor of $E^{1/2}/\rho$ indicates the best material for flexural shapes. Table 2.9 gives the results for a number of material systems based on these two measures and shows the mechanical advantages that can be derived for advanced composite structural elements and systems.

Table 2.9: Comparison of Axial and Flexural Efficiencies for Different Material Systems

			AXIAL EFFICIENCY		FLEXURAL EFFICIENCY	
Materials System	**E, GPa**	**ρ, g/cm^3**	**E/ρ**	**Ranking**	**$E^{1/2}/\rho$**	**Ranking**
HS Carbon/Epoxy	181	1.6	113.1	1	8.4	1
Carbon – PEEK	134	1.6	83.8	2	7.2	2
Kevlar/Epoxy	76	1.46	52.1	3	6.0	3
Mild Steel	200	7.8	25.6	4	1.8	5
E-Glass/Epoxy	38.6	1.8	21.4	5	3.5	4

(Seible et al, 1995)

3.0 DESIGN PRINCIPLES FOR COMPOSITE MATERIALS

3.1 DESIGN PHILOSOPHY

The advantages of advanced composite materials, including the potential to tailor their behavior according to specific needs, has led to increased research in civil infrastructure-related applications. The successful implementation of composites in all applications requires an understanding that design cannot follow the paradigms of metals or other conventional materials. The materials, configurations, and processes involved in designing with composites have intricate connections and interrelations. For example, reinforcement of cylindrical structural elements can be done with a number of techniques, but the final choice will be based on the columns basic shape, structural strengthening requirements and available materials.

Designing with advanced composite materials requires the engineer to make a number of decisions. Advanced composite design is not only the design of an element or structure, but starts with the selection of materials that will give the laminae properties allowing the composite to perform correctly. This design process involves topics such as anisotropic elasticity, strength of anisotropic materials, micro-mechanics, and manufacturing processes.

Specialists will likely limit their attention to one or two specialty areas such as constituent materials and design, micro-mechanics, or macro-mechanics. Although the design of composite materials and composite structures requires a background in advanced mechanics of materials, three-dimensional stress-strain relations, plate theory, and anisotropic elasticity, the actual implementation of composites for structural strengthening is much simpler. However, background in structural design and analysis is essential for successful designs of reinforced concrete structures incorporating composite materials.

The objective of this chapter is to introduce basic concepts related to composite materials. The information presented here cannot be regarded as guide for designing composites, but is rather to make the physical significance of the concepts understandable.

3.2 MECHANICS OF COMPOSITE MATERIALS

The design and analysis of composites, as opposed to conventional materials, are not supplemented with available design charts and guidelines to help the structural engineer. Although dependent upon the characteristics of the constituent materials, FRP composites can be tailored and designed to meet almost any desired specifications.

Unlike conventional materials, which have two elastic constants and two strength values, typical composites possess a large number of descriptive material parameters. The number of degrees of freedom associated with the number of descriptive parameters enables material optimization, but at the same time makes the analysis much more complex. In contrast, the optimization of conventional materials is typically limited to three degrees of freedom, usually the geometric parameters *(Kachlakev, 1997)*.

Composite materials are evaluated from two perspectives; micro-mechanical and macro-mechanical. Micro-mechanics examines the interaction of the constituent materials on a microscopic level. Macro-mechanics is the study of the composite material behavior when the material is presumed homogeneous and the effects of the constituent materials are treated as average properties of the composite *(Jones, 1975)*. For basic structural analysis, the materials are typically treated macro-mechanically. However, in order to study some of the effects of anisotropy, micro-mechanical analysis is often required. A schematic diagram of the various levels of analysis is shown in Figure 3.1.

The anisotropy of composites leads to mechanical behavior quite different from that of conventional materials. Isotropic materials subjected to a stress in one direction exhibit extension in the direction of the applied stress and contraction in the perpendicular direction. Shear stresses cause only shear deformations. For anisotropic materials, application of stress in one direction leads not only to extensions and contractions, but also produces shear deformations. Conversely, applied shear stress causes extension and contraction in addition to the shear deformation. This complex relationship between loading and deformation is referred to as "coupling" between the loading and deformation modes (see Figure 3.2).

Orthotropic materials are special subset of anisotropic materials. The distinguishing characteristics are related to the directionality of the material properties with the property being different for each axis. For example, when loaded in the "on-axis" direction (principal material direction), which coincides with the direction of fibers, extension in the direction of the applied load and contraction in the direction perpendicular to the load occurs. However, due to different properties in the two directions, the contraction may result in a deformation that is more or less than that of a similarly loaded isotropic material even though the isotropic material has the same elastic modulus as the composite in the direction of loading.

Additionally, in orthotropic materials the magnitude of the shear deformations is independent of the Young's modulus and Poisson's ratios. Thus, the shear modulus of an orthotropic material does not depend on other elastic constants.

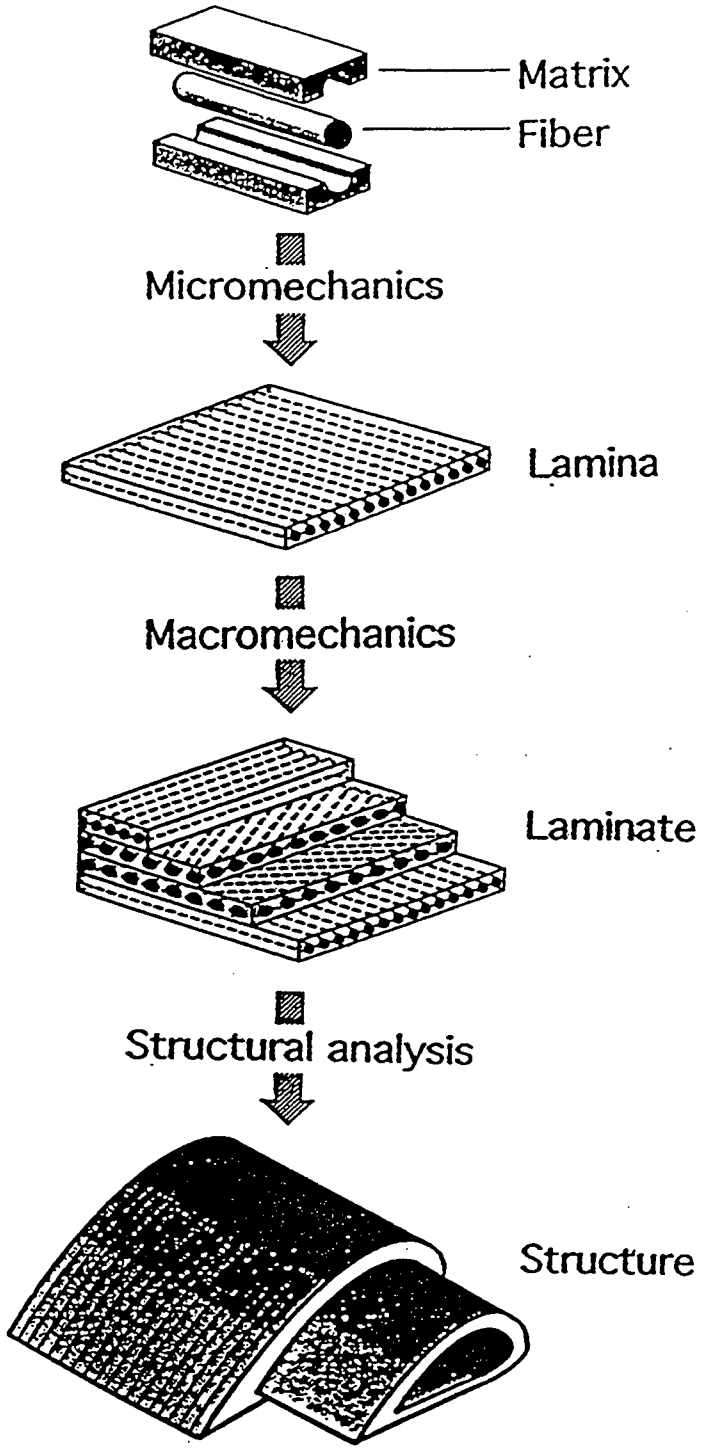

Figure 3.1: Structural Design Approach for Composites
(Daniel and Ishai, 1994)

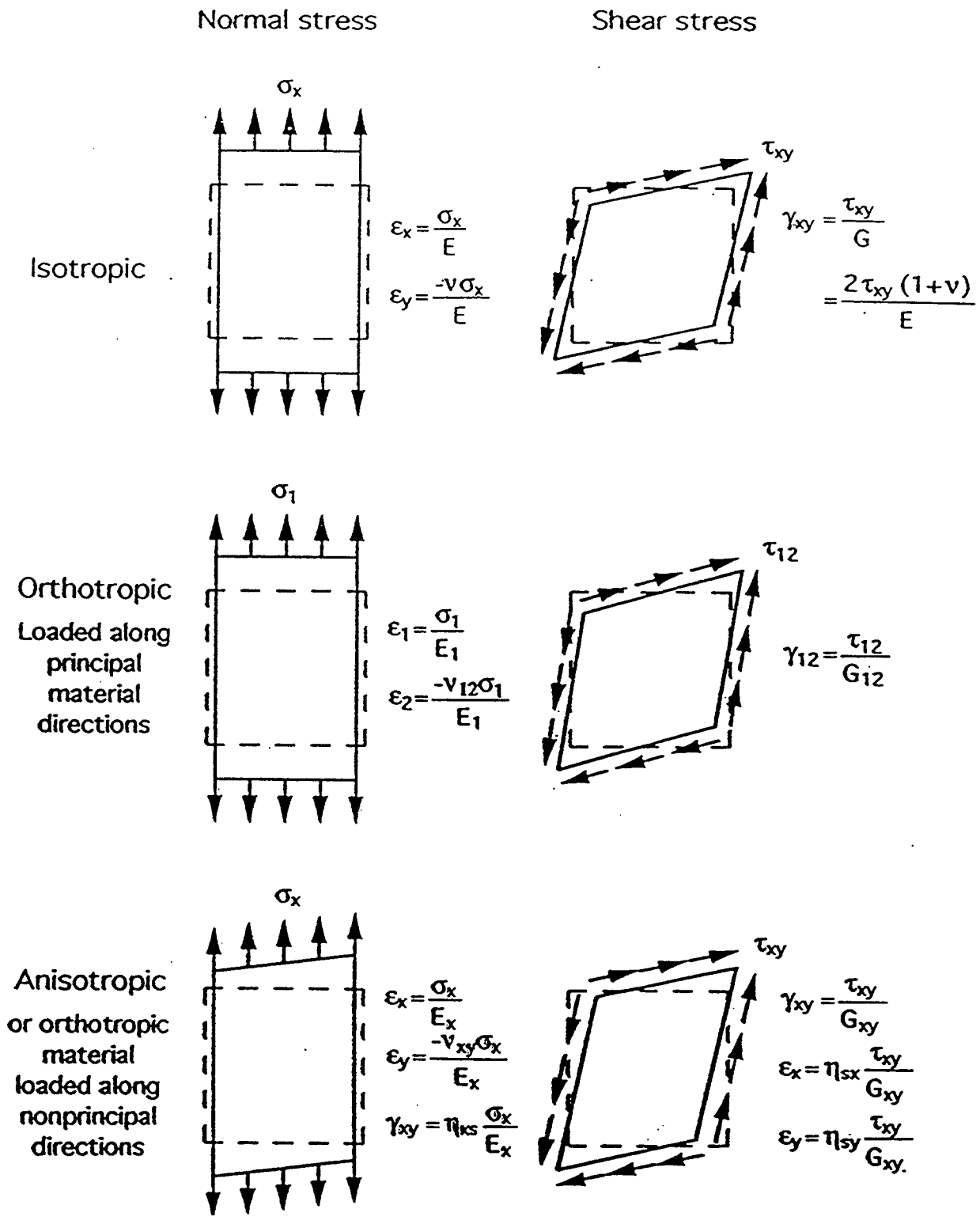

Figure 3.2: Mechanical Response of Various Types of Materials Subjected to Normal and Pure Shear Loading *(Daniel and Ishai, 1994)*

3.3 DESIGN PRINCIPLES

In the most general form of Hook's law, the state of stress at a point is represented by nine stress components σ_{ij} acting on the sides of an elementary cube with sides parallel to the xyz axes. Similarly, the state of deformations is represented by nine-strain components ε_{ij}. The stress and strain components, representing the behavior of an anisotropic material, are:

$$\sigma_{ij} = C_{ijkl}\,\varepsilon_{kl} \quad |_{i,j,k,l=1,2,3} \tag{3-1}$$

$$\varepsilon_{ij} = S_{ijkl}\,\sigma_{kl} \quad |_{i,j,k,l=1,2,3} \tag{3-2}$$

where:

σ – stress tensor
ε – strain tensor
C – stiffness matrix component
S – compliance matrix component

Note that:

$$\sigma_{kl} = S^{-1}_{ijkl}\,\varepsilon_{ij} \quad |_{i,j,k,l=1,2,3} \tag{3-3}$$

In Appendix A it is shown that there are 81 elastic constants needed to characterize an anisotropic composite material. However, since $\sigma_{ij} = \sigma_{ji}$ and $\varepsilon_{ij} = \varepsilon_{ji}$, the number of independent elastic constants is reduced to 36.

In the case of a specially orthotropic material (with three mutually perpendicular planes of material symmetry), the number of independent elastic constants is reduced to 9, as various stiffness and compliance coefficients are interrelated. Most of the composite materials for structural applications are analyzed assuming these conditions. Table 3.1 gives the number of independent constants for the various types of materials.

Table 3.1: Independent Elastic Constants for Various Types of Materials

Material	Independent Elastic Constants
General anisotropic material	81
Anisotropic material with symmetric stress and strain tensors	36
With elastic energy considerations	21
Specially orthotropic materials	9
Assuming transverse isotropy	5
Isotropic Materials	2

(Daniel and Ishai, 1994)

The stiffness and compliance components (C_{ijkl} and S_{ijkl}) have more physical than engineering meaning. The relationships between these mathematical constants and the engineering constants, i.e. elastic moduli and Poisson's ratios, for a two dimensional stress state are as follows *(Jones, 1975)*:

$$S_{11} = \frac{1}{E_1} \quad S_{12} = \frac{-\nu_{12}}{E_1} = \frac{-\nu_{21}}{E_2}$$
$$S_{22} = \frac{1}{E_2} \qquad S_{66} = \frac{1}{G_{12}} \tag{3-4a}$$

$$C_{11} = \frac{E_1}{1-\nu_{12}\nu_{21}} \quad C_{12} = \frac{E_2\nu_{12}}{1-\nu_{12}\nu_{21}}$$
$$C_{22} = \frac{E_2}{1-\nu_{12}\nu_{21}} \qquad C_{66} = G_{12} \tag{3-4b}$$

where:

E_1, E_2 – Young's moduli parallel and perpendicular to the fiber orientation
ν_{ij} – Poisson's ratio for strain in direction j when stressed in direction i
G_{12} – shear modulus

Further details regarding relationships between mathematical and engineering constants for a specially orthotropic materials subjected to tensile loading in the longitudinal and transverse direction are provided in Appendix A (Equations A-20 to A-23).

In order to design a composite material, the values of the independent constants are needed. The experimental determinations of the elastic constants and consequently the strength of a material are based on uniaxial stress states. However, the actual stress states of these materials are at least biaxial if not triaxial. Some of the biaxial strength theories are the maximum stress theory, maximum strain theory, the Tsai-Hill theory, and the Tsai-Wu theory. According to these theories the material, although orthotropic, must be assumed homogeneous *(Jones, 1975)*. Thus, some of the observed microscopic failure mechanisms cannot be accounted for.

Under off-axis loading, the stress imposed on the material must be transferred in the principal material directions. According to the maximum stress theory, the stresses in the principal material directions are obtained by *(Tsai, 1968)*:

$$\sigma_1 = \sigma_x \cos^2\theta \quad \sigma_1 = \sigma_x \sin^2\theta \quad \sigma_1 = \sigma_x \sin\theta\cos\theta \tag{3-5}$$

where:

θ – is the angle between the applied load and the fiber orientation
σ_x – is the stress in the direction of the applied load
σ_1 , σ_2 , τ_{12} – stresses in the principal material directions

In the maximum stress theory, the stresses in principle material directions (σ_1 , σ_2 , τ_{12}) must be less than the respective ultimate stresses (X_t, Y_t, S), otherwise fracture will occur.

$$\sigma_1 < X_t \quad \sigma_2 < Y_t \quad \tau_{12} < S \tag{3-6}$$

By inversion of Equation 3.5 and substitution of Equation 3.6, the maximum allowed uniaxial stress, σ_x is the smallest of:

$$\sigma_x < \frac{X_t}{\cos^2\theta} \quad \sigma_x < \frac{Y_t}{\sin^2\theta} \quad \sigma_x < \frac{S}{\sin\theta\cos\theta} \tag{3-7}$$

The maximum strain theory is similar to the maximum stress theory in that the strains are limited rather than stresses. Specifically, the material will fail if one or more of the following inequalities is not satisfied:

$$\varepsilon_1 < X_{\varepsilon t} = \frac{X_t}{E_1} \quad \varepsilon_2 < Y_{\varepsilon t} = \frac{Y_t}{E_2} \quad \gamma_{12} < S_\varepsilon = \frac{S}{G_{12}} \tag{3-8}$$

where:

$X_{\varepsilon t}$ – maximum normal strains in the x direction
$Y_{\varepsilon t}$ – maximum normal strains in the y direction
S_ε – shear strain;
X_t – maximum normal stresses in the x direction
Y_t – maximum normal stresses in the y direction
S – shear stress

The stress-strain relations are:

$$\varepsilon_1 = \frac{\sigma_1 - \nu_{12}\sigma_2}{E_1} \quad \varepsilon_2 = \frac{\sigma_2 - \nu_{21}\sigma_2}{E_2} \quad \gamma_{12} = \frac{\tau_{12}}{G_{12}} \tag{3-9}$$

Upon substitution of Equation 3-5 in Equation 3-9 and accounting for the failure inequalities shown in Equation 3-8, the maximum strain criterion can be expressed as:

$$\begin{aligned} \sigma_x &< \frac{X_t}{\cos^2\theta - \nu_{12}\sin^2\theta} \\ \sigma_x &< \frac{Y_t}{\sin^2\theta - \nu_{21}\cos^2\theta} \\ \sigma_x &< \frac{S}{\sin\theta\cos\theta} \end{aligned} \tag{3-10}$$

A flow chart for calculation of the elastic engineering constants in the general case of off-axis loading is illustrated in Figure 3.3.

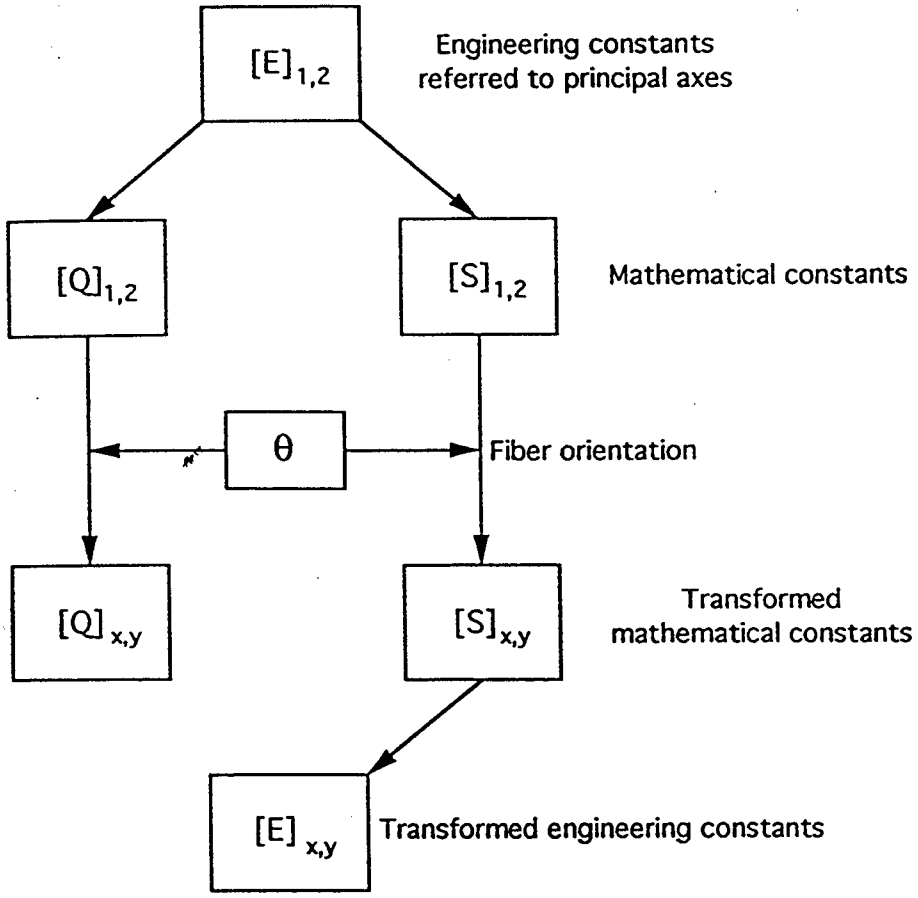

Figure 3.3: Flow Chart for Determination of Transformed Elastic Constants of Fiber-Reinforced Composite Material Under Off-Axis Loading
(Daniel and Ishai, 1994)

The constants E_1, E_2, ν_{12}, and G_{12} are obtained by "characterization" tests. Then, the relations in Equation 3-4a and 3-4b are used to obtain the reduced principal compliance and stiffness, S_{ij} and C_{ij}. Transformed stiffness and compliance S_{xy} and C_{xy} are calculated for the off-axis fiber orientation. Finally, the transformed engineering constants E_x and E_y are calculated with the equations in Appendix A.

3.4 MICRO-MECHANICAL PREDICTION OF ELASTIC CONSTANTS

Elastic constants of composites can be estimated by using the micro-mechanical approach. The parameters that determine the strength of composite are shape, size, orientation and concentration of the fibers, the matrix, and the bond between the fibers and matrix. A variety of methods have been used to predict the properties of constituent materials, namely: mechanics of materials, numerical, semi-empirical and experimental approaches *(Hashin, 1983)*.

The mechanics of materials approach is based on simplifying assumptions of either uniform strain or uniform stress in the constituents. This approach adequately predicts the longitudinal modulus and Poisson's ratio, since these properties are not sensitive to fiber shape and distribution *(Hashin, 1983)*. On the other hand, this approach underestimates the transverse and shear moduli. Since the other approaches are very time consuming and/or give unrealistic results, the mechanics of materials is the most widely used method. Two variations of this method are the parallel and series models.

The parallel model is recommended when the properties in the longitudinal direction are dominated by the fibers. The stiffness and strength are predicted using the rule of mixtures (Equations 3-11, 3-12, and 3-13). Assumptions made in the parallel model satisfy "isostrain" conditions, i.e., the strains in the reinforcement and matrix are equal, Equation 3-11. Also, ideal bond between them is assumed. Equations 3-12 and 3-13 can be used to estimate the longitudinal modulus of the composite lamina:

$$\varepsilon_c = \varepsilon_f = \varepsilon_m \tag{3-11}$$

$$\frac{\sigma_c}{\varepsilon_c} = \frac{\sigma_f V_f}{\varepsilon_f} + \frac{\sigma_m (1 - V_f)}{\varepsilon_m} \tag{3-12}$$

$$E_c = V_f E_f + \frac{E_m}{1 - V_f} \tag{3-13}$$

where:

- E_c – moduli of elasticity of the composite
- E_r – moduli of elasticity of the reinforcement
- E_m – moduli of elasticity of the matrix phase
- V_f – volume fractions of fibers
- V_m – volume fractions of fibers and matrix, respectively.
- ε_c, ε_f, ε_m – strains in the composite, fibers and matrix
- σ_c, σ_f, σ_m – stresses in the composite, fibers and matrix

The series model is the case when loading is normal to the fiber direction. The state of stress in the matrix surrounding the fibers is complex and is affected by interaction with neighboring fibers. The transverse modulus of fiber-reinforced composites is a matrix-dominated property and it is sensitive to local stresses. The series model assumes that $\sigma_c = \sigma_r = \sigma_m$, i.e. stresses resulting from a certain load in the composite system, reinforcement, and matrix phases are equal. Thus, the series model is also called "isostress" model (Equations 3-14, 3-15, and 3-16).

When the stress is applied in the direction perpendicular to both the matrix and the fibers, their loaded areas are also equal, i.e. $A_c = A_r = A_m$. Unlike the parallel model, the strains in the matrix and fibers are different. Equation 3-16 models the transverse modulus of elasticity of the composite system.

The series model is given by:

$$\varepsilon_c = \varepsilon_f V_f + \varepsilon_m V_m \tag{3-14}$$

$$\frac{\sigma_c}{E_c} = \frac{\sigma_f}{E_f} V_f + \frac{\sigma_m}{E_m} V_m \tag{3-15}$$

$$\frac{1}{E_c} = \sum \frac{V_i}{E_i} \tag{3-16}$$

Both the parallel and series models represent the limiting conditions of loading and fiber orientation. The actual properties vary between these extremes.

Elastic properties of composites also vary with fiber orientation. Typically, the elastic modulus of glass/epoxy composite decreases monotonically from a maximum at $\theta = 0^\circ$ to its minimum at $\theta = 45^\circ$, and increases again to a local maximum at $\theta = 90^\circ$. The shear modulus exhibits maximum at $\theta = 45^\circ$ and reaches its minimum at $\theta = 0^\circ$ and 90°. Poisson's ratio has minimums at $\theta = 0^\circ$ and $\theta = 90^\circ$, and peaks at approximately $\theta = 45^\circ$. Figures 3.4 and 3.5 show the elastic constants for a typical glass/epoxy composite as a function of the fiber orientation *(Daniel and Ishai, 1994)*.

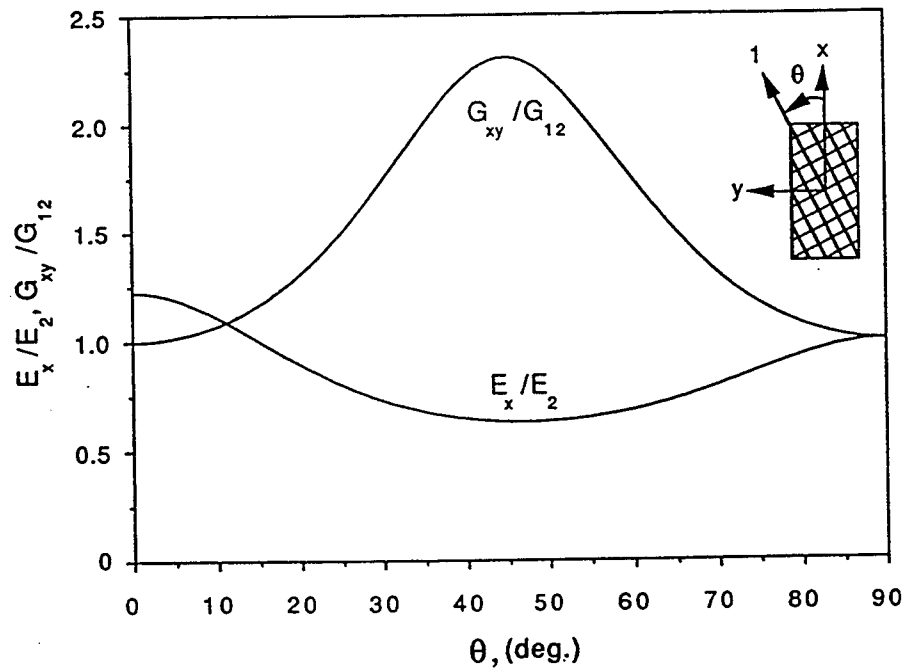

Figure 3.4: Young's Modulus and Shear Modulus of Glass/Epoxy as a Function of Fiber Orientation
(Daniel and Ishai, 1994)

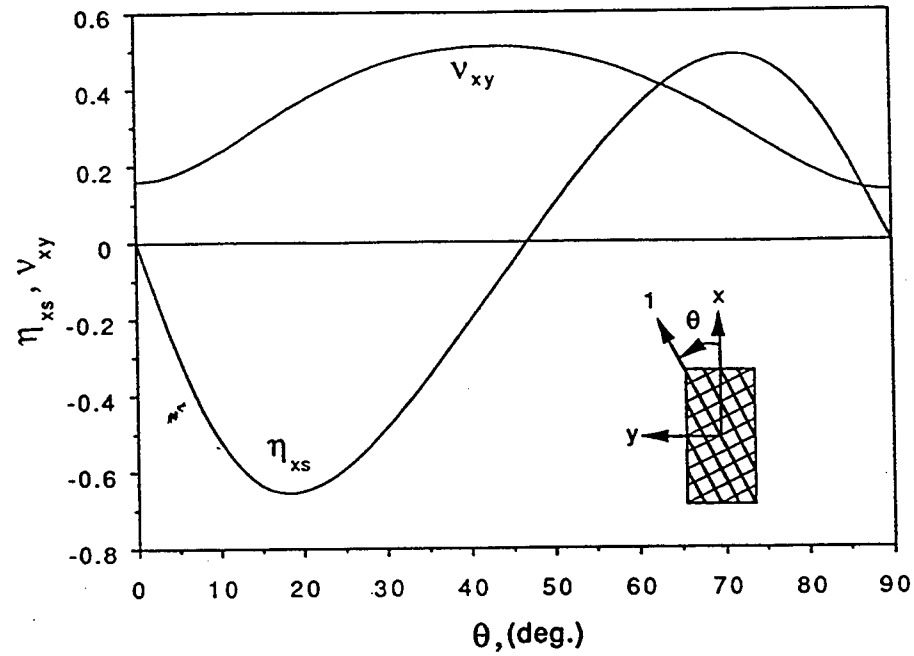

Figure 3.5: Poisson's Ratio and Shear Coupling Coefficient of Glass/Epoxy as a Function of Fiber Orientation
(Daniel and Ishai, 1994)

3.5 TEST METHODS FOR DETERMINATION OF MECHANICAL PROPERTIES OF FRP REINFORCEMENT

Currently ASTM is developing test methods for FRP materials. However, at this time there is no standard suite of ASTM test methods for quantifying structural performance and mechanical properties of FRP composites bonded to concrete. Certain ASTM standards are applicable to FRP materials. Thus, FRP composites may be tested in accordance with these methods as long as all exceptions to the method are listed in the test report.

Design and analysis of structures with composite materials requires reliable experimental data. A significant amount of reliable experimental data on the mechanical properties of the composite laminae and adhesives can be determined by using some or all of the tests listed in Table 3.1 *(ACI 440-F, 1997)*.

Table 3.1: Test Methods for FRP Material Systems Externally Bonded to Concrete

Property	Test Method
Tensile Strength, Strain, and Modulus of FRP Sheets	ASTM D 3039 or SACMA SRM 4-99
Fatigue Strength of FRP Sheets	N/A
Coefficient of Thermal Expansion of FRP Sheets	ASTM C 531 or E 851
Sheet to Sheet Adhesive Shear	ASTM C 531
Sheet to Concrete Adhesive Shear	ASTM C 531
Sheet to Concrete Adhesive Tension	ASTM C 531
Tensile Strength, Strain, and Modulus of FRP Shells	N/A
Fatigue Strength of FRP Shells	N/A
Coefficient of Thermal Expansion of FRP Shells	N/A
Shell to Concrete Adhesive Shear	N/A
Shell to Concrete Adhesive Tension	N/A
Shell to Shell Adhesive Shear	N/A
Stress Rupture of FRP Shells	N/A

In order to complement the suite of tests listed above some researchers have developed their own test procedures. Two of them follow.

A single-lap shear test specimen was developed at the University of Delaware for evaluating composite material plates bonded to concrete *(Finch et al, 1995)*. The test specimens consisted of 25 mm-wide FRP plates bonded to concrete blocks. The bond lengths varied from 50 mm to 200 mm. In the test setup, the concrete block is securely mounted to the bottom cross-head of a testing machine. The free end of the composite plate is clamped in a grip mounted on the top cross-head. A load is applied until the bond fails. From the load at failure, the shear bond strength can be determined. The test method can be used to evaluate the effects of surface preparation, type of adhesives, and concrete properties on average bond strength.

In order to study the interface characteristics between adhesive and concrete, Arduini et al *(1997)* carried out tension shear and compression tests. The shear tests were on prismatic and cubic concrete specimens. The test set-up is shown in Figure 3.6. After curing, the specimens were saw-cut at different angles, which varied from 20 to 70 degrees. The cut faces were rejoined with a layer of adhesive that was being evaluated .The bonded samples were taken to failure on a testing machine and the results were used to construct a Mohr-Coulomb failure envelope. From the envelope, the shear strength of the interface was found to be about 5 MPa (0.73 ksi).

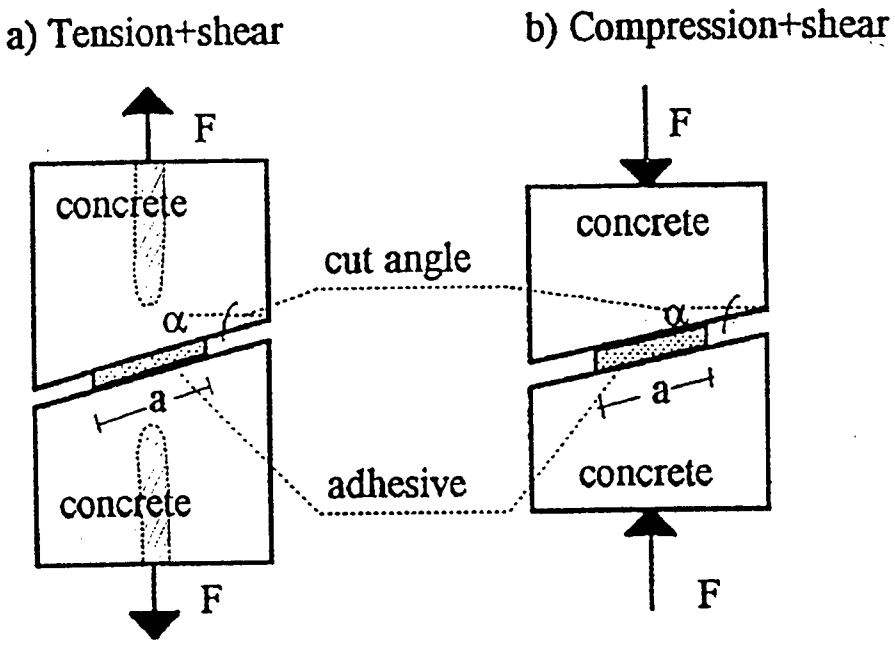

Figure 3.6: Tensile + Shear and Compression + Shear Concrete-Adhesive Specimens
(Arduini et al, 1997)

4.0 EXTERNAL REINFORCEMENT OF CONCRETE BEAMS USING FRP COMPOSITE MATERIALS

4.1 STRENGTHENING TECHNIQUES WITH CONVENTIONAL MATERIALS

Numerous researchers have studied strengthening of existing concrete structures through the use of externally bonded steel plates to increase the load-carrying capacity of concrete bridge girders. Most report promising results. However, some researchers report that epoxy-bonded steel plates alone will not increase the ultimate strength, though the stiffness is enhanced marginally *(Chan and Tan, 1996)*. Other researchers have reported that a shortcoming of this method is the possibility of corrosion at the epoxy-steel interface, which may affect the bond strength *(MacDonald and Calder, 1982)*. Some studies showed that, at higher temperatures, the epoxy can fail to transfer the shearing stresses from the steel plate to the concrete, with resultant crack propagation through the epoxy joint *(Van Gemert and Bosch, 1985)*.

Jones et al *(1982)* described the characteristics of under- and over-reinforced concrete beams with bonded steel plates. Five under-reinforced and three over-reinforced beams of the same dimensions were tested in four-point bending. The beams were strengthened with steel plates 1.5 mm to 10 mm thick. The study found that the composite action between the reinforced concrete beam and the glued steel plate was effective up to failure. The ultimate strength of both under- and over-reinforced beams increased significantly. The bending stiffness increased and the deflections decreased. The plates delayed the occurrence of the first crack, but had very little effect on crack spacing.

4.2 STRENGTHENING TECHNIQUES WITH COMPOSITE MATERIALS

4.2.1 Background

A survey conducted by the U.S. Army Corps of Engineers reported on composites repair technologies, upgrade and strengthening technologies, research, and demonstrations in the U.S., Western Europe and Japan. The survey revealed that in the U.S., the use of composite materials for structural retrofitting is still in the research and development stage *(Marshall and Busel, 1996)*. In Europe and Japan, these materials are being used in practical applications *(Nanni, 1997; Meier et al, 1992)*.

In an effort to overcome the structural disadvantages and construction difficulties of the steel plate technique, the Swiss Federal Laboratories for Testing and Research (EMPA) conducted an extensive project on "Post Reinforcement of Concrete Structures with Carbon Fiber-Reinforced Epoxies" *(Meier and Deuring, 1991)*. Restoration of real structures followed the research *(Meier et al, 1992)*.

Most projects conducted in Europe and Japan used carbon/epoxy sheet materials and laminates bonded to concrete. The most critical failure mode reported was bond failure accompanied by separation of the FRP laminate from the concrete substrate. Therefore, the bond strength of FRP to concrete was identified as a critical issue.

In order to promote faster development of the composite material systems in the U.S., the Construction Productivity Advancement Research Program (CPAR) was established in 1988. The program resulted in an agreement between the Corps of Engineering laboratories and private industry for cooperatively supporting composite research for structural applications.

Another study conducted by the Corps of Engineers found that civil works infrastructure is rapidly deteriorating and has long outlived its design life *(Marshall and Busel, 1996)*. Economically viable solutions to extend the useful life of the existing structures and to protect against earthquake damage are needed.

The goals of the ODOT project are to identify candidate material systems, study performance at the laboratory level, establish materials and installation performance specifications, and develop design guidelines to be used for each type of viable strengthening system. Demonstration projects, field tests and long term durability assessment will be considered as part of the project.

4.2.2 Some Early Evaluations

An extension of the steel plating method, which negates the corrosion problem, is to bond high-strength composite FRP plates or sheets to the tension face of concrete beams. Several researchers have studied the benefits of bonding non-corrosive composite materials to concrete *(Ritchie et al, 1991; Meier et al, 1992; Finch et al, 1995; Saadatmanesh and Ehsani, 1996)*. Some researchers have developed practical rehabilitation schemes for actual structures using graphite/epoxy plates *(Iyer et al, 1989; Rostasy et al, 1992)*.

Figure 4.1 shows a typical load-deflection diagram of simple steel-reinforced concrete beam without any external reinforcement, and then compares it to a similar beam strengthened with a 0.3 mm thick carbon FRP (CFRP) laminate *(Meier, 1992)*. The thin laminate nearly doubles the ultimate load carried by the beam. Furthermore, the deflection at ultimate load is only half of that of the unreinforced beam.

After the appearance of the first cracks in the concrete, the internal steel and external FRP carry the tensile stresses. As soon as the internal steel reaches its yield point, the FRP laminate continues to contribute to the additional increase of load. Finally, the laminate fails in a brittle manner, which results in a beam failure.

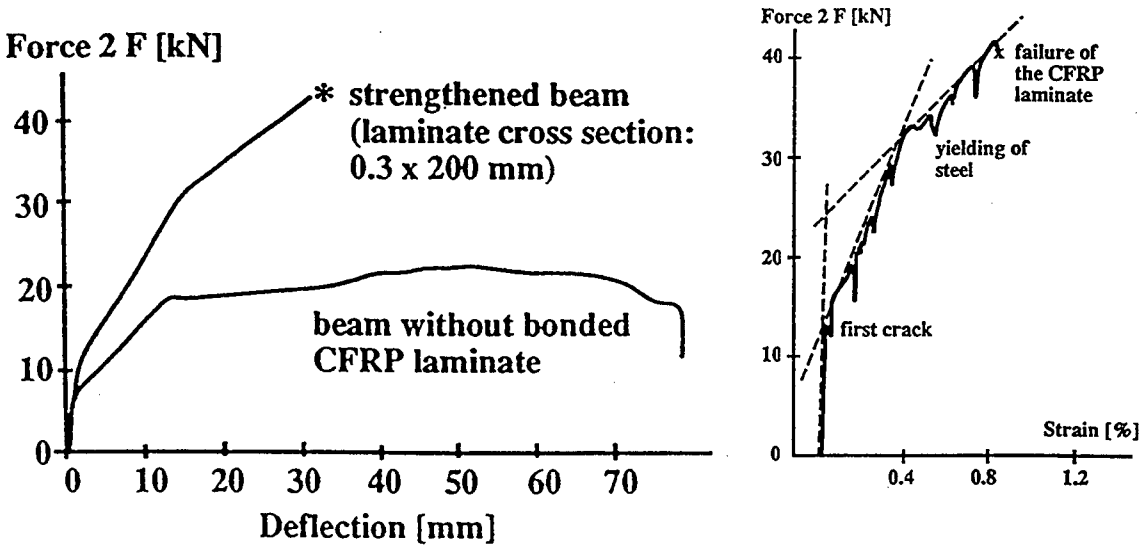

Figure 4.1: Load-Deflection Curve of Regular and CFRP-Strengthened Beam
(Meier and Kaiser, 1991, Las Vegas)

In order to demonstrate the effectiveness of FRP-strengthening, the Swiss Federal Laboratories conducted a study on strengthened and non-strengthened 200 mm x 150 mm x 2000 mm beams *(Meier and Kaiser, 1991; Meier, 1992)*. Initially, a non-strengthened beam was loaded with a force of 9.5 kN, which resulted in a few bending cracks with total crack width of 3.85 mm. The unloaded beam was then strengthened with 0.75 mm x 200 mm CFRP laminate and reloaded with force of 15 kN. As the load increased, additional cracks were observed, but the total crack width was reduced to 2.58 mm. The influence of externally bonded FRP laminates on the development of bending cracks is shown in Figure 4.2. The FRP reinforced beam achieved a more even distribution of the cracks and a smaller total crack opening.

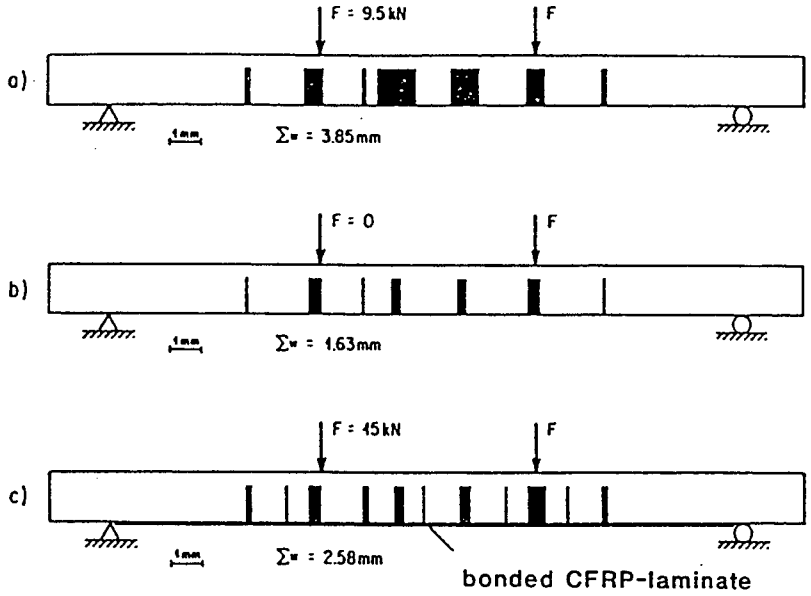

Figure 4.2: Crack Width in a Beam with and without External FRP Laminates
(Meier and Kaiser, 1991)

Sika AG of Zurich, Switzerland developed and tested a new CFRP strengthening system for concrete slabs, Sika CarboDur (Figure 4.3). The carbon FRP strips (1 mm to 2 mm thick and up to 500 m long) used with Sika CarboDur system are manufactured by pultrusion and have a tensile strength in the range of 3 kN/mm^2 in the direction of fibers. The system allows for strengthening of concrete slabs weakened by cut out openings that require crosswise-applied strips. The rigidity of the CFRP strips is such that they cannot be applied onto large concave surfaces. At strip crossings, adhesive 1.2 mm thick is applied. Carbon FRP strips are supplied on rolls up to 500 m long. Thus, an application that requires very long strips can be executed without lap joints. Two-component epoxy adhesives are used to bond the strips to the concrete. Good wetting of the concrete surface prior to plate bonding is essential. Particularly important is the smoothness of the adhesive layer in order to reduce the peak stresses. The adhesives requirements are listed in Table 4.1.

The system requires detailed surface preparation according to the principles described above. The bond strength between the CFRP and the concrete at the anchorage zones of the strips should have an average value of 2 N/mm^2 and no single value should be less than 1.5 N/mm^2.

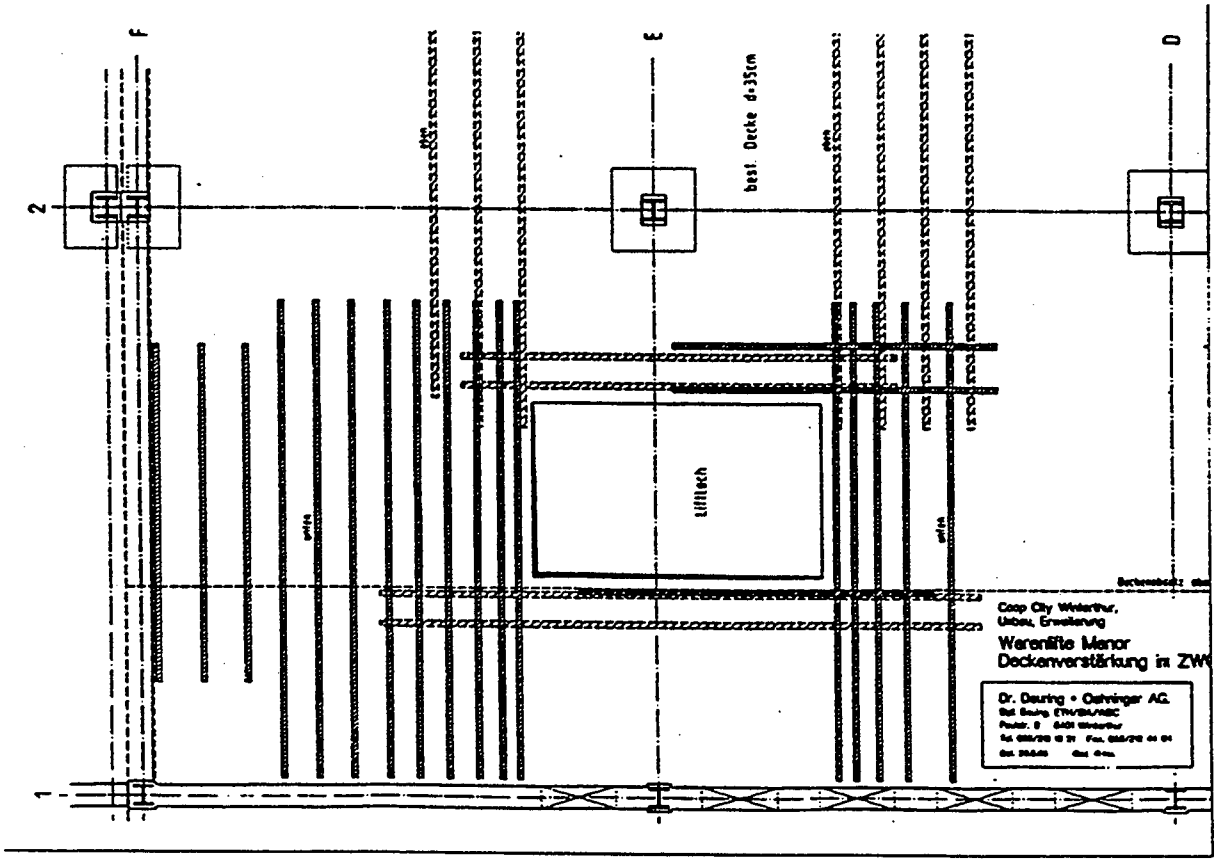

Figure 4.3: Layout of CFRP-Strips Strengthening with Sika Carbodur System
(Steiner, 1996)

Table 4.1: Characteristics of Sika CarboDur Epoxy Adhesives

Characteristics	Guide Values
Pot Life	40-80 min. at 20°C
Sag Flow	3-5 min. at 35°C
Squeezability	3000-4000 mm^2 at 15°C
Compressive Strength	75-100 N/mm^2
Tensile Strength	20-30 N/mm^2
Shear Strength	15-20 N/mm^2
Elastic Modulus	8-16 kN/mm^2
Shrinkage	0.04-0.08%
Adhesion to Wet Surface	4 N/mm^2
Glass Transition Point	50-70°C

(Steiner, 1996)

The strengthening technique used by Sika AG can be summarized as follows. The CFRP strips to be used are placed on a table and checked for possible damage. The bonding surface of the strips has to be cleaned with solvent. As a next step, homogeneously mixed epoxy is applied to the prepared concrete surface with trowel and leveled by scraping. This assures complete filling of the rough surface and wets the concrete completely. Next, the cleaned and completely dried CFRP strip is coated with epoxy adhesive, then applied to the concrete surface and fixed by light pressure. The adhesive layer should be about 2 mm thick, minimum 1 mm and maximum 5 mm. The extraordinary stability of the adhesive, as well as the light weight of the strips allows work without any clamping or supporting devices. Then the CFRP is pressed onto the concrete by means of rubber roller, squeezing the fresh epoxy out on both sides. Parallel CFRP strips are applied with a gap of 5 mm in between. The squeezed adhesive is removed with a painter's knife and the CFRP surface is cleaned.

For quality control purposes, steel discs or pieces of FRP strips are bonded to the concrete and pulled off after hardening. At least two prisms (4 x 4 x 16 cm) of adhesive, taken from the last mix of the day or from each different batch, must later be tested in a laboratory. The bonded FRP strips should be examined for hollow spots by light tapping.

If desired for aesthetic reasons, the outer face of the FRP strips can be painted or covered with cement mortars after priming the strip with a suitable bonding agent.

4.3 DESIGN MODELS AND APPLICATION TECHNIQUES

4.3.1 "Lack of Ductility" Problem Associated with FRP Strengthening

The scope of engineering use of any material depends primarily on its stress-strain profile. FRP materials can offer strength and stiffness several times higher than those of conventional metals. The strength and stiffness of FRPs depends on the type and volume of fibers and resin, which can be tailored according to design requirements. But the unique aspect of the stress-strain diagram for FRPs, which make them very different from metals, is the absence of yield plateau. This means that FRPs fail in a sudden brittle manner. The use of advanced composite plates, in lieu of steel, depends on how effectively the designer can accommodate and exploit the material in conjunction with the existing structural element, without sacrificing any of its desirable properties. Compromising on ductility at failure is a major concern, which has to be carefully considered when designing for FRP-strengthening.

The ductility of a reinforced concrete beam is a measure of its energy absorption capacity. Ductility mainly depends upon the distinct yielding level. Typically, ductility is defined as a ratio of deflection or curvature at ultimate strength to that at yield. Ductility of a structural member, in a broad sense, is an indication of its ability to undergo large strains before failure. From the mechanics of materials perspective, good ductility is also an indicator of a relatively high strain-energy absorption capacity of the member. Energy absorption in concrete beams can be estimated by considering the area under load-deflection or moment-curvature diagrams *(Vijay and GangaRao, 1996)*. Consideration of the serviceability-based energy level *(ACI 318-95)* with respect to the total energy in a moment-curvature plot provides a basis for addressing ductility and deformability in the design of FRP-strengthened concrete beams.

Interpretation of ductility of FRP strengthened concrete beams on the basis of conventional definitions may be misleading due to the linear stress-strain relation of FRP materials up to failure *(Vijay and GangaRao, 1996)*. An acceptable definition of ductility for FRP strengthened concrete beams should consider factors such as: uniform elongation of FRP laminates as compared to localized yielding of steel; confinement effects; and uniform crack location and spacing.

The ultimate strain and elastic modulus of glass FRP varies from 10800 to 19500 microstrain and 10.3 to 37.2 GPa, respectively. For carbon FRP these parameters vary from 7800 to 16200 microstrain and 54.5 to 305 GPa, respectively. In this context, an appropriate expression of ductility should not be a function of the FRP's ultimate stress and strain values. One attempt in to address this issue is the relative comparison in terms of strain-energy absorption, i.e. the area under the load-deflection curve.

A comparative study *(Swamy et al, 1996)* indicates that at any load level, the higher the FRP plate fraction area, the lower is the energy absorption capacity of the strengthened concrete member. In all strengthened beams, the load carrying capacity is increased substantially but the energy absorption capacity is reduced drastically at the equivalent load level. This is more pronounced for CFRP compared to GFRP plates.

One very clear distinction between CFRP and GFRP plate strengthened beams is the presence of a noticeable plastic region on the stress-strain plot for the latter. In real sense this is a pseudo-plastic region, because the steel rebars are in plastic stage but the external GFRP is still elastic. This is not the case when CFRP plates are used. Because of their higher stiffness and strength, the contribution of the external plate to the total tensile force is higher, which keeps the neutral axis down and delays or totally prevents the plastic deformation of the steel rebars.

4.3.2 Flexural Strengthening – Case Studies

One technique for flexural strengthening of existing reinforced concrete bridge elements is to apply externally bonded reinforcement to the tension side of the elements. Cracking and the ultimate moment of resistance are two important factors in flexural strengthening of reinforced concrete. In concrete elements there exists an envelope of potential structural enhancements, which is governed by the amount and distribution of internal reinforcement as well as the properties and geometry of the concrete. In particular, the tensile and shear strength of the cover concrete will limit stress transfer into the external reinforcement.

A study conducted at Oxford Brookes University, UK, describes the influence of various parameters on the flexural behavior of beams strengthened with externally bonded FRP reinforcement *(Hutchinson and Rahimi, 1996)*. These parameters include the concrete strength as well as the modulus and strength of FRP external reinforcement. Over thirty 2300 x 200 x 150 mm conventionally reinforced beams were fabricated and strengthened with epoxy-bonded unstressed CFRP and glass FRP (GFRP) laminates. Unidirectional pultruded Ciba Fibredux glass/epoxy and carbon/epoxy composite plates were used. The thickness of the cured laminate was between 0.4 and 1.8 mm. Representative properties of the materials are summarized in Table 4.2.

Table 4.2: Material Properties

Properties	Concrete	GFRP Composite	CFRP Composite	Epoxy Adhesive
Density, kg/m^3	2200	2200	1500	1500
Young's Modulus, $GN.m^{-2}$	25	36	127	7
Shear Strength, MNm^{-2}	6	–	80	23
Tensile Strength, MNm^{-2}	3	1074	1532	20
Compressive Strength, MNm^{-2}	55-69	–	–	70
Poisson's Ratio	0.2	0.3	0.3	0.3
Elongation at Break,%	0.15	3.1	1.21	0.7
Thermal Expansion, $10^{-6}C^{-1}$	10	8	-0.8	30

(Hutchinson and Rahimi, 1996)

The concrete beams were lightly sand blasted in order to remove the laitance and expose small and medium sized pieces of aggregate. A nylon peel layer was molded onto one surface of the composite during manufacture and was peeled off prior to bonding. Sikadur 31 PBA, a two-component cold-curing epoxy, was used. The unstressed composite plate was held against the concrete with a vacuum bag during curing to keep a uniform pressure over the bonded area. The resulting bond-line was about 2 mm thick. All of the beams with bonded external reinforcement performed significantly better than the controls. Test results are shown in Table 4.3. The GFRP provided significant ductility and reasonable strength. For the CFRP plates, the increased beam

enhancement was achieved at the expense of a loss of ductility with increasing thickness of CFRP.

Table 4.3: Results of Flexural Testing

FRP Reinforcement	FRP Cross Section, mm^2	Ultimate Deflection, mm	Ultimate Load, kN
None	0	53	26
Carbon	117	41	69
Carbon	60	38	54
Glass	270	33	60

(Hutchinson and Rahimi, 1996)

Five rectangular beams and one T-beam were tested at the University of Arizona, Tucson *(Saadatmanesh and Ehsani, 1996)*. Each beam was 4880 x 455 x 205 mm and was supported over a clear span of 4.57 m. The study investigated the effect of the original reinforcement ratio and the effect of shear cracking and shear reinforcement on the strength of composite reinforced beams. A 1.5 mm thick layer epoxy was used to attach 152 mm wide, 4.26 m long, and 6 mm thick glass FRP plates to the bottom of the beams.

The GFRP plates were tested under uniaxial tension. They exhibited linear-elastic behavior up to failure, with an average modulus of elasticity of 37 GPa and an average ultimate strength of 400 MPa. The lap shear strength of the epoxy was 14 to 15 MPa, elongation at failure was 40 percent, and curing time was 4 hours at room temperature.

The load vs. deflection curves of the strengthened and control beams indicated that plating increased the yield and ultimate loads by about 15 percent and 65 percent, respectively. The gain in ultimate flexural strength was more significant in beams with lower steel reinforcement ratios.

University of Toronto, Ontario, conducted research on the performance of conventionally reinforced concrete beams strengthened with bonded CFRP and GFRP plates *(Bonacci, 1996)*. The characteristics of the FRPs are given in Table 4.4. The failure modes are given in Table 4.5. Bond failure was the most common failure mechanism.

Table 4.4: FRP Properties

Property	Glass FRP	Carbon FRP
FRP Modulus, GPa	10-40	60-170
FRP Strength, MPa	200-750	700-1500

Two of the indices that can be used to compare strengthened beams to unstrengthened ones are strengthening ratio and deflection ratio. Strengthening ratio is defined as the strength of the beam with externally bonded FRPs divided by the strength of the control beam. Deflection ratio is defined as the centerline deflection at peak for the strengthened beam to that of the control beam. Strengthening ratios in this study varied from 1.0 (a bond failure with inadequate epoxy) to 4.3. Deflection ratios were from 0.1 to almost 1.0. Deflection ratio values near 1.0 were the result of having a small composite strengthened area or inadequate epoxy performance. Table 4.5 lists the strengthening ratios and failure modes. It appears that bond failure predominated in the high strengthening ratio cases. However, this cannot be generalized.

Table 4.5: Behavior of Failure Modes

	Failure Modes			
	Shear	**Compression**	**Fracture**	**Bond**
% of Specimens	8%	6%	22%	64%
Strengthening Ratio	1.38	1.55	2.01	4.35
Deflection Ratio	0.84	0.92	0.99	0.97
% of CFRP	0%	0%	33%	67%
% GFRP	18%	14%	11%	57%

Because of the brittle and complex nature of the failure modes, there is a need for safety factors when designing for strengthening with external FRP plates. Bonding failure depends on parameters that are not treated in analysis of conventional materials. Parameters such as epoxy thickness and mechanical response, preparation of the concrete surface before application of the epoxy, and sensitivity to faulting motions along existing cracks on the tension faces need to be considered. Also, there is concern that beams reinforced in this manner would have inadequate ductility. However, with proper design, externally strengthened beams can develop considerable deformation before failure. The design should assure flexurally balanced failures with shear and bond failure modes precluded. Shear, compression and bond failure result in a sudden failure mode, which is prohibited by the design codes.

Aramid/epoxy strengthened concrete slabs were tested at the University of Sherbrooke *(Demers et al, 1996)*. The ultimate strength of the aramid/epoxy-reinforced slabs was three times that of the plain concrete slab. The failure occurred with sufficient warning since the center deflection was larger than the clear span divided by 60. The failure of these slabs occurred by punch, and the composite sheet remained glued on all sides of the slab. Although the effective amount of fibers in each direction was the same for all reinforced slabs, there were some differences in their load-deflection response due to different reinforcement configurations. The study found that the fiber orientation, i.e. 0° and 90° or +/- 45°, has no significant effect on the overall behavior. However, this conclusion cannot be generalized.

Queen's University, Ontario collaborated with Royal Military College of Canada in an experimental testing program of large-scale prestressed concrete beams strengthened by unstressed and prestressed CFRP pre-preg sheets *(Wight et al, 1996)*. Mitsubishi Chemical fabricated sheets with a fiber volume fraction of 65 percent, and a fiber tensile strength of 235 GPa. The sheets were 0.2 mm thick, 300 mm wide and had an effective tensile modulus of elasticity of 125 GPa. Sheets were precut and bonded to the beam surface with a two-part epoxy.

The unstressed plate strengthening used alternate layers of epoxy and FRP sheets until the desired thickness was achieved. The first sheet applied to the beam was the longest and each subsequent layer was shorter than the preceding one.

The prestressed plate strengthening system consisted of steel round bar anchors bonded to the sheets and steel anchor assemblies fixed to the beam. The bar at one end of the FRP was fixed and the other bar was movable. When the sheet was fully prestressed with a hydraulic jack the movable bar was attached to the beam. The application of the FRP sheet resulted in an increase in the cracking load and a delay in the yielding of the reinforcing steel. A forty percent increase in the ultimate load of the control beam was observed in the beams with non-prestressed CFRP

sheets, whereas a 45-50 percent increase in the ultimate load was noted in the beams strengthened with prestressed sheets. The addition of non-prestressed FRP sheets delayed the yielding of the steel until a load of 30 percent higher than the control beam was attained. When prestressed sheets were bonded to the concrete beams, yielding occurred at a load 50 percent higher than that in the control beam.

Sharif et al *(1994)* investigated the strengthening effects of FRP plates on damaged, pre-loaded reinforced concrete beams. The beams were preloaded to develop central deflection corresponding to approximately 85 percent of their ultimate capacity.

The damaged beams were repaired using four different schemes as shown in Figure 4.4.

The results of the experiment suggested that shear and normal stresses in the FRP plates increase with increasing plate thickness, leading to premature failure by plate separation and concrete pull-out.

The steel anchor bolts prevented plate separation for the 3 mm plates and the beams failed due to diagonal tension cracks.

I-jacket plates provided the best strengthening system. This configuration eliminated plate separation and diagonal tension cracking, and developed the full flexural strength.

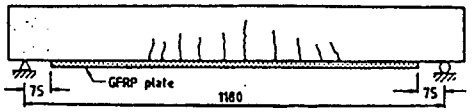

Various repair schemes for damaged beams: (a) Bonded fiberglass plate to beam soffit

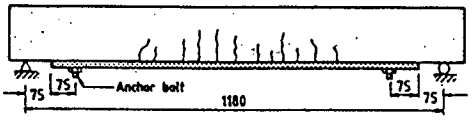

Various repair schemes for damaged beams: (b) Steel bolts anchoring bonded fiberglass plate

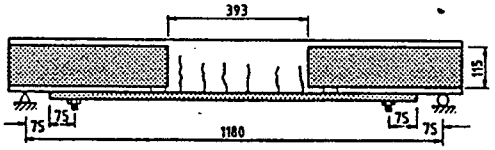

Various repair schemes for damaged beams: (c) Additional plates (wings bonded to beam sides)

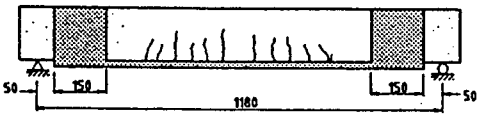

I-jacket fiberglass plate strengthening damaged beam: (a) Side view

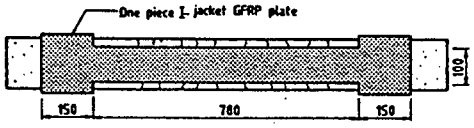

I-jacket fiberglass plate strengthening damaged beam: (b) Bottom view

Figure 4.4: Strengthening Schemes of Concrete Beams
(Sharif et al, 1994)

The study concluded that repaired concrete beams developed adequate flexural capacities to provide enough ductility despite of the brittleness of FRP plates. The procedures demonstrated the effectiveness of using externally applied FRP plates for strengthening damaged or upgrading of under-designed concrete beams.

A study conducted at the University of Sheffield investigated the differences between beams strengthened with GFRP plates and steel plates *(Swamy et al, 1996)*. The study found that the beams strengthened with steel carried more ultimate load and were stiffer than GFRP-strengthened beams, but the deflections at ultimate load of the GFRP-plated beams was larger. The study compared the beams' ductility based on their strain-energy absorption capacity. Differences between the performance of the beams are summarized in Table 4.6.

It was observed that the FRP- plated beam developed horizontal cracks at the concrete-FRP interface prior to failure. This is very detrimental to the effective stress transfer from the concrete to the external plate. The reason for this type of failure is the inability of the epoxy-concrete interface to remain intact when the external GFRP is undergoing large strains *(Swamy et al, 1996)*.

Table 4.6: Influence of the Plate Material

Beam Design	Plate Material	Ultimate Deflection mm	Ultimate Plate Strain μs	Ultimate Load kN
No Plate	None	32	–	200
Normal	Steel	30	4000	211
Normal	GFRP	33	6200	193
Special	GFRP	37	7000	232
Special	GFRP	49	10000	182

Contradictory results from specially designed GFRP plated beams indicated that bearing capacity can be increased considerably, while failure was more ductile then the un-plated beam. The results show that through special design considerations it is possible to increase the ductility at failure even when the bonded plate is a brittle material.

4.3.3 Shear Strengthening

A reinforced concrete beam must be designed to develop its full flexural strength to insure a ductile flexural failure mode under extreme loading. Hence, a beam must have a safety margin against other types of failure that are more dangerous and less predictable than flexural failure. Shear failure of reinforced concrete beam would have a catastrophic effect, should it occur. If a beam deficient in shear strength is overloaded, failure may occur suddenly without advanced warning of distress.

A study on strengthening reinforced concrete beams having deficient shear strength was conducted by Al-Sulaimani et al *(1994)*. Beams with different design shear strengths were damaged to a predetermined level, corresponding to appearance of the first shear crack, and then repaired with fiberglass plates. Different shear repair schemes were used, including GFRP shear strips, shear wings, and U-jackets in the shear span of the beams. These techniques are shown in Figure 4.5.

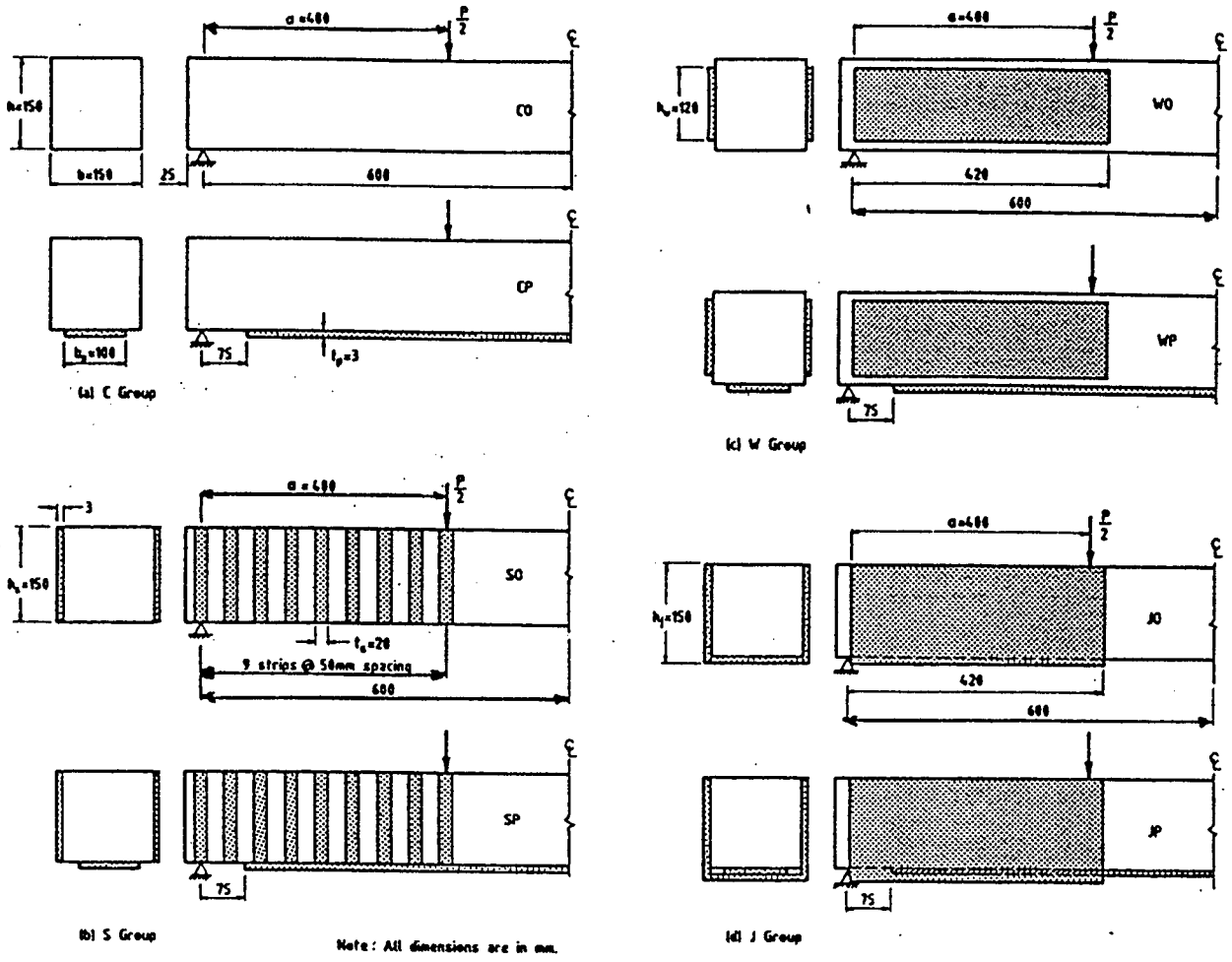

Figure 4.5: Repair Schemes
(Al-Sulaimani et al, 1994)

GFRP plates three millimeters thick were used in all schemes for external shear reinforcement. The GFRP material consisted of three layers of woven fiber-glass embedded in a polyester matrix and had an ultimate tensile strength of 200 MPa (29 ksi). Experimental data on strength, stiffness, deflection, and mode of failure were obtained, and comparison between the different shear schemes was made. The results showed that the increase in shear capacity was almost identical for strips and wings shear repair. They both increased shear capacity and restored degraded stiffness. However, the increase was not enough to cause the beams to fail in flexure. The failure of the strip and wing strengthening was by peeling.

The enhanced shear capacity provided by the U-jackets was sufficient to insure flexural failure in these beams. Thus, shear repair by jackets appears to be better than strips and wings schemes, since the continuity rendered by the geometry of the jacket minimizes the effects of stress concentrations present in the other two types of plates.

Shear reinforcing using CFRP sheets was studied in Japan *(Sato et al, 1996)*. CFRP sheets were glued to the sides and bottom of concrete beams with and without stirrups. Addition of CFRP sheets increased the shear strength of the specimens from about 50 to over 100 percent. Delimitation of the CFRP along the shear cracks was the failure mode in the beams without stirrups.

Chajes et al *(1995)* tested twelve under-reinforced T-beams to study the effectiveness of using externally applied composite materials as a method of increasing a beam's shear capacity. Woven fabrics made of aramid, E-glass, and graphite were bonded to the web of the T-beams using a two-component epoxy. The beams were tested in flexure, and the performance of the strengthened beams was compared to control beams with no external reinforcement. All of the beams failed in shear. The reinforced beams had an increase in ultimate strength of 60 to 150 and excellent resistance to composite peeling. The results are shown in Table 4.7.

Table 4.7: Contribution to the Shear Capacity of Various Externally Applied Fabrics

Beam Treatment	Concrete Shear Capacity, kips	Fabric Shear Capacity, kips	Ultimate Shear Capacity, kips
Control	4.23	—	4.23
Aramid	4.23	3.50	7.73
E-Glass	4.23	3.72	7.95
0/90 Graphite	4.23	3.85	8.08
45/135 Graphite	4.23	5.30	9.53

(Chajes et al, 1995)

4.3.4 External Prestressing

In some cases it may be necessary to provide additional camber in the concrete beam. This way, the serviceability of the structure can be improved and the shearing off of the FRP sheets, due to shear failure of the concrete, can be avoided *(Meier et al, 1992)*.

This type of prestressing is typically accomplished by cambering the girders with hydraulic jacks while in loose contact with an epoxy-coated composite plate. The jacks are removed when the epoxy has cured. This puts the composite plate in tension, preventing a complete elastic return of the girder.

This results in initial compression and tension stress in the girder, which oppose the stresses induced by gravity and external loads. The elimination of anchorage in this prestressing scheme precludes development of localized stresses in the anchorage zones.

Another technique for strengthening with prestressed sheets has been used by the Swiss Federal Laboratories *(Meier, 1991)* and is illustrated in Figure 4.6. The two far ends of the composite are cut when the adhesive has fully hardened and the sheet is then transformed into a pre-stressing element.

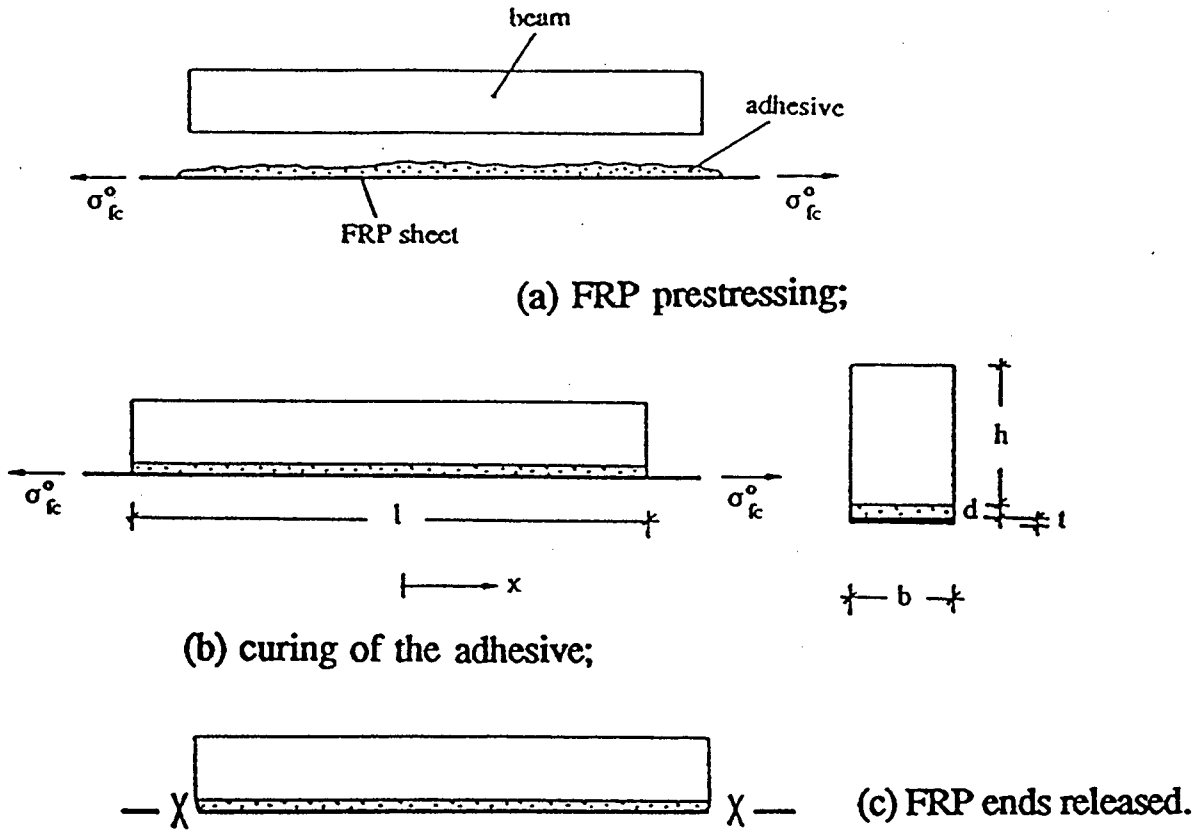

Figure 4.6: Procedure for Applying Prestressed FRP Sheet
(Triantafillou and Plevris, 1991)

When the pre-tensioning force is too high, failure of the system due to pre-tension release may occur at the two ends. This is caused by the development of high shear stresses in the concrete layer just above the FRP sheet. It can be avoided by limiting the prestress to approximately 50% of the ultimate. The study performed at EMPA, Switzerland *(Meier et al, 1992)* suggests that without special end anchorage, FRP sheets shear off from the end zones immediately if prestressed over 5% of their failure strength. On the other hand, technically and economically rational prestress is typically achieved at rate of 50% of the ultimate. Therefore, the design and construction of the end regions requires careful attention. The initial pretension calculations can be found in Triantafillou and Plevris (1991).

Karam *(1992)* proposed a technique that increases the efficiency of the anchorage zones by increasing the FRP area at the high shear regions hyperbolically. The hyperbolic profile of the end anchorage zone can be obtained by either successive sheet lamination to increase the thickness or by flaring the ends of the sheet to increase its width. The lamination solution is the most practical and the profile can be approximated by a series of equal steps, depending on the thickness of the sheet used. Another option is to increase the width of the FRP laminate, bonding the added area either to the bottom of the beam or to its sides. This will result in a decrease in the shear stresses, thus increasing the capacity and safety of the assembly.

A test program conducted at University of Arizona at Tucson, involved strengthening of concrete beam with GFRP plates *(Saadatmanesh, 1994)*. To simulate the loss of steel area due to corrosion, the test beam was significantly under-reinforced. External prestressing was applied to the beam by bonding the GFRP plate while the beam was held in a cambered position by jacking forces. The beam was initially loaded to approximately 110 kN and cyclically loaded until failure occurred between the FRP plate and concrete.

The resulting load-deflection curve showed that plating increased the yield and ultimate loads of the beam approximately 500 percent, and reduced the deflection approximately 250 percent. Additionally, GFRP plating reduced crack sizes and ductility in the beam at all load levels.

Before field application of this technique, further studies should be conducted to examine the creep behavior of the epoxy joint subjected to sustained cambering stresses. Also, effects of temperature and moisture on the epoxy joint should be examined.

The research conducted by Saadatmanesh et al *(1994)* was followed by analytical and parametric studies to evaluate the moments and curvatures for concrete girders externally prestressed with FRP plates *(Char et al, 1994)*. The analytical study was based on the same assumptions made in the classical theories of reinforced concrete members subjected to flexure, namely linear strain distribution, no creep or shrinkage, no shear deformations, and complete composite action between the FRP plate and concrete beam. The subsequent experiments showed agreement between the calculated and measured loads and strains. The parametric study investigated the effects of the initial camber and type of the composite plate on the moment-curvature relationship. CFRP and GFRP plates with typical properties and design were considered. A comparison of the moment-curvature relationships before and after strengthening revealed an increase in the maximum moment by a factor of 2 to 3 for GFRP plates, and 3.5 to 4.5 for CFRP plates.

Traintafillou and Plevris *(1992)* conducted a comprehensive study of short-term flexural behavior of reinforced concrete beams strengthened with bonded pretensioned composite laminates. The principal findings were as follows:

- A pretensioned laminate of a given thickness and unstressed laminate with greater thickness can be equally efficient in enhancing a member's mechanical properties.
- FRP sheets can be prestressed only to a certain degree. If the sheets are stressed beyond that level and then released, cracks are observed in the epoxy layer and near the ends of FRP sheets.
- To avoid sudden collapse, it is essential that the members be designed to fail in the compression zone first, followed by tensile fracture of the laminate.

The foregoing information is important to the development of composite strengthening of reinforced concrete beams. However, because of the added complications of prestressing in the field it would have limited use in the transportation environment.

4.3.5 Strengthening of Reinforced Concrete Beams with FRP Sheets

While most of the European institutions use exclusively rigid carbon or glass plates to enhance the bending capacity of RC beams, the Federal Institute for Materials and Testing (BAM) in Berlin, Germany, applied flexible CFRP prepreg unidirectional sheets to upgrade bending and shear capacity *(Limberger and Vielhaber, 1996)*.

In Japan and most recently in the United States, flexible CFRP sheets with thicknesses of 0.1 to 0.25 mm have been used in lieu of the 1 mm to 3 mm thick plates. The advantage of the flexible sheets is realized when curved structural elements require treatment. The disadvantage is that the cost of the rehabilitation is increased due to necessity of manually applying several plies. Typical properties of prepreg CFRP sheets are shown in Table 4.8.

Table 4.8: Technical Data of Prepreg CFRP Sheets

Type	Regular Modulus (RM)	High Modulus (HM)
Thickness, mm	0.097-0.167	0.095
Elastic Modulus, MPa	240000	650000
Tensile Strength, MPa	2500	2000
Ultimate Strain,%	0.1-0.14	0.3-0.4

(Mitsubishi Chemical Co., Japan)

It appears that the reduction of ductility typically associated with CFRP-plate beams can be avoided by using prepreg material with a combination of low modulus (LM) and high modulus (HM) fibers *(Limberger and Vielhaber, 1996)*. While the ultimate load is determined by the LM carbon fibers, the HM fibers contribute to improved serviceability and reduced crack width.

4.3.6 Reinforced Concrete Decks/Slabs Strengthened with FRP Materials

Research conducted by the Naval Facilities Engineering Service Center (NFESC) studied the use of FRP sheet to upgrade the decks of existing reinforced concrete piers and wharves. Laboratory tests on simply supported under-reinforced slabs were conducted to determine the effects of upgrading on moment capacity, shear strength, deflection, ductility and failure mode *(Malvar, 1996)*. The slabs were strengthened with one transverse and three longitudinal CFRP layers of Forca Tow Sheet *(Kliger, 1993)*. This sheet has unidirectional carbon fibers and was selected for this project because of its ease of application. Properties of the Forca Tow CFRP Sheets are listed in Table 4.9. Both laboratory and field specimens showed a punching-shear failure mode. Laboratory specimens reinforced with one CFRP layer in each direction exhibited an ultimate load increase of up to 47 percent. CFRP reinforced slabs showed increased ductility compatible to that of the non-strengthened slabs.

Table 4.9: Forca Tow Sheet FTS-C1-20

Property	Value
Laminate Type	Unidirectional Carbon
Fiber Weight/Area	200 g/cm^2
Tensile Strength	385 kN/m of width
Tensile Modulus	25.4 MN/m of width
Ultimate Strain	1.5%

The laboratory conducted tests showed that the CFRP sheets increased the load carrying capacity by 31 percent. The load capacity increase for the field specimens averaged 20 percent. However, the ultimate deflection was reduced 42 and 27 percent for the one-way and two-way CFRP flexural reinforcement, respectively.

4.3.7 Design Methodology

This section explains the behavior and basic steps for designing reinforced concrete beams externally strengthened with FRP plates. Assuming a known value of concrete strain in the extreme compression fiber (top of the beam), the depth of the neutral axis can be obtained from the equilibrium of forces across the cross-section of the beam (Figure 4.7).

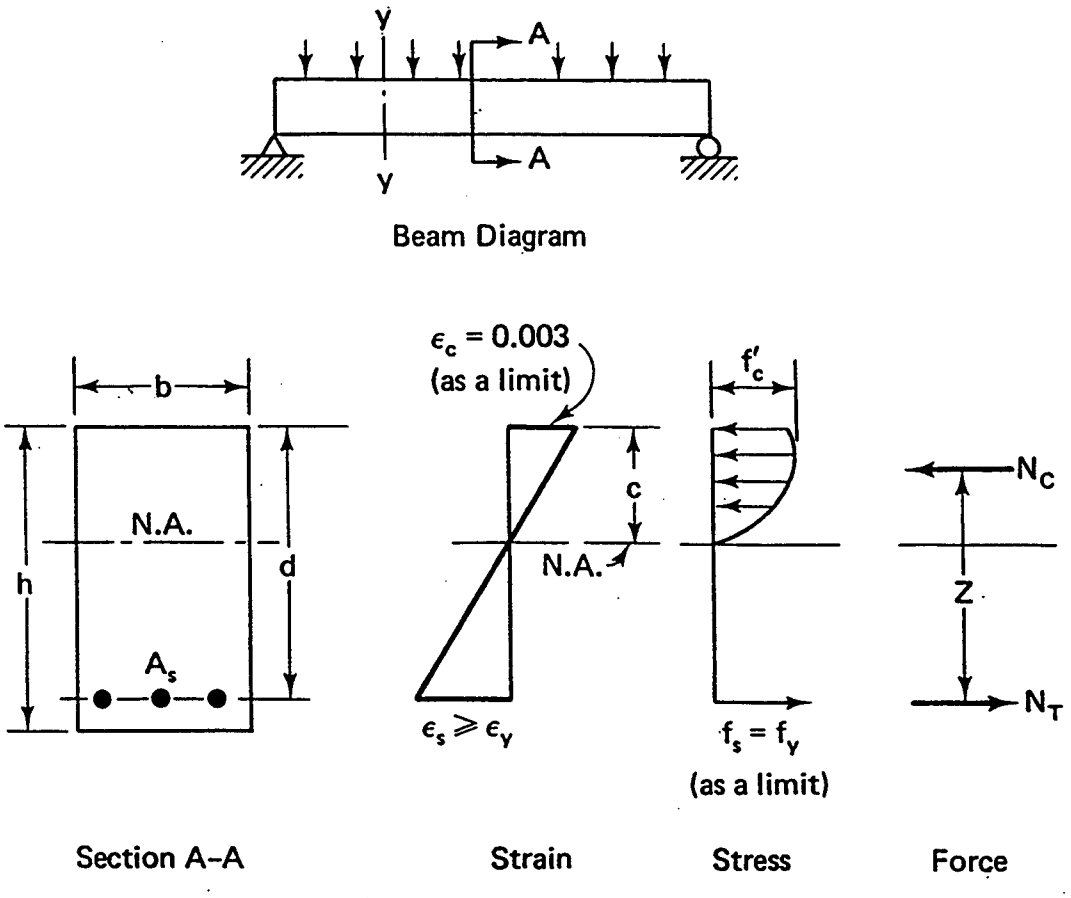

Figure 4.7: Beam Flexural Behavior at Near Ultimate Load

After the location of the neutral axis is determined, the strains in the concrete, the steel reinforcement bars, and the FRP plate can be calculated using the linear strain diagrams. It is assumed that the stress-strain curves for both steel and FRP material are idealized by Hognestad's parabola *(Park and Paulay, 1975)*. The stress-strain relation for steel is assumed to be elastic-perfectly plastic, and a linear relationship is assumed for FRP plates with ultimate stresses and strain depending upon the material used in the plate. The stresses in concrete, FRP, and steel bars are obtained from their idealized diagrams. The internal forces are then calculated multiplying the stresses by their corresponding areas. The moment capacity of the strengthened beam can be found by summarizing the moments of all internal forces about the neutral axis. Finally, the curvature can be calculated by dividing the strain in the extreme compression fiber by the distance to the neutral axis.

Similar design assumptions were adopted by Char et al *(1994)* who developed a computer program for calculating stresses and deflections of FRP strengthened beams. The merit of the design methodology was demonstrated by a numerical example that illustrated how a typical reinforced concrete bridge, originally designed for H15 truck loading, can be upgraded to H20 truck loading by bonding composite plates to the tension flange of the girders. Initially, the stresses in the steel and concrete were below the maximum allowed values for H15 loading when the bridge was loaded with live H15 truck loads, but exceeded the H15 values when under H20 loads.

Four retrofitting techniques were considered: bonding with GFRP plates; cambering the girder with GFRP plates; bonding with CFRP plates; and cambering the girder with the CFRP plates.

AASHTO standard specifications and design requirements were taken into account. The stresses in the beams strengthened with GFRP and CFRP plate but no camber were slightly higher than the allowable stresses provided by AASHTO. The cambered beams exceeded the required capacity of H20 loading by 150 percent.

A simplified approach for determining the flexural strength increase due to lamination is based on comparing it with the effects of additional steel reinforcement. The equivalent steel thickness, which is based on the thickness of the fibers only, is used in this design *(Thomas et al, 1996)*. Since the resin content and laminate thickness are not accurately controlled during strengthening, it would be difficult to obtain reliable strength and modulus values based on laminate composite area. Using the ACI or the AASHTO equations, the area of FRP laminate and the resulting moment capacity can be estimated. However, the merit of this approach is questionable and is not recommended for use by ODOT.

4.4 FATIGUE AND CREEP BEHAVIOR OF CONCRETE BEAMS WITH EXTERNALLY BONDED FRP SHEETS

At the present time, some of the important engineering properties of the FRP materials, such as strength and elastic modulus, are successfully predicted on the basis of simple mathematical models. Toughness, fatigue performance, and time-dependent behavior are much more difficult to forecast. Fiber-reinforced composites are heterogeneous and they exhibit complex behavior under cyclic loading. In a laminated composite, the state of stress and strain are multi-axial even under simple tensile loads. This is due to the inter-laminar shear and normal stresses between the layers. Moreover, fiber/matrix composite systems are often rate sensitive *(Ellyin and Kujawski, 1992)*. Damage modes in composites generally do not combine to form a single dominant crack in a self-similar manner, as in the case of metals. In a laminate, a complex damage state is observed under cyclic loading. For example, in multidirectional laminate cracks in 90^{o} plies usually occur first. Then an increase in density occurs, leading subsequently to delamination or transverse cracking in closely oriented plies. Final fracture occurs when 0^{o} plies fail.

In contrast to metals, the fatigue strength of FRP materials decreases with increasing compressive stress. Another significant difference observed between metals and composite materials is their response to a notch *(Ellyin and Kujawski, 1992)*. FRPs have high notch sensitivity to static or low cycle fatigue, and relatively low sensitivity to high cycle fatigue. These differences must be taken into account when the combined behavior of an FRP-concrete beam system is investigated.

A study conducted at West Virginia University investigated the effect of sustained load on concrete beams externally reinforced with CFRP. The research focused on the rate of increase in concrete creep strains due to sustained four-point loading. The reinforcing material was carbon Fiber Tow Sheets, type FTS-C1-20, manufactured by Tonen Corporation, Japan. The design thickness of a single ply was 0.11 mm, while the total thickness of the strengthening sheets varied from 0.6 to 1.0 mm. The Tow Sheet had a tensile strength of 382 N/mm, a tensile modulus of 23×10^{4} N/mm, and ultimate strain at failure of 1.5% *(Ligday et al, 1996)*. Two concrete beams, one unwrapped and one wrapped with Carbon Tow Sheet, were tested under sustained load (50% of the ultimate) for a duration of 50 days. The study found that the external wrap on the concrete beam significantly decreases the rate of creep strain. In this particular study, the creep reduction factor was calculated to be 0.3. However, these results should not be generalized.

The effect of repeated loading on the performance of concrete members strengthened by externally bonded advanced composites was studied by the Wright Laboratory Airbase Survivability Section, Wright Patterson Air Force Base, Ohio. CFRP external reinforcement laminates were attached to the specimens using a high-performance epoxy adhesive. The CFRP was three-ply and unidirectional, having a tensile strength and modulus of elasticity of 2270 MPa and 138 GPa, respectively. The specimens were tested under non-reversed fatigue loading, having loads ranging up to 90 percent of the maximum static load, applied at a rate of 20 Hz for two million cycles *(Muszynski and Sierakowski, 1996)*.

Additionally, toughness was measured using Japanese standard JCI-SF4 that determines the total area under the load-deflection curve to the point where the maximum deflection occurs.

The study also evaluated the endurance limit of the specimens. Endurance limit is defined as the maximum fatigue flexural stress at which the concrete (plain or reinforced) can withstand two million cycles of fatigue loading, expressed as a percentage of the modulus of rupture of plain concrete *(Wu et al, 1989)*. The endurance limit of CFRP reinforced beams was greater than 250 percent that of the control specimens.

The results of this study showed that the CFRP external reinforcement increased the load carrying capacity by a factor of 3 and the toughness of non-reinforced concrete beams by a factor of 40. Furthermore, the static flexural strength and toughness after fatigue loading were approximately the same as the non-fatigued control CFRP reinforced concrete samples.

The behavior of 4.7 x 0.2 x 0.15 m reinforced concrete beam subjected to fatigue loading was investigated at the Swiss Federal Laboratories *(Meier et al, 1992; Kaiser, 1989)*. The steel reinforcement consisted of two 8 mm bars in the tension and compression zones. The beam was post-strengthened with hybrid (carbon/glass FRP) sheets that had tensile strength and elastic modulus of 960 MPa and 80 GPa, respectively. A sinusoidal fatigue loading was applied at a frequency of 4 Hz. The fatigue failure initiated after 480,000 cycles in the first steel rod, and after 560,000 cycles in the second one. In comparison, the FRP sheet failed after 805,000 cycles.

This experiment provides insight into the failure mechanism of hybrid (steel rods/FRP sheet) beam reinforcing system, and shows how much the FRP sheet can withstand after failure of the steel reinforcement.

A second fatigue test was conducted on a beam with a 6.0 m span under more realistic conditions. The goal was to verify that bonded FRP sheets can withstand very high humidity and temperature combined with fatigue loading *(Meier et al, 1992)*. The beam was strengthened with CFRP sheets, thus increasing the static strength by 32 percent. After strengthening the beam was subjected to 10.7 million cycles of fatigue loading. Crack development was observed after 2 million cycles. Upon the completion of 10.7 million cycles, the test was continued in a climatically controlled room, at temperature of 40°C and 95 percent relative humidity. After 12 million cycles, the steel reinforcement failed, while the CFRP sheet did not present even the slightest problems. After 14.09 million cycles, cracking initiated and rapidly grew into the external FRP reinforcement which led to failure.

4.5 LOW TEMPERATURE RESPONSE OF RC BEAMS STRENGTHENED WITH FRP SHEETS

Low temperature testing is an important area of research because many mature technologies developed for warmer climates can fail when applied in cold regions. Although not typical for Oregon, a temperature range from -46°C to 38°C is not uncommon for the northern parts of the Unites States and Canada *(Baumert et al, 1996)*. Experiments on tensile loading of unidirectional FRP at low temperatures *(Dutta, 1990)* have shown that the longitudinal tensile strength decreases. This contradicts the commonly accepted notion that at low temperatures, material strength increases.

Behavior of composites is primarily governed by the fiber properties. After the beginning of fiber failure, the additional tensile load that can be applied to the composite will depend upon how efficiently the high local stresses around the broken fibers are transferred to the neighboring fibers. The properties of the matrix and the interface govern this stress transfer mechanism. At low temperatures most of the polymers show increased yield stress *(Kreibich et al, 1979)*. The reduced ability of the matrix to yield causes the load distribution across the fibers to be less uniform. Thus, at low temperatures, some fibers will share more load than others and will fail earlier, causing progressive failure to the other fibers. However, the actual load sharing process within the laminates is very complex and not fully understood *(Jones, 1975)*.

Another concern is that the differences in the coefficient of thermal expansion between concrete and unidirectional laminate may cause significant adhesive shear stress in the end of the FRP plates. Researchers from Switzerland developed a model to predict the temperature change that would cause adhesive bond damage. To investigate the effect of freeze/thaw, six beams were subjected to 100 cycles of 20°C to -25°C before being tested to failure *(Baumert, 1996)*. Half of the beams were cracked prior to application of the laminates. It was expected that water would enter the cracks and expand with subsequent freezing, resulting in peeling of the laminates. All frozen beams were brought to room temperature before testing. A comparison of the ultimate loads sustained by the frozen beams, with those of the control beams, showed no detrimental influence from the freeze/thaw cycles.

Baumert et al *(1996)* reported results of a plain concrete beams strengthened with CFRP tested at 21°C and -27°C. At both temperatures, the failure occurred by shear peeling off the CFRP sheets. For plain concrete beam tests, the addition of CFRP sheets appears to have a little effect on the magnitude of the first crack development. At low temperature, a significant increase in the first crack load was observed, without noticeable change in beam stiffness. It appears that the main reason for strength increase of FRP-strengthened unreinforced beams at low temperatures is the concrete strength increase.

4.6 ANALYSIS OF THE FAILURE MECHANISM OF RC BEAMS STRENGTHENED WITH FRP PLATES

As a result of FRP repair, the mode of failure of a flexural member may change from ductile to brittle *(Arduini et al, 1997)*. Brittle shear failure in concrete may substantially reduce the nominal expected flexural capacity based on standard design computations. Furthermore, changing the thickness of the FRP plate, the bonded length, or adding shear reinforcement significantly modifies the crack distribution pattern along the beam and changes the failure mechanism.

FRP-strengthened concrete beams can fail in several ways when loaded in bending. The following collapse mechanisms are the most widely recognized:

- steel yield-FRP rupture when the ultimate strain of the material is reached. If both, steel and FRP area fractions, are quite small, steel yielding may be followed by rupture of the composite sheet.
- steel yield-concrete crushing when the maximum compressive strength is reached. If the FRP area fraction is high and steel fraction area is small, failure is typically due to concrete crushing, while steel may yield or not, depending on its area fraction.
- shear failure of the concrete when the ultimate shear strength is reached. If both FRP and steel fractions are high, the concrete will reach its maximum capacity before the steel yields and before the composite sheet ruptures.
- debonding or local adhesive failure when the ultimate tensile strain of the adhesive is reached. The bond between the FRP and concrete may fail.

Stress-strain distribution of various failure modes is shown in Figure 4.8. Internal equilibrium and the ultimate bending moment calculations for the various failure modes are given in Triantafillou and Plevris, 1991.

Figure 4.9 illustrates how the failure mechanism depends on the quantity of the external FRP reinforcement.

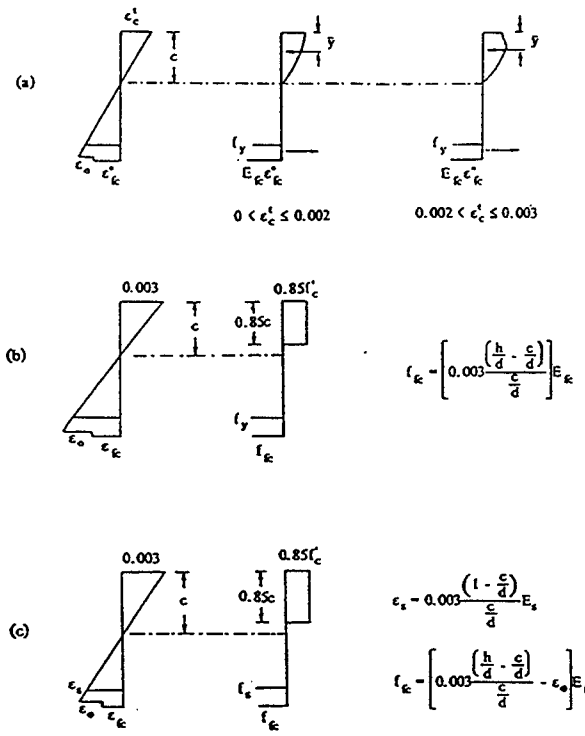

Strain and stress distribution at a section when the flexural strength is reached: (a) steel-yield-FRP rupture; (b) steel yield-concrete crushing; and (c) compression failure.

Figure 4.8: Stress-Strain Distribution at Failure
(Triantafillou and Pvevris, 1991)

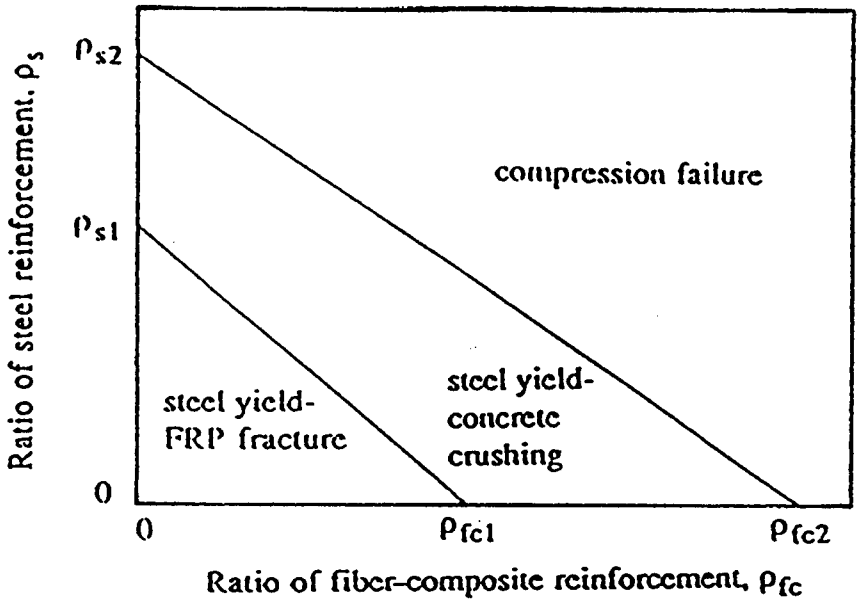

Figure 4.9: Influence of the FRP Reinforcement on the Failure Mechanism
(Triantafillou and Plevris, 1991)

Different failure modes of a beam strengthened with FRP plate are illustrated in Figure 4.10. The most typical type of failure is by rupture, i.e., either by a plate tensile failure or by concrete crushing in the compression zone. However, possibility of premature failure exists at the FRP-concrete interface due to separation of the plate. While the composite sheet is loaded on tension, the adhesive is loaded primarily in shear. The debonding occurs because of:

- Imperfections in the spreading of the adhesive;
- Flexural cracking of the concrete;
- Peeling-off of the composite when the beam face is not perfectly flat;
- Fatigue loads.

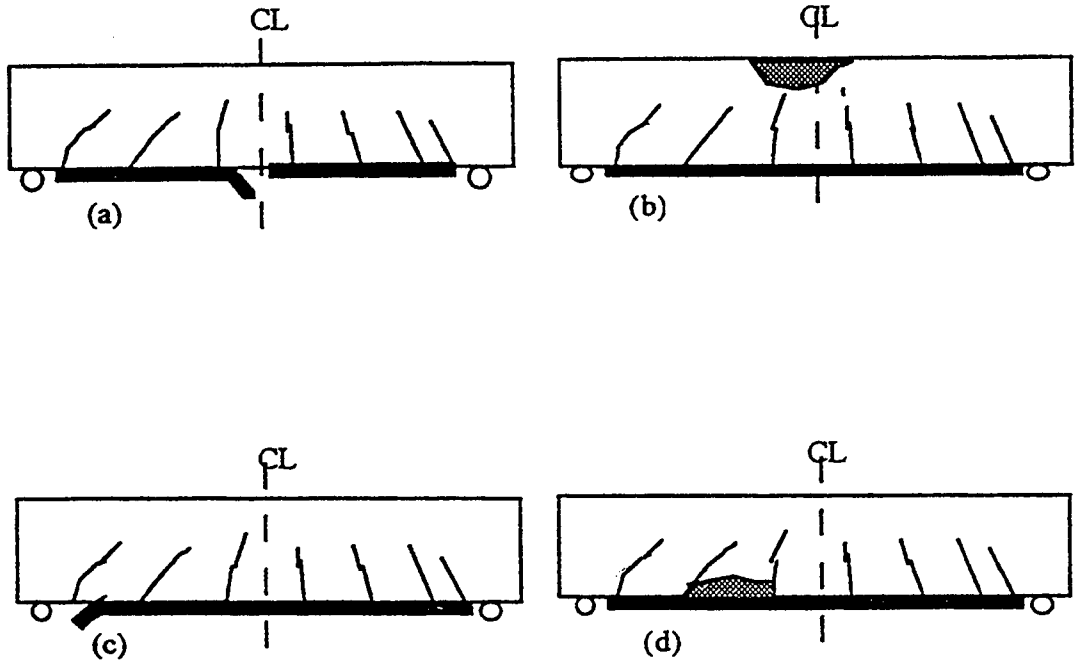

Figure 4.10: Different Failure Modes in RC Beams Strengthened with FRP Plate
(Varastwhpour and Hamelin, 1996)

In 1984 to 1989, CFRPs were successfully employed for the first time in Switzerland for post-strengthening purposes *(Meier et al, 1992)*. The research work showed the validity of the strain-compatibility method in the analysis of cross sections. The calculation of flexure in reinforced concrete elements post-strengthened with CFRP sheets was performed analogous to conventional reinforced concrete.

The work showed that the possible occurrence of shear cracks may lead to a peel-off of the strengthening sheet. Thus, the shear crack development represents a dimensional criterion.

Flexural cracks are typically spanned by the FRP sheets and do not influence the load capacity of the repaired structure. Compared to un-strengthened beams, FRP-retrofitted beams usually develop much finer cracks.

The following failure modes were common:

- Tensile failure of the CFRP sheet. Although the sheets failed suddenly, the failure was always announced in advanced by cracking sounds.
- Concrete failure in the compression zone (punch failure) and shearing of the concrete in the tensile zone.
- Continuous peeling-off of the FRP sheets due to uneven concrete surface. The study found that for thin sheets (less than 1 mm), applied by vacuum bagging, an extremely even concrete surface is required.
- Inter-laminar shear within the CFRP sheets.

The following modes are not likely, but theoretically possible *(Meier et al, 1992)*:

- Cohesive failure within the adhesive;
- Adhesive failure at the CFRP sheet/adhesive interface;
- Adhesive failure at the CFRP/concrete interface.

These findings are related to the specific materials employed in this study and cannot be generalized.

Laboratory and field tests show that FRP composites used for strengthening RC beams exhibit greater moment bearing capacity and smaller deflections. By adding external reinforcement to a RC structure, the stiffness of the structure changes. The governing equations of RC beams must be modified to consider the effect of FRP sheet on the nominal moment capacity of the structure. The main equation of the superposition model is *(Bhutta and Al-Qadi, 1995)*:

$$M_n = M_{rc} + M_{frp} \qquad \textbf{(4-1)}$$

The following assumptions are made: the bond between FRP and concrete beam is perfect, and the RC behavior is elasto-plastic in nature.

A typical stress-strain diagram of a hybrid concrete beam externally reinforced with FRP plate is in Figure 4.11.

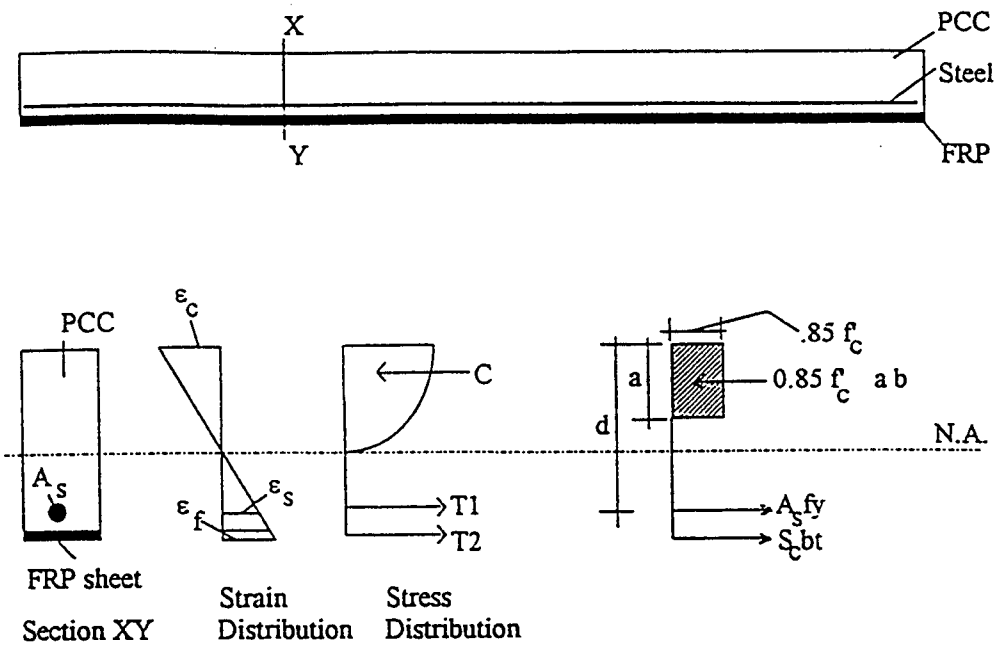

Figure 4.11: Stress-Strain Distribution of Hybrid Beam
(Bhutta and Al-Qadi, 1995)

The "generalized stiffness" is a function of the dimensions and constituent properties of the individual materials in the hybrid section. Composite laminate theory can be used for analysis of orthotropic materials *(Jones, 1975)*. This theory can address complex structures with multiple material configuration, such as reinforced concrete structures externally reinforced with FRP composites. Using this approach Bhutta and Al-Qadi *(1995)* studied the effect of composite thickness on the improvement in moment capacity. Analytical results are presented in Figure 4.12 for Kevlar FRP (KFRP), CFRP and GFRP. All FRP plates were 0.025 mm thick.

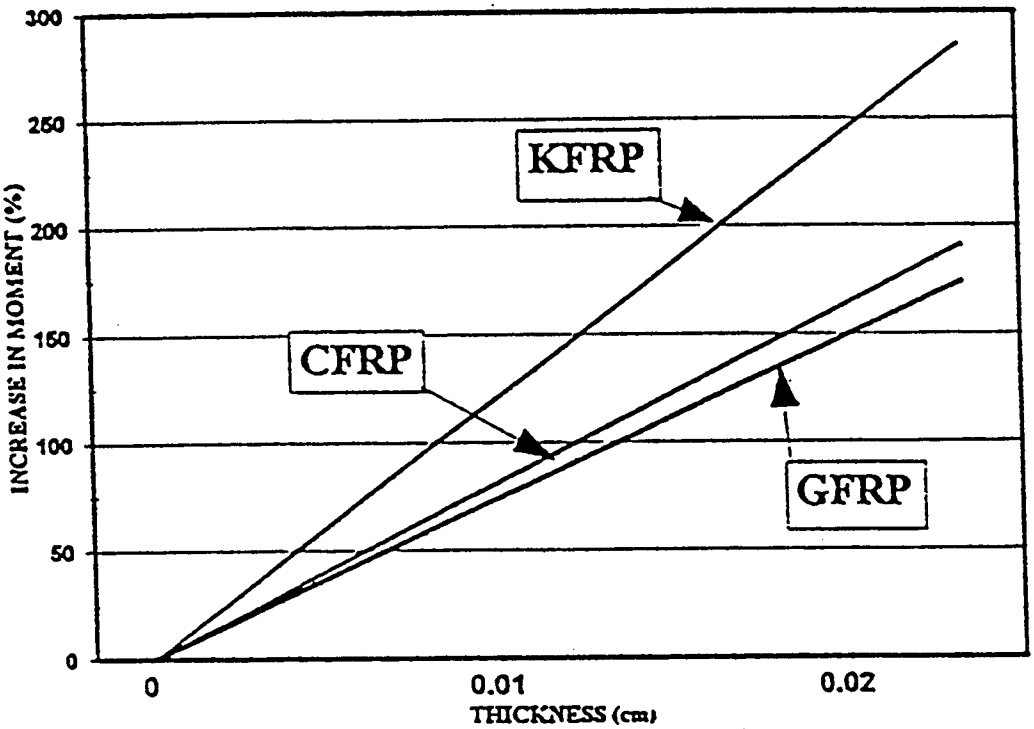

Figure 4.12: Percentage Increase in Moment Capacity
(Bhutta and Al-Qadi, 1995)

Models for stiffness and deflection of a simply supported hybrid beam were developed based on the composite laminate theory. The theory was modified to handle isotropic materials (concrete and steel reinforcing bars) and orthotropic materials (FRP). Sensitivity analysis was performed to evaluate the safety factor for hybrid beams as compared to RC beams.

KFRP showed the highest increase in moment capacity (280%), because of its high strain-to-failure value. On the other hand, CFRP has a high elastic modulus, but its strain at failure is low. The percentage increase in the moment capacity of CFRP plated beam was 190%. The smallest increase (170%) was found for GFRP. The analysis showed that the ability of the beam to handle moment is strongly dependent on the strength characteristics and the thickness of the FRP sheet. The deflection response of the hybrid beam, strengthened with 0.25 mm thick FRP provides a factor of safety of approximately 1.5 times that of a conventional RC beam.

A theoretical study of FRP beams strengthened with FRP plates was conducted at the Claude Bernard University, Lyon, France *(Varastehpour and Hamelin, 1996a)*. The authors assumed that the mechanical behavior of RC beams strengthened with FRP plates strongly depends on the interaction at the plate/concrete interface. It was found that the plate/concrete bond slip depends on the surface treatment. The non-linear analysis developed in this study appears to provide a good method for predicting the flexural strength of the beam and failure modes. The two failure modes defined in this paper are interface failure due to a coupling shear and normal stresses, and rupture of the concrete layer between the reinforcing bars and the FRP plate. The analytical method provides estimation of the shear stresses distribution.

The analytical results were checked by experiment *(Varastehpour and Hamelin, 1996b)*. CFRP plates with nominal thickness of 0.31 mm, elastic modulus of 117 GPa, and ultimate strength of 1350 MPa were used for strengthening. Three different geometries for FRP strengthening were used (Figure 4.13).

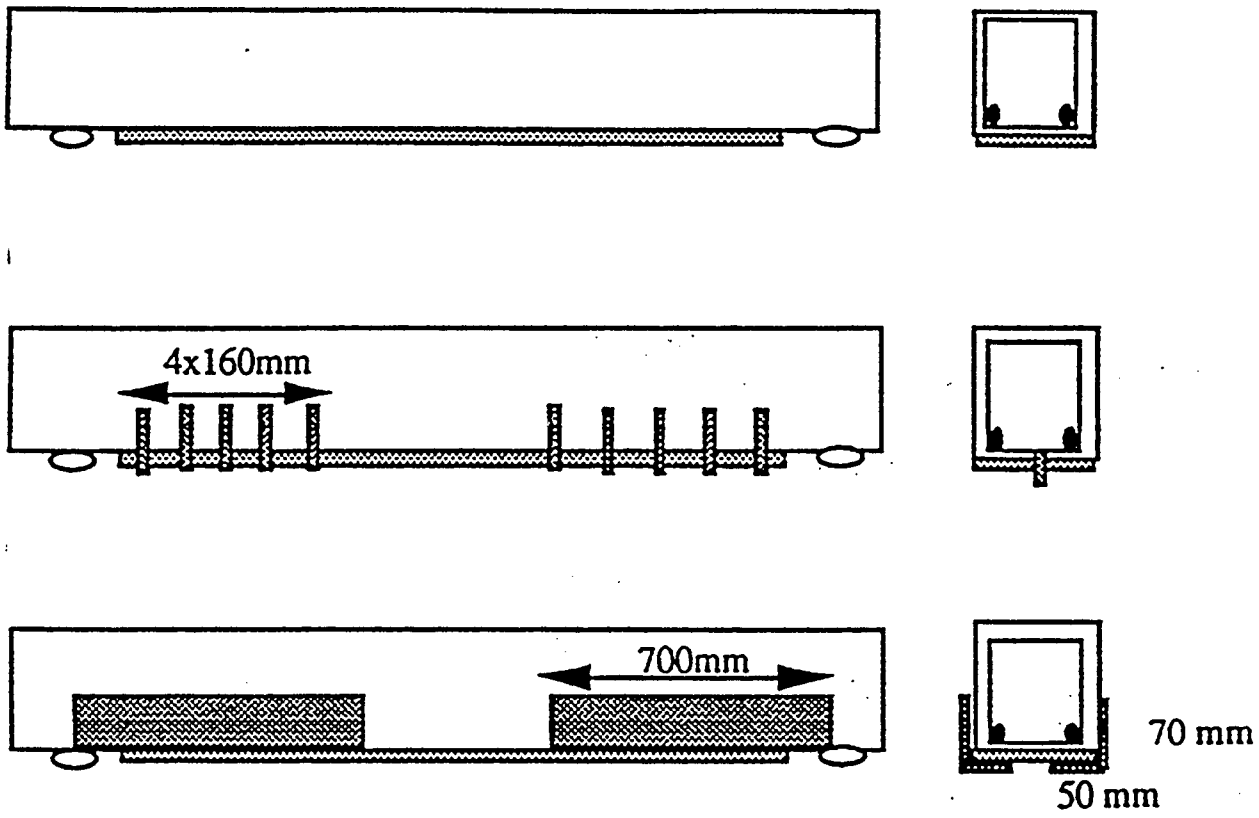

Figure 4.13: Different Methods for Strengthening RC Beams with FRP Plate
(Varastehpour and Hamelin, 1996b)

The first method used eight layers of woven textiles that were bonded by polymerization in situ, as illustrated in Figure 4.14.

A 2.5 mm thick CFRP plate was used for the second method. The plate was held in contact with the beam by vacuum bagging while the adhesive cured for one day.

The third method used mechanical anchorages made of composite materials that were 12 mm in diameter and 60 mm long. The CFRP plate was bonded to the anchorages with an adhesive (Sikadur, with elastic modulus of 8500 MPa, compressive strength of 75 MPa, and tensile strength of 25 MPa). It was placed in the shear spans, between the supports and the concentrated loads. For all beams, the ultimate measured loads were lower than the computed ones, due to premature failure on the beams. Results are presented in Table 4.10.

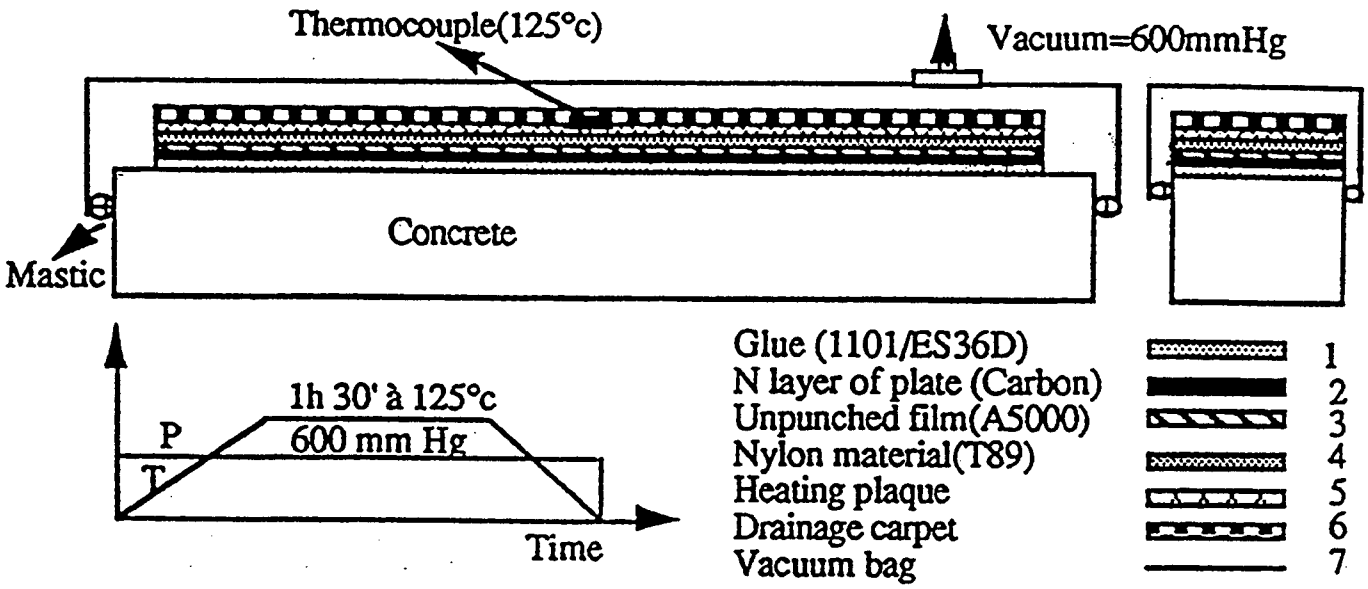

Figure 4.14: Plate Bonding by Polymerization in Situ Method and External Set Up
(Varastehpour and Hamelin, 1996b)

Table 4.10: Test Results

Beam	Ultimate Load (KN)			Ultimate Plate Strain (mm/mm x 10^{-3})			% over control beam	Failure Mode
	Exp	The	Exp/The	Exp	The	Exp/The		
Control	125	114	1.09	–	–	–	–	Concrete Crush
Polymerization in situ	195	238	0.82	3.53	5.5	0.64	56	Bond
Bonding by Glue	200	238	0.84	3.27	5.5	0.66	60	Bond
Glue + Mechanical Anchorage	188	238	0.79	3.31	5.5	0.31	50	Bond

(Varastehpour and Hamelin, 1996b)

The addition of the L-shape plates (Figure 4.13) bonded to the sides of the beam allowed for development of a full flexural strength of the beam.

4.7 OTHER TECHNIQUES FOR STRENGTHENING CONCRETE BEAMS USING FRP MATERIALS

The University of British Columbia investigated a novel technique for repair using a thin coat of GFRP composite applied by spraying *(Banthia et al, 1996)*. Test beams were sprayed on the tension side with a 3 mm thick coat composite with randomly distributed chopped fibers. The fiber volume fraction was kept at a low 8%, which was not expected to provide a significant change in the basic properties of the matrix. The beams were notched in order to simulate structural damage. Two polymers, polyurethane and polyester, were pre-mixed. The strength and modulus of the polymer after setting were 27 MPa and 4 GPa, respectively. The properties of the E-glass fibers were: tensile strength of 2410 MPa, modulus of elasticity of 69 GPa, elongation at break of 3.5%, and a density of 2.45 g/cm^3. The chopped fibers were 9.5 mm in length and about 10 μm in diameter. Typical test results are presented in Table 4.11.

Table 4.11: Results from RC Beams Strengthened with Sprayed FRP Composite

Beam Type	Load First Crack, kN	Maximum Load, kN	Fracture Energy, Nm (joules)
Un-notched, Plain	16.33	16.88	0.33
Un-notched with FRP	17.59	22.70	20.47
Notched, Plain	5.21	5.60	0.11
Notched with FRP	6.75	18.35	9.67

(Banthia et al, 1996)

For un-notched beams, the FRP coating led to an increase of 36% of the ultimate load. The fracture energy increased approximately 70 times. In the case of notched beams the increase in maximum load and fracture energy were 3 and 87 times, respectively. The low aspect ratio of fibers and the random distribution allowed fibers to fail by pull-out in addition to fracturing, and led to higher ductility.

This technique has a high potential for repair and retrofit. However, use of E-glass fibers in direct contact with the alkaline sub-base concrete is not recommended. The matrix has to be insensitive to UV attack. Finally, the use of higher fiber volume (up to 50%) may lead to significant improvement of the strength and modulus of the resulting composite.

4.8 FIELD APPLICATIONS

4.8.1 Canada

A study started in 1996 by the University of Alberta, and Alberta Transportation and Utilities, Canada resulted in construction and four-year durability investigations of a concrete bridge strengthened with CFRP sheets. The study emphasized the increase of shear capacity of bridge girders, construction processes and initial costs.

The bridge, located on a secondary highway, with an average annual daily traffic of 3000 vehicles, is near Edmonton, Alberta. The bridge has three 18 m spans, with 10 girders in each span. One span was selected for the project. When the monitoring is complete the span will be dismantled and the girders will be tested to failure in a laboratory. *(Alexander and Cheng, 1996)*

Two approaches to concrete surface preparation were used. Six beams were prepared according to specifications that called for grinding and patching, while the surface preparation for the other four was left to the discretion of the contractor.

Two CFRP sheets layouts were used. The sheets were placed on the inside girder surface so that the carbon fibers were perpendicular to the girder length. Six of the girders were reinforced continuously from one end to the other, while the other four had 25 cm sheets with 5 cm spacing between them.

One advantage of the FRP strengthening method is that the repair work can be done from below the deck, with very little disturbance to the traffic. However, vibrations during construction, especially from large trucks, may cause sheets to slip and not develop adequate bond to the concrete. To examine this effect, five girders were reinforced while the entire bridge was open to traffic, while the other five were strengthened while the lane above was closed to traffic. Since the girders were only covered with asphalt pavement, the traffic had very little effect on the girders beneath the closed lane.

Table 4.12 gives the costs to rehabilitate the span. The unit area costs were $\$428/m^2$ or $\$39/ft^2$.

Table 4.12: Construction Cost (Canadian Dollars) Using CFRP Sheets

Item	Span Cost, $	Bridge Cost, $
Man Power	7,500	22,750
CFRP Materials	11,000	33,000
Traffic Control	3,500	7,000
Miscellaneous	4,000	8,000
Total Cost	26,000	70,500

If the whole bridge had been strengthened, a reduction in CFRP material cost may have been realized. Further, if traffic control had been eliminated and the CFRP reinforcement reduced to a minimum, the total cost for this bridge could have been around $50,000. In comparison, an alternative method using external steel stirrups would put the cost at about $100,000 *(Alexander and Cheng, 1996)*. That method would require closing the bridge for one month, removing the bridge deck, coring through the girder flanges, placing the stirrups, and replacing the bridge deck.

The study concluded that for issues such as simplicity of construction, convenience to users, and total cost of rehabilitation, the CFRP method is superior to the steel rehabilitation method.

4.8.2 United States

Rehabilitation of the T-beams of a concrete bridge using externally bonded FRP laminates was performed in rural Alabama *(Tedesco et al, 1996)*. The structure consisted of thirteen 10.34 m, simple spans. Each span had four reinforced concrete T-beams, all of which exhibited significant flexural cracking due to truck load traffic over 30 years.

The concrete surfaces were prepared by leveling with power grinders, roughening by sandblasting and pressure washing to remove any remaining dust and dirt which might adversely

affect bonding. The surfaces of the concrete and the FRP laminates were cleaned with methyl ethyl ketone immediately before application.

Three CFRP laminates 3.4 m long, 266 mm wide, and 1 mm thick were installed on the bottom of each beam. The CFRP laminates had an elastic modulus of 125 GPa and a tensile strength of 1200 MPa. GFRP laminates 3.4 m long, 356 mm wide and 1 mm thick were installed on the sides of the beam stems. The laminates had an elastic modulus of 21 GPa and a tensile strength of 450 MPa. Splice plates of 0.9 m were used to maintain structural continuity in the CFRP and GFRP laminates.

The bridge response was quantified by measuring the vertical deflections and strains in the primary flexural reinforcement, concrete, and on the surface of the FRP laminates before and after strengthening. Measurements were made under static and dynamic loading conditions using a three-axle truck with a gross vehicle weight of 381 kN (85,000 # on three axles). The length between the front and rear axles was 7.1 m.

The girders had a 10% reduction in midspan deflection and similar decreases in rebar stress. Periodic monitoring has shown continued integrity of the bond between the concrete and FRP laminates, as well as improved overall serviceability.

4.8.3 Japan

Of all countries, Japan has the largest number of field applications in strengthening concrete beams with FRP materials *(Nanni, 1995)*. Two petrochemical companies, Tonen and Mitsubishi Chemical, have literature describing design guidelines, construction, and field applications (Tonen, 1994; Mitsubishi Chemical, 1994).

Research in Japan has centered on the strength and ductility enhancement capabilities of FRP strengthened systems. Nanni *(1995)* describes several field applications of externally bonded FRP reinforcement. These projects used commercially available products, such as Forca Tow Sheet supplied by Tonen Corporation and Replark by Mitsubishi. Forca Tow Sheet uses dry type carbon fibers and is available in three grades, 3.9 to 5.9 kN/cm (2.2 to 3.4 kip/in.) tensile strength, and 259 to 627 kN/cm (148 to 358 kip/in.) tensile modulus. Mitsubishi's Replark is a prepreg offered in two grades, 3.4 to 5.8 kN/cm (1.9 to 3.3 kip/in.) tensile strength and 240 kN/cm (137 kip/in.) tensile modulus. The thicknesses of both products are in the 1 to 3 mm (0.04 to 0.12 in.) range.

The retrofit projects included strengthening to increase the load rating of the structure (Hiyoshikura Bridge, Tokando Highway), arresting steel reinforcement corrosion with rehabilitation (Wakayama, Central Japan) and strengthening to accommodate larger windbreak walls (Hata Bridge, Southern Japan). In all cases a 30 to 40 percent reduction of tensile strains in the steel reinforcement was confirmed.

The basic steps used in most of the retrofitting projects in Japan were concrete surface preparation such as cleaning and crack sealing, rust proofing existing steel reinforcement, smoothing (grouting), application of prime coat, application of resin undercoat; attachment of the FRP sheets, curing, and application of finish coats *(Nanni, 1995)*.

4.8.4 Europe

Numerous projects involving FRP bridge strengthening were successfully completed in Europe. A commercial project took place in Italy during the second half of 1997 to strengthen highway bridge girders near Terracina, Rome *(Nanni, 1997)*. The objective of the project was to compensate for the loss of prestressing caused by corrosion of the strand. Replark, Mitsubishi Chemical's CFRP material system, was adopted for the project. The repair sequence included removal of the deteriorated materials, restoration of the original cross section of the concrete with no-shrinkage mortar, protection of the steel reinforcement with a passivating coat, surface preparation, application of the FRP sheets, and a finish coat. Three sheets with 0 degree fiber orientation, 0.33 m wide and 3 m long, were bonded to the bottom of the beams. Additionally, four strips with 90 degree fiber orientation, 0.16 m wide and 3.0 m long, were wrapped around the sides and bottom of the beams.

The 228-meter long Ibach bridge, located in Lucerne, Switzerland was the first structure in the world strengthened with CFRP. The structure's prestressing tendons were accidentally damaged during installation of new traffic signals *(Meier et al, 1992)*. Repair using CFRP plates was completed in three nights and the bridge remained open to traffic during the entire work.

The bridge was repaired with three CFRP sheets per beam. Each sheet was 5 m x 150 mm x 1.75 mm, with a fiber content of 55 percent, axial Young's modulus of 129 GPa, and a axial tensile strength of 1900 MPa *(Meier and Deuring, 1991)*. A loading test with a 840 kN vehicle demonstrated that rehabilitation was very satisfactory. The repair work of the Ibach Bridge is an excellent demonstration of the simplicity and cost effectiveness of advanced composite materials for bridge repair.

Although the CFRP materials used in this project were approximately fifty times more expensive per kilogram, and nine times more expensive by volume than steel, the unquestionably superior properties of the CFRP plates justify their higher price *(Meier and Deuring, 1991)*. The repair would have required 175 kg of steel and only 6.2 kg of CFRP was used. Additionally, the repair work was carried out from a mobile platform, thus eliminating the need for scaffolding and closing traffic. Furthermore, material cost was only 20% of the total. Ease of handling strongly reduced the labor price as well. Thus, the high price of the CRFP does not seem outrageous.

The Technical University of Braunschweig, Germany, directed the strengthening of the Kattenbusch Bridge *(Rostasy, et al, 1992)*. The bridge is a continuous post-tensioned double box girder structure with eleven 36.5 m spans that had wide cracks at the joints. The cracks had broken through the bottom of the box and reached the webs of the girders. The main cause of the cracks was the temperature restraint in the summer, which was not considered in the design. As a result, an abrupt increase of the dynamic steel stresses with increased temperature was observed. Hence, additional reinforcement to control the crack width and to reduce the dynamic steel stresses was necessary. The work was performed in 1987.

Composite strengthening was selected as the means to increase the stiffness of the bottom slab. Ten mm thick GFRP plates were glued to the concrete members with adhesives commonly used for bonding of steel plates to concrete (see Table 6.1). Ninety-five percent of the fibers in the laminate were unidirectionally oriented, and the fiber content was 51 percent. The laminate had

a Young's modulus of 39 GPa, and a tensile strength of 700 MPa. In addition to laboratory tests, load tests of the bridge before and after strengthening were performed with 22-ton trucks. Figure 4.15 shows the measured reduction of stress by external strengthening in the lowest tendons. The maximum stress change was between 20 and 30 MPa. The bridge functions perfectly today *(Rostasy et al, 1992)*.

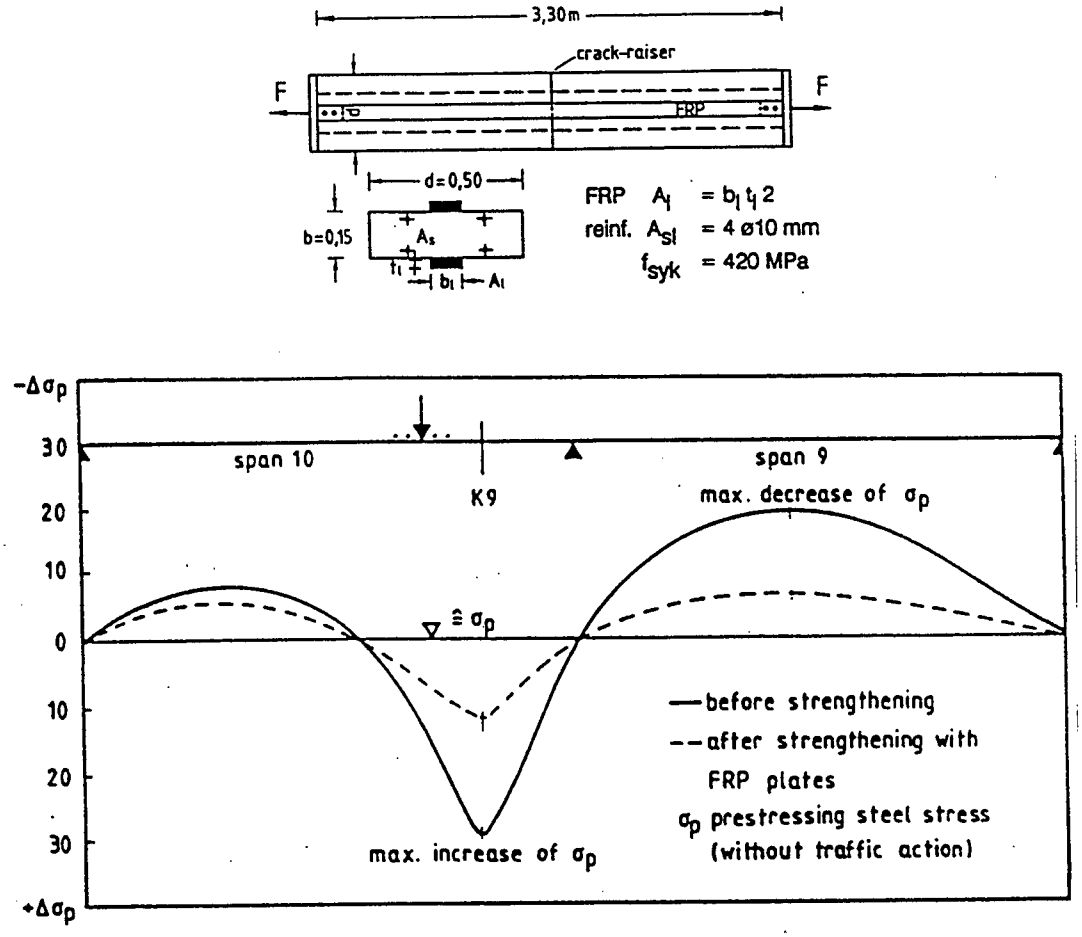

Figure 4.15: Measured Stress Reduction Due to GFRP Lamination
(Rostasy et al, 1992)

4.9 SUMMARY

Much of the material in this chapter relates to taking composite strengthened reinforced concrete elements to failure. This information is very important to researchers who will be studying the failure mechanisms of composite reinforced structural elements. It will have less relevance for designers in the bridge strengthening community. Their primary concern will be how well the composite strengthened elements perform when loads on the elements are significantly below ultimate. Thus, the key advantages of FRP composites, for future designers, will be:

- advanced composite materials to reinforce concrete beams offer strength and shear enhancement significantly beyond that of traditional materials;
- they are lighter and easier to handle;
- composites have excellent corrosion resistance;
- their very low chemical reactivity;
- ability to custom design the composite's properties by varying the type, orientation and volume concentration of fibers;
- ability to easily control the number and orientation of layers for each individual application.

A perceived disadvantage in using these materials is their cost. Costs will decrease as the industrial demand increases. Even today, if costs are based on the total project rather than on materials cost, composites can be very competitive.

Other concerns, not directly covered in the preceding sections are resistance to UV and microbial degradation.

The following variables influence the response of FRP laminate bonded beams:

- size of the beam;
- thickness and area of the FRP composite;
- type of adhesive;
- type of composite;
- type of loading (static or dynamic);
- under- or over-reinforced beam;
- crack or non-cracked beams before plate bonding;
- prestressed or non-stressed main reinforcement;
- action of corrosion;
- weather;
- age.

The following sequence can be assumed to occur during static loading of FRP reinforced beams:

1) Elastic response predominates until tensile cracking of the beam occurs. At this point the neutral axis shifts upward and is accompanied by a change of the load-displacement curve.
2) After tensile cracking occurs, the beam remains elastic, the load is shifted to the concrete compression area, and the FRP holds the cracked concrete in place.
3) At maximum load bond failure usually occurs and the beam collapses.

Beams strengthened with very stiff FRP plates (6 mm and greater) exhibit a brittle failure mechanism, usually observed at the end of the linear elastic range. A large increase in stiffness is obtained by using thick plates. However, the fibers are underutilized and are subjected to very low stress, 1/7 to 1/4 of ultimate.

For beams strengthened to intermediate stiffness, the cracks localize at the end of the plates. In these cases, shear failure is typically observed.

Beams that are reinforced with thin glass plates exhibit ductile behavior. The first stiffness reduction typically occurs due concrete cracking in the tensile zone followed by shear cracking at the plate ends.

Adhesive selection is critical to good performance because it is responsible for the stress transfer from the concrete to the reinforcing materials. Some properties of good adhesives are:

- Proper viscosity – entrained and entrapped air must be minimized during the mixing and bonding phase;
- Rapid polymerization time to minimize the repair time and reduce the chance of being weakened by vibration or flexure during cure;
- Good adhesion to both the concrete and FRP plates.

4.10 DESIGN EXAMPLES

4.10.1 Flexural Design – Calculation of FRP Strengthened Beam Bending Resistance

Currently there are no design procedures for external reinforcement with FRP composites. In the near future ACI Committee 440 will provide engineers with guidelines for strengthening concrete structures with FRP composites. Until then, each designer must conduct his or her own review of the design concepts.

The design examples provided herein follow a logical step-by-step process based on conventional reinforced concrete design. Appropriate assumptions regarding FRP allowable strains and stresses are an integral part of the design process. Although the design follows the ACI fundamentals and European experience, additional knowledge is needed for success. These topics include, but are not limited to, the following:

- Composite behavior near ultimate loads;
- Brittle versus ductile failure modes;
- Strength loss due to elevated or low temperatures of the adhesive;
- Creep of GFRP laminates; and
- Thermal compatibility between FRP composites and concrete.

The procedures are provided only for illustration of the material presented in this chapter and cannot be regarded as a working guideline for the strengthening of concrete members with FRP laminates.

Typically, conventionally reinforced beams are designed so that concrete failure occurs when the yield point of steel is reached. The failure is normally preceded by crack formations and large deflections. By controlling the reinforcing ratio, undesired brittle modes of failure can be prevented.

The ultimate strength of a beam strengthened with FRP laminates cannot be calculated the same way, because the behavior of the composite materials is linear-elastic to failure and they do not have a plastic deformation reserve. Thus, the maximum bending resistance of the hybrid concrete-steel-FRP section is typically reached when the laminate failure occurs and before the concrete failure.

The calculation of bending resistance is based on the following assumptions, which also apply to conventionally reinforced concrete sections:

- Idealized stress-strain diagram for concrete, steel and FRP laminate;
- The tensile resistance of concrete is neglected;
- The strains are distributed across the section height proportionally to the distance from the neutral axis;
- The position of the forces and the neutral axis remains constant;
- Due to external influences, the ratios of maximum to medium strains are described by the composite factors K_L and K_S, for the FRP and steel reinforcement, respectively.

Figure 4.16 shows the forces used for calculation of the ultimate moment M_R on the rectangular cross-section.

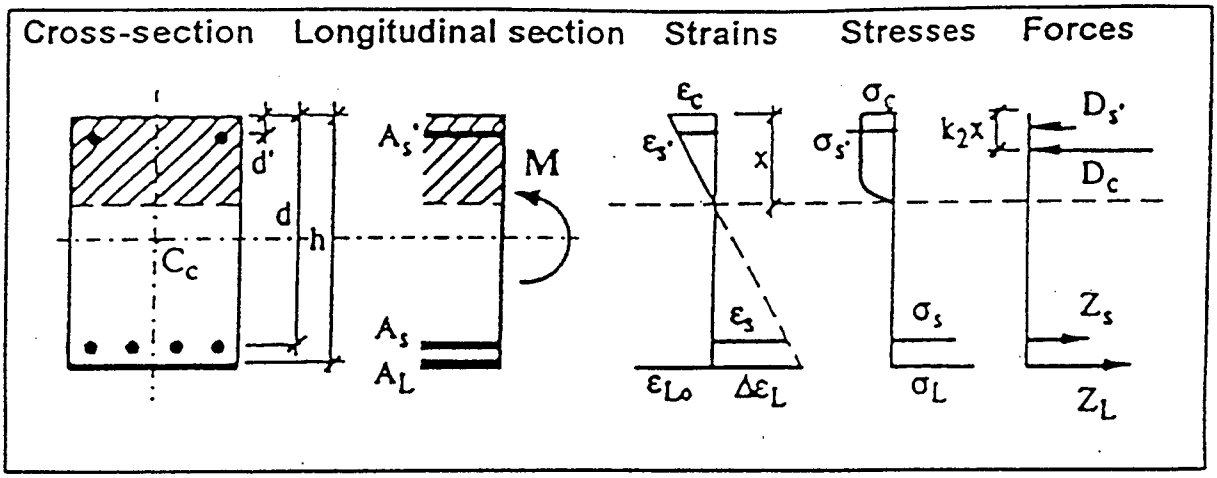

Figure 4.16: Rectangular Beam Cross-Section: Calculation of the Ultimate Moment of Resistance

4.10.1.1 *Design Based on the European Experience and Design Codes*

4.10.1.1.1 Assumptions

- The governing failure mode is rupture of the laminate;
- The steel reinforcement has yielded before FRP rupture.

4.10.1.1.2 Equilibrium Conditions

$$\Sigma Z = 0 \Rightarrow Z_L + Z_S - D_C = 0 \qquad \text{and} \tag{4-1}$$

$$\Sigma M = 0 \Rightarrow M_R - Z_L(h - k_2 c) - Z_S(d - k_2 c) = 0 \tag{4-2}$$

where: $D_C = k_1 b c f_c'$

4.10.1.1.3 Determination of k_1 and k_2 Coefficients

For extreme fiber concrete strain $\varepsilon_c < 0.2\%$, k_1 and k_2 are determined as follows:

$$k_1 = \frac{1000\left(-500\varepsilon_c^{\,2} + 3\varepsilon_c^{\,2}\right)}{6} \tag{4-3}$$

$$k_2 = \frac{1-(4-750\varepsilon_c)}{(6-1000\varepsilon_c)} \tag{4-4}$$

For extreme fiber concrete strain $0.2\% < \varepsilon_c < 0.3\%$, k_1 and k_2 are determined as follows:

$$k_1 = 1 - \frac{1}{1500\varepsilon_c} \tag{4-5}$$

$$k_2 = 1 - \frac{0.5 - \left(3*10^6 \varepsilon_c\right)^{-1}}{1 + \left(-1500\varepsilon_c\right)^{-1}} \tag{4-6}$$

4.10.1.1.4 Location of the Neutral Axis of the Cross Section

$$\varepsilon_c = \frac{k_L(\varepsilon_{LU})c}{h-c} \tag{4-7}$$

$$c = \frac{f_{LU}A_l + f_Y A_S}{k_1 b f_c'} \tag{4-8}$$

Note that the concrete strain is expressed as a function of the laminate strain and the distance to the neutral axis.

4.10.1.1.5 Calculate M_R

Since the magnitude of the concrete strain is not known, use both expressions for k_1. Then, the concrete strains based on both models are found, and the appropriate mathematical model is identified and used to calculate k_2 and the ultimate moment capacity.

$$M_R = Z_S(d-k_2c) + Z_L(h-k_2c), \text{ or} \quad \textbf{(4-9)}$$

$$M_R = f_{LU} A_L(h-k_2c) + f_Y A_S(d-k_2c) \quad \textbf{(4-10)}$$

4.10.1.1.6 Check the Average Strains at Failure

Once the ultimate moment capacity is determined, all the underlying assumptions need to be checked. This includes a check to confirm that the concrete is not stressed beyond its crushing limits (ε_c is less than 0.003), and verify that steel has yielded, but did not fracture.

4.10.1.1.6.1 Bond Coefficients k_L and k_S

$0.65 \le k_L \le 0.80$ (typically 0.70)

$0.90 \le k_S \le 1.00$ (typically 0.90)

4.10.1.1.6.2 Strains in the FRP Laminate

$$\Delta\varepsilon_{Lm} = k_L \Delta\varepsilon_{Lmax} = k_L \varepsilon_{LU} \Rightarrow \sigma^L{}_{max} = \sigma^L{}_{ult} \quad \textbf{(4-11)}$$

4.10.1.1.6.3 Strains in the Steel reinforcement

$$\Delta\varepsilon_{Sm} = k_S \Delta\varepsilon_{Smax} \Rightarrow \sigma^S{}_{max} > \sigma^S{}_y \quad \textbf{(4-12)}$$

$$\varepsilon_{Sy} < \varepsilon_{S\,max} = \frac{\varepsilon_S}{k_s} \Rightarrow \varepsilon_S = \frac{\Delta\varepsilon_{Lm}(d-c)}{h-c} \quad \textbf{(4-13)}$$

4.10.1.1.6.4 Strain in Concrete

$$\varepsilon_c = \frac{\Delta\varepsilon_{Lm} c}{h-c} \quad \textbf{(4-14)}$$

where $\varepsilon_c < 0.003$

4.10.1.2 Numerical Example

The figure below illustrates the geometry of the beam and the position of the reinforcement.

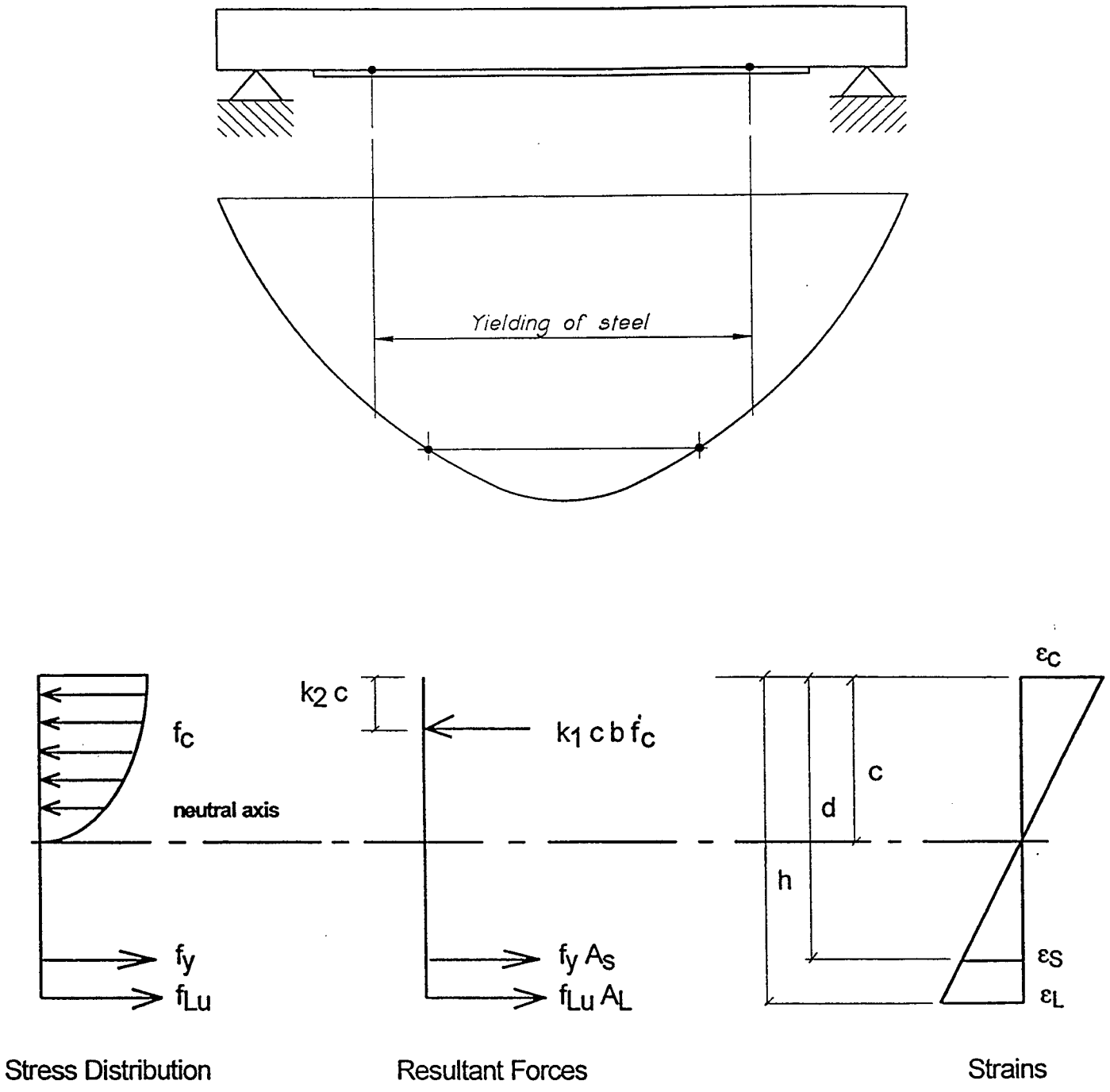

Figure 4.17: Beam Cross Section, Numerical Example

4.10.1.2.1 Design Goal

Provide additional moment capacity and stiffness on the existing reinforced concrete beam.

4.10.1.2.2 Reinforcement Details and Assumptions

4.10.1.2.2.1 Concrete Section

f_c'= 4,000 psi
b=6 in.
h=6 in.
d= 3.81 in.

4.10.1.2.2.2 Steel Reinforcement

A_S=0.11 in^2 (one No.3 steel rebar A60)
d_S=0.375 in.
fy=36 ksi
ε^{max}_S =0.12%

4.10.1.2.2.3 FRP Reinforcement

f_{Lult}=348 ksi
ε^{ult}_L =1.4%
f_{Lmax}=240 ksi (design value)
ε^{max}_L =0.98%
b_L=5 in.
t_L= 0.004 in.
A_L=0.02 in^2

4.10.1.2.2.4 Determination of the Concrete Strain

Solve the following system of equations:

$$\varepsilon_c = \frac{\varepsilon_{Lult} c}{h - c}, \text{ and}$$

$$c = \frac{f_{LU} A_l + f_Y A_S}{k_1 b f_c'}$$

- Case One: $\varepsilon c < 0.002$

$$\varepsilon_c = \frac{\dfrac{\varepsilon_{Lult}\left(f_{Lult}A_L + f_yA_S\right)}{\dfrac{1000}{6}\left(-500\varepsilon_c^2 + 3\varepsilon_c^2\right)bf_c'}}{h - \dfrac{\left(f_{Lult}A_L + f_yA_S\right)}{\dfrac{1000}{6}\left(-500\varepsilon_c^2 + 3\varepsilon_c^2\right)bf_c'}}$$

Based on the initial assumptions for all variables included in the above equation,

$\varepsilon_c = -1.146*10^{-3}$ in/in. Use $\varepsilon_c = 0.0012$ in/in.

After substitution, $k_2 = 0.354$ and $k_1 = 0.48$.

Position of the neutral axis: c = 0.76 in.

Check Strains: Check to confirm that the concrete has not been stressed beyond its crushing point, and steel yielded, but did not fracture.

$$\varepsilon_c = \frac{\varepsilon_{Lult}c}{h-c} = \frac{(0.014)(0.76in)}{6in - 0.76in} = 0.002 \text{ in/in.} < 0.003 \Rightarrow \text{O.K.}$$

$$\varepsilon_S = \frac{\varepsilon_{Lm}(d-c)}{h-c} = \frac{(0.014)(3.81in - 0.76in)}{6in - 0.76in} = 0.008 \text{ in/in.} \Rightarrow \text{O.K.}$$

- Case Two: $0.002 < \varepsilon_c < 0.003$

$\varepsilon_c = 0$

This case is not applicable for the selected beam geometry, reinforcement quantity, FRP thickness, and material properties of concrete, steel and FRP.

4.10.1.2.2.5 Maximum Bending Resistance

$M_R = f_{LU}\, A_L(h-k_2c) + f_Y\, A_S(d-k_2c) =$
$[6-(0.354)(0.76 \text{ in.})](0.02 \text{ in}^2)(240 \text{ ksi}) +$
$[(3.81 \text{ in.})-(0.354)(0.76 \text{ in.})](0.11 \text{ in}^2)(36 \text{ ksi})$

$M_R = 27.5 + 14 = 41.53$ kips-in $= 3.5$ kips-ft

4.10.1.2.2.6 Strengthening Ratio

$$M_R^{str} / M_R^{unstr} = 1.7$$

4.10.1.3 The ACI Based Design of FRP Strengthened RC Beam

4.10.1.3.1 Assumptions

The assumptions are the same as in the European code-based design plus the following:

4.10.1.3.1.1 Concrete and Steel Reinforcement

$E_S = 29{,}000$ ksi
$\varepsilon_{Sy} = 0.002$ in/in.
$f^{ult}_{SY} = 60$ ksi

4.10.1.3.1.2 FRP Laminate

$E_L = 22{,}500$ ksi

The retrofit is based on 80% of the bottom face (5 in.) covered with one layer of CFRP.

$$A_L = 0.8bt_L = (0.8)(6 \text{ in.})(0.004 \text{ in.}) = 0.0192 \text{ in}^2$$

4.10.1.3.1.3 FRP Position Below the Bottom of the Beam

$y_L = -0.004$ in

4.10.1.3.1.4 Equilibrium Conditions

$$T=C \Rightarrow f^{ult}_{SY} A_S + f_L A_L = (0.85)(f_c')(a)(b)$$

where a = compression zone depth (in.)

$$(0.11 \text{ in}^2)(36 \text{ ksi})+(0.0192 \text{ in}^2)(22{,}500 \text{ ksi})(0.014) = (0.85)(4 \text{ ksi})(a)(6 \text{ in.})$$

$$a = 0.62 \text{ in.}$$

$c = a / \beta = 0.73$ in. (β=0.85 for $f_c' < 4000$ psi)

4.10.1.3.1.5 Calculate the Concrete Strain Based on the Ultimate Fiber Strain

$$\varepsilon_c^{ult} = \frac{\varepsilon_{Lult} c}{h-c} = \frac{(0.014)(0.73\,\text{in.})}{(6\,\text{in.} - 0.73\,\text{in.})} = 00194 \text{ in/in. } < 0.003 \Rightarrow \text{O.K.}$$

4.10.1.3.1.6 Moment Capacity Provided by the CFRP Laminate

$M_R = \phi M_n = \phi[A_L f_L (d_L - a/2)]$

Where $d_L = h + t_L = 6 + 0.004 = 6.004$ in.

$\phi M_n = (0.9)(0.0192 \text{ in.})(22{,}500 \text{ ksi})(0.014)(6.004 \text{ in.} - 0.31 \text{ in.})$
$\phi M_n = 31$ kips-in $= 2.6$ kips-ft

4.10.1.3.1.7 Serviceability and Deflections

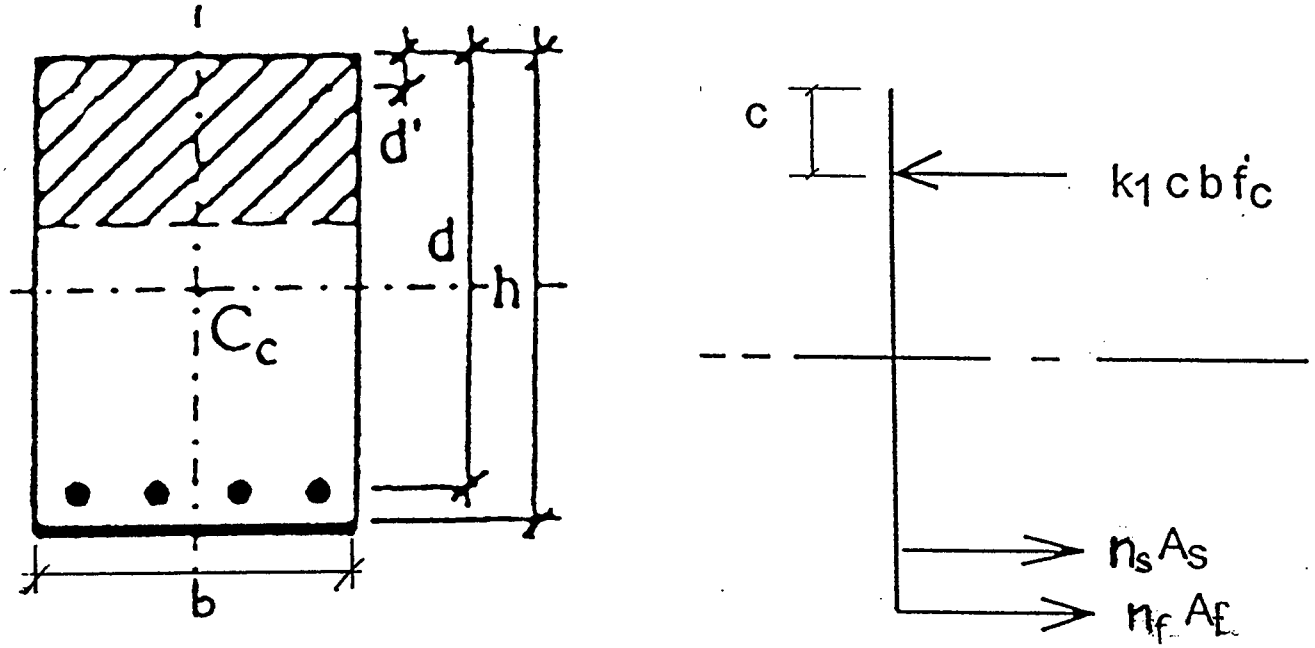

Figure 4.18: Beam Cross Section, Serviceability and Deflections

Calculations of the transformed moments of inertia are based on the modular ratios with respect to the concrete modulus.

$$E_c = 57{,}000\sqrt{f_c'} = 57{,}000\sqrt{4000} = 3605 \text{ ksi}$$

$$n_S = \frac{E_S}{E_c} = \frac{29000}{3605} = 8.04$$

$$n_L = \frac{E_L}{E_c} = \frac{22500}{3605} = 6.24$$

Table 4.13: Transformed Moments of Inertia Calculations

	n_iA_i (in^2)	y_i (in)	$n_iA_iy_i$	y_i (in)-calc.	$I=bc^3/12$ (in^4)	$n_iA_i^2$ (in^4)
Concrete	6(c)	c/2	$3c^2$	0.506	0.518	1.555
Steel	(8.04)(0.11)	c-d= c-3.81	0.8844c-3.37	-2.80	–	6.934
CFRP	(6.24)(0.0192)	c-h=c-6.004	0.12c-0.72	-4.992	–	2.986

$\Sigma I + Ay^2 = 11.993 \cong \underline{12 \text{ in}^4}$

4.10.1.3.1.8 Determine the Position of the Neutral Axis

By definition, the position of the neutral axis is the distance to the centroid when $\Sigma A_i y_i = 0$

$$3c^2 + 0.8844c - 3.37 + 0.12c - 0.72 = 0$$

$$3c^2 + 1.0044c - 4.09 = 0$$

$$c = 1.012 \text{ in.}$$

4.10.1.3.1.9 Calculate the Midspan Deflection

Calculations are based on the moment of inertia (Σ I), and the maximum moment capacity of the beam ($M_R = \phi M_n$).

$$\Delta_{CL} = \frac{\frac{5}{48}\sum M_R L_{CLR}^{\ 2}}{E_c I}$$

where:

L_{CLR} – beam length, (in.)

For this example: $L_{CLR} = 21$ in.

$$\Delta_{CL} = \frac{\frac{5}{48}(31.3kips - in)(21in)^2}{(3605ksi)(12in^4)}$$

$$\Delta_{CL} = 0.0332 \text{ in.}$$

4.10.2 Shear Strength Enhancement of RC Beams Using FRP Laminates

The most important feature for proper shear design using FRP materials, whether glass or carbon, is the strain compatibility between the composite laminate and the concrete. Rational shear strengthening designs are limited to 0.4% due to strain issues. This strain limitation is due to concrete limitations and it is independent of FRP material type.

The design example outlined in this chapter is strain based design. They are other possible approaches, based on ultimate strength and strain values which will result in different and sometimes uncertain failure modes. The strain based design approach is conservative compared to the other approaches, but it can be performed easily and does not require advanced knowledge in composite materials mechanics and behavior.

The shear strengthening design procedure is provided only for illustration and cannot be regarded as a woking guideline for strengthening of concrete members with FRP laminates.

4.10.2.1 Necessary Assumptions

f_{Lj} – Allowable jacket stress, (ksi)
E_j – Elastic modulus of FRP jacket (ksi)
ε_{uj} – Allowable jacket stress for shear (ksi)
t_j – FRP jacket thickness (in.)
f_{ty} – Transverse steel tensile strength (ksi)
L_{clr} – Beam clear length (in.)

4.10.2.2 Check Existing Shear Capacity

If steel shear reinforcement is provided:

$$V_{cap} = \frac{A_v f_{ty} d}{s} \quad \textbf{(4-15)}$$

If no shear reinforcement is provided

$$V_{cap} = 2\sqrt{f'_c} bd \quad \textbf{(4-16)}$$

4.10.2.3 *Calculate Needed Shear Capacity*

$$V_{cap} = \frac{A_v f_{ty} d}{s'} \tag{4-17}$$

where:

s' – new shear reinforcement spacing (in.)

4.10.2.4 *Calculate Shear Capacity Shortfall*

$$V_{Sj} = V_S - V_{cap} \tag{4-18}$$

4.10.2.5 *Calculate the Required FRP Jacket Thickness*

$$t_j > \frac{V_{Sj}}{2 f_{Lj} d(\cot 45)} \tag{4-19}$$

45 degree shear crack inclination has been assumed.

4.10.2.6 *Required Bond Length Development*

The development length is needed to prevent shear rupture of concrete. The concrete bond stress is limited to 200 psi. Development length must be provided beyond the point determined to carry the tensile force.

$$\sigma_b = \frac{T_L}{A_b} \tag{4-20}$$

$$A_b = (b_L)(l_d) \tag{4-21}$$

$$E_w = E_L(t_j) \tag{4-22}$$

$$T_L = E_w(b_L)(0.004) = E_L t_L(b_j)(0.004) \tag{4-23}$$

where 0.004 is the concrete strain limit

4.10.2.7 Numerical Example

4.10.2.7.1 Assumptions

6in. x 6in. concrete beam with no shear reinforcement provided
d = 3.81 in.
ε_{uj} = 0.004 in/in.
E_{uj} = 22,500 ksi
f^{ult}_L = 240 ksi
t_L = 0.004 in.
L_{clr} = 21 in.

4.10.2.7.2 Calculate the Allowable FRP Jacket Stress

$$f_{Lj} = \frac{f^{ult}{}_L \varepsilon_{uj}}{\varepsilon^{ult}{}_L} = \frac{(240ksi)(0.004in/in)}{0.014in/in} = 68 \text{ ksi}$$

4.10.2.7.3 Check Shear Capacity

$$V_{cap} = V_c = 2\sqrt{f'_c}bd = 2\sqrt{4000psi}(6in.)(3.81in.) = 2.89 \text{ kips}$$

Since no shear reinforcement is provided, ACI Code Section 11.5.5.1 requires that the maximum allowable shear force is:

$$\text{Max.}V_U = 0.5\ \phi\ V_c = (0.5)(0.85)(2.89\text{kips}) = 1.23 \text{ kips}$$

4.10.2.7.4 Calculate the Needed Shear Capacity

Since the required shear force is not known in this example, it will be calculated based on the tensile resistance (capacity) of the beam. According to the theory:

$$0.707\ V + 0.707\ V = T$$

where:

V – shear force in the beam (kips)
T – tensile force in the beam (kips)

$$T = f^{ult}{}_{SY}\ A_S + f^{ult}{}_L\ A_L$$
$$= (0.11\ in^2)(60\ ksi) + (0.02\ in^2)(240\ ksi) = 11.4 \text{ kips}$$

Thus: $V_S = 11.4 / 1.414 = 8.06$ kips (use 8.1 kips)

4.10.2.7.5 Calculate Shear Capacity Shortfall

$V_{Sj} = V_S - V_{cap} = 8.1 - 2.89 = 5.21$ kips

4.10.2.7.6 Calculate the Required FRP Jacket Thickness

$$t_j > \frac{V_{Sj}}{2f_{Lj}d(\cot 45)} = \frac{5.21}{2(68ksi)(3.81in.)(1.0)}$$

$t_j > 0.01$ in

Individual layer thickness t_L = 0.004 in. The required number of layers is 2.5. Use three layers.

Note: The beam was first strengthened for flexure and then for shear. The calculation of the maximum tensile force included the flexure capacity of CFRP laminate 0.004 in. thick applied to the tensile face of the beam. This explains the large quantity of shear reinforcement needed in this example.

4.10.2.7.7 Required Bond Length Development

$$\sigma_b = \frac{T_L}{A_b}$$

$E_w = E_L\, t_j$

$T_L = E_w\, b_L\, (0.004) = E_L t_j\, b_L\, (0.004)$

where 0.004 is the concrete strain limit

$\sigma_b = 200$ psi

$$0.2 \text{ ksi} = \frac{(22500 \text{ ksi})(0.01 \text{ in.})\,(5 \text{ in.})\,(0.004)}{(5 \text{ in.})(l_d)}$$

$l_d = 4.5$ in.

4.10.3 List of Variables

a compression zone depth (in.)
A_b bond area of FRP laminate (in^2)
A_L cross-section area of FRP laminate (in^2)
A_S cross-section area of tension steel reinforcement (in^2)
b width of the concrete section (in.)
b_L width of the FRP laminate (in.)
c distance from the top of the section to the neutral axis (in.)
C resultant compressive force in the cross section (kips)
d effective depth of the concrete section (in.)
D_c compressive force in concrete (kips)
d_s steel rebar diameter (in.)
E_c elastic modulus of concrete (ksi)
E_L elastic modulus of FRP laminate (ksi)
E_S elastic modulus of steel (ksi)
E_w FRP elastic modulus per unit width (kips/in. width)
f_c' concrete compressive strength (ksi)
f_{Lj} allocable jacket stress, (ksi)
f_{LU} (f_{Lult}) ultimate strength of FRP laminate (ksi)
f_{ty} transverse steel tensile strength (ksi)
f^{ult}_{sy} steel ultimate strength (ksi)
f_y steel yield strength (ksi)
h height of the concrete section (in.)
k_1 variable used to determine the magnitude of concrete compressive force
k_2 variable used to determine the location of concrete compressive force
k_L FRP bond coefficient
k_S steel bond coefficient
L_{CLR} beam length (in.)
l_d bond development length (in.)
M_n nominal moment capacity of the beam (kips-ft)
M_R maximum moment capacity of the beam (kips-ft)
s center-to-center spacing of the shear reinforcement (in.)
T resultant tensile force in the cross section (kips)
t_j FRP jacket thickness (in.)
t_L FRP laminate thickness (in.)
T_L tensile force provided at strain of 0.4% , limit for shear (kips/in.)
V_c shear resistance provided by the concrete (kips)
V_{cap} existing shear capacity of the beam (kips)
V_S needed (design) shear capacity of the beam (kips)
V_{Sj} shear reinforcement shortfall (kips)
Z_c compressive force in concrete (kips)
Z_L tensile force in FRP laminate (kips)
Z_S tensile force in steel (kips)

β reduction coefficient used to determine the position of the neutral axis
ϕ reduction factor
Δ_{CL} midspan deflection (in.)
σ_b bond stress of concrete (psi)
σ^L_{ult} ultimate stress of FRP laminate (psi)
σ^S_{max} ultimate stress of steel (psi)
ε_c strain in concrete (in/in.)
ε_L strain in FRP laminate(in/in.)
ε_{LU} ($\varepsilon^{max}_L = \varepsilon^{ult}_L$) strain in FRP laminate at ultimate stress (in/in.)
ε^{max}_S (ε^{ult}_S) ultimate strain in steel (in/in.)
ε_S strain in steel (in/in.)
ε_{uj} allowable jacket stress for shear (ksi)
ε^{ult}_c maximum allowable strain in concrete (in/in.)

5.0 EXTERNAL REINFORCEMENT OF CONCRETE COLUMNS USING FRP COMPOSITE MATERIALS

5.1 INTRODUCTION

Many concrete bridge columns designed before the new seismic design provisions were adopted in 1970 have low shear strength and low flexural strength and ductility. These problems, combined with environmental deterioration, have contributed to catastrophic bridge failures in resent earthquakes *(Cercone and Korff, 1997)*. Post earthquake analysis of the seven freeway bridges that collapsed during the Northridge earthquake revealed that they could have survived if they had been retrofitted to withstand seismic forces.

The work of some researchers has indicated that increasing the confinement in the potential plastic hinge regions of the column will increase the apparent concrete compressive strength and ductility *(Saadatmanesh and Ehsani, 1994)*. Therefore, strengthening techniques typically involve methods for increasing the confining forces either in the potential plastic hinge regions or over the entire column.

An unwrapped concrete column loaded in compression will fail by developing a crack network and shear cones in the column. In order to visualize the failure mechanism associated with confined concrete columns, it is important to think of the wrapped column as a system of concrete cores loaded in compression and concentrically wrapped with a tensile-loaded jacket. The existence of the jacket, which provides a high degree of confinement, can prevent or delay the initiation and propagation of the internal cracking mechanism.

Until recently, the steel jacketing of bridge columns was the only retrofitting method widely approved. This technique is effective in preventing columns from collapsing due to shear or flexural failure. However, installation is labor intensive, time consuming, and requires heavy equipment to handle the steel. Another problem is that the installation requirements rather than the confinement requirements determine the thickness and weight of the steel jackets. In order to prevent buckling under its own weight during lifting, the steel jacket has to be extremely heavy and strong. Thus, the resulting retrofit projects are typically expensive and use an excessive amount of material *(Cercone and Korff, 1997)*.

Advanced composite materials have unique mechanical and durability characteristics that complement column strengthening. Research by the Advanced Composites Technology Transfer Consortium (ACTT) at the University of California, San Diego (UCSD) has shown that seismically deficient bridge columns can be wrapped with FRP materials in an automated fashion, further reducing the time requirements as compared to equivalent steel jacket installations. Recent developments in automated manufacturing and application processes for FRP column wrapping has shown that this type of structural enhancement is cost effective *(Seible, et al, 1995)*.

5.2 COLUMNAR CONFINEMENT OF CONCRETE WITH ADVANCED COMPOSITE MATERIALS

Existing concrete column failure theories show that a small amount of columnar confinement will dramatically increase a column's strength and ductility *(Harmon and Slattery, 1992)*. This approach could be related to the use of spiral reinforcement in steel reinforced columns. The spiral reinforcement provides no additional strength to the concrete, but greatly increases the column's ductility. Since the concrete that covers the spiral reinforcement will spall before failure is reached, its contribution to the strength increase is insignificant.

FRP materials properties are best exploited when the application requires directional, tensional restraints. Together with the FRP's ability to conform to existing substrates, this makes them a very viable material for post columnar strengthening. Further, FRP reinforcement on the outside of a column requires no cover and is corrosion resistant.

Harmon and Slattery *(1992)* demonstrated the effectiveness of using CFRP on high strength concrete cylinders to create compression members with both high strength and high ductility. The CFRP wraps had a tensile strength and elastic modulus of 3500 MPa and 235 GPa, respectively, and were applied at various thicknesses to achieve different volumetric reinforcing ratios. Figure 5.1 shows the axial strain versus stress results from the study. The stress-strain curves were bilinear with a pseudo-yield stress higher than the failure stress of the unreinforced cylinders. As the reinforcing ratio increases, the ultimate failure stress increases significantly but has only a minor effect on the yield stress.

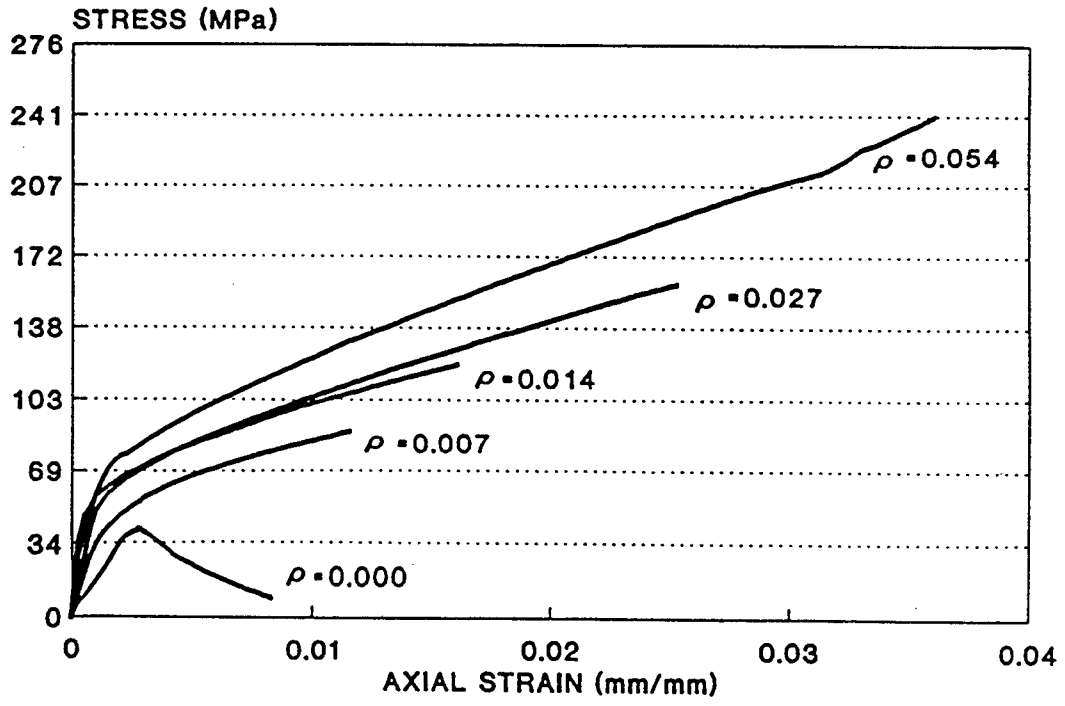

Figure 5.1: Stress vs. Axial Strain
(Harmon and Slattery, 1992)

Figure 5.2 shows the typical effect of cylinder confinement with FRP materials on the transverse strain. It can be seen that the circumferential strains increase dramatically after the failure stress of the unwrapped cylinder was reached. The circumferential transverse strains decreased as the circumferential reinforcement was increased.

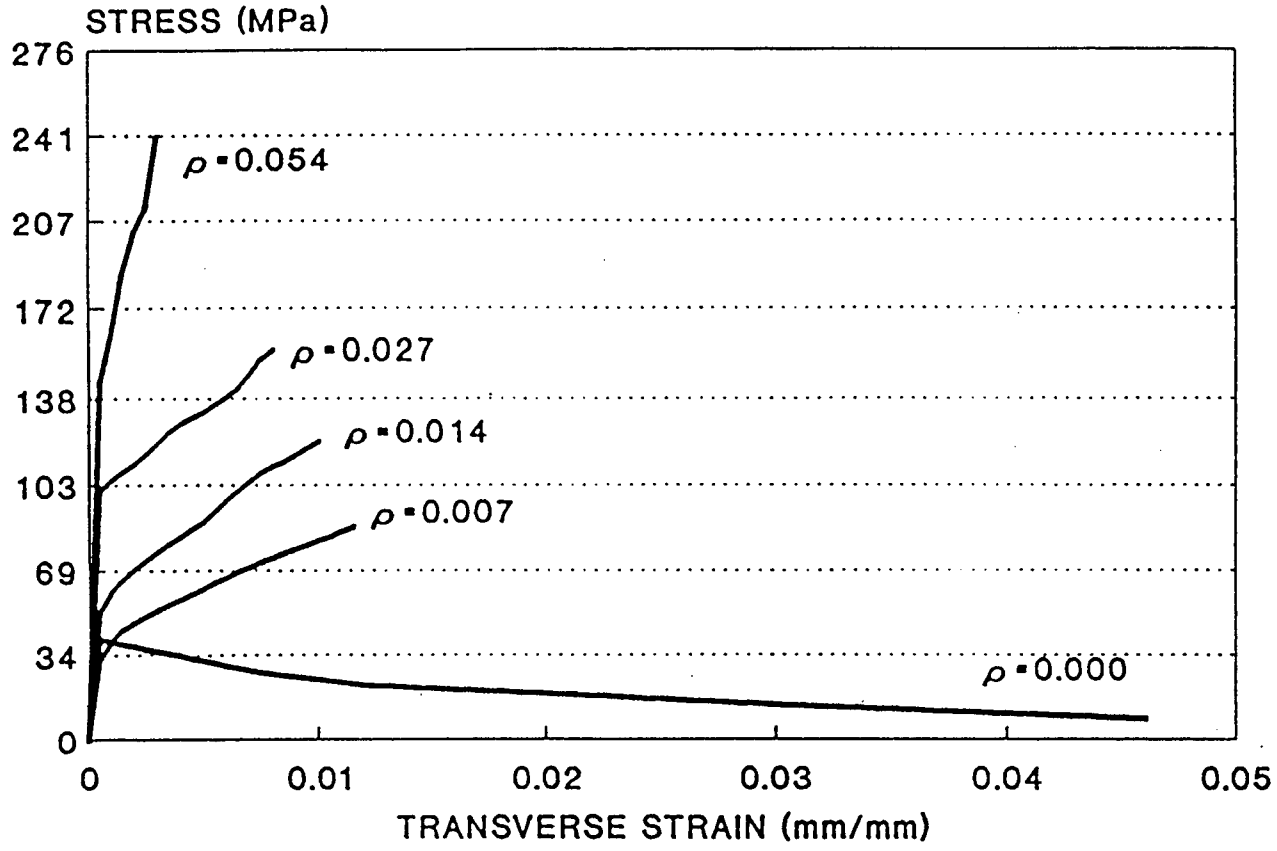

Figure 5.2: Stress vs. Transverse Strain
(Harmon and Slattery, 1992)

This study also showed that the benefit of concrete confinement with advanced FRP materials is roughly independent of the concrete's compressive strength (Figure 5.3). Other researchers studying the effect of concrete compressive strength on bond strength made similar observations *(Kachlakev, 1997; Lundy and Kachlakev, 1996)*. This phenomenon seems to be due the large differences in material properties and mechanical response between concrete and FRP composites. The failure stress of FRP reinforced cylinders increased approximately 40 MPa for each percent increase in the confinement reinforcing ratio.

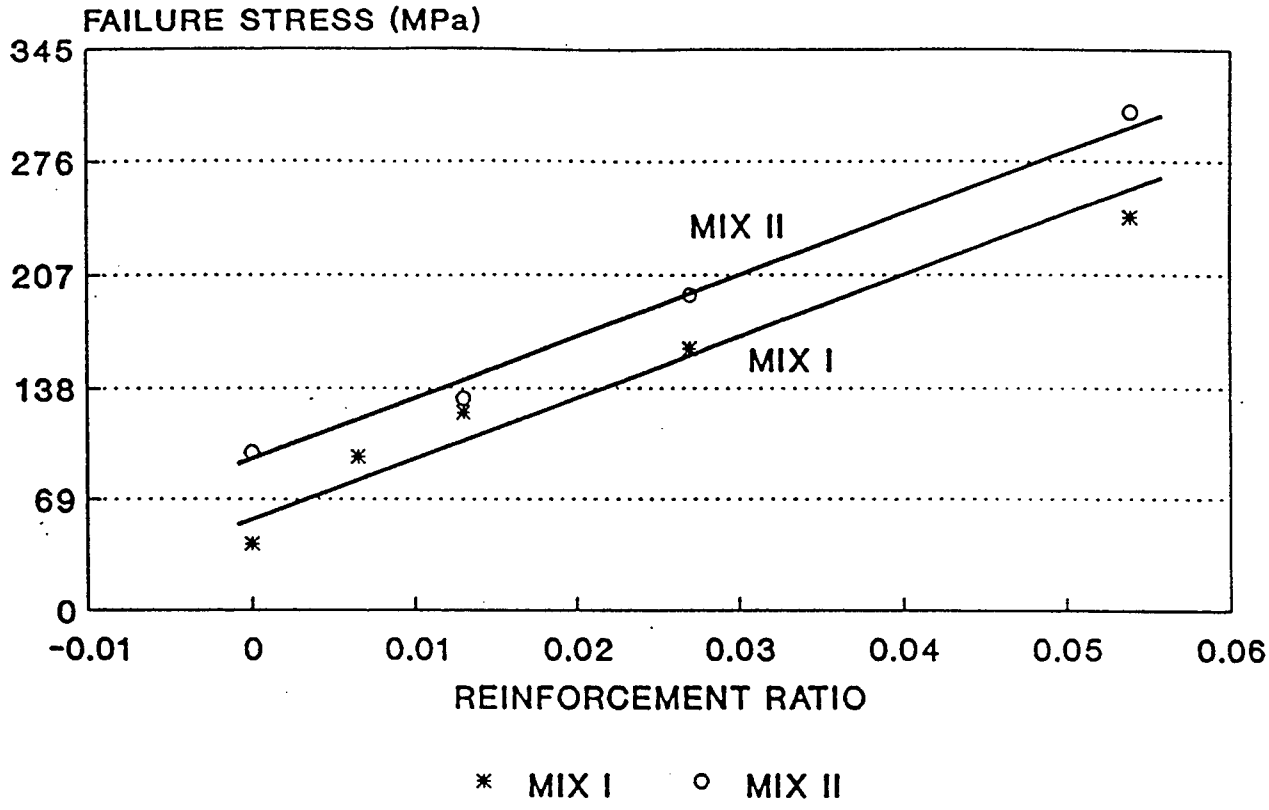

Figure 5.3: Failure Stress vs. Reinforcement Ratio
(Harmon and Slattery, 1992)

5.3 STRENGTHENING OF CONCRETE COLUMNS WITH EXTERNALLY APPLIED FRP – CASE STUDIES

5.3.1 California Department of Transportation (CALTRANS)

CALTRANS adopted the steel-jacket approach for retrofitting columns after the Whittier earthquake in 1987. It began by investigating the effects of steel jackets to increase the shear and flexural capacity of columns on the 5000 bridges that were in need of some form of replacement or retrofit. *(Cercone and Korff, 1997)* After the Loma Prieta earthquake in 1989, the column-retrofit program was accelerated.

Recently, CALTRANS approved a few mechanically and hand-applied fiberglass techniques as viable alternatives to standard steel jacketing *(Cercone and Korff, 1997)*. By writing specifications focused on the end results, CALTRANS left it to the industry to find the most efficient ways of achieving the desired goals.

5.3.2 University of California, San Diego (UCSD)

A high-strength fiber/epoxy column wrapping system, developed by Hexcel Fyfe Company, Del Mar, California, has been tested at UCSD *(Fyfe, 1994)*. Five full-scale columns were evaluated for flexural and shear performance. Three of the specimens were circular, 2 ft diameter by 12 ft high columns, and the other two were rectangular columns, 19.25 in. x 28.27 in. x 12 ft high.

The columns' ductility ratio, "μ" was used as a measure of performance. Ductility ratio, ductility factor, or displacement ductility is defined as the ratio of the lateral strain at failure to the strain when the steel is at the yield point. The control columns had a ductility ratio (μ) of 2 with shear failure occurring at $\mu = 3$. The strengthened columns exhibited stable response up to $\mu = 10$ with very little degradation between successive cycles at each ductility value measured. The exceptionally good results indicate that there is great potential for this jacketing method.

The lap splice flexural area is the column area that is most subject to flexural affects and has a lap splice condition. This is a location where inelastic flexural action must develop to provide the ductile response necessary to enable the bridge to withstand seismic action.

A second set of tests on 0.4 scale bridge columns was done with carbon fiber jackets in the lap-spliced flexural area. The CFRP jackets were installed using an automated winding machine. The advantage of the automated carbon fiber jacket installation is that the installation and curing time is approximately one-quarter of the installation time for comparable steel jackets. Further, a full height shear retrofit can be just as effective as steel jackets *(Seible et al, 1995)*, as shown in Figure 5.4. A jacket thickness of only 0.4 mm (0.015 in.) was required over the shear critical central region of the column to prevent brittle shear failure.

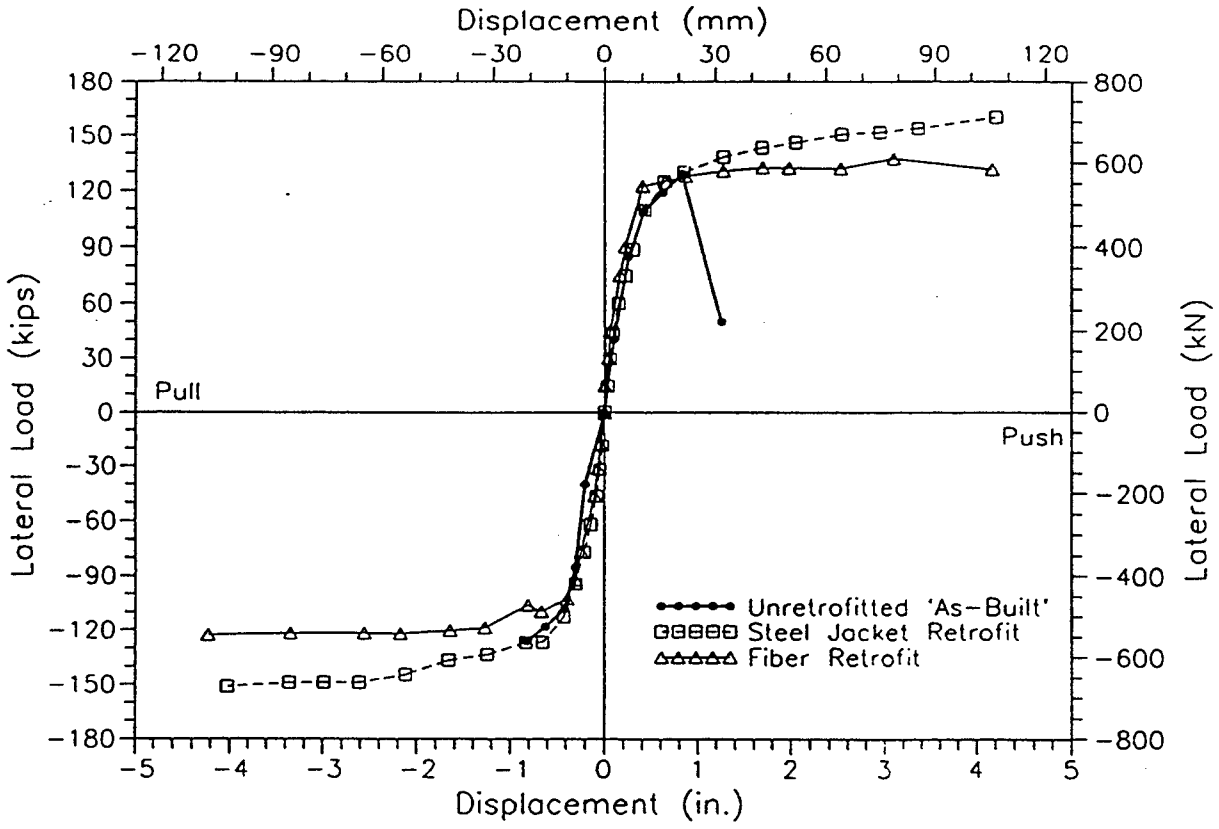

Figure 5.4: Comparison of Load Displacement Envelopes for Steel and Carbon Jackets
(Seible et al, 1995)

The "hysteresis cycle" was stable up to a displacement ductility of 10.5, at which point the test was terminated due to physical testing limitations. These hysteresis curves, also known as hysteresis loops or circles, are lateral load-displacement diagrams. Lateral load-deflection relationships are typically shown for different lateral displacement values. A decrease in the sustained load at the same displacement is referred to as degradation of the hysteresis behavior and is an indication of failure. Comparison between the performance of columns retrofitted with 0.4 mm carbon and 5 mm steel jackets is shown in Figure 5.4. Both cases showed similar improvement when compared to the control.

The steel-jacketed columns exhibited a slightly higher initial stiffness and lateral load carrying capacity. This might be due to the isotropic nature of the steel jackets, resulting in more stiffness and load capacity at the column ends. However, stiffness and capacity increases are not critical in column retrofits since shear control is sought. Thus, the carbon jackets with only horizontal or hoop directional strength and stiffness meet the requirements for columns.

For evaluation of steel jacket techniques, six large-scale columns were fabricated using pre-1971 reinforcing design. An undamaged and a post-damaged column were retrofitted with steel jackets in order to determine whether a damaged column can be salvaged after an earthquake. The study concluded that columns without retrofitting degraded rapidly while the steel jacketed columns attained μ values greater than 6.

Priestley researched an alternative method of retrofitting, using a combination of "active" and "passive" confinement provided by a jacket of fiberglass/epoxy composite material *(Priestley et al, 1992)*. Active refers to pressure injection of epoxy or cement grouts into the area between the composite and the concrete while passive refers to conventional application procedures. The columns were reinforced so that the flexural plastic hinge regions were fully covered.

The process of pressure grouting induces large hoop strains in the composite jacket. The process is maintained, with a little loss of pressure, until the grout has hardened. A second, passive layer of the composite material is placed over the portion of the plastic hinge in the region where high longitudinal compression strain in the column indicates a need for extra confinement. It was expected that the active confinement process would improve the seismic performance when compared to passive confinement, since the expansion of the concrete core, which is necessary to activate confinement in a passive system, is not essential in an actively confined system.

Three different designs, based on combinations of active and passive GFRP layers and grouts, were evaluated.

The first one consisted of an active E-glass/epoxy layer 2.44 mm thick and was epoxy pressure-grouted to an active confinement stress of 1.72 MPa. In addition, a passive wrap of high modulus fiberglass/epoxy was extended over the bottom part of the column in order to increase the potential confining pressure in the critical region at the column base.

The thickness of the active wrap in the second retrofit was reduced to 1.22 mm and the active pressure stress was reduced to 0.69 MPa. The other components of the system were the same as in the previous case.

The most significant change in the third retrofit was the use of cement, rather than epoxy.

The first scheme was the most effective and had stable hysteresis cycles with a displacement ductility value of about 8. Structural degradation of the fiberglass/epoxy jacket did not occur until displacement ductility levels were significantly higher than the ductility levels attainable with equivalent steel jacketed columns *(Chai et al, 1991)*. This may be due to the more effective confinement at the column base, combined with plasticity in the column, resulting from the lower stiffness of the retrofitting material.

The second retrofit was very similar to the first, except that the structural degradation was due to bond failure. Although the pressure was not sufficient to eliminate the bond failure, it resulted in a friction force, which restricted the movement in both the vertical and horizontal direction.

Problems were experienced with the cement grouting on the third retrofit, resulting in circumferential fracture of the active wrap at about 1.4 MPa grout pressure. It was not felt that this was a fault of the use of cement grout, but was probably related to the fluctuations in the pumping pressure since much higher pumping speeds were used for the cement grout.

Similar tests on shear strengthened columns were performed by the same authors *(Priestley et al, 1992)*. The columns were strengthened at the top and bottom with 1.14 mm thick GFRP wraps and pressure grouted with 0.69 MPa cement grout. Passive wrap, with varying thickness from 2.28 mm to 3.43 mm, was installed over the center 1.2 m of the column. The reinforced columns had exceptionally stable hysteresis cycles with little or no strength and stiffness degradation up to a displacement ductility of 8.

The shear resistance degraded with increasing ductility, even for regions outside the hinge zones. The peak shear force was approximately 20 percent higher than the controls. The enhanced performance was due to the ability of the glass fiber/epoxy jacket to deform to a curved surface in the compression zone. The high elastic strain in the jacket material resulted in significant membrane action, thus resisting the collapse in the compression zone until very large displacement ductility levels were obtained. The study concluded that the glass FRP strengthening increases the shear strength of the concrete columns by converting the brittle shear failure mode to ductile flexural deformations.

Two tests were conducted on a new type of fiber-glass-epoxy composite material made of high-modular and regular glass fibers *(Zamichow, 1991)*. The first test had the column wrapped with eight layers of the composite. Four layers were used for the second test. A vertical load of 1816 kN (400 kips) was applied while a cyclic lateral load provided displacements of 2.54 to 254 mm (1 to 10 in.). The columns were cycled far beyond their yield point, which probably exceeded any displacement expected in a large earthquake. Even though the concrete crushed and some steel reinforcing bars ruptured in tension during the test, the fiber wrap remained intact.

5.3.3 University of Arizona, Tucson

Columns strengthened with glass and carbon-reinforced composite straps were evaluated *(Saadatmanesh et al, 1994)*. The main variables in the study were:

- Different concrete mix designs;
- FRP materials;
- Strap thickness; and
- Clear spacing between straps.

The ultimate axial load carried by the columns strengthened with E-glass straps was increased by 82 to 103 percent, depending upon the strength of the unconfined concrete, and by 151 to 171 percent for the columns wrapped with carbon FRP straps.

The ductility ratio increased almost linearly with increasing strap thickness. However, the rate of increase of ductility ratio decreased with the increase in the clear spacing between straps.

The maximum moment capacity increased by 45 to 53 percent for the columns strengthened with E-glass straps, and by 79 to 87 percent for the columns strengthened with carbon fiber straps. The increase in moment capacity was less than the increase in the ultimate axial load. This appears to be an advantage since the majority of the columns requiring strengthening lack adequate ductility, not flexural capacity. Increase in ductility, without increasing the moment capacity would help to prevent a brittle failure.

Analysis of these results by Saadatmanesh et al *(1994)* found that the rate of increase in ultimate load, ductility, and maximum moment capacity decreased for increasing concrete compressive strength. This behavior is typical for FRP materials and can be explained by the "size effects law" *(Kachlakev, 1997; Kachlakev and Lundy, 1995)*.

The relationship between the specimen size and the nature of failure is referred to as "size effect law." In the presence of non-linearly distributed cracking, the failure of the specimen is not simultaneous. The failure occurs through propagation of the failure zone across the specimen. Thus, while one part of the specimen has already failed, another part is approaching its maximum load carrying capacity. The larger the structure or specimen, the more pronounced the non-simultaneous nature of failure, since a larger amount of energy flows into the zone that is currently failing *(Kachlakev, 1997)*.

Four columns with prefabricated FRP wraps were tested to failure under "reversed inelastic cyclic loading" at a level that is considered higher than a severe earthquake. The loading cycles were divided into two phases. The load control phase was applied until the longitudinal bars reached yield. The second phase was a controlled displacement load.

The columns were repaired with a prefabricated GFRP composite wrap that was 0.8 mm thick and had 50.2 volume percent fiber. Each wrap had a tensile strength of 532 MPa, and tensile modulus of 17,755 MPa. The design called for six or eight wraps per strap.

Improvement in the column's response to the controlled displacement load was observed. Typical behavior of the original and repaired columns is shown in Figure 5.5. At the displacement ductility of 3, where the original columns failed, no structural degradation was observed in the repaired columns. The hysteresis cycle of the repaired columns was stable up to a displacement ductility of 6. The repaired columns had twice the stiffness and a lower rate of stiffness degradation than control columns.

The strength of the repaired columns increased about 30%. The study concluded that the GFRP wrap straps were very effective for flexural strengthening and ductility enhancement of severely damaged columns.

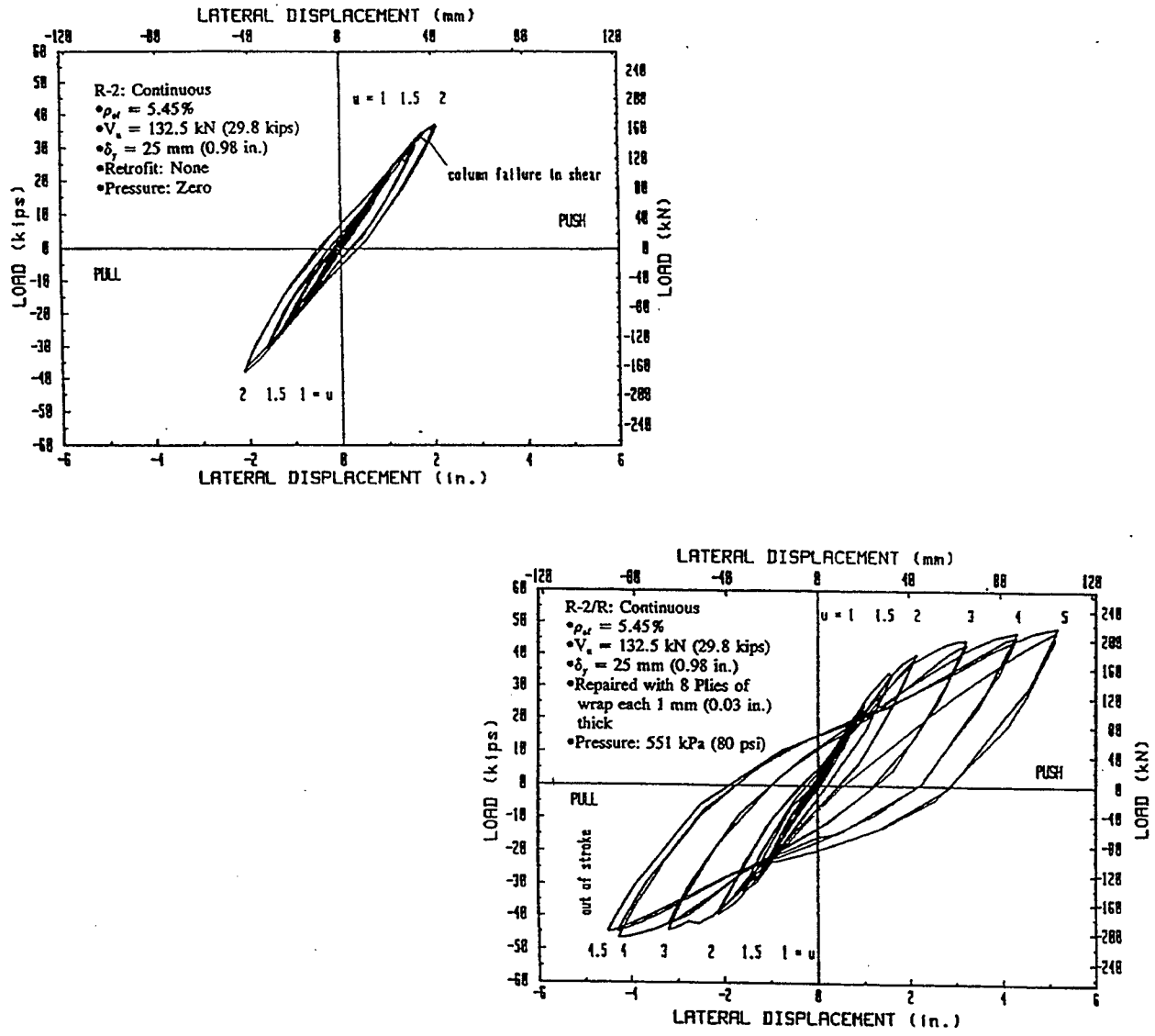

Figure 5.5: Load vs. Displacement Response of Columns Before and After Repair
(Saadatmanesh et al, 1997)

5.3.4 University of South Florida and Florida DOT

A group of tests were completed in which steel-reinforced concrete members obtained from two model bridges were strengthened using CFRP laminates. Six 6.1 m (20 ft) long beams were loaded past the yield point of the steel reinforcement to simulate severe service distress. They were then repaired by bonding CFRP laminates and tested to failure. The study showed increase in ultimate strength of up to 50 percent.

Additionally, extensive experimental and analytical study showed that CFRP-strengthened concrete columns can produce performance equal to high-performance concrete (15-20 ksi strength and 0.02-0.04 strain) from normal-strength concrete (3-5 ksi strength and 0.003-0.004 strain) *(Shahawy et al, 1996)*. The external reinforcement acts as confinement and protective jacket, as well as shear and flexural reinforcement. The FRP wrap increased the initial peak of the stress-strain curve by 30 percent, while the ultimate failure was about 3 time that of the unconfined specimens.

5.3.5 Japan

Researchers from Japan tested ten 200 mm x 200 mm x 1 m columns that had been strengthened with carbon fiber wraps and subjected to cyclic lateral loads *(Katsumata et al, 1988)*. It was concluded that:

- CFRP confinement increased seismic capacity;
- Ultimate displacement and energy dissipation increased approximately linearly with the carbon fiber volume; and
- Carbon fiber volume and the quantity of the steel hoop reinforcement could be correlated by using the effective strength ratio of the materials.

The Technological Research Center of Tokyu Construction Company, Sagamihara, Japan conducted a study on concrete columns that had been strengthened with FRP materials *(Yamamoto, 1992)*. The objectives of the study were to determine the increase of the apparent concrete strength and to investigate the shear and flexural behavior.

The thickness of the CFRP was varied from 0.6 to 1.00 mm, while the thickness of GFRP was 3.00 mm. The GFRP had a tensile strength 119 MPa, and Young's modulus 13.2 GPa, while the CFRP had a tensile strength 752 MPa and modulus of 78 GPa. Results from the tests are shown in Table 5.1.

Table 5.1: Shear-Flexural Strengthening Effects of GFRP and CFRP

SPECIMEN	Initial Rigidity (kN/mm)	Yielding Rigidity (kN/mm)	Flexural Cracking (kN)	Shear Cracking (kN)	Yielding Strength (kN)	Ultimate Strength (kN)	Ultimate Displace-ment (Radian)
Non-strengthened	36.3	10.2	19.6	68.6	104	112	1/50
CFRP	33.8	11.6	19.6	80.4	108	114	1/12.5
GFRP	35.6	10.9	19.6	68.6	105	119	1/18

(Yamamoto, 1992)

Note that the strengthening effects provided by the CFRP and GFRP are very similar. Thus, it seems safe to conclude that the CFRP provides about three times strengthening of GFRP for equal thickness and similar concrete strength. Also, the flexural strengths are the same among the specimens. From a standpoint of seismic retrofitting, it is actually desirable that existing RC columns are strengthened without increasing the flexural strength. It appears that the uniaxial strength of FRP-strengthened concrete increased up to three times above that of the non-strengthened concrete depending upon the percentage of the FRP strengthening ratio. Shear-flexural tests show that the ductility of the strengthened columns is considerably improved.

While the non-strengthened columns collapsed at relative displacement of 1/50, FRP strengthened columns endured up to 1/12.

5.4 THEORETICAL BACKGROUND AND ANALYSIS OF FRP WRAP-STRENGTHENED CONCRETE COLUMNS

The unreinforced concrete typically exhibits linear elastic behavior until failure. Once the brittle material begins to crack, failure is catastrophic. Concrete cylinders confined with a composite wrap generally display a two-stage failure process: the response is elastic up to a stress level slightly higher than the failure strength of the unreinforced concrete, then the response is non-linear until failure. This mechanism has been confirmed by experimental studies *(Hoppel et al, 1995)*. A typical stress-strain curve is shown in Figure 5.6. The non-linear response begins at point A and the point of failure is labeled B.

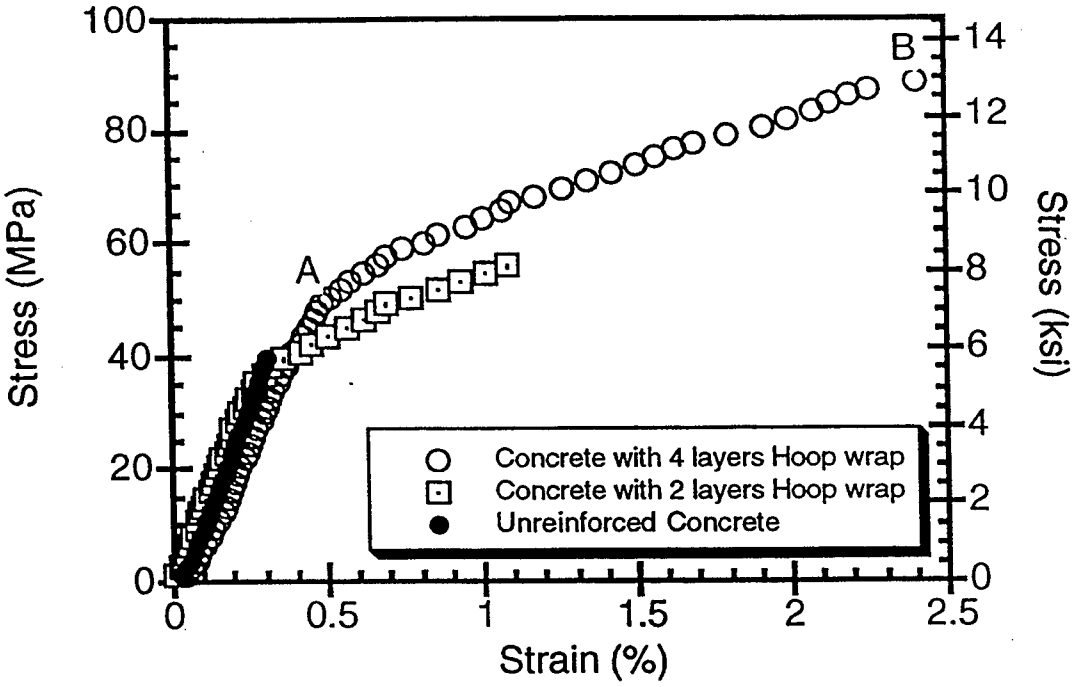

Figure 5.6: Stress-Strain Curve of Unreinforced Concrete Cylinder with Hoop Wrap *(Hoppel et al, 1995)*

It appears that the concrete began to fail at point A and beyond that point, the composite wrap held the cylinder together. For the design of concrete structures wrapped with composites, both points A and B are important. The stress at which the concrete begins to fail represents the design limitations of the structure for axial stress. The failure point represents the maximum stress that the structure can support. The difference between point A and point B is a measure of the ductility of the column.

Other researchers suggest that the stress-strain response of confined concrete has three distinct phases *(Shahawy et al, 1996)*. In the first phases, the behavior of the confined column is similar to plain concrete. With increases in micro cracking, a transition zone is entered in which the wrap exerts a lateral pressure on the concrete. The third phase, when the composite wrap is fully activated, is where the stiffness is stabilized. The response in this phase is mainly dependent on the stiffness of the composite.

Bridge columns designed in the 1950's and 1960's commonly had lap splices of longitudinal reinforcement at the base *(Priestley et al, 1992)*. This is a location where inelastic flexure must develop to provide the ductile response necessary for the bridge to survive catastrophic failure during a seismic event. However, the lap splices, as designed, break down under cyclic inelastic action such as that experienced with seismic loading. This is accompanied by a reduction in flexural strength and energy absorption. Failure of the lap splices can be inhibited if adequate confining pressure is provided in the region of the lap splices and across the potential splitting cracks.

In order to avoid development of the fracture surface within the lap-splice region during a cyclic or seismic event, a critical confining pressure f_l is needed.

$$f_l > \frac{A_b f_y l_s}{\frac{0.5\pi D}{n} + 2(d_b + c)} \tag{5-1}$$

where:

A_b – the area of one of the spliced bars;
f_y – steel yield strength;
l_s – splice length
D – diameter of the longitudinal reinforcement pitch circle;
n – number of bars in the column
d_b – rebar diameter;
c – concrete clear cover.

With FRP composite wrap, having a thickness t_a and elastic modulus E_a, stressed to produce an active confining pressure f_a in the column, and additional passive wrap with thickness t_p and elastic modulus E_p, the forces' equilibrium requires that:

$$t_a E_a + t_p E_p \geq 500(f_l - f_a) \tag{5-2}$$

Using the above equation, the design thickness, t_a and t_p, and the active pressure f_a can be determined, if the confining pressure f_l and composite properties E_a and E_p are known.

Richart *(1928)* and Yamamoto *(1992)* recommend that the strength of concrete, for a given confining stress be expressed by the following equation:

$$f_p = f_c + k\sigma_p \tag{5-3}$$

where:

f_p – strength of the confined concrete, MPa,
f_c – strength of the non-confined concrete, MPa,
k – coefficient,
σ_p – confining stress, MPa, and is expressed as follows:

$$\sigma_p = \frac{2a_w f_t}{sD} \tag{5-4}$$

where:

a_w – sectional area of FRP;
f_t – tensile strength of FRP;
s – spacing of FRP strips (if applicable) ;
D – diameter of the concrete column or the longest side of a rectangular concrete beam .

The increase in strength is typically proportional to the FRP strengthening ratio. The values for k, as estimated by Yamamoto, 1992, are 3.5 for cylinders and 0.6 for prisms. Better estimates can be obtained by the least squares method or other techniques.

The FRP reinforcing ratio can be calculated from the following equation *(AIJ, 1988)*:

$$Q_{u,\min} = \left(\frac{0.092 k_u k_p (180 + F_c)}{\frac{M}{Qd} + 0.12} + 2.7\sqrt{p_{wl}\sigma_{wl} + p_{w2}\sigma_{w2}} + \frac{0.1N}{bD} \right) bj \tag{5-5}$$

where:

$Q_{u,\min}$ – minimum shear strength;
k_u – correction factor related to the effective depth of the cross section;
k_p – correction factor related to the tensile reinforcement ratio;
F_c – concrete compressive strength;
M – design moment;
Q – design shear force;
d – effective depthof the concrete;
p_{wl} – percentof shear reinforcement;
p_{w2} -percent of FRP reinforcement;
σ_{wl} – yield strength of the shear reinforcement;
σ_{w2} – yield strength of the FRP reinforcement;
N – axial load normal to the cross section;
b – width of the cross section;
D – depth of the cross section;
j – effective depth.

Due to the brittle behavior of FRP, it is preferable to use 70 percent or less of the ultimate FRP tensile strength, when estimating the FRP strengthening ratio for existing RC columns. In the near future the ACI 440 Committee will recommend the maximum percentage of the ultimate tensile strength which must be used in the design.

When the column reinforcement is not spliced in the plastic hinge region, confinement may still be necessary to ensure adequate ductility. FRP composite jacket thickness can be estimated from energy considerations and ductility *(Priestley and Seible, 1991)*. The critical parameters are the ultimate compression strain of the concrete to be confined (E_{cu}), the ultimate tensile strength (f_j) and strain (ε_j) of the jacket material, the confined concrete strength (f'_{cc}), and the effective volumetric ratio provided by the composite jacket (ρ_s).

$$E_{cu} = 0.004 + \frac{0.5\rho_s f_j \varepsilon_j}{f'_{cc}} \tag{5-6}$$

and

$$\rho_s = \frac{4(t_a + t_p)}{D} \tag{5-7}$$

In some cases the bridge columns need to be reinforced to prevent failure in shear. With shear failure the force-deformation behavior is typically characterized by degradation of lateral strength, stiffness, and energy absorption capacity. A retrofit design for columns requires enhancement of the shear strength, so that the shear strength exceeds the flexural strength, thus enabling ductile flexural action to develop. For circular FRP jackets, the enhancement of column's shear resistance is given by Priestley et al, 1992:

$$V_{sj} = \left[\left(t_a E_a + t_p E_p \right) \varepsilon_p + \frac{f_a D}{2} \right] \frac{\pi D \cos \theta}{2} \tag{5-8}$$

where:

θ – the angle between the column axis and the principle diagonal compressive strut (to be taken 30°)

For rectangular FRP jackets, the shear strength enhancement can be calculated as follows:

$$V_{sj} = t_p E_p \varepsilon_p h \cot \theta \tag{5-9}$$

where:

h – column section dimension in the direction being strengthened.

5.5 FACTORS INFLUENCING THE PERFORMANCE OF FRP-STRENGTHENED COLUMNS

The factors that may affect the behavior of concrete columns strengthened with FRP composite wraps are: column composition, column geometry, current condition, loading, and environmental conditions. The effects of some of these parameters have been demonstrated by different case studies in Section 5.3. The influence of other parameters can be addressed from a mechanics of composites and reinforced concrete structures approach.

Hoppel et al *(1995)* evaluated the sensitivity of the axial stress at failure to the elastic modulus of the composite wrap on concrete cylinders. The stresses at failure with glass fiber reinforced epoxy wraps and high modulus graphite fiber reinforced epoxy wraps were calculated using the assumption of perfect bonding between wrap and the cylinder. The results are shown in Figure 5.7.

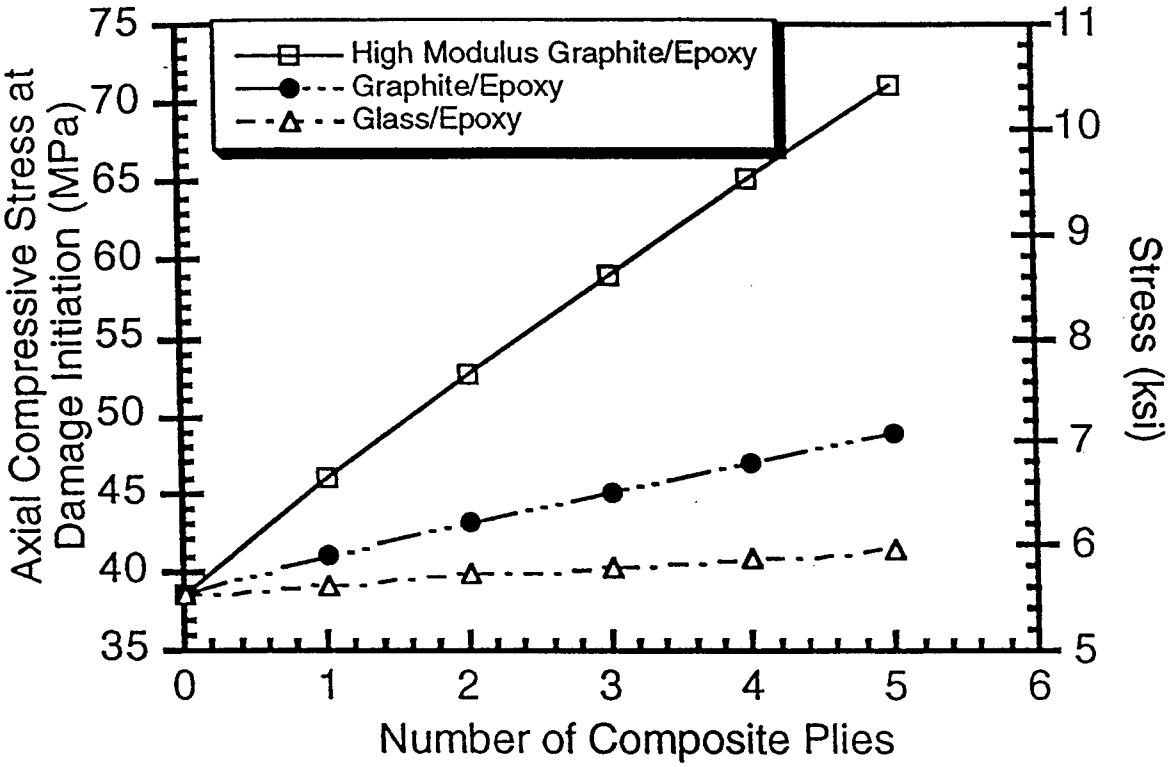

Figure 5.7: Predicted Axial Compressive Stress of Concrete Cylinders with Composite Wraps *(Hoppel et al, 1995)*

The high modulus CFRP creates a high confining pressure, leading to much higher axial stress when the core fails. The more compliant GFRP wrap does not provide as high a confining pressure, and shows very little strength increase over the unconfined core.

There are some disadvantages associated with the use of high modulus CFRP as a hoop wrap for concrete columns. If the wrap is bonded to the column, the radial stress in the column will be proportional to the difference between the Poisson's ratio of the concrete and the Poisson's ratio of the wrap. If they are close (as in case of GFRP and concrete), the stress in the column will approach zero. If the Poisson's ratio of the wrap is much greater than that of the concrete (as in the case of CFRP wrap), the wrap will induce radial tension in the concrete, which may cause failure at the epoxy-concrete interface. Since this is the main type of failure mode observed by researchers, the advantages and disadvantages of high modulus materials for hoop wraps have to be carefully considered.

Shahawy evaluated the stiffness degradation of FRP wrapped concrete columns by subjecting standard test cylinders strengthened with CFRP to cyclic loading. Good energy absorption was achieved. More importantly, while the hysteresis loops become wider for loads beyond the unconfined compressive strength of the concrete, stiffness degradation was not as severe as that of steel-encased concrete. *(Shahawy et al, 1996)*

Howie and Karbhari *(1995)* studied the effect of fiber orientation on strengthening of columns. Unreinforced concrete specimens were wrapped with composite CFRP jackets. Nine different fiber orientations were selected as shown in Table 5.2. The test specimens were instrumented and compression tested to failure. The test results show that the stress-strain relationships are bilinear. The first linear portion has a slope similar to that of unwrapped, plain concrete, while the slope of the second portion was substantially less. The physical properties obtained by using the different wraps are shown in Table 5.2. The thickest lay-up with 0° orientation had the highest average stress and a relatively high modulus. The +/- 45° wrap had the highest elastic modulus value. These results coincide with expectations based on the laminate theory.

Table 5.2: Properties of Carbon Wraps Depending on the Fiber Orientation

Type of Lay-up	Stress MPa	Deformation mm	Modulus GPa
$[0^{\circ}]$	755	3.39	73.3
$[0^{\circ}]_2$	1047	2.73	70.6
$[0^{\circ}]_3$	1105	2.57	77.5
$[0^{\circ}]_4$	1352	4.32	95.7
$[90^{\circ}/0^{\circ}]$	660	2.22	39.9
$[0^{\circ}/90^{\circ}/0^{\circ}]$	822	2.89	54.0
$[+45^{\circ}/-45^{\circ}]$	50	7.21	71.1
$[90^{\circ}/+45^{\circ}/-45^{\circ}/0^{\circ}]$	388	5.02	27.7
$[+45^{\circ}/-45^{\circ}]_2$	68	10.0	587.0

It seems that the increase of the load-carrying ability and the damage characteristics of the strengthened concrete samples strongly depends on the type of fiber architecture in the wrap. It will take less energy to split the matrix between two parallel fibers (90° orientation relative to the direction of load) than to fracture the fibers. The samples containing 90° and +/- 45° showed more examples of different damage types, which suggests that, as the wraps architecture increases in complexity, so does the nature of damage associated with them. The matrix-dependent damages are usually hoop splits, interlayer bond loss, and fiber rotations, while vertical tears, broken fibers, and holes in the wrap are fiber-dependent failure modes *(Jones, 1975)*.

The increase in load-carrying capacity as a function of fiber orientation is shown in Figure 5.8. The results show that the best orientation for increasing the load carrying capacity is the one that contains the largest amount of fibers in the hoop direction.

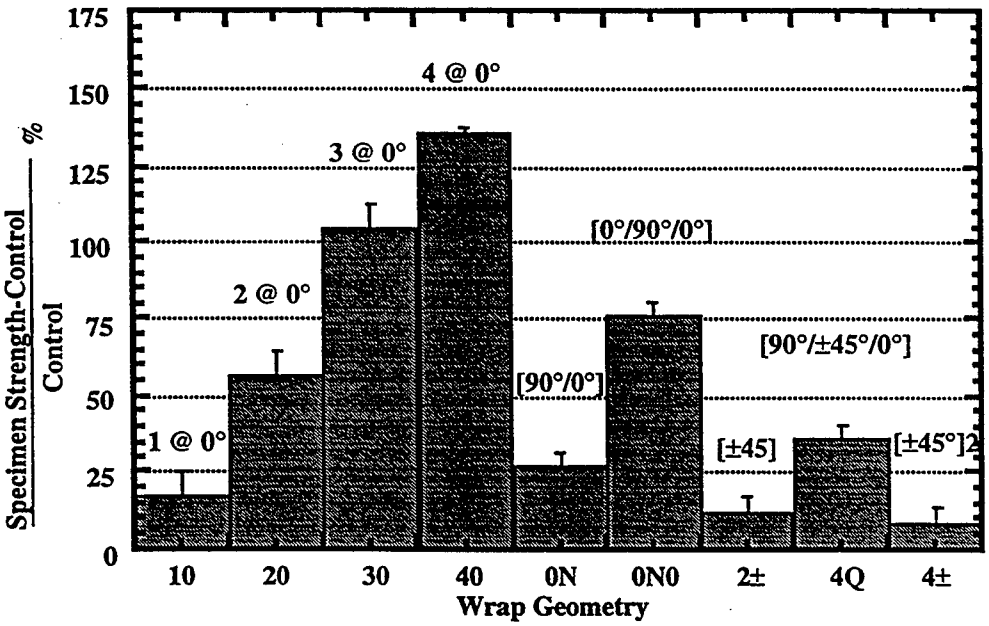

Figure 5.8: Increase in Load Carrying Capacity as a Function of Wrap Orientation
(Howie and Karbhari, 1995)

5.6 FREEZE-THAW RESPONSE OF FRP WRAPPED COLUMNS

Most of the research work to date has focused on strength and ductility of FRP-strengthened columns. Few studies have investigated the effect of freeze-thaw on the behavior of concrete columns wrapped with FRP sheets.

Karbhari and Eckel *(1993)* tested plain concrete cylinders that were wrapped with FRP and subjected them to –18°C temperature in sea water and fresh water. The results showed increased brittleness of the FRP fibers at low temperatures and fiber degradation in seawater. The CFRP wraps were superior to glass and aramid wraps.

Study conducted at Queen's University, Canada investigated CFRP sheets for strengthening concrete columns under cyclic freeze-thaw conditions *(Soudki and Green, 1997)*. Carbon fibers with an individual layer thickness of 0.16 mm and a tensile strength of 237 kN/m were used. Concrete cylinders measuring 150 x 300 mm and wrapped with one or two CFRP layers were compared to unwrapped cylinders. The overall response of the wrapped concrete cylinders was found to be superior to that of unwrapped specimens subjected to similar environmental conditions. The axial strength of the unwrapped cylinders subjected to cyclic freeze-thaw action was 46% lower than that of unwrapped cylinders kept at room temperature. The specimens strengthened with one layer of CFRP showed a 57 percent increase in compressive strength. The addition of a second CFRP layer increased the strength by 87 percent when compared to control cylinders tested under similar conditions.

The strength of a cylinder with a two-layer wrap, tested under freezing conditions, had the same strength as an unwrapped cylinder kept and tested at room temperature. Unlike the cylinders kept and tested at room temperature, the cylinders subjected to freeze-thaw and tested under freezing conditions had a catastrophic mode of failure. The wraps suddenly broke off in a series of hoops. The concrete within the wrap had mini-cracking but remained intact.

Freeze-thaw action significantly reduced the stiffness and strength of CFRP strengthened cylinders, but the CFRP wraps appeared to be efficient in strengthening columns subjected to freeze-thaw when compared to plain concrete cylinders under similar conditions.

5.7 SYSTEMS FOR FRP STRENGTHENING OF BRIDGE COLUMNS

There are numerous material systems available on the market today suitable for use in column strengthening *(Nanni, 1997)*. Among them are:

- Forca Tow Sheet and Replark, manufactured in Japan by Tonen and Mitsubishi Chemical;
- Composite Carbon Wrap, manufactured by XXSys Technologies, USA;
- Tyfo S, by Fyfe Co., USA;
- SnapTite, manufactured by NCF Industries, USA;
- QuakeWrap, by Structural Rehabilitation Corp., USA;
- Hadrshell by DuPont, USA;
- CarboDur by Sika Corp., Zurich, Switzerland.

One of the bridge column seismic retrofit systems approved by CALTRANS is the Robo Tech, developed by XXsys Technologies, Inc., San Diego. The system uses 3.6 GPa (520,000 psi) high strength carbon fibers with an elastic modulus less than 5% of steel, resulting in greater lateral deflection under load and corresponding higher ductility. This is essential, because the most resent CALTRANS bridge design guide requires minimum column ductility from 4 μ to 6 μ to assist lateral motions *(Cerkone and Korff, 1997)*.

Currently, there are two types of Robo Tech wrapper systems. One is designed for encasing structures up to 1.2 m (4 ft) in diameter and 9 m (30 ft) high, with a wrapping speed of 30 m (100 linear ft) of FRP material per minute. The other system retrofits columns up to 2 m (7 ft) in diameter and several hundred feet high, with a wrapping speed of 120 m (400 linear) ft per minute. The Robo Tech rotates around the column in two axes, producing a hoop-wrapped jacket.

The technology is fully computerized, which assures wrapping without any deviations. By using continuous fibers, there are no joints, seams or other potentially weak spots.

Prior to retrofitting, cracks, holes and sharp protrusions in the columns are repaired. Depending on the type of strengthening (flexural or shear), the column sections are wrapped to a specified thickness. For flexural strengthening, typical wrap thickness is about 4 mm (0.16 in.) at the top, tapering to 2 mm (0.08 in.) at the bottom. Curing with a radiant heater completes the process. After the column is finished, the Robo-Wrapper generates a report that shows the location and quantity of materials.

Recently, XXsys Technology has been awarded a subcontract to retrofit 176 rectangular columns of the Arroyo Seco Bridge on Route 134 in Pasadena, California. This is the first seismic retrofit using composites on an historic arch bridge *(Infrastructure, 1997)*. The resulting carbon jackets are expected to be two to four times stronger than steel. Steel jacketing cannot be used on this bridge because it would be very thick and would alter the aesthetics of the bridge. The only options on this project were complete column reconstruction or the use of advanced materials to add strength with minimal weight.

A high strength fiber/epoxy system for wrapping columns was developed by Hexcel Fyfe Company (now Fyfe Co., LLC), Del Mar, California *(Fyfe, 1994)*. The method uses an elastomeric bladder with injection ports. The bladder is placed around the column and a high strength fiber material is circumferentially wrapped around it. The fibers are impregnated with an epoxy especially developed for this system. After the initial setting of the epoxy, the bladder is filled with cement grout at 0.3 to 1.6 MPa(50 to 240 psi), post-tensioning the fibers. The fiber elongation is limited to less than 33 percent of the nominal epoxy elongation in order to prevent premature failure. The composite has 0% creep at that stress level.

Fifteen projects have been completed with the Hexcel Fyfe Company system. Among them is a bridge on Highway 5 in Los Angeles, where total of fifteen columns were wrapped. The diameter of the columns varied from 1.2 to 1.8 m (4 to 6 ft) and the height from 5.5 to 15m (18 to 50 ft). This bridge, located 32 km (20 miles) from Northridge, did not suffer any damage in the 1994 Northridge earthquake.

A bridge on Highway 101 near Santa Barbara, California had two 1.5 m (5 foot) columns with a circular upper section and square lower flexural area, and was successfully wrapped with this system.

Ninety-six columns on a bridge near Sparks, Nevada, needed flexural section retrofitting. Forty-eight of the columns were inside a casino that had been built under the bridge. The successful wrapping of these columns demonstrated the ability of system to be applied in tight spaces.

A repair on short columns that transfer the load from a reinforced concrete deck to a reinforced concrete arch in a viaduct near Spoleto, Italy was done using the Replak material system manufactured by Mitsibishi Chemicals *(Nanni, 1997)*. The columns, 1.65 m (5.4 ft) tall and having a cross section of 0.4 x 0.4 m (15.7 x 15.7 in.), exhibited severe distress and concrete spalling due to steel reinforcement corrosion. After removal of the deteriorated material and restoration to the original shape with non-shrink mortar, the columns were strengthened with a single layer of CRFP sheets applied in the transverse direction. The design configuration of these columns was such that the column ends acted as hinges. A circumferential CFRP wrap provided confinement without adding any bending stiffness or moment capacity at the hinge location.

An effective technique for repairing damaged concrete columns was developed at the Structural Engineering Laboratory, University of Arizona *(Saadatmanesh et al, 1997)*. They developed an FRP wrap of high-strength E-glass fibers woven to form a fabric-like material of specified width and length. The fabric is placed on a mylar sheet and saturated with polyester resin. Then the sheet is rolled around a mandrel that is the size and shape of the column to be repaired. The material is then oven cured for 40 minutes at 160°F. After curing, the mylar is removed from the fabric and the pre-formed sheet is flexible enough to be wrapped around circular or rectangular columns.

The column repair consists of removing all loose concrete and replacing everything that was removed or missing. Next, 3 mm rubber spacers are bonded to the column surface to create a gap for post-pressurization. The wraps are placed over the spacers and adhered to each other with a thin layer of two-component, low viscosity epoxy. The final step of the repair is to pressure-inject epoxy into the gap between the composite wrap and the concrete surface. Hose-type clamps at the top and bottom of the repair zone prevent epoxy leakage during pressurizing. The various steps of a repair are shown in Figure 5.9.

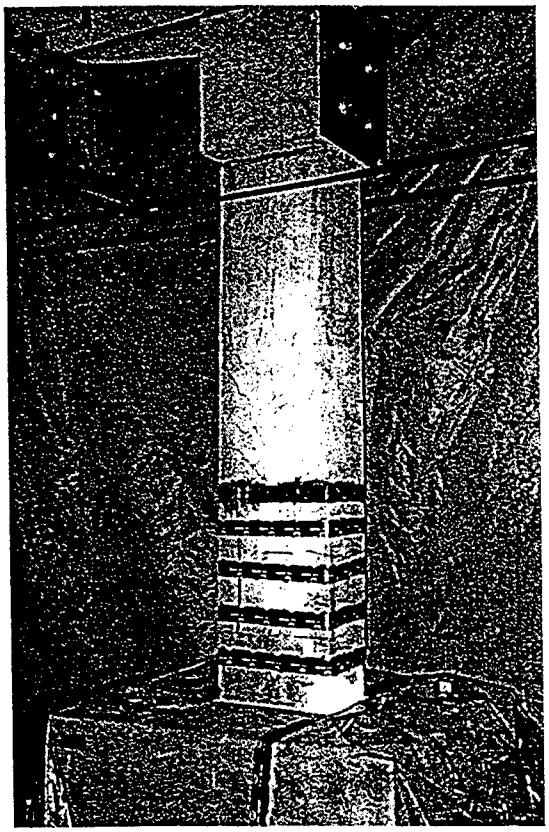

a) Replacement of Spalled Concrete and Reshaping the Column

b) Wrap of Glass FRP in Multiple Layers around the Failure Zones

c) Pressurizing the Gap Between the FRP Composite and Concrete Surface with Epoxy Resin

Figure 5.9: Various Steps of Repair Operation
(Saadatmanesh et al, 1997)

5.8 SUMMARY

Research has indicated that advanced composite jacketing for upgrading bridge columns is at least as effective as steel jacketing. With developments in manufacturing and installation processes, advanced composites rehabilitation and strengthening techniques became cost-competitive, even with the relatively high present costs for the fibers and resin.

The composite jackets strengthen a concrete column in two ways. First, the jacket provides confining pressure, which increases the stress at which the concrete begins to fail. Secondly, once the concrete failure initiates, the composite wrap holds the column together and allows it to deform while retaining structural integrity.

The advantages of strengthening concrete columns with FRP straps are:

- Increased ductility as a result of the confinement, the concrete will tend to fail at higher strain levels, resulting in significant increases in ductility.
- Increased strength the lateral pressure exerted by the confinement will increase the apparent compressive strength of the column, resulting in a higher load carrying capacity and providing extra support against buckling of the longitudinal steel.
- Low weight the low density of composites significantly simplifies the construction process and reduces cost.
- Reduced construction time strengthening with steel jackets of a typical 4-ft diameter, 22-ft high circular column required 2.4 days, excluding excavation and painting. Two columns of similar size can be retrofitted using FRP wraps in one day with a significant reduction of construction cost.
- Low maintenance – composite retrofit wrapping is more durable than steel jackets by a factor of 2 to 4. Because of their resistance to electrochemical deterioration, FRP wraps do not corrode and are not affected by salt spray and other aggressive environmental factors.
- Esthetics – FRP composites are very thin and do not significantly alter the geometric appearance of columns.

5.9 DESIGN EXAMPLES

Currently there are no design procedures for external reinforcement with FRP composites. In the near future ACI Committee 440 will provide engineers with guidelines for strengthening concrete structures with FRP composites. Until then, each designer must conduct their own review of the design concepts.

The design examples provided herein follow a logical step-by-step process based on conventional reinforced concrete design. Appropriate assumptions regarding FRP allowable strains and stresses are an integral part of the design process. Although the design follows the ACI fundamentals and the UCSD experience, additional knowledge is needed for success. These topics include, but are not limited to, the following:

- composite behavior near ultimate loads;
- brittle versus ductile failure modes;
- strength loss due to elevated or low temperatures of the adhesive;

- creep of GFRP laminates; and
- thermal compatibility between FRP composites and concrete.

The procedure is provided only for illustration of the material presented in this chapter and cannot be regarded as a guideline for the strengthening of concrete members with FRP laminates.

The determination of the FRP jacket thickness for the different column regions are based on the previously outlined column failure modes.

5.9.1 Shear Strengthening

The column shear failure is primarily associated with a strength and dilation deficiency. The column shear strength can be increased by hoop or horizontal reinforcement with FRP jackets, having fibers oriented at 90 degrees relative to the longitudinal axis of column. The basis of the shear design strengthening is to limit the column dilation in the loading direction to dilation strains of 0.4%.

The shear capacity of the retrofitted column is calculated as:

$$V_n = V_c + V_s + V_p + V_j > \frac{V_o}{\phi_V}, \tag{5-10}$$

where:

V_n – nominal shear capacity of the retrofitted column;
Vc – shear capacity contribution from the concrete;
Vs – shear capacity contribution from the horizontal shear reinforcement;
Vp – shear capacity contribution due to axial load;
V_j – shear capacity contribution of the FRP jacket;
V_o – column shear demand based on full flexural overstrength in the potential plastic hinges.

5.9.1.1 Jacket Thickness for Circular Columns

The jacket thickness for strengthening of circular columns can be determined by the following equation:

$$t_j = \frac{\left(\frac{V_o}{\phi_V}\right) - \left(V_c + V_s + V_p\right)}{\left(\frac{\pi}{2}\right) 0.004 E_j D} \sim \left(\frac{1}{E_j D}\right) C_v^C \tag{5-11}$$

5.9.1.2 Jacket Thickness for Rectangular Columns

The jacket thickness for strengthening of rectangular columns can be determined by the following equation:

$$t_j = \frac{\left(\frac{V_o}{\phi_V}\right) - \left(V_c + V_s + V_p\right)}{2(0.004)E_j D} \sim \left(\frac{1}{E_j D}\right) C_v^R \qquad \textbf{(5-12)}$$

where:

ϕ_v – shear capacity reduction factor (typically $\phi_v = 0.85$);
E_j – elastic modulus of the FRP jacket;
D – column dimension in the loading direction;
C^i_v – remaining general coefficient for rectangular and circular columns.

5.9.1.3 Concrete Shear Capacity Contribution

5.9.1.3.1 Inside The Plastic Hinge Region

The concrete shear capacity contribution inside the plastic hinge region is calculated as follows:

$$V_c^i = k\sqrt{f_c'}\, A_e \qquad \textbf{(5-13)}$$

5.9.1.3.2 Outside The Plastic Hinge Region

The concrete shear capacity contribution outside the plastic hinge region is calculated as follows:

$$V_c^o = 3\sqrt{f_c'}\, A_e \qquad \textbf{(5-14)}$$

where:

k – coefficient;
f_c' – concrete compressive strength (psi);
A_e – concrete effective area.

Derivation of k coefficient is shown in Figure 5.10.

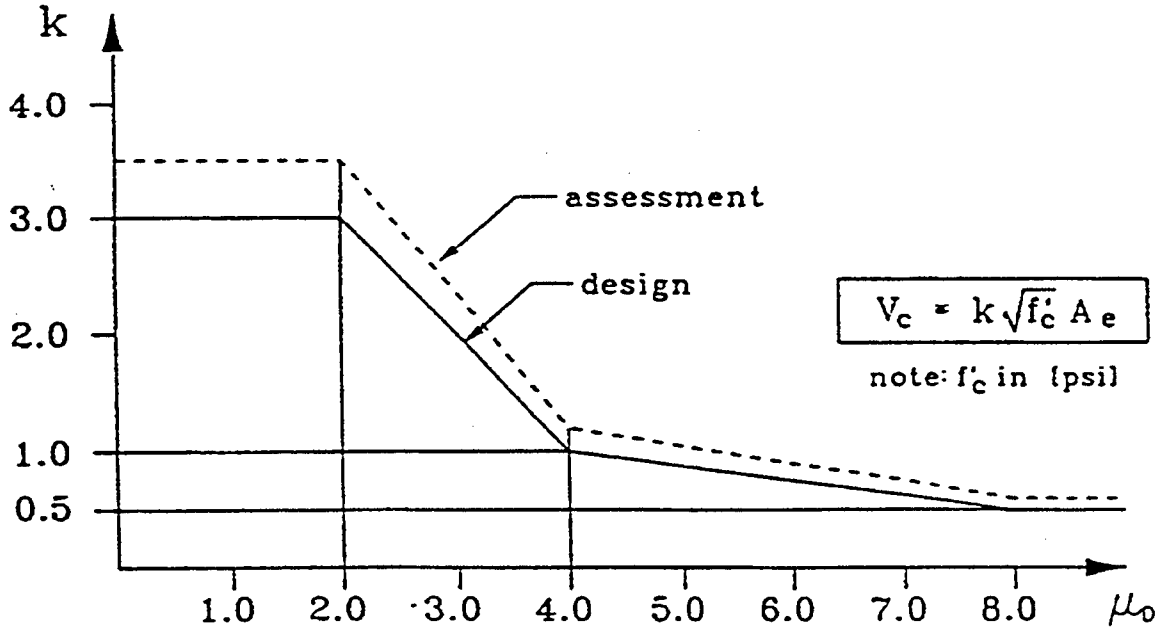

Figure 5.10: Concrete Shear Capacity

5.9.1.4 Steel Shear Capacity Contribution

5.9.1.4.1 Circular Columns

The shear capacity contribution of the internal steel reinforcement is calculated as follows for circular columns:

$$V_s = \left(\frac{\pi}{2}\right)\frac{\left(A_h f_{hy} D'\right)}{s}\cot\theta \qquad \textbf{(5-15)}$$

5.9.1.4.2 Rectangular Columns:

The shear capacity contribution of the internal steel reinforcement is calculated as follows for rectangular columns:

$$V_s = n\frac{\left(A_h f_{hy} D'\right)}{s}\cot\theta \qquad \textbf{(5-16)}$$

where:

n	number of transverse tie legs in loading direction;
A_h	area of one leg of horizontal hoop reinforcement;
s	hoop/tie spacing (spiral pitch);
D'	distance center to center of the shear leg ends (see Figure 5.11);
θ	angle between direction of the shear cracks and vertical column axis.

5.9.1.5 Axial Load Shear Capacity Contribution

The contribution of the axial load shear component is calculated such as:

$$V_p = P\tan\alpha \qquad \textbf{(5-17)}$$

where:

tanα = (D - c)/2L for single curvature bending conditions;
tanα = (D - c)/L for double curvature bending conditions;
P axial load applied to the column.

See Figure 5.12 for an illustration.

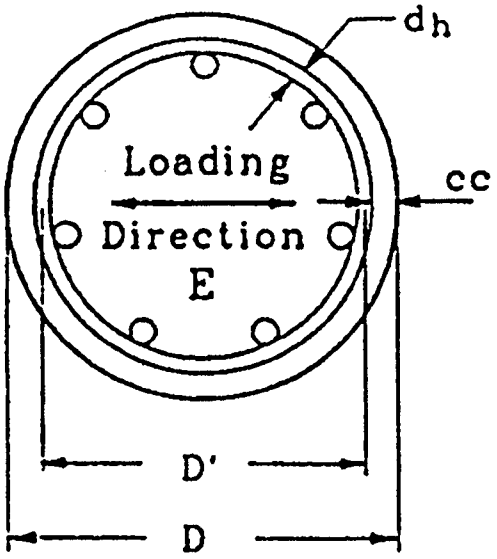

a) Circular Columns

$D' \quad D - 2cc - d_h$

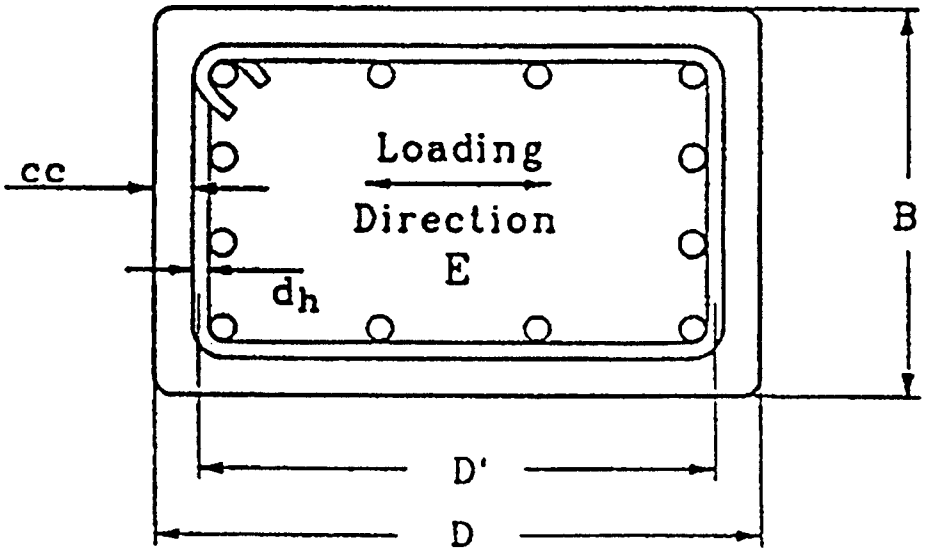

b) Rectangular Columns

Figure 5.11: Effective Column Dimensions

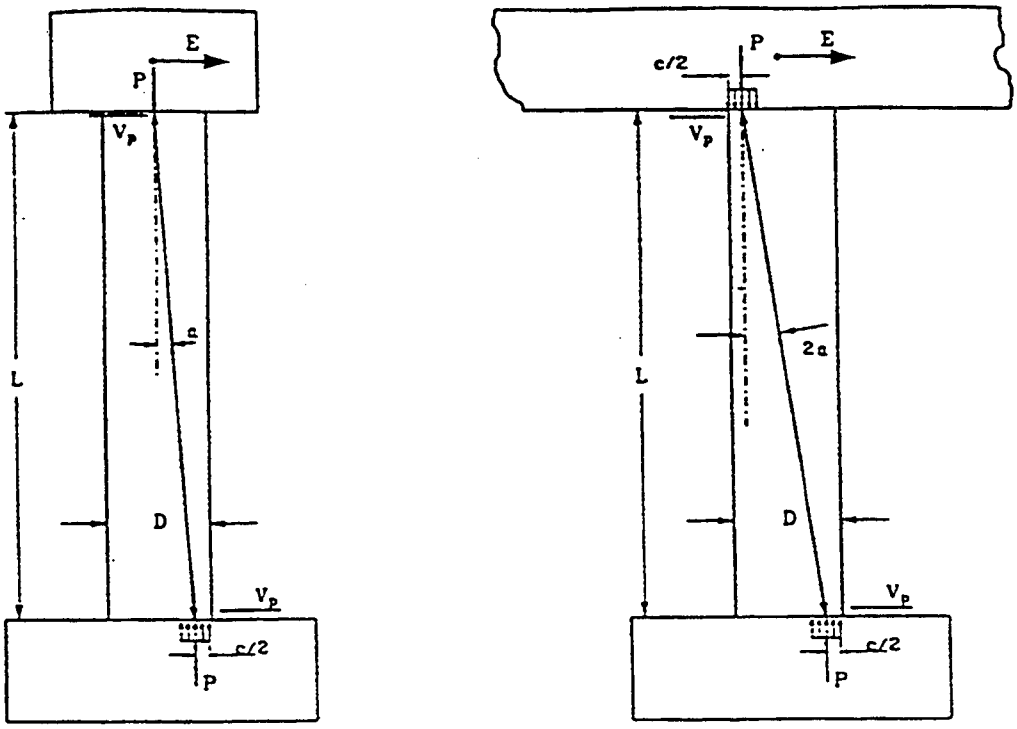

Figure 5.12: Axial Load Shear Component

5.9.1.6 Shear Capacity of FRP Jackets

5.9.1.6.1 Circular Columns:

The shear capacity of the FRP jackets is calculated as follows for circular columns:

$$V_j = \left(\frac{\pi}{2}\right) f_{jd} t_j D \cot\theta \qquad \textbf{(5-18)}$$

5.9.1.6.2 Rectangular Columns:

The shear capacity of the FRP jackets is calculated as follows for rectangular columns:

$$V_j = 2 f_{jd} t_j D \cot\theta \qquad \textbf{(5-19)}$$

where:

θ – angle between shear cracks and column axis;
f_{jd} – design stress of the FRP jacket in the hoop direction ($f_{jd} \cong 0.004\ E_j$).

The design thickness of the FRP jacket for shear is checked such that:

$$V_j \geq \left(\frac{V_o}{\phi_V}\right) - \left(V_c + V_s + V_p\right) \qquad \textbf{(5-20)}$$

5.9.2 Flexural Hinge Confinement for Circular Columns

The inelastic deformation capacity of the flexural plastic hinge regions can be increased by confining the column with FRP jacket in the hoop direction. The expression of the required jacket thickness for circular columns can be based on: a) equal energy approach at failure or b) steel reinforcement buckling.

5.9.2.1 Based on Equal Energy at Failure

$$t_j = \frac{\rho_j D}{4} = \frac{0.09 D\left(\varepsilon_{cu} - 0.004\right) f'_{cc}}{\phi_f f_{ju} \varepsilon_{ju}} \sim \frac{D}{f_{ju} \varepsilon_{ju}} C_f \qquad \textbf{(5-21)}$$

where:

f'_{cc} confined concrete compressive strength which depends on the effective lateral confining stress and nominal concrete strength (typically $f'_{cc} \cong 1.5 f'_c$);
f_{ju} ultimate strength capacity of the FRP jacket in hoop direction;
ε_{ju} ultimate strain at failure of the FRP jacket in hoop direction;
ϕ_f flexural capacity reduction factor (typically, $\phi_f = 0.9$);
ε_{cu} ultimate concrete strain which depends on the provided level of confinement;
ρ_j transverse reinforcement ratio;

D – column dimension in the loading direction;
C_f – remaining general coefficient.

The ultimate concrete strain can be determined as

$$\varepsilon_{cu} = 0.004 + \frac{2.8\rho_j f_{ju}\varepsilon_{ju}}{f'_{cc}} \quad \textbf{(5-22)}$$

The ultimate concrete strain can also be obtained from

$$\varepsilon_{cu} = \Phi_u c_u \quad \textbf{(5-23)}$$

where:
Φu – ultimate section curvature;
c_u – depth of the neutral axis.
Both, Φ_u and c_u can be determined from the moment-curvature analysis of the cross-section and in turn related to the ductility factor of the column.

$$\mu_\Delta = 1 + 3\left(\frac{\Phi_u}{\Phi_y}\right)\left(\frac{L_p}{L}\right)\left(\frac{1-0.5L_p}{L}\right) \quad \textbf{(5-24)}$$

where:
$L_p = 0.08L + 0.022f_{sy}\, d_b$,
μ_Δ – column ductility factor;
L – shear span of the plastic hinge;
L_p – semi-empirical plastic hinge length;
Φ_y – section yield curvature;
f_{sy} – yield strength of the main column reinforcement;
d_b rebar diameter of the main column reinforcement.

5.9.2.2 Based on Rebar Buckling [if $\frac{M}{VD} > 4$]:

In order to ensure that the rebar buckling in the plastic hinge does not the control the flexural failure mode, an additional check has to be performed for slender columns, if M / (V.D) > 4, where, M – maximum column moment; V – maximum column shear force; D – column dimension in the loading direction.

$$t_j = \frac{nD}{E_j} \sim \frac{D}{E_j} C_b \quad \textbf{(5-25)}$$

where:
E_j – FRP elastic modulus in (ksi);
n – number of column rebars for slender columns with $\frac{M}{VD} > 4$.

The required FRP jacket thickness is directly proportional to the column diameter and inversely proportional to the FRP elastic modulus in the hoop direction.

5.9.3 Flexural Hinge Confinement for Rectangular Columns

Due to the limited research data available, the design of FRP jackets for strengthening rectangular columns is based on the empirical assumption of doubling the equivalent circular column jacket.

The circular FRP jackets provide confinement by radial pressure forces, generated by the jacket curvature, and the tensile hoop strains in the jacket, generated by the expansion of the plastic hinge. Circular FRP jackets can be used for shear strengthening of rectangular columns by adding precast concrete segments to the columns (see Figure 5.13). Thus, an equivalent column diameter D_e can be derived, and the jacket thickness calculations can follow those outlined for circular columns, using the equivalent column diameter D_e.

If the column depth-to-width aspect ratio is less than 1.5, rectangular FRP jackets could be used. It is recommended that the theoretical thickness of the rectangular jackets be twice that of an equivalent circular column with diameter D_e *(Seible and Karbhari, 1997)*.
The effective circular FRP jacket diameter can be calculated as

$$D_e = R_1 + R_2 \tag{5-26}$$

where:

$R_1 = \frac{b^2}{a}$, and $R_3 = \frac{a^2}{b}$,

R_1 – radius of curvature in "x" direction of the column cross-section (see Figure 5.13);
R_3 – radius of curvature in "y" direction of the column cross-section (see Figure 5.13);
a – half of the FRP jacket diameter in "x" direction;
b – half of the FRP jacket diameter in "y" direction.

The shape of the FRP jacket can be approximated with oval by the mean of the following equations:

$$a = kb \tag{5-27}$$

$$b = \sqrt{\left(\frac{A}{2k}\right)^2 + \left(\frac{B}{2}\right)^2} \tag{5-28}$$

$$k = \left(\frac{A}{B}\right)^{\frac{2}{3}} \tag{5-29}$$

where:

A – dimension of the rectangular column in "x" direction;
B – dimension of the rectangular column in "y" direction.

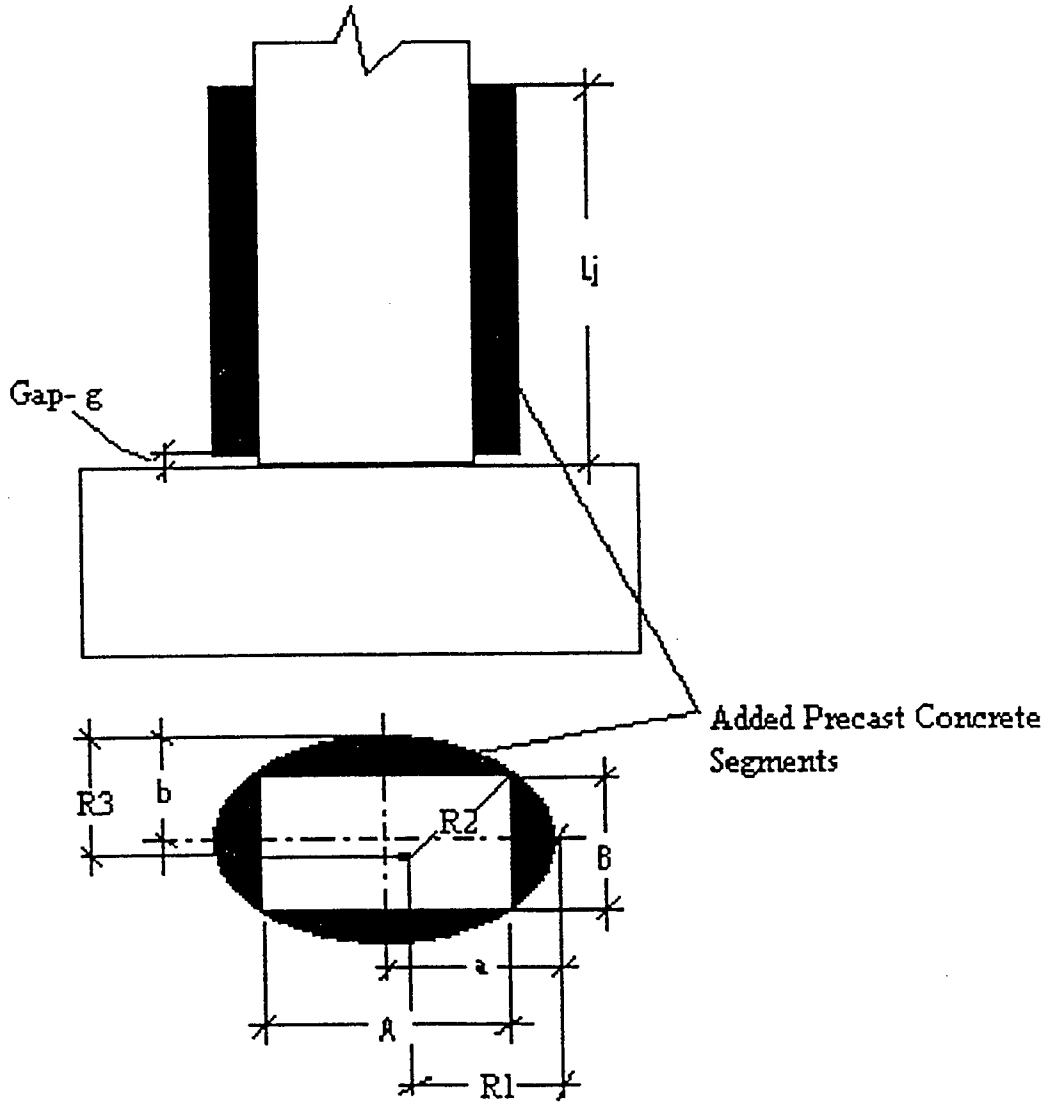

Figure 5.13: Flexural Plastic Hinge Design for Rectangular Columns

5.9.4 Lap Splice Clamping

Lap splice clamping (see Figure 5.14) is necessary to prevent splitting of the concrete adhered to the starter bars and slip of the column reinforcement relative to each other. In order to prevent those failure mechanisms, a sufficient lateral pressure f_l is required. Experiments suggest *(Seible et al, 1995)* that lap splice debonding and relative slippage starts when hoop strains are between 1000 and 2000 με.

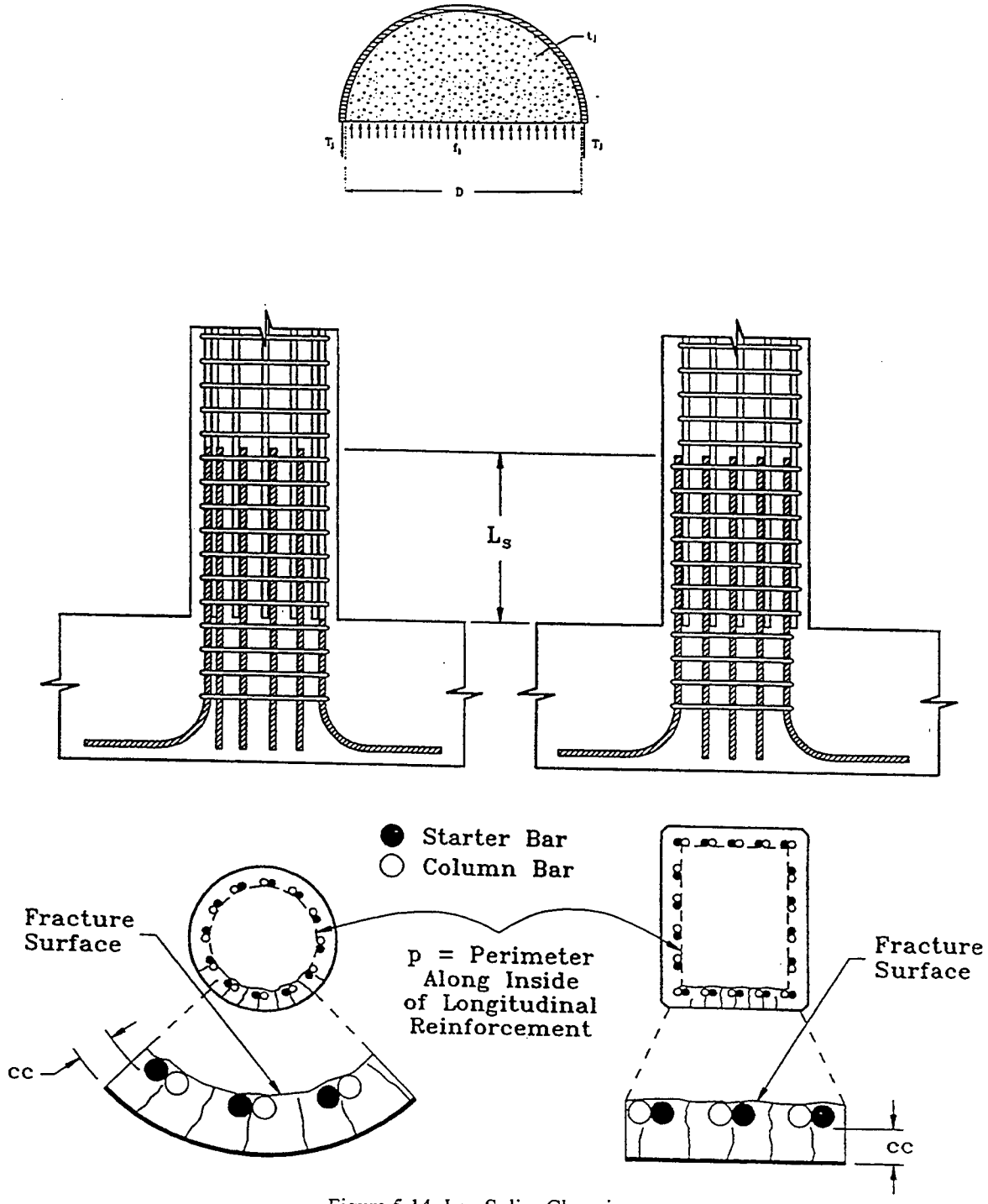

Figure 5.14: Lap Splice Clamping

In order to limit the dilation hoop strain of the FRP jacket to 1000 με ($f_j = 0.001\ E_j$), the FRP thickness must be derived such as:

$$t_j = 500\left(\frac{D(f_1 - f_2)}{E_j}\right) \tag{5-30}$$

where:

t_j – FRP jacket thickness;
f_l – lateral clamping pressure over lap splice L_p;
f_h – horizontal stress level at a strain of 0.1%, provided by the hoop reinforcement;
D – circular column diameter;
E_j – FRP jacket elastic modulus in hoop direction.

The lateral pressure can be calculated such that

$$f_1 = \frac{A_s f_{sy}}{\left(\frac{p}{2n} + 2(d_b + cc)\right)L_s} \sim \left(\frac{D}{E_j}\right)C_s \tag{5-31}$$

where:

A_s – area of the main column reinforcement bars;
f_{sy} – yield strength of the main column reinforcement;
p – perimeter of the column cross-section along the lap spliced bar location;
n – number of spliced bars along perimeter p;
cc – concrete clear cover of the main column reinforcement;
d_b – diameter of the main column reinforcement;
C_s – remaining coefficient.

Table 5.3 shows relative FRP jacket thicknesses for three FRP systems with hypothetical mechanical properties. The relative FRP jacket thickness is calculated for the four column failure modes, i.e., shear failure, plastic hinge failure, rebar buckling, and lap splice failure. System 1 intended to represent towpreg CFRP jackets, typically used in automated winding; System 2 represents Kevlar/epoxy FRP jacket; and System 3 is a representation of GFRP composite jackets, typically used in prefabricated adhesively bonded shells. The values are normalized with respect to System 1.

Table 5.3: Comparison of Hypothetical FRP Jacket Thicknesses

		Normalized FRP Jacket Thickness			
System	**Mechanical Properties**	**Shear Strength**	**Plastic Hinge Confinement**	**Bar Buckling Restraint**	**Lap Splice Clamping**
System 1	E_j = 124 GPa; f_{ju} = 1380 MPa; ε_{ju} = 1%	1	1	1	1
System 2	E_j = 76 GPa; f_{ju} = 1380 MPa; ε_{ju} = 1.5%	1.6	0.7	1.6	1.6
System 3	E_j = 21 GPa; f_{ju} = 655 MPa; ε_{ju} = 2.5%	6.0	0.9	6.0	6.0

(Seible and Karbhari, 1997)

Note that strengthening for shear, rebar buckling and lap splice clamping is driven by the FRP jacket modulus in the hoop direction and favors higher moduli materials, such as CFRP. Strengthening for plastic hinge confinement can be achieved more efficiently with a lower modulus and higher strain capacity materials, such as GFRP.

5.9.5 Numerical Design Examples

5.9.5.1 Design Goal

Provide a shear retrofit of rectangular column in double bending with CFRP jacket. Convert the brittle shear failure to a ductile flexural failure. Target displacement ductility of $\mu_\Delta \geq 8$. Steel rebars are spliced 381 mm (15 in) above the column base.

5.9.5.2 Assumptions

- column length (L) = 1.219 m (4 ft);
- maximum moment (M_{yi}) = 650 kN-m (5752.5 kip-in);
- shear contribution of concrete inside the plastic hinge (V^i_c) = 53.4 kN (12 kips);
- shear contribution of concrete outside the plastic hinge (V^o_c) = 302.5 kN (68 kips);
- shear contribution of the transverse reinforcement (V_s) = 93.4 kN (21 kips);
- shear contribution of the axial load (V_p) = 104.5 kN (23.5 kips)
- shear reduction capacity factor (ϕ_v) = 0.85
- FRP jacket elastic modulus (E_j) = 125,000 N/mm^2 (18.1 x 10^6 psi)
- strength of the FRP jacket in hoop direction (f_{ju})= 1300 MPa (188.5 ksi)
- FRP deformation capacity in hoop direction ε_{ju} = 1 %
- lateral clamping pressure by the hoop reinforcement (fh) = 0.2 MPa (29 psi)
- column dimension in loading direction (A or D) = 600 mm (23.6 in)
- column dimension in the other direction (B) = 500 mm (19.7 in)
- transverse steel yield strength f_{sy} = 330.4 MPa (44 ksi)
- column main shear reinforcement diameter (d_b) = 19 mm (0.75 in)
- section yield curvature (Φ_y) = 0.0055 mm (2.16 x 10^{-4} in)
- depth of the neutral axis (c_u) = 0.12 mm
- concrete compressive strength (f_c') = 35 MPa (5076 psi)
- concrete clear cover (cc) – 25.4 mm (1 in)
- number of spliced bars (n) = 25
- lap splicing length (L_s) = 381 mm (15 in)
- area of one main reinforcing bar (A_s) = 284 mm^2 (0.44 in^2) No. 6, A36 steel bar
- perimeter of the column cross-section along inside the spliced bars location (p)

5.9.5.3 Shear Strength Requirements

Maximum expected plastic shear demand, based on overstrength V_o:

$$V_o = 1.5\, V_{ji} = 1.5 \left(\frac{M_{ji}}{L}\right) = 1.5 \left(\frac{650}{1.219}\right) (650 / 1.219) = 800 \text{ kN } (179.85 \text{ kips})$$

Determination of FRP jacket thickness inside the plastic hinge region (t^i_j):

$$t_j^i = \frac{\left(\frac{V_o}{\phi_V}\right) - \left(V_c^i + V_s + V_p\right)}{2(0.004)E_j D}$$

$$= \left[\frac{\left(\frac{800}{0.85}\right) - (53.4 + 93.4 + 104.5)}{2(0.004)(125000)(600)}\right] 10^3$$

= 1.15 mm (0.045 in)

Determination of FRP jacket thickness outside the plastic hinge region (t^o_j):

$$t_j^o = \frac{\left(\frac{V_o}{\phi_V}\right) - \left(V_c^o + V_s + V_p\right)}{2(0.004)E_j D}$$

$$= \left[\frac{\left(\frac{800}{0.85}\right) - (302.5 + 93.4 + 104.5)}{2(0.004)(125000)(600)}\right] 10^3$$

= 0.75 mm (0.03 in)

5.9.5.4 Flexural Plastic Hinge Confinement Requirements

The confinement of the plastic hinge will be designed using a rectangular jacket with twice the FRP thickness required for an equivalent circular jacket having an effective diameter of D_e.

Effective diameter D_e:

$$k = \left(\frac{A}{B}\right)^{\frac{2}{3}} = \left(\frac{600}{500}\right)^{\frac{2}{3}} = 1.13$$

$$b = \sqrt{\left(\frac{A}{2k}\right)^2 + \left(\frac{B}{2}\right)^2} = \sqrt{\left(\frac{600}{2(1.13)}\right)^2 + \left(\frac{500}{2}\right)^2} = 364.7 \text{ mm (14.36 in)}$$

a = kb = (1.13)(364.7) = 412.08 mm (16.22 in)

$$R1 = \frac{b^2}{a} = \frac{364.7^2}{412.08} = 322.8 \text{ mm (12.71 in)}$$

$$R3 = \frac{a^2}{b} = \frac{412.08^2}{364.7} = 465.6 \text{ mm (18.33 in)}$$

$$De = R1 + R3 = 322.8 + 465.6 = 788.4 \text{ mm (31.04 in)}$$

Expected plastic hinge length Lp:

$$L_p = 0.08L + 0.022 f_{sy} d_b = 0.08 \times 1219 + 0.022 \times 303.4 \times 19 = 224.3 \text{ mm (8.83 in)}$$

Required curvature ductility $\mu\Phi$ (in order to achieve displacement ductility $\mu\Delta = 8$) :

$$\mu_\Phi = 1 + \frac{\mu_\Delta - 1}{3\left(\frac{L_p}{L}\right)\left(1 - \frac{0.5L_p}{L}\right)}$$

$$= 1 + \frac{8-1}{3\left(\frac{224.3}{1219}\right)\left[1 - 0.5\left(\frac{224.3}{1219}\right)\right]} = 14.97$$

Use $\mu_\Phi = 15$

Required concrete ultimate strain value:

$$\varepsilon_{cu} = \Phi_u c_u = \mu_\Phi \Phi_y c_u = 15(0.0055)(0.12) = 0.0099$$

FRP jacket thickness required to assure the determined concrete strain:

In the primary confinement region:

$$t_j^1 = \frac{0.09 D_e (\varepsilon_{cu} - 0.004) f'_{cc}}{\phi_f f_{ju} \varepsilon_{ju}}$$

$$= \left[\frac{0.09(788.4)(0.0099 - 0.004)(1.5)(35)}{0.9(1300)(0.01)}\right]2 = 3.76 \text{ mm (0.148 in)}$$

In the secondary confinement region:

$$t_j^2 = \frac{t_j^1}{2} = 1.88 \text{ mm (0.074 in)}$$

5.9.5.5 *Rebar Buckling Restraint*

Since $\frac{L}{D} = \frac{1219}{600} = 2.032 < 4$, the anti-rebar buckling criteria do not need to be checked.

5.9.5.6 *Lap Splice Clamping Requirements*

$p = 2[A - 2(cc + d_b) + B - 2(cc + d_b)]$

$p = 2[600 - 2(25.4 + 19) + 500 - 2(25.4 + 19)] = 1845$ mm (73.63 in)

Required clamping pressure (f_l):

$$f_l = \frac{A_s f_{sy}}{\left(\frac{p}{2n} + 2(d_b + cc)\right)L_s} = \frac{(284)(330.4)}{\left(\frac{1845}{2(25)} + 2(19 + 25.4)\right)381}$$

$f_l = 1.96$ MPa (0.284 ksi)

Thickness of the FRP jacket (t^s_j):

$$t^s_j = 500\left(\frac{D(f_1 - f_2)}{E_j}\right) = 500\left(\frac{600(1.96 - 0.2)}{125000}\right) = 4.22 \text{ mm (0.17 in)}$$

5.9.5.7 *Summary of FRP Jacket Thickness Specifications*

For an example, see Figure 5.15.

$L^i_v = 1.5\ D = 900$ mm (35.43 in) $\rightarrow t^i_j = 1.15$ mm (0.045 in)

$L^o_v = L - 2\ L^i_v = 600$ mm (23.62 in) $\rightarrow t^o_j = 0.75$ mm (0.03 in)

$L^t_{c1} = L^b_{c1} = 0.5\ D = 300$ mm (11.81 in) $\rightarrow t^1_j = 3.76$ mm (0.148 in)

$L^t_{c2} = L^b_{c2} = 0.5\ D = 300$ mm (11.81 in) $\rightarrow t^2_j = 1.88$ mm (0.074 in)

$L_s = 381$ mm (15 in) $\rightarrow t^s_j = 4.22$ mm (0.17 in)

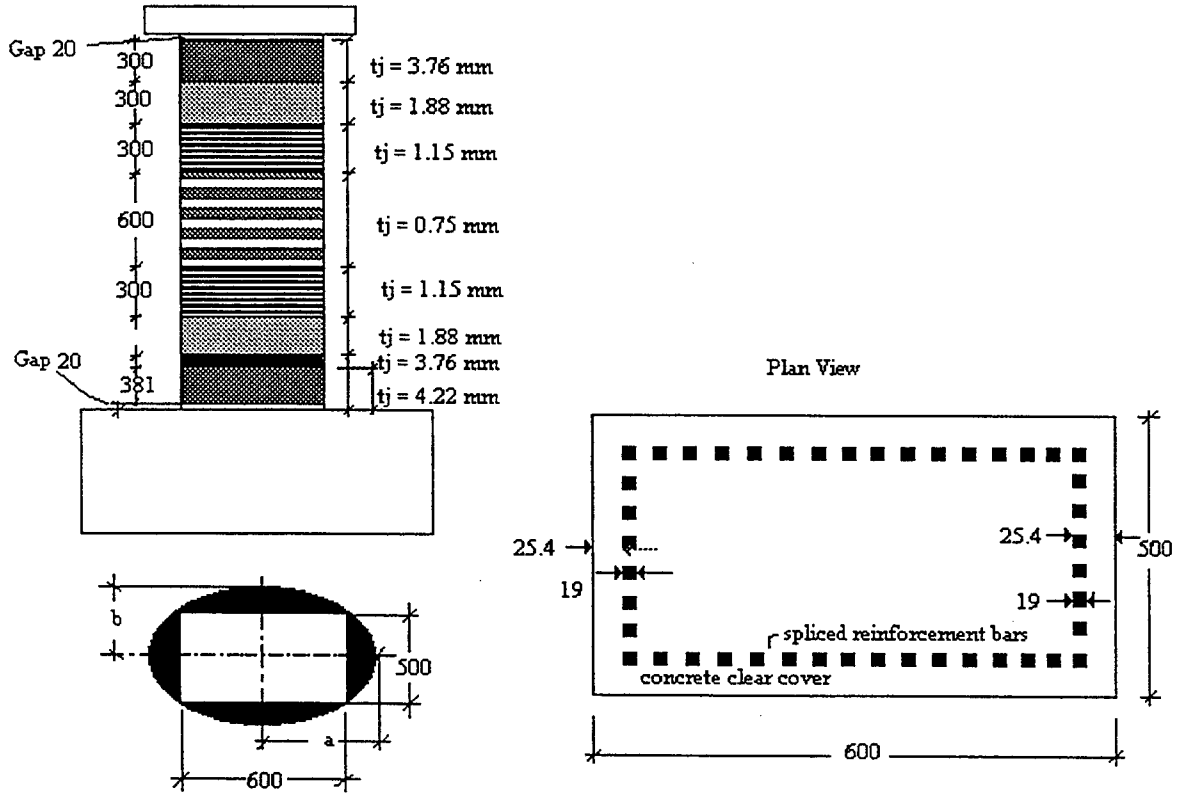

Figure 5.15: Summary of FRP Jacket Lay-Outs

5.9.6 List of Variables

a	half of the FRP jacket diameter in "x" direction
A	dimension of the rectangular column in "x" direction
A_e	concrete effective area
A_h	area of one leg of horizontal hoop reinforcement
A_s	area of the main column reinforcement bars
b	half of the FRP jacket diameter in "y" direction
B	dimension of the rectangular column in "y" direction
cc	concrete clear cover of the main column reinforcement
C_f	remaining general coefficient
C^i_v	remaining general coefficient for rectangular and circular columns
C_s	remaining coefficient
c_u	depth of the neutral axis
D	column dimension in the loading direction
D'	distance center to center of the shear leg ends
d_b	diameter of the main column reinforcement
E_j	FRP jacket elastic modulus in hoop direction
f_c'	concrete compressive strength
f_{cc}'	confined concrete compressive strength
f_h	horizontal stress level
f_{jd}	design stress of the FRP jacket
f_{ju}	ultimate strength capacity of the FRP jacket in hoop direction
f_l	lateral clamping pressure over lap splice
f_{sy}	yield strength of the main column reinforcement
k	coefficient
L	shear span of the plastic hinge
L_p	semi-empirical plastic hinge length
n	number of spliced bars along column perimeter; or number of transverse tie legs in loading direction
p	perimeter of the column
P	axial load applied to the column
R_1	radius of curvature in "x" direction of the column cross-section
R_3	radius of curvature in "y" direction of the column cross-section
s	hoop/tie spacing (spiral pitch)
t_j	FRP jacket thickness
V_c	shear capacity contribution from the concrete
V_j	shear capacity contribution of the FRP jacket
V_n	nominal shear capacity of the retrofitted column
V_o	column shear demand
V_p	shear capacity contribution due to axial load
V_s	shear capacity contribution from the horizontal shear reinforcement

θ angle between direction of the shear cracks and vertical column axis
μ_Δ column ductility factor
μ_Φ required column curvature ductility
ε_{cu} ultimate concrete strain which depends on the provided level of confinement
ϕ_f flexural capacity reduction factor
ρ_j transverse reinforcement ratio
ε_{ju} ultimate strain at failure of the FRP jacket in hoop direction
Φ_u ultimate section curvature
ϕ_v shear capacity reduction factor
Φ_y section yield curvature

6.0 CONSTRUCTION CONSIDERATIONS AND DURABILITY OF THE RETROFITTED SYSTEMS

6.1 RELIABILITY ASSESSMENT AND CONDITION EVALUATION OF EXISTING BRIDGE STRUCTURES

6.1.1 Background

Reliability is defined as the probability that an item will consistently perform a required function under given environmental and operational conditions for a stated period of time. Reliability is a probabilistic measure that has been used to evaluate performance of structures in various engineering applications. Quantitative reliability analysis includes a detailed evaluation of important factors contributing to a structure's failure and the associated relative uncertainties.

The quality of condition assessments of bridges depends on the accuracy and precision of inspection methods. Condition assessments are estimated both as mean values and as lower bounds *(Hearn et al, 1996)*. These estimates are incorporated in evaluations of the strength and safety of bridges. The disparity between mean values and lower bound values of strength and safety is a measure of the quality of the inspection. Performance prediction models currently used in bridge maintenance processes are based on visual inspection database information *(DeStefano and Grivas, 1996)*. These models typically result in a high degree of prediction uncertainty due to subjective inspection techniques and various environmental and operational factors affecting the deterioration of the structures.

In the United States, bridge conditions are reported as qualitative condition ratings. Data from bridge inspections must indicate the current strength of bridge members, and load demand. Load capacity of a bridge member is a comparison of member strength with load demand. Safety is a similar comparison that includes recognition of variability in strength and in demand. Strength of members can be estimated from data on normalized loss together with original design information. Damage is defined as a normalized loss of any type. For concrete, damage is associated with the normalized area of spalls, and size and spacing of cracks. For steel members and reinforcing bars, damage is defined as the loss in thickness or in diameter.

Three parameters – material, cross section, and condition – define each bridge member *(Hearn and Frangopol, 1996)*. From these data, member strength can be estimated. Each member has a known location, and therefore load demand in it can be estimated.

When the statistical variance of the design variables and loads are known, the probability of failure associated with given state of stress can be evaluated. In reality, this is done in terms of a reliability index, defined as a probability of failure. Currently, the codes for reinforced concrete structures are based on a reliability index of three combinations of dead and life loads. The following equations are used in the analysis:

$$\beta_t = \frac{S_m - S_t}{\left(\sigma_{S_m}{}^2 + \sigma_{S_p}{}^2\right)^{\frac{1}{2}}} \qquad \textbf{(6-1)}$$

where:

$\beta(t)$ – Reliability Index at age *t* years;
σ – Standard Deviation.

$$P_{f(t)} = \Phi(-\beta), \qquad \textbf{(6-2)}$$

where:

$P_{f(t)}$ – Probability of Failure at age *t* years.

$$R(t) = 1 - P_{f(t)}, \qquad \textbf{(6-3)}$$

where:

R(t) – Reliability of the bridge at age *t* years.

Typical performance prediction curves are shown in Figure 6.1.

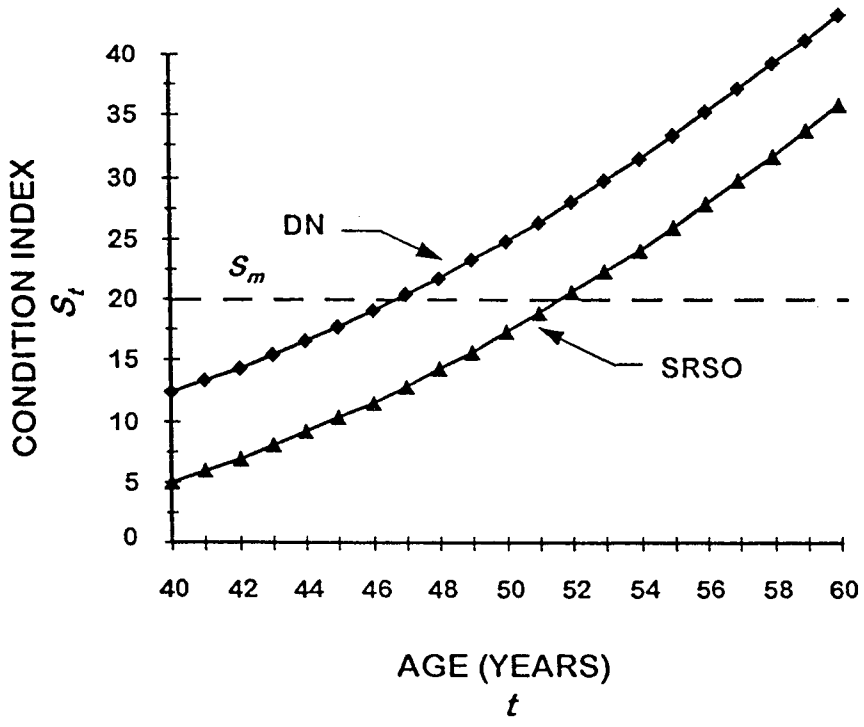

Figure 6.1: Performance Prediction Curves
(DN–Do nothing SRSO–Strip, repair, seal, overlay)
(DeStefano and Grivas, 1996)

6.1.2 Reliability of FRP Materials

Typically, the behavior of FRP materials is studied by modeling the composites as a chain of *m* short bundles, with each bundle containing *n* short fibers. Within each bundle, the load originally carried by the failed fibers is redistributed among the non-failed fibers according to the load-sharing rules. Following the chain-of-bundles FRP model, Harlow and Phoenix *(1981)* showed that the probability of failure H for a composite laminate under stress σ can be described by the following equation:

$$H_{m,n}(\sigma) = 1 - \exp mn\left(\frac{\sigma}{\sigma_o}\right)^{\rho} \tag{6-4}$$

where:

σ_0 and ρ – scale and shape parameters.

For unidirectional FRP laminate (the most widely used for strengthening purposes) with volume V, *mn* can be substituted for V. Thus:

$$H_V(\sigma) = 1 - \exp V\left(\frac{\sigma}{\sigma_o}\right)^{\rho} \tag{6-5}$$

Regarding the material selection, it is commonly believed that, given their superior properties over other materials, FRP laminates offer the highest potential for strengthening concrete structures. Typically, studies deal with both material properties and geometric parameters in a deterministic manner, i.e., the statistical nature of their variability is not taken into account. In some cases, the properties of the FRP may vary due to imperfection in the manufacturing processes and/or construction shortcomings. These variations may have direct impact on rehabilitation design and safety margins. However, this should not endanger the structure, since the design factors of safety for FRP materials are greater than those of conventional materials. Typically, values of 50% or less of the ultimate strength/strain characteristics of FRP materials are used as design inputs.

6.1.3 Reliability of FRP-Strengthened Concrete Members – Case Studies

If properly designed, FRP strengthened concrete beams are supposed to fail in bending *(Triantafillou and Plevris, 1992)* in one of the following failure mode sequences: steel yielding-FRP rupture, or steel yielding-concrete crushing. However, in the case of thick CFRP laminates, concrete crushing in a catastrophic manner is possible. Bond failure between the FRP plate and concrete is another possible failure mode. Debonding is highly dependent on the quality control during construction and the properties of the specific adhesive employed. If both are sufficient, debonding, at least in theory, will be preceded by other failure mechanisms. Shearing of the concrete between the steel and external FRP reinforcement is hard to quantify. However, this failure mechanism can be avoided by confining the two ends of the laminate by clamping *(Plevris et al, 1995)* or by other similar techniques *(Sharif et al, 1994)*.

Research conducted at Massachusetts Institute of Technology focused on short and long term behavior characteristics of concrete beams strengthened with FRP laminates *(Plevris et al, 1995)*. The study aimed to establish a strength reduction factor for a given probability of failure and to study the effect of each design variable on the reliability of strengthening bridge elements with FRP. The flexural capacity of the strengthened beam was thought to depend on beam geometry, amount of steel reinforcement and FRP laminate, and strength and elastic modulus of concrete, reinforcing steel rebars and FRP plates. The geometric and material properties were treated as independent random variables. Concrete strength, FRP failure strain, and FRP area fraction were the most influential properties on the variability of the beam strength. Reliability-based design was studied and two strength reduction factors were derived to achieve a reliability factor of three (required by the current codes). The analysis indicated a general strength reduction factor (beam strength) $\Phi = 0.85$ and partial strength reduction factor for the FRP laminate strength $\Phi_{fc} = 0.95$ ($\Phi = \Sigma\phi_i$, where ϕ_i is a strength reduction factor for design variable "i").

The study concluded that the cross section dimensions of the beam, FRP laminate length, and the initial strain have no significant effect on reliability against flexural failure.

6.2 SELECTION OF COMPOSITE SYSTEM

Although composites have generally being considered to have very good environmental durability, it must be remembered that this characteristic depends ultimately on the selection of fibers, matrix and processing method used.

The choice of fiber system should be predicated on the specifics of application, structural safety, stress levels likely to be faced by the retrofit system, and its design life. The choice of strengthening system could also affect the condition of the deteriorated area, because a change in the electrical resistivity of the system due to addition of the repair material could cause acceleration of the corrosion process in reinforcing steel. Whereas it is accepted that carbon fibers are inert to most exposure type durability tests *(Karbhari et al, 1996)*, glass fibers need to be protected through an application of resin. Some studies pointed out the potential for extreme degradation of glass-fiber composite when left unprotected *(Sen et al, 1993)*. Rather than use such data to dismiss the use of glass fibers for external applications, appropriate stress level limits and safety factors must be determined.

The choice of adhesive used for application of a composite retrofit/repair will depend on a number of factors, including the method of application. If the composite is prepared "in-situ" using a wet lay-up process, the bond between the concrete and the composite will be defined by the resin system used. The resin will serve both as an adhesive and matrix. In some cases, the resin could be modified by addition of fillers to increase its viscosity in order to enable it to act as a primer, sealing off surface cracks and unevenness. Prefabricated FRP laminates are attached to the concrete surface with an adhesive rather than the with resin system itself. The difference between the wet lay-ups and prefabricated laminates is that in the latter case there are two distinct interfaces, i.e., between the concrete and the adhesive, and between the adhesive and the composite.

Irrespective of the case, the durability of the adhesive is critical to the performance of the composite-retrofitted concrete structure. The degradation of strength and modulus values of the adhesive chosen for the retrofit must be examined through a broad range of temperatures and environmental exposures. Selection of an inappropriate adhesive system could result in a disaster.

6.3 CONCRETE SURFACE PREPARATION AND COMPOSITE SYSTEM INSTALLATION REQUIREMENTS

6.3.1 Background

The most important factors influencing the quality of the strengthening are the mechanical properties of the FRP laminates, the bond characteristics at the FRP-concrete interface, and preparation of the concrete surface prior to FRP bonding.

The effect of different surface treatments with epoxy resins was studied at Claude Bernard University *(Varastehpour and Hamelin, 1996b)*. Significantly different behavior was obtained from different combinations of materials (glue, plate and surface treatments). Figure 6.2 shows the difference of shear stress – strain response of various adhesives.

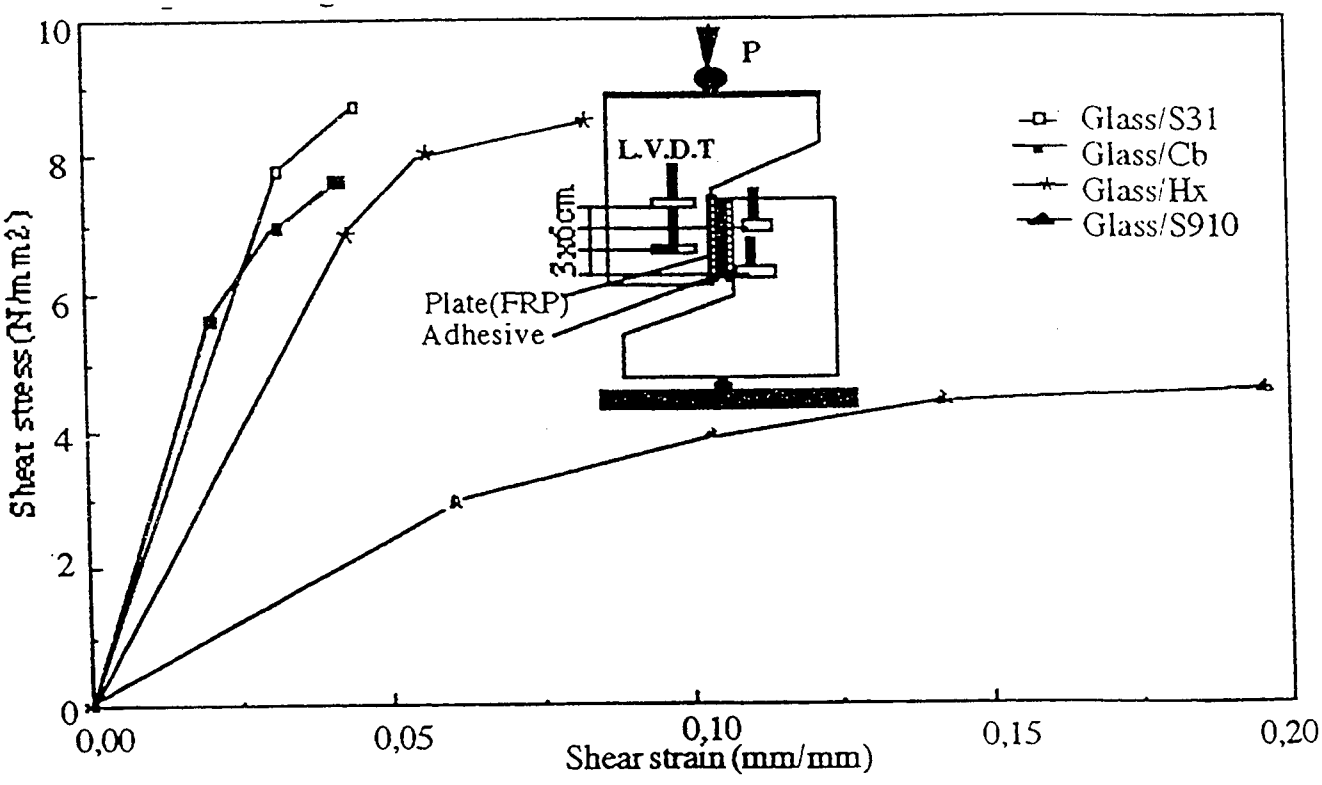

Figure 6.2: Interface Shear Stress vs. Shear Strain
(Varastehpour and Hamelin, 1996b)

The success of strengthening depends on the performance of the epoxy resin mortar used. A study conducted at University of Arizona showed that tough epoxies are the most suitable for concrete strengthened with GFRP laminates *(Saadatmanesh, 1994)*. The study used a two-component, rubber-toughened epoxy with a consistency similar to that of a cement paste, having lap shear strength of 15 MPa, maximum elongation at failure of 40 percent, and curing time of 4 hours at room temperature.

Tonen Corporation (Japan) investigated the influence of concrete surface preparation, the rigidity of carbon fiber sheets (CFS) and number of lamination layers on bonding to concrete. High strength and high modulus CFS were examined. The concrete surface was prepared by ordinary sand blasting and water jetting. In the case of water jetting, epoxy type putty was used to smooth the rough concrete surface *(Yoshizawa et al, 1996)*. The test results showed that fracture occurred near the interface of concrete and CFS. When the bonding length was increased from 100 mm to 150 mm, maximum tensile strength remained almost unaffected. However, longer bond length provides better resistance to shear cracking. Surface treatment by water jetting showed bond strength two times higher than for surface treatment by ordinary sanding. Additionally, the maximum load resisted by water jet-treated and strengthened beams was 1.7 times higher than that of unreinforced beams. No noticeable difference was recognized by using different water jet pressures or different primers. The bond strength of high modulus CFS was approximately 50 percent higher than that of low modulus, high strength CFS. Increasing the numbers of CFS laminate layers from one to three resulted in almost 100 percent increase in bond strength.

6.3.2 Surface Preparation Technological Operations

The purpose of the surface preparation is to create optimal adhesion conditions for maximum bond between the materials to be jointed. Cleaning of the surface removes existing foreign matter such as dirt, dust, oil, and grease. A sound and solid base is a precondition for good bonding. Since it is mostly older structures that require strengthening, it is important to detect and remove potentially weak spots. Adhesion to exposed aggregates is generally better than to the hardened cement paste. Therefore, it is recommended that existing cement paste be removed by sandblasting or similar techniques, and that the aggregate be exposed as gently as possible. Visual check of the treated surface for foreign matter and inclusions in the concrete surface is a part of the quality control. The evenness of the surface must be checked by a metal batten. On a basic length of 2 meters, the unevenness must not exceed 10 mm *(Steiner, 1996)*. Large defective and uneven areas must first be repaired and leveled with an epoxy resin mortar. This operation must be carried out at least one full day before the bonding work in order to allow proper time for curing and hardening of the epoxy mortar.

For any composite system to perform properly, the sheets must be adequately bonded to the substrate. Experience gained by researchers shows that "the surface preparation is 90 percent of the job" *(Thomas et al, 1996)*. Surface preparation can be divided into a few simple operations:

1. Before installation of the FRP system, the deteriorated concrete structure must be repaired. Existing cracks should be injected with epoxy resin. Spalling concrete should be removed and the original cross section of the concrete member restored with no-shrinkage mortar.

2. Corners and sharp angles of the structure should be smoothed because these areas are prone to delamination. External angles should be rounded to at least 10 mm (0.5 in.) radius, and internal angles should be smoothed by placing an epoxy mortar into the corner.

3. Laitance and other bond inhibiting contaminants must be removed, usually by sand blasting or high pressure water jetting. Depending upon the composite system to be applied, condition of the concrete surface, and contractors experience, one method might be more effective than the other.

4. An epoxy primer is then brushed or rolled onto the clean surface. This is usually a two-component, high-viscosity epoxy system. When the primer has dried, all shallow imperfections on the surface must be filled with an epoxy filler.

   In many cases, the use of protective coatings and resin reach layers can postpone the evaporation of moisture containing alkalis through the resin to the interface and fiber surface. This raises concerns about fiber degradation *(Karbhari et al, 1996)*. Regarding possible degradability of glass fibers in high-alkalinity environments, retrofits designed with glass are appropriate if one adheres to precautions in terms of materials selection and design stress levels.

5. The initial resin coat is applied to the prepared surface using a paint roller or similar device. With the resin still wet, the sheet must be positioned onto the surface and de-airated using either a ribbed roller or spatula, or vacuum bagging when technologically required. Then, a second layer of resin is applied onto the sheet. The process is repeated for multiple layers until the design thickness is reached.

6. Initial drying of the composite laminate is usually achieved within a few hours and cures overnight. However, this will vary from one system to another. Common practice is to allow at least three to five days for complete cure before the structure is fully loaded.

Some researchers recommend slightly different procedures for surface preparation. Research conducted in EMPA, Switzerland states that some adhesives that are already used to bond steel plates to concrete beams can be applied to FRP composites *(Meier and Kaiser, 1991)*. Typical properties of the adhesives used in Switzerland are shown in Table 6.1. In order to ensure a strong bond, EMPA researchers suggest removing the resin-rich surface layer from prefabricated FRP laminate by sanding, and treating the concrete surface by grit-blasting or similar methods. No primers are recommended. The laminates are degreased with detergent treatment to remove soluble contaminants and resin particles. The pressure required to bond the laminate to concrete beam is applied by vacuum bag or through lightweight clamps.

Table 6.1: EMPA Adhesive Properties

Property	XB-3074	Sikadur 31
Modulus (N/mm^2)	6200	8500
Bending Strength (N/mm^2)	25	35
Compressive Strength (N/mm^2)	75	65
Tensile Strength (N/mm^2)	24	17
Density (g/cm^3)	1.67	1.65

(Meier and Kaiser, 1991)

Generally, the following characteristics of structural adhesives are very important: strong adhesion to the elements to be bonded; strong cohesion; little tendency to creep under permanent load, and; resistance to humidity and alkalinity *(Steiner, 1996)*.

Evaluation of the bond characteristics of FRP plates-adhesive-concrete was the main objective of a study conducted at the University of Delaware in conjunction with Delaware Department of Transportation *(Finch et al, 1995)*. The study evaluated the effect of different adhesives on bond strength. Results indicated that bond strength much greater that concrete shear strength could be achieved depending on the adhesive.

In order to test the effect of surface preparation on bond strength, three different preparation techniques were used: bonding the FRP plate directly to the "as cast" concrete; mechanically abrading (sandblasting) the concrete surface prior to bonding; and mechanical abrading plus consequent treating with primer prior to FRP bonding. The last method was shown to be the optimum preparation technique *(Finch et al, 1995)*.

6.3.3 Additional Factors Influencing the Quality of Strengthening

Most of the up-to-date knowledge about FRP strengthening has been gained through research conducted worldwide. When a research study is carried out, the specimens are typically prepared and tested in a laboratory that has a warm, dry and consistent environment. Unfortunately, these conditions cannot be compared to the harsh climate that a real bridge must endure. Freeze/thaw cycles and moisture are factors likely to affect the structural performance of FRP strengthened members *(Alexander and Cheng, 1996)*.

Freeze/thaw cycles induce stresses into every structure and material that is exposed to temperature changes. In the case of CFRP composites, these stresses are due to the difference in the coefficient of thermal expansion between the concrete ($\alpha = 11.6 \times 10^{-6}$ strain/°C) and the CFRP ($\alpha = 0.7 \times 10^{-6}$ strain/°C). Although laboratory tests have shown that these additional stresses do not cause substantial problems, they should be taken into consideration *(Alexander and Cheng, 1996)*. In the case of GFRP composites, the freeze/thaw-induced stresses are less problematic because of the similarity of the thermal expansion coefficients of concrete and GFRP.

Bridge decks are usually very permeable, allowing rainwater to leach onto and into the concrete girders below. If the water freezes while in the girder, large hydraulic forces may build up, weakening the bond between the FRP and concrete.

6.4 BOND BETWEEN FRP LAMINATES AND CONCRETE

Composite plates offer significant advantages over traditional materials, such as high stiffness- and strength-to-weight ratios, corrosion resistance and light weight. However, long-term durability and effectiveness of the bond between FRP composites and concrete are two aspects of the design and construction processes that need to be carefully considered. The adhesion and bond between the two materials depends on a number of external and internal variables of the system's response. Parameters affecting the bond are schematically illustrated in Figure 6.3.

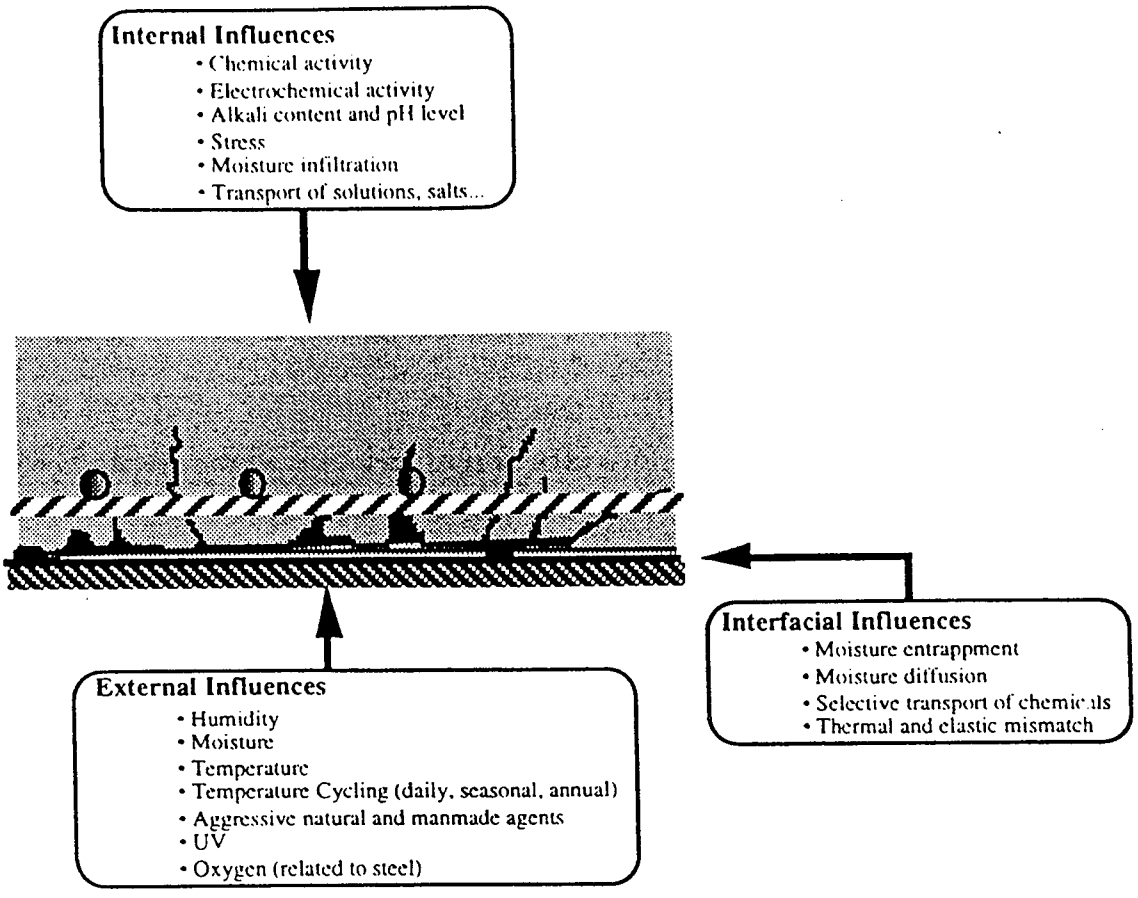

Figure 6.3: Variables Influencing the Bond Between FRP Laminates and Concrete
(Karbhari et al, 1996)

The strength and effectiveness of any assembly depends largely on the cohesive strength of the adhesive and the degree of adhesion. Two mechanisms of adhesion typically associated with bond strength are mechanical interlocking and chemical adhesion. When bonding composites to concrete, mechanical interlocking is by far the dominant mechanism. The major source of adhesion is the interlocking of the resin into the irregularities of the concrete surface. The rougher and deeper surface created by abrasion (sandblasting, grinding, etc.) allows the resin to penetrate into these irregularities thus, forming a strong interfacial layer.

Failure at the interface of composite plate and concrete can be associated with one or combination of the five modes shown in Figure 6.4.

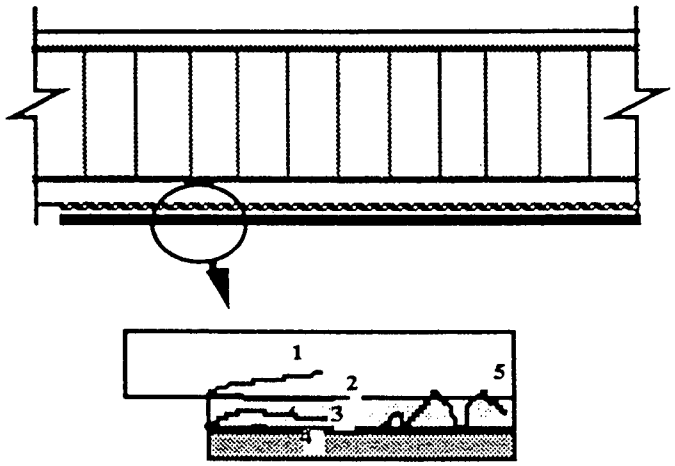

1: Peel failure into concrete
2: Interfacial failure between concrete and adhesive
3: Cohesive failure in the adhesive
4: Interfacial crack between the adhesive and the composite
5: Alternating crack path between the two interfaces

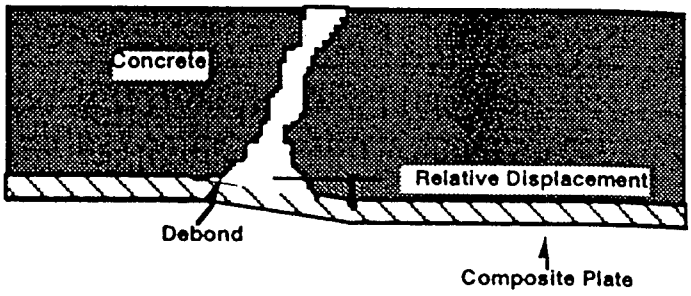

Figure 6.4: Failure at the Concrete-FRP Plate Interface
(Karbhari et al, 1996).

The transition zones at the ends of the plate are subject to sudden changes represented by a region of high shear and small but rapid changes in bending moments. This combination causes high bond stresses on the adhesive/FRP plate and adhesive/concrete interfaces. This type of failure is more likely to occur when thick composite plates are used, due to higher stress concentrations at the ends. With thin sheets, vertical displacement from shear or flexural cracks could cause bond failure in regions away from the plate ends. The use of primer epoxy and repair of pre-existing cracks may substantially reduce the possibility of failure.

6.5 MICROBIAL DEGRADATION OF FRP COMPOSITES

FRP materials, with their high strength-to-weight ratio, improved corrosion resistance, and better mechanical properties, seem to be an ideal candidate for replacing conventional metals as structural materials. However, there are various degradation mechanisms that have to be carefully considered. These mechanisms include degradation of FRP composites due to bacterial attack, moisture absorption, and sensitivity to acids. Knowledge of the effect of microorganisms on the integrity of composite materials is essential for a comprehensive evaluation of microbial damage and for the development of resistant materials *(Gu et al, 1997)*.

Possible mechanisms for microbiological degradation of composites include: direct attack of the resin by acids or enzymes, blistering due to gas evolution, and polymer destabilization caused by sulfides *(Sampath et al, 1997)*.

The constituents of FRP materials such as matrix resin, additives, and fibers may be susceptible to microbial growth, resulting in potential damage to the resin and delamination of the fibers from the resin matrix. Composites contain a range of chemicals to improve their mechanical properties, such as plasticizers, flame retardants, catalysts, and colorants. These chemicals may be used as carbon and energy sources by microorganisms.

Contamination with microorganisms could also occur during the manufacturing process *(Thorp, 1994)*. Fibers may promote fungal colonization by serving as capillaries for transporting nutrients from susceptible regions or external surfaces, thus stimulating extensive microbiological invasion. The attachment of a natural population of bacteria to the FRP materials suggests that bacteria may utilize chemicals from the surface of the fibers. Similar processes are observed on epoxy polyamide primers and polyurethane coatings.

The success or failure of an FRP composite is governed by the degree of adhesion between the fiber surface and the resin matrix. Localized weakening of this bond by microorganisms could result in bond failure and delamination when the composite is stressed. This may significantly affect the mechanical properties and physical integrity of the composite.

Sampath et al *(1997)* investigated the susceptibility to degradation of GFRP composites exposed to aggressive environments. The effects of water absorption, bacterial attack, and acids on composites were investigated by monitoring the changes in weight and dimensions measured at regular intervals. Specimens were immersed in distilled water after conditioning for six hours. The tests were performed at different temperatures: 40°C, 80°C, and 100°C until cracks were detected visually. Composite samples exposed to a temperature of 80°C exhibited an increased rate of water absorption in comparison to the specimens maintained at 40°C. However, GFRP samples exposed to temperature of 100°C showed an initial increase in weight followed by a subsequent decrease. Table 6.2 shows the reduction in tensile strength and elastic modulus values due to absorption of water.

Table 6.2: Effect of Water Absorption on Mechanical Properties of Vinyl Ester Composites

Test	Load at Break (kN)	Displacement at Break (mm)	Strain at Break (%)	Stress at Break (Mpa)	Elastic Modulus (Mpa)
Unexposed	12.87	3.2	2.1	97.87	7,092
Water, 40°C	11.6	2.3	1.53	91.33	7,059
Water, 80°C	10.86	2.15	1.43	85.51	7,029
Water, 100°C	9.86	2.05	1.37	77.67	6,950

(Sampath et al, 1997)

The microbial attack on GFRP composites and isophthalic ester were studied using an oil degrading bacteria (ODB), selected bacteria community (SBC), and sulfate reacting bacteria (SRB) cultures. The organisms were isolated from seawater.

In all cases the composites were colonized by the bacteria. Fiber pull-out and matrix cracking because of bacteria attack were distinct. After exposure for twenty-one days, the vinyl ester showed cracks, pores, and surface roughness. Specimens exposed to SBC for the same amount of time exhibited much drastic damage. Figure 6.5 shows the damage to the glass fiber itself when exposed to SBC. Well-woven glass fibers exhibited a complete shattering of their pattern after ten days of exposure.

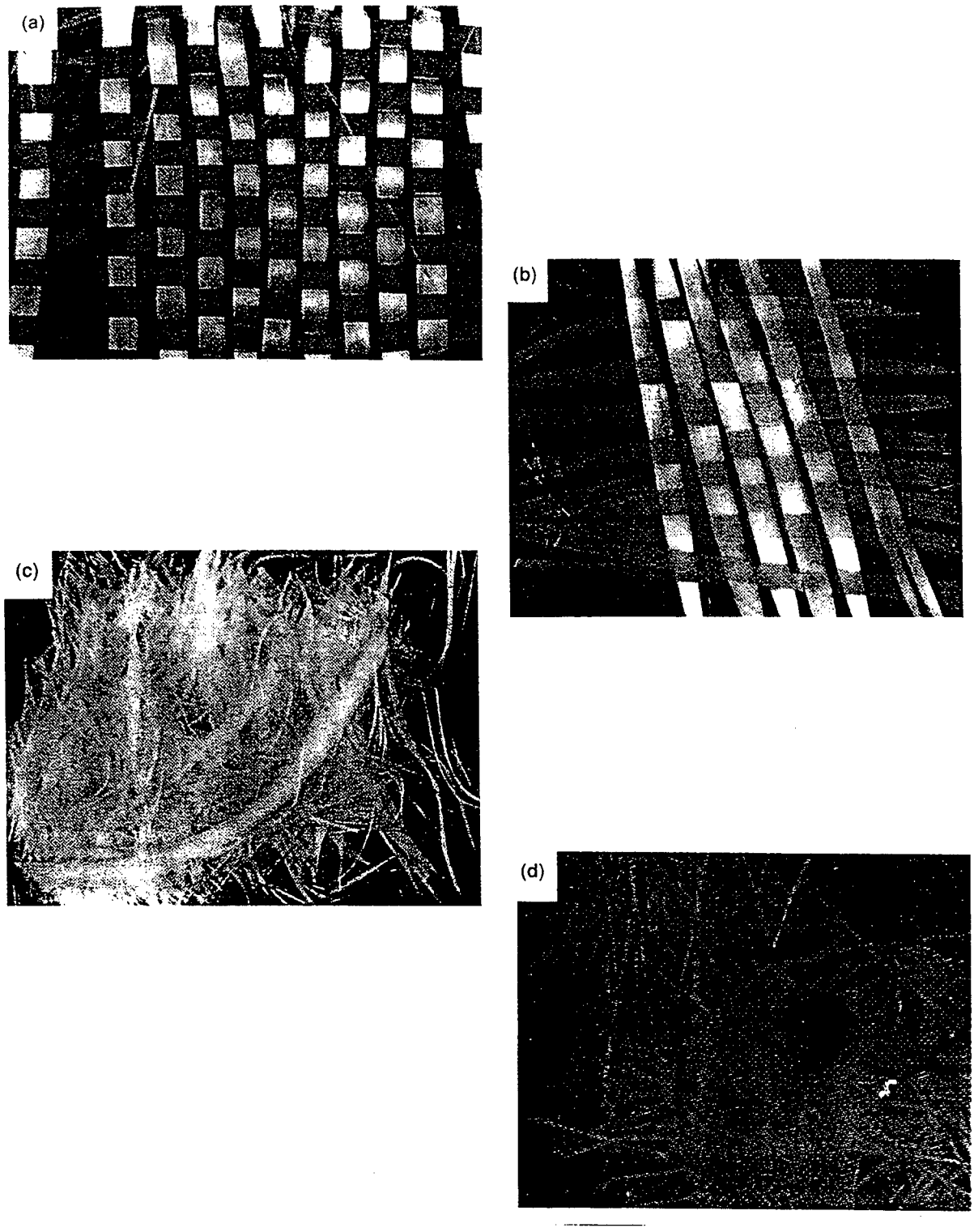

Figure 6.5: Fiberglass Damage by Bacteria Attack
a) Fiberglass without exposure b) Fiberglass exposed to culture medium, alone, and with SRB after
c) Fiberglass exposed to SRB after 10 days
d) Fiberglass exposed to SRB after 21 days.
(Sampath et al, 1997)

The study concluded that irrespective of the environment – water, acid, or bacterial – the main cause of degradation appears to occur through moisture absorption. The diffusion of water into the matrix promotes initial weight gain, followed by weight loss from surface peeling, leaching out of additives, or other reasons. All of these effects are enhanced by increased temperature or the presence of acid. Once the moisture diffuses into the resin, it attacks the fibers, resulting in fiber pull-out, breaking, or fiber dislocation. In the presence of bacteria, disruption of fiber-matrix bonding occurs, resulting in fiber pull-out. However, it is not clear whether the bacteria attacks and colonizes the resin, resulting in crack development, or if moisture absorption leads to crack development, followed by bacterial attack. Acknowledging the fact that most structural composites use specially developed, water-repellent resin systems, it is safe to conclude that the bacteria attacks should not be a problem if the second possibility reflects reality. However, detailed studies of the resin system to be used in each individual project are recommended.

Gu et al *(1997)* conducted a study describing the utilization of composite constituents as nutrients for microflora. The objectives were to determine how the carbon and glass fibers and epoxy resin are attacked by microorganisms, and to monitor the electrochemical behavior of these composites inoculated with fungal consortia under laboratory conditions. The samples were autoclaved to extract soluble organisms and then inoculated with fungal consortium. The incubation was performed at 22°C and ambient pressure in the dark. After one month of incubation, aliquots for growth were measured spectrometrically at 600 nm.

After inoculation of the composites with fungal consortium, higher fungal growth was observed in the samples containing composite extracts compared to the control samples (see Figure 6.6). The results suggest the availability of organic carbon from the composite materials for microbial growth. This is the first indicator of the nutritional relationship between the FRP deterioration and the growth of fungi.

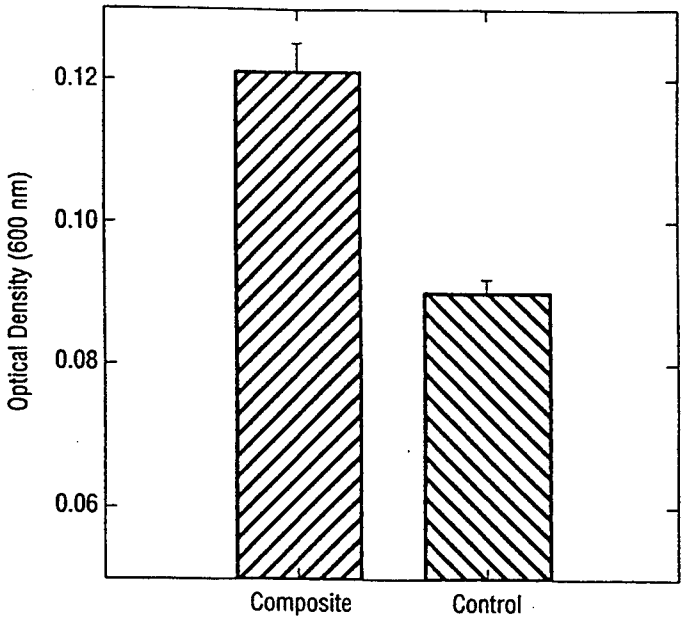

Figure 6.6: Microbial Growth on Composites after 30 Days of Incubation
(Gu et al, 1997)

Scanning electron microscopy (SEM) study indicated fungal colonization of the composites and local fungal penetration into the resin, particularly for the composites consisting of polyamide resin reinforced with glass fibers. The composites were also reported to be susceptible to a bacterial attack.

Electrochemical Impedance Spectroscopy (EIS) test of inoculated composites, conducted over 179 days, showed large deviations from the initial spectrum. A decrease of impedance was observed, indicating a decrease of pore resistance of the composite matrix or increase of pore size and pore numbers. The deterioration of the inoculated composites was continuous. However, the samples held under sterile conditions showed minimum change in impedance.

Because the vinyl esters, starch derivatives, and acetylated celluloses widely used in composites are biodegradable, delamination of fibers from the resin matrices is likely to occur as a result of microbial decomposition of these chemicals. Such failures may be avoided by using chemicals for the resin composition that are resistant to microbial attack or by incorporating a biocide. Organisms in resins that may support the growth of microorganisms can be either eliminated or inactivated by incorporation of a biocide in the resin matrix formation. Elimination of microbial contamination during composite manufacturing process would provide additional protection against biological degradation.

6.6 SHIPPING, STORAGE, HANDLING AND FIRE PROTECTION

6.6.1 Shipping, Storage and Handling

Shipping composite materials usually requires a special protection of their surface. These materials have to be handled with care according to manufacturer's prescriptions. The handling is easy due to their light weight. Storage and other requirements are typically specified by each manufacturer and cannot be generalized. Overall, shipping, storage and handling requirements are similar to those for conventional construction materials.

Instructions regarding safety of handling the FRP materials should be provided to the workers through actual demonstration. The workers should be trained side by side with experts, gaining hands-on experience.

6.6.2 Fire Protection

Composites are highly attractive materials for a variety of structural uses, but their organic resins are potentially flammable and subject to loss of strength in a fire. This vulnerability is coupled with the potential for internal delaminations from mechanical loading, which in turn will alter the composite thermal properties. Thus, the general problem of composites response to fire is very complex and not completely understood.

Fire exposure problems with FRP composites are similar to those encountered with epoxy bonded steel plates. At elevated temperatures, epoxies soften and degrade, and suffer significant strength reduction *(Thomas et al, 1996)*. This shortcoming could be addressed by use of fire suppression sprinkler systems or fire retarding products over the epoxy FRP system. Another approach, taken by resin manufacturers, is resin formulation changes that lead to fire-resistant matrix systems. In either case, the effect is depression of the heat release and limitation of the lateral fire spread.

In 1994 the EMPA performed a series of bending tests on strengthened beams exposed to high temperature (652°C, 1205°F). Six 5.2 m x 400 mm x 300 mm beams were loaded the maximum standard permissible short time load. One beam was post-strengthened with steel plates (75 mm wide, 8 mm thick), and one beam acting as the control was not plated. Four beams were strengthened with CFRP strips (74 mm wide, 1 mm thick). After eight minutes of exposure to 1205°F, the steel plate debonded from the beam. During the test, the fibers of the CFRP-strengthened beams started to burn at the surface of the strip, thus causing a slow decrease in stiffness. The CFRP composites debonded from the beam after one hour. The study concluded that the main reason for the superior behavior of the CFRP composites compared to that of the steel plates is their low thermal conductivity in the lateral direction.

6.7 QUALITY CONTROL AND QUALITY ASSURANCE

Thorough training of workers and contractors enhances the quality of any strengthening project. The designer is responsible for determining typical fiber lay-up for each laminate. The manufacturer is required to select the final laminate material and proportions of materials within the defined geometry to satisfy the short and long term strength, stiffness, durability and fire resistance requirements of the established specifications.

Quality of the FRP laminates for external reinforcement of structural elements is checked by continuous standard mechanical testing of samples of the material from each shipment supplied by the manufacturer.

A detailed resin specification must be available for each strengthening application. The resin specification includes physical properties, keeping properties, packaging, labeling, quality control and batch acceptance. It is anticipated that filled resin will be supplied to the contractor and bridge owner, and therefore tolerances covering viscosity, volatation, gel time, and density are specified for quality assurance purposes.

Fiber grades and their physical properties must be specified by the manufacturer in a fashion similar to the resin. Specifications of pigments and ultra violet absorbers must be provided. Other additives such as fillers, flame retarding substances and low profile additives are permitted as long as performance requirements are achieved. A surface protection is generally specified on exposed surfaces.

During the strengthening operations using the wet process (in-situ FRP composition), the level of FRP prestressing and the respective strains must be monitored and kept in the prescribed limits. Maximum prestress level and losses in prestressing must be carefully observed when prestressed external FRP sheets are used.

A type approval process is required before FRP composites are applied to the bridge members. This process consists of obtaining certificates of conformity for constituent materials and carrying out a series of tests on laboratory prepared samples to demonstrate satisfactory performance. The type of tests and the extent of the study may vary according to clients' and designers' preferences and the complexity of the planed rehabilitation. Typically the test data include the following:

- Short term flexural strength and stiffness;
- Long term flexural strength and stiffness;
- Ultimate tensile strength;
- Durability tests.

More sophisticated research may include ultrasonic C-scan tests to check for fiber debonding before and after mechanical testing.

A detailed specification of the manufacturing process such as pultrusion, if pre-fabricated laminates are to be used, must be prepared covering handling and storage of materials, cutting of sections, quality control, packaging and labeling.

Requirements for physical properties of the final product must be specified in terms of appearance, selection of test samples for destructive testing, mechanical properties, allowable tolerances, and quality control. Minimum acceptable requirements must be specified for strength, stiffness, and fiber content, all to be established by destructive testing on each batch, series, or shipment of the material. These tests typically examine tensile properties, flexural properties, compression properties, and interlaminar shear strength.

6.8 COST EFFECTIVENESS

Advanced composite materials are now being used successfully in a wide range of structural applications around the world. Most of these applications are prototype structures that are demonstrating the capability of the materials to achieve the designer's objective. However, the cost effectiveness of composite reinforcement is an important consideration rarely addressed by the prototype structures.

Cost effectiveness is a primary concern in bridge engineering. Selection of cost effective techniques for bridge repair is a complex task. The criteria adopted by the clients in the decision making process vary widely and are unpredictable *(Head, 1992)*. First cost is one of the most important considerations used in the decision making process. If the design is fully specified around a particular retrofitting system, the client will need to be assured that an element of competition is present in the manufacturing procurement. However, designs are often linked to particular manufacturing technique available from limited sources. Although a disadvantage from a standard point of view, this approach allows for better utilization of the properties of composite materials. Advanced composite solutions for bridges are very unlikely to use nationally or internationally standardized products as in the steel industry, because there are so many ways in which different fibers and resin systems can be combined.

Whole life cost analysis, which accounts for predicted inspections and maintenance costs over the lifetime of the bridge, are usually preferred by the clients. Advanced composite materials compare favorably with steel in such analyses. These materials, having a life-to-maintenance ratio of over 40 years, are clearly beneficial as long as inspection costs are minimized *(Head, 1992)*. Recent developments in intelligent structures technology allows remote inspection and condition monitoring by optical fibers embedded in the composite, which can reduce the inspection costs. The Canadian *(Rizkalla and Mufti, 1996)* and the European *(Miesseler and Wolff, 1991)* experiences are good examples of the importance of "smart" structures in the future.

When the cost effectiveness of a strengthening scheme is evaluated, traffic disruption and accident costs caused by inspection and maintenance over the lifetime of the bridge have to be considered. Disruption and accident costs must be assessed against delay times and accident statistics. The net present value of these costs must be added to the whole life cost to provide a comparative cost for deciding on the bridge strengthening form. Traffic disruption costs for busy highways can be a very high proportion of the capital cost. The low maintenance of rehabilitation offered by FRP composites will greatly reduce the capital costs over the life of the bridge.

Because lightweight composite materials offer shorter construction times, they can significantly contribute to delay reductions, an important aspect of the client's choice. Additionally, these materials have much to offer to an environmentally conscious client, particularly by replacing the use of hardwoods and of natural resources used in steel manufacturing, and by requiring less energy consumption.

Apart from design and safety requirements, the selection of a repair strategy is based on the anticipated cost reduction. In spite of the higher materials cost, repair of concrete structures with FRP laminates can provide substantial cost savings and performance benefits. The initial cost of the carbon fibers is about 10 times higher than structural steel, estimated per weight of the material. However, considering the specific example application of bridge strengthening performed by EMPA, Switzerland, where 94 kg of steel were replaced with 4.5 kg of CFRP, the price difference does not seem so extreme *(Meier and Kaiser, 1991)*.

It should be kept in mind that the material cost is usually only twenty percent of the total cost for strengthening applications *(Meier, 1992)*. An example that demonstrates the economic advantages of composites is the use of epoxy carbon sheets for repair of column-beam connection shear cracking in southern Florida. The application of advanced composites resulted in a thirty-five percent direct cost savings to the owner, attributed to the diminished labor costs compared with conventional methods *(Thomas et al, 1996)*. Another repair project, dealing with slab-column joint distress, had an estimated cost savings of sixty percent using composite wraps instead of conventional methods such as steel plate jackets, steel tension strapping or enlargement of the columns *(Thomas et al, 1996)*.

The material costs of fibers and resin constituents are a greater proportion of total cost than the constituents of steel and concrete. This means that design methods have to be very sophisticated to avoid conservatism or material wastage. However, design costs of advanced composite strengthening applications are typically very high due to the complexity of the design process and the need to optimize material content. Design costs of concrete and steel structures may typically be two to four percent of the construction or rehabilitation cost, whereas with advanced composites design may account for at least ten to twenty percent *(Head, 1992)*. Design cost reduction can be achieved through the use of standard systems. The American Concrete Institute (ACI 440 Committee) and other institutions in the United States and abroad are currently developing standards for reinforcing rods, prestressing cables, and strengthening. However, it is difficult to generalize strengthening since each case is unique.

Since materials and design costs are high, it is paramount that manufacturing costs are minimized. Automated processes with low labor input, such as pultrusion, are ideally suited to meet these demands. Labor intensive manufacturing methods used in the aerospace and defense industries are unlikely to be cost effective for civil engineering applications. Additionally, the use of composite materials can avoid the labor intensive repair practices that prevail in steel and concrete bridges. The weight of the composite retrofitting systems can be as little as ten percent that of conventional systems. This allows the structures to be repaired or upgraded with much lower craneage and transportation costs, as well as reduced construction times. Structures can be repaired or upgraded in days rather than months.

In conclusion, it is clear that advanced composite strengthening systems have a good chance of success in competition with conventional materials.

7.0 CONCLUSIONS AND RECOMMENDATIONS

Strengthening of structures becomes necessary because of inadequacies that affect the strength or serviceability of the whole structure or some of its members. Inadequacies may be due to inherent deficiencies in the structure such as design or construction error, or to factors such as deterioration or corrosion that develop over time. Structural inadequacies may also arise from changes in use of the structure, increased service load requirements, code changes, or necessary seismic upgrade.

Development of a strengthening strategy involves many different considerations: durability, time frame, cost-effectiveness, constructability, labor, and environmental issues all must be taken into account. Regardless of the strengthening technique used, the most important step in the planning of any strengthening or repair work is a detailed structural analysis of the existing structure. After a proper evaluation of the original structural design, field conditions, serviceability requirements and the current condition, the load-carrying capacity of the structure is assessed. This information is used to determine whether or not corrective work is required, and if so, the type of repair or strengthening that is best for the structure.

There are several types of structural strengthening: flexural strengthening of beams, increase of beam shear capacity, column strengthening, load transfer between members (primarily shear), as well as various combinations of these methods. The techniques used for strengthening usually are interrelated. Regardless of the type of strengthening, the main objective is to provide continuity of structural action between the existing and the new system, to ensure load transfer and provide composite action. The design engineers must acknowledge that adding strength to a structural member will normally also result in increased stiffness, which might be undesirable under certain conditions (for instance, during earthquakes).

Advanced composite materials offer unique mechanical and durability characteristics that can affect the bridge infrastructure renewal. Recent developments in automated manufacturing and application processes of advanced composite structural components indicate that these new materials are becoming very competitive in civil engineering applications, both structurally and economically.

The main advantages to using FRP materials are:

- Better handling due to reduced weight;
- Enhanced durability due to their very low chemical reactivity and corrosion resistance;
- Possibility of manufacturing tailor-made products of varying types, orientation and volumetric content of fibers, and number of layers for each individual application.

FRP composites provide an attractive alternative to conventional strengthening techniques for repair or upgrade of concrete structures. The role of FRP composites in such applications is analogous to the role played by steel in steel-reinforced concrete. The capability of fibers to resist loads in tension is used to increase the flexure, shear, or compression capacity of the structure, depending on how the fibers are oriented. For instance, if increase of the flexural strength of a beam is desired, FRP composites are externally applied to the tensile face of the beam, so that the fibers are parallel to the longitudinal member axis. To serve as shear reinforcement for a beam, composites are applied to the shear zone with fibers usually oriented at 45 degrees relative to the longitudinal reinforcement, as in the case of conventional steel stirrups. To increase the compressive strength of a concrete column, the FRP composites are oriented circumferentially in order to contribute to the confinement capacity. However, these typical solutions are not definitive, and the most appropriate positioning of the FRP laminates will depend upon each individual application.

The literature review indicates that most research investigators have addressed testing with very few references to parametric design concepts. Independent tests, studying similar variables have been carried out at different institutions. In view of the inevitability of specimens and loading conditions being not identical, the data cannot be synthesized in an effective manner to formulate detailed design recommendations. The only realistic way to obtain reliable data showing the influence of material type, fiber orientation, laminate thickness and application schemes is to conduct a parametric design study.

The benefits of FRP composites used for strengthening depend both on their constituent materials and application techniques. Fibers (reinforcement) and resin are the two main constituents of any FRP composite. For strengthening design purposes the performance of the FRP laminates (the final product) is the main interest. However, knowledge about the properties of the constituent materials is critical to several aspects of the overall process, including the initial selection of a strengthening system, quality control, and performance evaluation of the hybrid reinforced concrete-FRP structure.

The three most commonly used fibers for external concrete strengthening are glass, carbon and aramid. A few companies dominate the worldwide production of fibers within each category. Differences within the materials from the same category exist due to production processing, surface treatments or additives used to promote durability or adhesion. Performance differences also arise from the form of fiber configuration. The three most widely used forms for external strengthening are tows (bundles consisting of large fiber volume), unidirectional sheets (made out of parallel tows) and fabrics (woven, knitted, or stitched). The form of material configuration affects the rate of saturation with resin, ease of application and conformation to the concrete substrate to be strengthened. Selection of type and form of fibers will depend upon design, construction and economic considerations.

The role of the resin in FRP composites is to transfer the load between fibers and from the existing structural member to the fibers. The three most widely used resins for external strengthening are epoxy, vinylester and polyester. Differences within a resin category exist from one strengthening system to another. This is because different resin manufacturers formulate products with different additives to optimize desirable application and enhance performance. The systems using polyester or vinyl ester resins are typically combined with glass fiber reinforcement. Epoxy-based systems are generally available with glass, carbon, and aramid fibers.

The epoxy resins possess very good mechanical properties and the best adhesion to fibers from the three categories. Polyesters are low-cost resins with generally poor mechanical properties compared to those of other resins. Their main disadvantage is high shrinkage during cure. Polyesters can be successfully used in external strengthening applications in a form of prefabricated jackets. In such applications their curing shrinkage is offset and does not affect the end product. Vinyl esters possess chemical properties of both polyesters and epoxies, and exhibit characteristics of both. As with polyesters, use in prefabricated jackets reduces the effect of vinyl ester's high volumetric changes.

As constituent materials of FRP composites, the fibers and resins are integrally linked. Their combined performance should be the main consideration of the design engineer. If a specific strengthening application is likely to encounter a particular environmental condition (high alkalinity, UV radiation, etc.), then fibers susceptible to that condition should be paired with a resin having a good resistance against the environmental condition. An external strengthening system should be able to withstand the combined effects of loads and environment.

The performance of FRP composites depends to a large degree on the application method being adopted. External strengthening systems using the same types of fibers and resin may have only slight resemblance to each other during application. After application, however, even FRP systems with little in common may perform similarly. There are five application schemes that may be used for external strengthening of existing reinforced concrete structures, namely: rigid plates, prefabricated jackets, wound tows, pultruded strips (FRP sheets), and wet lay-ups *(Fancher, 1997).*

The rigid plating technique is analogous to steel plate bonding. The cured composite laminate is cut to the required dimensions and then affixed with an adhesive to the prepared surface of the member to be strengthened.

Prefabricated FRP jackets are large-diameter, thin-wall tubes formed and cured in factory conditions, and containing a longitudinal slit. Their main application is to confine columns with insufficient compressive strength. During application, the jackets are wrapped around the column to be strengthened. An adhesive is either spread or pumped between the concrete surface and the FRP jackets. Usually, these jackets have very high quality of FRP laminate. However, the prefabrication in a factory-controlled environment of each individual column affects the final cost of the strengthening project. Typically, they are economically feasible, if a large number of columns having the same geometry are upgraded.

Wound tows are used to build the composite laminate "in-situ" conditions by mechanically coiling them around a concrete column. The tows may be impregnated in a resin bath in the field, or may arrive at the job site already preimpregnated (prepreg). The fibers or the prepreg are applied around the column by a wrapping device, i.e., a platform carrying the fiber bundles, resin bath and the working crew, which rotates and moves up and down the column. This technique is easily adaptable to almost any shape and side of column. Additionally, the method provides a continuous wrap with no joints or overlapping, thus assuring the highest possible quality of the FRP laminate. Possible limitations are the workspace available around the column and the wrapper installation time.

Pultruted strips consist of continuous fibers and uncured resin pulled through a die to form a strip with a constant cross-section. The whole manufacturing process is completed in a factory. In the field, the cured strip is bonded to a prepared surface of the member to be strengthened. The laminates may be ordered in any desired length and width, depending upon the geometry of the beam to be strengthened. Possibly, this is the most suitable technique for flexural strengthening of beams, assuring high quality as well as ease of application. The cost of the pultruded laminates can be a limiting factor.

Wet lay-ups are a dry fabric or sheet having only a small amount of factory-applied resin. In the construction field, the dry fabric is saturated with resin, and placed by hand to form a composite laminate. The field saturation may be mechanical or by hand. The number of fabric layers may vary according to the design thickness of the laminate. The wet lay-ups are by far the most adaptable technique to existing structural members and can be used for strengthening of both beams and columns. However, this method is the most labor intensive, and requires a very experienced crew to perform the work. Proper orientation of the fabric, saturation with resin, removal of the air pockets, and initial pretensioning (10-12 lb/f) are critical to the performance of the concrete-FRP member.

No single combination of fiber, resin, and application method could be regarded as best for every external strengthening job. The choice among FRP options may be guided first by the shape and function of the structural element to be strengthened, physical restrictions of the work area, time availability, and scale of the job. Until environmental conditions have been evaluated and service load requirements have been calculated, the most suitable FRP system may not be apparent. The system to choose is not necessarily the one using the least expensive materials that meet the load requirements. Selection of a particular strengthening system should be based on the specific site conditions and the desired level of strengthening (structural design). An appropriate selection process must consider both individual materials (fibers and resin) and their combination (final product). For the bridge owners it is imperative to consider only materials for which test data is available. Table 7.1 summarizes the advantages and limitations of the different application techniques.

Table 7.1: Comparison of FRP Application Techniques

	STRENGTH	POSSIBLE LIMITATIONS
Plate	• Factory-controlled resin impregnation and cure insures high strength with low variability.	•Laminate can be applied only to flat surface. •Laminate must be cleaned prior to application. •Laminate must be bolted or held in place until banding agent begins to harden.
Prefabricated Jacket	• Factory-controlled resin impregnation and cure insures high strength with low variability. • Application is relatively quick.	•Method is suitable only for columns or industrial chimneys. Irregular geometries may cause application difficulties. •Preformed shells require manufacturing lead time and must be custom fitted to a column. •Sections of installation must be masked off to protect from adhesive running out of higher sections under clamping pressure.
Wound Tow	• Factory-controlled resin impregnation provides excellent fiber saturation and good fiber-resin ratio control. • Strict alignment of fibers is possible with automated winding. • Oven curing in the field produces denser cross-linking than ambient cure methods and consequently, higher service temperature limits.	•Method is suitable only for outside surfaces of columns or industrial chimneys. Irregular geometries may cause application difficulties. •Only a handful of robotic winders exist; equipment malfunction in the field may result in job delays. •Set-up time for automated winder may make method suitable only for very large-scale jobs. •Winding and curing equipment may be difficult to maneuver within tight confines and at extreme heights.
Pultruded Strip	• Factory-controlled resin impregnation and cure insures high strength with low variability. • Application is relatively easy.	•Strip is more flexible than rigid plate but not as flexible as fabric or fiber sheet. Limited flexibility restricts geometries accommodated and increases work space requirements. •Preparation of uneven surfaces must be completed in advance. Surface flatness is critical to insure good bond. •Strip must be cleaned with solvent prior to application.
Wet Lay-up	• Method is suitable for fabrics or unidirectional sheets in a range of fiber materials and grades. • Structural elements of various geometries and for various load conditions can be treated. • Application is relatively easy. • Confined work spaces are easily accommodated, as are member openings and fixtures.	•Unless prepreg content is minimal, fiber may require special handling to maintain intended stage of partial cure prior to installation. •For some systems, recommended substrate preparation includes grinding both before and after application of primer and putty.
Mechanical Saturation, Wet Lay-up	• Method is suitable for fabrics or unidirectional sheets in a range of fiber materials and grades. • Structural elements of various geometries and for various load conditions can be treated. • Mechanical saturation facilitates fiber wet-out.	•Large quantities of wet, mechanically saturated fabric may present handling and application challenges.

(Fancher, 1997)

It is natural for new technology to find its first use in cases of rehabilitation or damage restoration, i.e., when the client is faced with a problem that needs an immediate solution. As the technology matures, a field application that is equally viable and important is that of damage prevention. If the preservation of priceless historical heritage in addition to the repair of unsafe modern structures is considered, it becomes evident that the future of the new material systems and strengthening techniques is boundless. However, at this time there are a few factors that limit the application of FRP materials for both strengthening and new construction.

The typical approach in U.S. engineering practice is that of designers using materials and methodologies that: a) are covered by nationally or locally accepted specifications and design codes and b) have been used for many years. It must be recognized that although the traditional U.S. approach of designers designing and contractors building is well established, it limits the acceptance of new materials and technologies. It seems that adoption of a "design-build" approach to strengthening structures with new materials will be beneficial to everyone. Under this approach, an engineer and contractor team performs the structural design and also does the strengthening work *(Ballinger, 1997)*.

It should be recognized that each of the FRP systems available on the market today has been developed through extensive research. Thus, for each system there are significant materials and performance test data. In turn, these data have been used to develop company guidelines and design adds that can be used to design structural strengthening or repair. Furthermore, the data from such research is used as a cornerstone in the ACI efforts to develop standards for design with FRP materials. Thus, the lack of design and construction specifications will soon be overcome by the preparation of new codes and standards.

It must also be recognized that at this point there are no ASTM specifications for FRP materials. Moreover, there are no nationally accepted methods of inspection of individual materials or the laminates made from them. Before proper ASTM specifications are developed, test and inspection methods developed by the manufacturer for each particular FRP system may be used. Also, some of the ASTM practices designed for plastics are applicable to structural composites as well. This does not contradict the typical U.S. approach of "risk and liability" accepted by owners of the structures, design engineers and contractors. The FRP systems available today are not sold on the open market to contractors as "commodity products." Throughout the world, these materials are only made available to contractors who have aligned themselves with one of the FRP strengthening systems' manufacturers. This approach is typical for new products and techniques and targets assurance of the manufacturer's reputation more than anything else. As time goes by, more and more contractors will be able to perform bridge strengthening with FRP materials, since the installation is fairly simple.

Regardless of the manufacturer, strengthening with FRP systems includes the following basic steps:

- Repair of the deteriorated concrete structure before installation of the FRP system.
- Smoothing of corners and sharp angles on the structural member.
- Removal of laitance and other bond inhibiting contaminants by sand blasting, high pressure water jetting or other technique.
- Application of epoxy primer onto the clean surface. This is usually a two-component, high-viscosity epoxy system.
- Application of the initial resin coat to the prepared surface after the epoxy primer is dry.
- With the resin still wet, the FRP material is positioned onto the surface and de-aerated with roller or vacuum bagging. Then a second layer of resin is applied onto the sheet. The process is repeated for multiple layers until the design thickness is reached.
- The resin usually dries within a few hours. Common practice is to allow at least 3 to 5 days for complete cure before the structure is loaded.

Finally, the potential benefits of using FRP materials have to be weighed against the level of risk and liability. The following measures are suggested for bridge owners when FRP strengthening systems are considered:

- Data from inspection of the manufacturing process for the materials that will be used must be available to owners and, subsequently, inspectors.
- The manufacturer should supply the owner with system-specific design guidelines that are being used in the system's development process. Materials and structural test data must be furnished as well.
- Structural engineers who design the strengthening must be provided with system-specific design aids and guidelines. They also must have sufficient background in composite materials and structural repair with externally bonded FRP reinforcement.
- The contractors who are authorized by the manufacturer must furnish to the bridge owner their quality assurance program and guarantee proper installation according to the manufacturer's requirements and engineer's design.
- An independent laboratory must evaluate samples of the composite FRP material taken from the job site. The test data must be supplied to all involved parties, so that they may individually confirm that the materials installed have the same properties as those assumed by the design engineer, the contractor, the owner, and government officials.

8.0 REFERENCES

ACI 319-95, American Concrete Institute, Building Code Requirements for Reinforced Concrete, The American Concrete Institute, Detroit, MI.

ACI 440-F, "Guidelines for Selection, Design, and Installation of Fiber Reinforced Plastic (FRP) Systems for Externally Strengthening Concrete Structures", The American Concrete Institute, ACI Committee 440-F, Draft document, 1997.

AIJ, 1988. Standard for Structural Calculation of Reinforced Concrete Structures, Architectural Institute of Japan, 1988.

Al-Sulaimani, G., Sharif, A., Basundul, I., Baluch, M., and Ghaleb, B., "Shear Repair for Reinforced Concrete by Fiberglass Plate Bonding", ACI Structural Journal, The American Concrete Institute, July-August, 1994.

Alexander, J., G., S., and Cheng J., J., R., "Field Application and Studies of Using CFRP Sheets to Strengthen Concrete Bridge Girders", Advanced Composites in Bridges and Structures, 2nd International Conference, Proceedings, Montreal, Quebec, August, 1996.

Arduini, M., D'Ambrisi, A., and Di Tommaso, "Shear Failure of Concrete Beams Reinforced with FRP Plates", "Infrastructure: New Materials and Methods of Repair" (Editor K. Basham), Proceedings of the Third Materials Engineering Conference, San Diego, CA, 1994.

Arduini, M., Di Tommaso, A., and Nanni, A., "Brittle Failure in FRP Plate and Sheet Bonded Beams", ACI Structural Journal, The American Concrete Institute, July-August, 1997.

Ballinger, G. A., "Development of Composites in Civil Engineering", Advanced Composites in Bridges and Structures, 1st International Conference, Proceedings, Las Vegas, Nevada, 1991.

Ballinger, G.,"Acceptance and Use of FRP Sheet Strengthening Systems", Concrete Repair Bulletin, International Concrete Repair Institute, July/August 1997.

Banthia, N., Yan, C., and Nandakumar, N., "Sprayed Fiber Reinforced Plastics (FRPs) for Repair of Concrete Structures", Advanced Composites in Bridges and Structures, 2nd International Conference, Proceedings, Montreal, Quebec, August, 1996.

Baumert, M.E., Green, M.F., and Erki, M.-A., "A Review of Low Temperature Response of Reinforced Concrete Beams Strengthened with FRP Sheets", Advanced Composites in Bridges and Structures, 2nd International Conference, Proceedings, Montreal, Quebec, August, 1996b.

Bhutta, S.A., and Al-Qudi, I.L., "Hybrid Composite Beam:Analytical Model", "Infrastructure Repair Methods", Proceedings, Third Materials Conference, ASCE, 1995.

Billmeyer, F. W., Textbook of Polymer Science, 3rd Edition, New York, Wiley Interscience, 1984.

Bonacci, J. F., "Strength, Failure Mode and Deformability of Concrete Beams Strengthened Externally with Advanced Composites", Advanced Composites in Bridges and Structures, 2nd International Conference, Proceedings, Montreal, Quebec, August, 1996.

Cercone, L., and Korff, J., "Putting the Wraps on Quakes", Civil Engineering, July 1997.

Chai, Y., Priestley, M., Seible, F., "Seismic Retrofit of Circular Reinforced Concrete Bridge Columns", ACI Structural Journal, The American Concrete Institute, V.88, No.5, Sept./Oct. 1991.

Chajes, M., Januszka, T., Mertz, D., Thomson, T., and Finch, W., "Shear Strengthening of Reinforced Concrete Beams Using Externally Applied Composite Fibers", ACI Structural Journal, May/June 1995, The American Concrete Institute.

Char, M., Saadatmanesh, H., and Ehsani, M., "Concrete Girders Externally Prestressed with Composite Plates", PCI Journal, May-June, 1994.

Cjan, K.S., and Tan, T.H.,"Repair and Strengthening with Adhesive-Bonded Plates", Repair and Strengthening of Concrete Members with Adhesive Bonded Plates, the American Concrete Institute, SP-165, 1996.

Daniel, I. M., and Ishai, O., Engineering Mechanics of Composite Materials, Oxford University Press, 1994.

Demers, M., Hebert, D., Gauthier, M., Labossiere, P., and Neale, K.W., "The Strengthening of Structural Concrete with An Aramid Woven Fiber/Epoxy Resin Composite", Advanced Composite Materials for Bridges and Structures, Second International Conference, M.El-Bardry, Editor, Proceedings, August, 1996, Montreal, Canada.

Demers, M., Hebert, D., Gauthier, M., Labossiere, P., and Neale, K.W., "The Strengthening of Structural Concrete with An Aramid Woven Fiber/Epoxy Resin Composite", Advanced Composites in Bridges and Structures, 2nd International Conference, Proceedings, Montreal, Quebec, August 1996.

DeStefano, P., and Grivas, D., "Bridge Deck Performance and Rehabilitation: A Reliability-Based Analysis", 4th Materials Conference, "Materials for the New Millennium" Editor K. Chong, American Society of Civil Engineers, Washington, D.C., November 1996.

Dussek, I.J., "Strengthening of Bridge Beams and Similar Structures by Means of Epoxy-Resin-Bonded External Reinforcement", Transportation Research Record 785, Transportation Research Board, Washington, D.C., 1980.

Dutta, P.K., "CRREL Research on Materials in Cold Environments", U.S. Army Corps of Engineers, SR 90-42, 1990.

Ellyin, F., and Kujawski, D., "Fatigue Testing anf Life Prediction of Fiberglass-Reinforced Composites", Proceedings of the First International Conference on Advanced Composite Materials in Bridges and Structures (Editors Neale and Labossiere), Sherbrooke, Quebec, Canada, 1992.

Fancher, N.,"External Strengthening with FRP Composites", Concrete Repair Bulletin, International Concrete Repair Institute, July/August 1997.

Faza, S.S., GangaRao, H.V.S., and Barbero, E.J., "Fiber Composite Wrap for Rehabilitation of Concrete Structures", Repair and Rehabilitation of the Inffastructure of the Americas, H.A. Toutanji, Editor, The National Science Foundation, 1994.

Federal Highway Administration, "National Bridge Inventory in Highway Bridge Replacement and Rehabilitation Program, Eleventh Report of the Secretary of Transportation to the United States Congress", Washington, D.C., April, 1993.

Finch, W.W., Chajes, M.J., Mertz, D.R., Kaliakin, V.N., and Faqiri, A., "Bridge Rehabilitation Using Composite Materials", 3rd Materials Conference, Proceedings, "Infrastructure Repair Methods", American Society of Civil Engineers, 1995.

Fitch, M.,"Determination of the End of Functional Service Life for Concrete Bridge Decks", Transportation Research Board 74th Annual Meeting, Washington, D.C., Paper No. 950454, 1995.

Fyfe, E. R., "New Concept for Wrapping Columns with a High Strength Fiber/Epoxy System", "Infrastructure: New Materials and Methods of Repair" (Editor K. Basham), Proceedings of the Third Materials Engineering Conference, San Diego, CA, 1994.

Gu, Ji-Dong, Lu, C., Mitchell, R., Thorp, K., and Crasto, A., "Fungal Degradation of Fiber-Reinforced Composite Materials", Materials Performance, Vol.36, No.3, March 1997.

Harlow, D.,and Phoenix, S., "Probability Distributions for the Strength of Composite Materials", International Journal of Fracture, Vol.17, No.6, 1981.

Harmon, T.G., and Slattery, K.T., "Advanced Composite Confinement of Concrete", Proceedings of the First International Conference on Advanced Composite Materials in Bridges and Structures (Editors Neale and Labossiere), Sherbrooke, Quebec, Canada, 1992.

Hashin, Z., "Analysis of Composite Materials – A Survey", Journal of Applied Mechanics, Vol.50, 1983.

Head, P.R., "Design Methods and Bridge Forms for the Cost Effective Use of Advanced Composites in Bridges", Proceedings of the First International Conference on Advanced Composite Materials in Bridges and Structures (Editors Neale and Labossiere), Sherbrooke, Quebec, Canada, 1992.

Hearn, G. and Frangopol, D., "Segment-Based Reporting for Elemet-Level Bridge Inspections", Proceedings of the Fourth National Workshop on Bridge Research in Progress, June 17-19, 1996, Buffalo, New York.

Hearn, G., Frangopol, D.,and Marshall, S.,"Design of Bridge Inspection Programs for Structural Reliability", Proceedings of the Fourth National Workshop on Bridge Research in Progress, June 17-19, 1996, Buffalo, New York.

Hoppel, C., Bogetti, T., Gillepie, J., and Karbhari, V., "Analysis of a Concrete Cylinder with a Composite Hoop Wrap", "Infrastructure: New Materials and Methods of Repair" (Editor K. Basham), Proceedings of the Third Materials Engineering Conference, San Diego, CA, 1994.

Howie, I., and Karbhari, V.M.," Effect of Materials Architecture on Strengthening Efficiency of Composite Wraps for Deteriorating Columns in the North-East", "Infrastructure: New Materials and Methods of Repair" (Editor K. Basham), Proceedings of the Third Materials Engineering Conference, San Diego, CA, 1994.

Hutchinson, A.R., and Rahimi, H., "Flexural Strengthening of Concrete Beams with Externally Bonded FRP Reinforcement", Advanced Composites in Bridges and Structures, 2nd International Conference, Proceedings, Montreal, Quebec, August, 1996.

Infrastructure, "XXSys Technologies Contracted to Retrofit Historic Arch Bridge", High-Performance Composites, July/August, 1997.

Iyer, S.L., Sivaramakrishnan, C., Atmatam, S., "Testing of Reinforced Concrete Bridges for External Reinforcement", Proceedings of the Structural Congress, ASCE, May 1989.

Johnson, R.P., and Tail, C.J., "The Strength in Combined Bending and Tension of Concrete Beams with Externally Bonded Reinforcing Plates", Building and Environment, 16(4), 1981.

Jones, R., Swamy, R., and Ang, T., Under and Over-Reinforced Concrete Beams Strengthened with Steel Plates", The International Journal of Cement Composites and Lightweight Concrete, Volume 4, No.1, pp. 19-31, February 1982.

Jones, R., Swamy, R.N., and Charif, A., "Plate Separation and Anchorages of Reinforced Concrete Beams Strengthened by Epoxy-Bonded Steel Plates", The Structural Engineer, Part A, 66(12), June 1988.

Jones, R.M., Mechanics of Composite Materials, Hemisphere Publishing Corporation, 1975.

Kachlakev, D.I., "Bond Strength Investigations and Structural Applicability of Composite Fiber-Reinforced Polymer (FRP) Rebars", Ph.D. Dissertation, Oregon State University, Corvallis, Oregon, May, 1997.

Kachlakev, D.I., and Lundy, J.R., "Bond Strength Investigations of Glass Fiber-Reinforced Plastic Rebars in Concrete", Proceedings, IVth International Conference on Advanced Materials, Cancun, Mexico, August, 1995.

Karam, G.N., "Optimal Design for Prestressing with FRP Sheets in Structural Members", Proceedings of the First International Conference on Advanced Composite Materials in Bridges and Structures (Editors Neale and Labossiere), Sherbrooke, Quebec, Canada, 1992.

Karbhari, V., and Eckel, D., "Effect of a Cold-Region-Type Climate on the Strengthening Efficiency of Composite Wraps for Columns", Technical Report, University of Delaware, Center for Composite Materials, Newark, Delaware, 1993.

Karbhari, V., Seible, F., and Hegemier, G., "On the Use of Fiber Reinforced Composites for Infrastructure Renewal – A Systems Approach", 4th Materials Conference, "Materials for the New Millennium" Editor K. Chong, American Society of Civil Engineers, Washington, D.C., November, 1996.

Katsumata, H., Kobatake, Y., and Tekada, T., "Study with Carbon Fiber for Earthquake-Resistant Capacity of Existing Reinforced Concrete Columns", Proceedings of the Ninth World Conference on Earthquake Engineering, Tokyo, Japan, 1988.

Klaiber, F.W., Dunker, K.F., and Sanders, W.W., "Strengthening of Single-Span Steel Beam Bridges", Journal of Structural Engineering, American Society of Civil Engineers, Vol.108, No. 12, 1982.

Kliger, H."A New Reinforced Fiber Sheet Material for Repair of Civil Engineering Concrete Structures", High-Performance Composites for Civil Engineering Applications, SAMPE Regional Seminar, La Jolla, CA, September, 1993.

Krebich, U.T., Lohse, F., and Scmid, R., "Polymers in Low Temperature Technology", Non-Metallic Materials and Composites at Low Temperatures, New York, Plenum Press, 1979.

Kretsis, G., "A review of the Tensile, Compressive, Flexural and Shear Properties of Hybrid Fiber-Reinforced Plastics", Composites, Vol.18, No1, January, 1987.

Kujawski, D., and Ellyin, F., "Rate/Frequency-dependent Behavior of Fiberglass/Epoxy Laminates in Tensile and Cyclic Loading", Composites, Vol.26, No.10, 1995.

Ligday, F.J., Kumar, S.V., and GangaRao, H.V.S., "Creep of Concrete Beams with Externally Bonded Carbon Fiber Tow Sheets", Advanced Composites in Bridges and Structures, 2nd International Conference, Proceedings, Montreal, Quebec, August, 1996.

Limberger, E., and Vielhaber, J., "Experimental Investigations on the Behavior of CFRP-Prepreg Strengthened Structural RC Elements", Advanced Composites in Bridges and Structures, 2nd International Conference, Proceedings, Montreal, Quebec, August, 1996.

Lundy J.R., and Kachlakev, D.I., "Evaluation of the Bond Strength of Glass FRP Rebars in Concrete", 4th Materials Conference, "Materials for the New Millennium" Editor K. Chong, American Society of Civil Engineers, Washington, D.C., November, 1996.

MacDonald, M.D., and Calder, A.J.J., "Bonded Steel Plating for Strengthening Concrete Structures", International Journal of Adhesives, Vol.2, No.2, 1982.

Malvar, L.J., Warren, G.E., and Inaba, C.M., "Large Scale Tests on Navy Reinforced Concrete Pier Decks Strengthened with CFRP Sheets", Advanced Composites in Bridges and Structures, 2nd International Conference, Proceedings, Montreal, Quebec, August, 1996.

Marshall, O.S., and Busel, J.P., "Composite Repair/Upgrade of Concrete Structures", 4th Materials Conference, "Materials for the New Millennium" Editor K. Chong, American Society of Civil Engineers, Washington, D.C., November, 1996.

McConnell, V.P., "Bridge Column Retrofit-Hybrid Woven Unifabric", High Performance Composites, September/October, 1993.

McConnell, V.P., "Infrastructure Update", High Performance Composites, May/June, 1995.

Meier U., and Kaiser, H., "Strengthening of Structures with CFRP Laminates", Proceedings of ASCE Specialty Conference, "Advanced Composite Materials in Civil Engineering Structures", Editor S. Iyer, Las Vegas, Nevada, 1991.

Meier, U., "Carbon Fiber-Reinforced Polymers: Modern Materials in Bridge Engineering", Published by the International Association for Bridge and Structural Engineering, CH -8093 Zurich, Switzerland, (in English), Reprint from Structural Engineering International, 1992.

Meier, U., and Deuring, M., "The Application of Fiber Composites in Bridge Repair", Strasse und Verkehr (in English), No. 9, 1991.

Meier, U., Deuring, M., Meier, H., and Schwegler, G., "Strengthening of Structures with CFRP Laminates: Research and Applications in Switzerland", Proceedings from the 1st Conference on Advanced Composite Materials in Bridges and Structures (Editors Neale and Labossiere), Canadian Society of Civil Engineers, Montreal, Canada, 1992.

Miesseler, H.-J., and Wolff, R., "Experience with Fiber Composite Materials and Monitoring with Optical Fiber Sensors", Proceedings of ASCE Specialty Conference, "Advanced Composite Materials in Civil Engineering Structures", Editor S. Iyer, Las Vegas, Nevada, 1991.

Mitsubishi Chemical, "REPLARK: Carbon Fiber Prepreg for retrofitting and Repair Method", Manufacturer Publication, Tokyo, Japan, 1994.

Moukwa, M., "Molecular Structure and Performance of Thermosetting Resins Used in Advanced Composite Materials", Advanced Composites in Bridges and Structures, 2nd International Conference, Proceedings, Montreal, Quebec, August, 1996.

Muszynski, L.C., and Sierakowski, R.L., "Fatigue Strength of Externally Reinforced Concrete Beams", 4th Materials Conference, "Materials for the New Millennium" Editor K. Chong, American Society of Civil Engineers, Washington, D.C., November, 1996.

Nanni, A., "CFRP Strengthening", Concrete International, June 1997, The American Concrete Institute.

Nanni, A., "Concrete Repair With Externally Bonded FRP Reinforcement", Concrete International, The American Concrete Institute, June 1995.

Plevris, N., Triantafillou, T., and Veneziano, D., "Reliability of RC Members Strengthened with CFRP Laminates", Journal of Structural Engineering, The American Society of Civil Engineers, July 1995.

Prevris, N., Triantafillou, T., and Veneziano D., "Time Dependent Behavior of RC Members Strengthened with FRP Laminates", Journal of Structural Engineering, pp.1037-1044, 1995.

Priestley, M.J.N., Seible, F., and Fyfe, E., "Column Seismic Retrofit Using Fiberglass/Epoxy Jackets", Proceedings of the First International Conference on Advanced Composite Materials in Bridges and Structures (Editors Neale and Labossiere), Sherbrooke, Quebec, Canada, 1992.

Purvis, R., Babaei, K., and Clear, K., "Life-Cycle Cost Analysis for Protection and Rehabilitation of Concrete Bridges Relative to Reinforcement Corrosion", Strategic Highway Research Program, Report No. SHRP-S-377, Washigton, D.C., 1994.

Reddy, D.V., Gervois, G.B., and Carlsson, L.A., "Laminate Bonding for Concrete Repair and Retrofit", 4th Materials Conference, "Materials for the New Millennium" Editor K. Chong, American Society of Civil Engineers, Washington, D.C., November, 1996.

Rizkalla, S. and Mufti, A. "Recent Innovations for Concrete Highway Bridges", 4th Materials Conference, "Materials for the New Millenium", Editor K. Chong, American Society of Civil Engineers, Washington, D.C., vol. 2, page 1063, November, 1996.

Rostasy, F.S., Hankers, C., and Ranisch, E.-H., "Strengthening of R/C and P/C Structures with Bonded FRP Plates", Proceedings of the First International Conference on Advanced Composite Materials in Bridges and Structures (Editors Neale and Labossiere), Sherbrooke, Quebec, Canada, 1992.

Rostasy, F.S., Hankers, C., and Ranisch, E.H.,"Strengthening of RC- and P/C-Structures with Bonded FRP Plates, "Advanced Composite Materials in Bridges and Structures", CSCE, Sherbrooke, Canada, 1992.

Saadatmanesh H., Ehsani, M., and Wei, An, "Analytical Study of Concrete Girders Retrofitted with Epoxy-Bonded Composite Laminates", Repair and Strengthening of Concrete Members with Adhesive Bonded Plates, the American Concrete Institute, SP-165, 1996.

Saadatmanesh, H., Alberecht, P., and Ayyub, B.M., "Experimental Study of Prestressed Composite Beams", Journal of Structural Engineering, American Society of Civil Engineers, Vol.115, No. 9, 1989.

Saadatmanesh, H., and Ehsani, M., "Experimental Study of Concrete Girders Retrofitted with Epoxy-Bonded Composite Laminates", Repair and Strengthening of Concrete Members with Adhesive Bonded Plates, the American Concrete Institute, SP-165, 1996.

Saadatmanesh, H., Ehsani, M., and Jin, L., " Repair of Earthquake-Damaged RC Columns with FRP Wraps", ACI Structural Journal, The American Concrete Institute, March-April, 1997.

Saadatmanesh, H., Ehsani, M., and Li, M., "Strength and Ductility of Concrete Columns Externally Reinforced with Fiber Composite Strips", ACI Structural Journal, Vol. 94, No.4, July/August 1994, The American Concrete Institute.

Sampath, P., Khanna, A.S., and Ganti, S.S., "Environmentally Influenced Degradation of Fiber-Reinforced Composites", Materials Performance, Vol.36, No.5, May 1997.

Sato, Y., Ueda, T., Kakuta, Y., and Tanaka, T., "Shear Reinforcimg Effect of Carbon Fiber Sheet Attached to Side of Reinforced Concrete Beams", Advanced Composites in Bridges and Structures, 2nd International Conference, Proceedings, Montreal, Quebec, August, 1996.

Seible, F., Hegemier, G., and Karbhari, V., "Advanced Composite for Bridge Infrastructure Renewal", Forth International Bridge Engineering Conference, Proceedings, Vol.1, August 29-30, 1995, San Francisco, California.

Sen, R., and Shahawy, M., "FRP Research for Highway Applications in Florida", "Infrastructure: New Materials and Methods of Repair" (Editor K. Basham), Proceedings of the Third Materials Engineering Conference, San Diego, CA, 1994.

Sen, R., Liby L., Spillett, K., and Shahawy, M., "Bridge Rehabilitation Using Advanced Composites", 39th International SAMPE Symposium, April 11-14, 1994.

Shahawy, M., Mirmiran, A., and Samaan, M., "Hybrid Colunms of FRP and Concrete", 4th Materials Conference, "Materials for the New Millennium" Editor K. Chong, American Society of Civil Engineers, Washington, D.C., November, 1996.

Sharif, A., Al-Sulaimani, G., Basunbul, I., Baluch, M., and Ghaleb, B., "Strengthening of Initially Loaded Reinforced Concrete Beams Using FRP Plates", ACI Structural Journal, March / April, 1994.

Sierakowski, R., Ross, C., Tedesco, J., and Hughes, M., "Concrete Beams With Externally Bonded Carbon Fiber Reinforced Plastic (CFRP) Strips", "Infrastructure: New Materials and Methods of Repair" (Editor K. Basham), Proceedings of the Third Materials Engineering Conference, San Diego, CA, 1994.

Solomon, S.K., Smith, D.W., and Cusens, A.R., "Flexural Tests of Steel-Concrete-Steel Sandwiches", Magazine of Concrete Research, 28(94), March 1976.

Soudki, K.A., and Green M.F., "Freeze-Thaw Response of CFRP Wrapped Concrete", Concrete International, The American Concrete Institute, August, 1997.

Steiner, W., "Strengthening of Structures with CFRP Strips", Advanced Composite Materials for Bridges and Structures, Second International Conference, M.El-Bardry, Editor, Proceedings, August, 1996, Montreal, Canada.

Swamy, R.N., Lynsdale C.J., Mukhopadhyaya, P., "Effective Strengthening with Ductility:Use of Externally Bonded Plates of Non-Metallic Composite Materials", Advanced Composites in Bridges and Structures, 2nd International Conference, Proceedings, Montreal, Quebec, August, 1996.

Tedesco, J.W., Stalling, M., El-Mihilmy, M., and McCauley, M., "Rehabilitation of Concrete Bridges Using FRP Laminates", 4th Materials Conference, "Materials for the New Millennium" Editor K. Chong, American Society of Civil Engineers, Washington, D.C., November, 1996.

Thomas, J., Kline, T., Emmons, P., and Kliger, H., "Externally Bonded Carbon Fiber for Strengthening Concrete", 4th Materials Conference, "Materials for the New Millennium" Editor K. Chong, American Society of Civil Engineers, Washington, D.C., November, 1996.

Thomas, J, Morey, K., "Design Considerations and Application Techniques for Strengthening", Concrete Repair Bulletin, International Concrete Repair Institute, July/August 1997.

Tonen, "FORCA Tow Sheet Technical Notes", Manufacturer Publication, Tokyo, Japan, 1994.

Triantafillou, T., and Plevris, N., "Flexural Behavior of Concrete Structures Strengthened with Epoxy-Bonded Fiber Reinforced Plastics", International Seminar on Structural Repair/Strengthening by the Plate Bonding Technique, Proceedings, University of Sheffield, England, September 1992.

Triantafillou, T.C., and Plevris, N., "Post-Strengthening of R/C Beams with Epoxy-Bonded Fiber Composite Materials", Proceedings of ASCE Specialty Conference, "Advanced Composite Materials in Civil Engineering Structures", Editor S. Iyer, Las Vegas, Nevada, 1991.

Tsai, S. W., Fundamental Aspects of Fiber Reinforced Plastic Composites, Wiley Interscience, New York, 1968.

Van Gemert, D.A., and Vanden Bosch, M.C.J., "Repair and Strengthening of Reinforced Concrete Structures by Means of Bonded Steel Plates", Proceedings, International Conference on Deterioration, Bahrain, 1985.

Varastehpour, H., and Hamelin, P., "Analysis and Study of Failure Mechanism of RC Beam Strengthened with FRP Plate", Advanced Composites in Bridges and Structures, 2nd International Conference, Proceedings, Montreal, Quebec, August, 1996a.

Varastehpour, H., and Hamelin, P., "Experimental Study of RC Beam Strengthened with FRP Plate", Advanced Composites in Bridges and Structures, 2nd International Conference, Proceedings, Montreal, Quebec, August, 1996.

Vijay, P.V., and GangaRao, H.V.S., "A Unified Limit State Approach Using Deformability Factors in Concrete Beams Reinforced with GFRP Bars", 4th Materials Conference, "Materials for the New Millennium" Editor K. Chong, American Society of Civil Engineers, Washington, D.C., November, 1996.

Wight, R., G., Green, M., F., and Erki, M.-A., "Post-Strengthening Prestressed Concrete Beams with Prestressed FRP Sheets", Advanced Composites in Bridges and Structures, 2nd International Conference, Proceedings, Montreal, Quebec, August, 1996.

Yamamoto, T., "FRP Strengthening of RC Columns for Seismic Retrofitting", Proceedings of the Earthquake Engineering Tenth World Conference, Balkema, Rotterdam, 1992.

Yoshizawa, H., Myojo, T., Okoshi, M., Mizukoshi, M., and Kliger, H., "Effect of Sheet Bonding Condition on Concrete Members Havinf Externally Bonded Carbon Fiber Sheet", 4th Materials Conference, "Materials for the New Millennium" Editor K. Chong, American Society of Civil Engineers, Washington, D.C., November, 1996.

Zamichow, N., "S.D. Research May Butress State's Bridges", Los Angeles Times, July 26, 1991.

APPENDIX A

GENERAL ANISOTROPIC MATERIALS

GENERAL ANISOTROPIC MATERIALS[1]

The state of stress in a continuous media is completely determined by the stress tensor τ_{ij} and the state of deformation by the strain tensor e_{ij}. Assume that when an elastic medium is maintained at a fixed temperature there is a one-to-one analytical relationship between the τ_{ij} and e_{ij} and that the stresses vanish when the strains are all zero. Then the stress-strain relationship may be written in linear form

$$\tau_{ij} = c_{ijkl} e_{kl} \Big|_{i,j,k,l=1,2,3} \qquad \textbf{(A-1)}$$

In general c_{ijkl} will vary from point to point in the medium. However, if the c_{ijkl} are independent of the position of the point, c_{ijkl} are constants, and the medium is called "elastically homogenous." Eq. A-1 is a natural generalization of Hooke's law and is used as the basis for the linear theory of elasticity.

The components τ_{ij} are symmetric, thus the interchange of the indices i and j does not alter the formula, so that $c_{ijkl} = c_{jikl}$. From here it follows that the last two indices are also symmetric, $c_{ijkl} = c_{ijlk}$, consequently, the components e_{kl} are symmetric. The consequence of this symmetry is that the 81 constants in Eq. A-1 are reduced to, at most, 36 independent constants.

Equation A-1 may now be simplified by introducing the notation

$$\tau_{11} = \tau_1 \quad \tau_{22} = \tau_2 \quad \tau_{33} = \tau_3 \quad \tau_{23} = \tau_4 \quad \tau_{31} = \tau_5 \quad \tau_{12} = \tau_6$$
$$e_{11} = e_1 \quad e_{22} = e_2 \quad e_{33} = e_3 \quad 2e_{23} = e_4 \quad 2e_{31} = e_5 \quad e_{12} = e_6$$

And write the six equations (A-1) in the form

$$\tau_1 = c_{11}e_1 + c_{12}e_2 + c_{13}e_3 + c_{14}e_4 + c_{15}e_5 + c_{16}e_6$$
$$\cdots\cdots\cdots\cdots\cdots\cdots\cdots\cdots\cdots\cdots\cdots\cdots\cdots\cdots$$
$$\tau_6 = c_{61}e_1 + c_{62}e_2 + c_{63}e_3 + c_{64}e_4 + c_{65}e_5 + c_{66}e_6$$

Or, in compact form

$$\tau_i = c_{ij}e_j \qquad \textbf{(A-2)}$$

Since the matrix c_{ij} is non-zero there exists C_{ij} such that

$$e_i = C_{ij}\tau_j$$

The constants c_{ij} in Eq. A-2 are called the *elastic constants*, or *moduli*, of the material. Since the strains e_i are dimensionless, the c_{ij} have the same dimensions as the stress components.

[1]This portion of the appendix is based on the "Mathematical Theory of Elasticity," by Sokolnikoff, McGraw-Hill, 1956, pp. 58-64.

The maximum number of the independent elastic constants is 36, but this number reduces to 21 whenever there exists a quadratic potential function W, called the strain-energy density function,

$$W = \frac{1}{2} c_{ij} e_i e_j, \tag{A-3}$$

With the property,

$$\frac{\partial W}{\partial e_i} = \tau_i. \tag{A-4}$$

Since the quadratic form of Eq. A-3 is symmetric with respect to e, and it then follows from Eq. A-4 that

$$\tau_i = c_{ij} e_j,$$

Where $c_{ij} = c_{ji}$.

Consider a substance that is elastically symmetric to the x_1x_2-plane. This symmetry is expressed by the invariance of c_{ij} under the transformation

$$x_1' = x_1, \quad x_2' = x_2, \quad x_3' = -x_3.$$

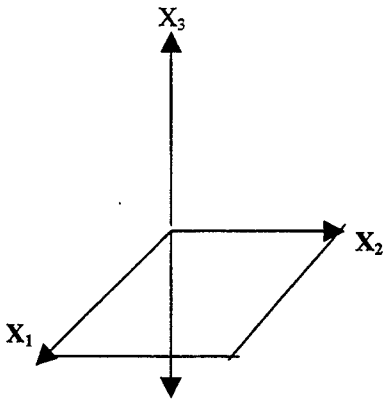

The table of direction cosines of this transformation is

	X_1	X_2	X_3
x'_1	1	0	0
x'_2	0	1	0
x'_3	0	0	-1

Now: $e'_{\alpha\beta} = l_{\alpha i} l_{\beta j} e_{ij}$ and $\tau'_{\alpha\beta} = l_{\alpha i} l_{\beta j} \tau_{ij}$

where l_{kl} are the values in the direction cosines table. The subscripts correspond to the variable subscripts. The set of quantities e_{ij} and τ_{ij}, transforming according to the two equations above, are said to represent a Cartesian tensor of rank 2.

Solving the two equations it is seen that (recall the simplified notation and Eq. A-2)

$$\tau'_i = \tau_i, \quad e'_i = e_i, \quad i = 1,\ 2,\ 3,\ 6$$

$$\tau'_4 = -\tau_4 \quad e'_4 = -e_4 \quad \tau'_5 = -\tau_5 \quad e'_5 = -e_5 .$$

The first equation of A-2 becomes

$$\tau'_1 = c_{11} e'_1 + c_{12} e'_2 + c_{13} e'_3 + c_{14} e'_4 + c_{15} e'_5 + c_{16} e_6$$

or

$$\tau_1 = c_{11} e_1 + c_{12} e_2 + c_{13} e_3 - c_{14} e_4 - c_{15} e_5 + c_{16} e_6 .$$

By comparison, $c_{14} = c_{15} = 0$. Similarly, by considering the 5 remaining equations of A-2

$$c_{24} = c_{25} = c_{34} = c_{35} = c_{64} = c_{65} = 0,$$
$$c_{41} = c_{42} = c_{43} = c_{46} = c_{51} = c_{52} = c_{53} = c_{56} = 0.$$

For a material with elastic symmetry about the x_1x_2 plane, the matrix of the coefficients in equation A-2 can be written as

$$\begin{vmatrix} c_{11} & c_{12} & c_{13} & 0 & 0 & c_{16} \\ c_{21} & c_{22} & c_{23} & 0 & 0 & c_{26} \\ c_{31} & c_{32} & c_{33} & 0 & 0 & c_{36} \\ 0 & 0 & 0 & c_{44} & c_{45} & 0 \\ 0 & 0 & 0 & c_{54} & c_{55} & 0 \\ c_{61} & c_{62} & c_{63} & 0 & 0 & c_{66} \end{vmatrix} \qquad \textbf{(A-5)}$$

Since τ_{ij} and e_{ij} are tensors of rank two, then, from the mathematics of tensor analysis, equation A-1 can be written in the form

$$\tau_{ij} = c_{ij}^{kl} e_{kl} \quad i,\ j,\ k,\ l = 1,\ 2,\ 3,$$

valid in all coordinate systems, then it follows that the c_{ij}^{kl} are components of a tensor of rank 4.

Under the coordinate transformation from $X \rightarrow X'$ the c_{ij}^{kl} transform according to the law

$$c_{ij}^{'kl} = \frac{\partial x_\alpha}{\partial x_i'} \frac{\partial x_\beta}{\partial x_j'} \frac{\partial x_k'}{\partial x_\gamma} \frac{\partial x_l'}{\partial x_\delta} c_{\alpha\beta}^{\gamma\delta}$$

If the c_{ij}^{kl} are invariant under a given coordinate transformation ($c_{ij}^{'kl} = c_{ij}^{kl}$),

then the transformation characterizes elastic symmetry and the $\frac{\partial x_i}{\partial x_j'}$ are the direction cosines.

Now consider symmetry with respect to the x_1x_2 plane. The c_{ij} are again invariant under the new transformation

$$x_1' = -x_1, \quad x_2' = x_2, \quad x_3' = x_3.$$

By applying previous considerations

$$c_{16} = c_{26} = c_{36} = c_{45} = c_{54} = c_{61} = c_{62} = c_{63} = 0.$$

Note that elastic symmetry in two mutually orthogonal planes implies symmetry in the third orthogonal plane. Thus equation A-5 reduces further and the matrix of the c_{ij} for orthotropic media takes on the following form.

$$\begin{vmatrix} c_{11} & c_{12} & c_{13} & 0 & 0 & 0 \\ c_{21} & c_{22} & c_{23} & 0 & 0 & 0 \\ c_{31} & c_{32} & c_{33} & 0 & 0 & 0 \\ 0 & 0 & 0 & c_{44} & 0 & 0 \\ 0 & 0 & 0 & 0 & c_{55} & 0 \\ 0 & 0 & 0 & 0 & 0 & c_{66} \end{vmatrix} \qquad \textbf{(A-6)}$$

If $c_{ij} = c_{ji}$, as previously discussed, there are thirteen essential constants in array A-5 and nine in array A-6.

SPECIALLY ORTHOTROPIC MATERIALS UNDER PLANE STRESS

Equation A-2 can now be written as

$$\begin{bmatrix} \tau_1 \\ \tau_2 \\ \tau_3 \\ \tau_4 \\ \tau_5 \\ \tau_6 \end{bmatrix} = \begin{vmatrix} c_{11} & c_{12} & c_{13} & 0 & 0 & 0 \\ c_{12} & c_{22} & c_{23} & 0 & 0 & 0 \\ c_{13} & c_{23} & c_{33} & 0 & 0 & 0 \\ 0 & 0 & 0 & c_{44} & 0 & 0 \\ 0 & 0 & 0 & 0 & c_{55} & 0 \\ 0 & 0 & 0 & 0 & 0 & c_{66} \end{vmatrix} \begin{bmatrix} e_1 \\ e_2 \\ e_3 \\ e_4 \\ e_5 \\ e_6 \end{bmatrix} \qquad \textbf{(A-7)}$$

In most structural applications composite materials are used in the form of thin laminates loaded in the plane of the laminate. Thus, composite laminates can be considered to be under plane stress with the stress components in the out-of-plane direction being zero. Let the X_3 plane represent the out of plane direction and recall that:

$$\tau_{11} = \tau_1 \quad \tau_{22} = \tau_2 \quad \tau_{33} = \tau_3 \quad \tau_{23} = \tau_4 \quad \tau_{31} = \tau_5 \quad \tau_{12} = \tau_6$$
$$e_{11} = e_1 \quad e_{22} = e_2 \quad e_{33} = e_3 \quad 2e_{23} = e_4 \quad 2e_{31} = e_5 \quad e_{12} = e_6.$$

Thus: $\tau_3 = \tau_4 = \tau_5 = 0$ and array A-7 becomes

$$\begin{bmatrix} \tau_1 \\ \tau_2 \\ 0 \\ 0 \\ 0 \\ \tau_6 \end{bmatrix} = \begin{vmatrix} c_{11} & c_{12} & c_{13} & 0 & 0 & 0 \\ c_{12} & c_{22} & c_{23} & 0 & 0 & 0 \\ c_{13} & c_{23} & c_{33} & 0 & 0 & 0 \\ 0 & 0 & 0 & c_{44} & 0 & 0 \\ 0 & 0 & 0 & 0 & c_{55} & 0 \\ 0 & 0 & 0 & 0 & 0 & c_{66} \end{vmatrix} \begin{bmatrix} e_1 \\ e_2 \\ e_3 \\ e_4 \\ e_5 \\ e_6 \end{bmatrix} \qquad \textbf{(A-8)}$$

Or in expanded form

$$\tau_1 = c_{11}e_1 + c_{12}e_2 + c_{13}e_3$$

$$\tau_2 = c_{12}e_1 + c_{22}e_2 + c_{23}e_3$$

$$0 = c_{13}e_1 + c_{23}e_2 + c_{33}e_3$$

$$c_{44} = c_{55} = 0$$

$$\tau_6 = c_{66}e_6$$

where the c_{ij} are the elastic moduli.

RELATIONSHIPS BETWEEN ELASTIC MODULI AND ENGINEERING CONSTANTS

From engineering considerations the stress components can be estimated by:

$$\begin{aligned} e_1 &= \frac{\tau_1}{E_1} \\ e_2 &= \frac{-\upsilon_{12}}{E_1}\tau_1 \\ e_3 &= \frac{-\upsilon_{13}}{E_1}\tau_1 \end{aligned} \qquad \text{(A-9)}$$

$$e_4 = e_5 = e_6 = 0$$

Where:

E_1 is Youngs modulus in the X_1 direction
υ_{12} is the Poisson ratio in the X_1X_2 direction
υ_{13} is the Poisson ratio in the X_1X_3 direction

If a specially orthotropic material is subjected to uniaxial tensile loading in the longitudinal direction, X_1, we have:

$$\begin{aligned} e_1 &= \frac{\tau_1}{c_{11}} \\ e_2 &= \frac{\tau_1}{c_{12}} \\ e_3 &= \frac{\tau_1}{c_{13}} \end{aligned} \qquad \text{(A-10)}$$

$$\tau_4 = \tau_5 = \tau_6 = 0$$

Solving equations A-9 and A-10 for c_{ij} in the X_1 direction

$$c_{11} = E_1 \quad c_{12} = c_{21} = -\frac{\upsilon_{12}}{E_1} \quad c_{13} = c_{31} = -\frac{\upsilon_{13}}{E_1} \qquad \text{(A-11)}$$

$$\tau_1 = E_1 e_1 - \frac{\upsilon_{12}}{E_1} e_2 - \frac{\upsilon_{13}}{E_1} e_3 \qquad \text{(A-12)}$$

Similarly, for the X_2 direction

$$c_{22} = E_2 \quad c_{21} = c_{12} = -\frac{\upsilon_{21}}{E_2} \quad c_{23} = c_{32} = -\frac{\upsilon_{23}}{E_2} \qquad \text{(A-13)}$$

$$\tau_2 = -\frac{\upsilon_{12}}{E_2} e_1 + E_2 e_2 - \frac{\upsilon_{23}}{E_2} e_3 \qquad \text{(A-14)}$$

The stress-strain equations, from Daniel and Ishai, 1994, for anisotropic materials using generalized form of Hooke's law are:

$$\sigma_{ij} = C_{ijkl}\,\varepsilon_{kl} \quad |_{i,j,k,l=1,2,3} \tag{A-15}$$

$$\varepsilon_{ij} = S_{ijkl}\,\sigma_{kl} \quad |_{i,j,k,l=1,2,3} \tag{A-16}$$

Where:

σ is the stress tensor
ε is the strain tensor
C is the stiffness matrix component
S is the compliance matrix component

Note that:

$$\sigma_{kl} = S^{-1}_{ijkl}\,\varepsilon_{ij} \quad |_{i,j,k,l=1,2,3} \tag{A-17}$$

Equations A-15 and A-16 are each nine equations with nine unknowns, which are related by equation A-17, and reduces to:

$$\begin{bmatrix}\sigma_1\\ \sigma_2\\ \sigma_3\\ \tau_4\\ \tau_5\\ \tau_6\end{bmatrix} = \begin{vmatrix}C_{11} & C_{12} & C_{13} & 0 & 0 & 0\\ C_{12} & C_{22} & C_{23} & 0 & 0 & 0\\ C_{13} & C_{23} & C_{33} & 0 & 0 & 0\\ 0 & 0 & 0 & C_{44} & 0 & 0\\ 0 & 0 & 0 & 0 & C_{55} & 0\\ 0 & 0 & 0 & 0 & 0 & C_{66}\end{vmatrix} \begin{bmatrix}\varepsilon_1\\ \varepsilon_2\\ \varepsilon_3\\ \nu_4\\ \nu_5\\ \nu_6\end{bmatrix}$$

$$\begin{bmatrix}\varepsilon_1\\ \varepsilon_2\\ \varepsilon_3\\ \nu_4\\ \nu_5\\ \nu_6\end{bmatrix} = \begin{vmatrix}S_{11} & S_{12} & S_{13} & 0 & 0 & 0\\ S_{12} & S_{22} & S_{23} & 0 & 0 & 0\\ S_{13} & S_{23} & S_{33} & 0 & 0 & 0\\ 0 & 0 & 0 & S_{44} & 0 & 0\\ 0 & 0 & 0 & 0 & S_{55} & 0\\ 0 & 0 & 0 & 0 & 0 & S_{66}\end{vmatrix} \begin{bmatrix}\sigma_1\\ \sigma_2\\ \sigma_3\\ \tau_4\\ \tau_5\\ \tau_6\end{bmatrix}$$

From engineering considerations we have:

$$\begin{aligned} \varepsilon_1 &= \frac{\sigma_1}{E_1} \\ \varepsilon_2 &= \frac{-\upsilon_{12}}{E_1}\sigma_1 \\ \varepsilon_3 &= \frac{-\upsilon_{13}}{E_1}\sigma_1 \\ \nu_4 &= \nu_5 = \nu_6 = 0 \end{aligned} \qquad \textbf{(A-18)}$$

and

$$\begin{aligned} \sigma_1 &= C_{11}\varepsilon_1 + C_{12}\varepsilon_2 + C_{13}\varepsilon_3 \\ \sigma_2 &= C_{12}\varepsilon_1 + C_{22}\varepsilon_2 + C_{23}\varepsilon_2 \\ 0 &= C_{13}\varepsilon_1 + C_{23}\varepsilon_2 + C_{33}\varepsilon_3 \\ \tau_4 &= 0 \\ \tau_5 &= 0 \\ \tau_6 &= C_{66}\nu_6 \end{aligned} \qquad \textbf{(A-19)}$$

If a specially orthotropic material is subjected to uniaxial tensile loading in the longitudinal direction, σ_1, we have:

$$\begin{aligned} \varepsilon_1 &= S_{11}\sigma_1 \\ \varepsilon_2 &= S_{12}\sigma_1 \\ \varepsilon_3 &= S_{13}\sigma_1 \\ \tau_4 &= \tau_5 = \tau_6 = 0 \end{aligned} \qquad \textbf{(A-20)}$$

Then from A-19 and A-20 we have:

$$S_{11} = \frac{1}{E_1}, \quad S_{12} = S_{21} = -\frac{\upsilon_{12}}{E_1}, \quad S_{13} = S_{31} = -\frac{\upsilon_{13}}{E_1} \qquad \textbf{(A-21)}$$

If a material element is subjected to uniaxial tensile loading in the in-plane transverse direction, σ_2, we have:

$$\begin{aligned} \varepsilon_1 &= S_{12}\sigma_2 = -\frac{\nu_{21}}{E_2}\sigma_2 \\ \varepsilon_2 &= S_{22}\sigma_2 = \frac{\sigma_2}{\tau_{2\,1}} \\ \varepsilon_3 &= S_{23}\sigma_2 = \frac{-\nu_{23}}{E_2}\sigma_2 \\ \nu_4 &= \nu_5 = \nu_6 = 0 \end{aligned} \qquad \textbf{(A-22)}$$

Then:

$$S_{22} = \frac{1}{E_2}, \quad S_{12} = S_{21} = -\frac{\upsilon_{21}}{E_2}, \quad S_{13} = S_{31} = -\frac{\upsilon_{23}}{E_2} \qquad \textbf{(A-23)}$$

OREGON DEPARTMENT OF TRANSPORTATION
Research Report User Survey

We need your opinion! Your input is invaluable to us as we strive to produce more useful reports for our customers. By completing this brief questionnaire, you are helping to improve the overall quality of the research program. We hope you will take a minute to give us your thoughts. After filling out the evaluation below, fold the page in thirds with the address on the back showing, tape it shut, and drop it in the mail!

Report Title: **Strengthening Bridges Using Composite Materials (Final Report)**
Report Number: FHWA-OR-RD-98-08 Publication Date: March 1998

Your name, title, and organization (optional): _____

1. Which parts of the report did you read? *(Check all that apply)*
   - ❑ All
   - ❑ Abstract
   - ❑ Table of Contents
   - ❑ Introduction
   - ❑ Body
   - ❑ Conclusions and Recommendations
   - ❑ Appendices
   - ❑ Other _____

2. Overall, how useful did you find the report? *(Check only one)*
   ❑ Very useful ❑ Somewhat useful ❑ Not very useful ❑ Not at all useful

3. How will you use the information in this report? *(Check all that apply)*
   - ❑ As reference material
   - ❑ Will use information in other research
   - ❑ To implement recommendations
   - ❑ Will not use information
     ↳ Why? _____
   - ❑ Other _____

4. Implementation of the recommendations would have the following impacts: *(Check one box per row)*

	Very Positive	*Positive*	*Somewhat Positive*	*No Impact*	*Negative*	*Don't Know*
Safety	❑	❑	❑	❑	❑	❑
Cost	❑	❑	❑	❑	❑	❑
Service	❑	❑	❑	❑	❑	❑

5. How would you rate the technical content of the report? *(Check only one)*
   ❑ Excellent ❑ Good ❑ Fair ❑ Poor ❑ Don't Know

6. How would you rate the report's readability? *(Check only one)*
   ❑ Excellent ❑ Good ❑ Fair ❑ Poor ❑ Don't Know

7. Additional comments: _____

Fold here

Research Unit
Transportation Development Branch
200 Hawthorne SE Ste. B-240
Salem, OR 97310

Fold here